Impulsive Control and Synchronization of Chaos-Generating-Systems with Applications to Secure Communication

by

Anmar Khadra

A thesis
presented to the University of Waterloo
in fulfillment of the
thesis requirement for the degree of
Doctor of Philosophy
in
Applied Mathematics

Waterloo, Ontario, Canada, 2004

I hereby declare that I am the sole author of this thesis. This is a true copy of the thesis, including any required final revisions, as accepted by my examiners.
I understand that my thesis may be made electronically available to the public.

Anmar Khadra

Abstract

When two or more chaotic systems are coupled, they may exhibit synchronized chaotic oscillations. The synchronization of chaos is usually understood as the regime of chaotic oscillations in which the corresponding variables or coupled systems are equal to each other. This kind of synchronized chaos is most frequently observed in systems specifically designed to be able to produce this behaviour.

In this thesis, one particular type of synchronization, called impulsive synchronization, is investigated and applied to low dimensional chaotic, hyperchaotic and spatiotemporal chaotic systems. This synchronization technique requires driving one chaotic system, called response system, by samples of the state variables of the other chaotic system, called drive system, at discrete moments. Equi-Lagrange stability and equi-attractivity in the large property of the synchronization error become our major concerns when discussing the dynamics of synchronization to guarantee the convergence of the error dynamics to zero. Sufficient conditions for equi-Lagrange stability and equi-attractivity in the large are obtained for the different types of chaos-generating systems used.

The issue of robustness of synchronized chaotic oscillations with respect to parameter variations and time delay, is also addressed and investigated when dealing with impulsive synchronization of low dimensional chaotic and hyperchaotic systems. Due to the fact that it is impossible to design two identical chaotic systems and that transmission and sampling delays in impulsive synchronization are inevitable, robustness becomes a fundamental issue in the models considered. Therefore it is established, in this thesis, that under relatively large parameter perturbations and bounded delay, impulsive synchronization still shows very desired behaviour. In fact, criteria for robustness of this particular type of synchronization are derived for both cases, especially in the case of time delay, where sufficient conditions for the synchronization error to be equi-attractivity in the large, are derived and an upper bound on the delay terms is also obtained in terms of the other parameters of the systems involved.

The theoretical results, described above, regarding impulsive synchronization, are reconfirmed numerically. This is done by analyzing the Lyapunov exponents of the error dynamics and by showing the simulations of the different models discussed in each case.

The application of the theory of synchronization, in general, and impulsive synchronization, in particular, to communication security, is also presented in this thesis. A new impulsive cryptosystem, called induced-message cryptosystem, is proposed and its properties are investigated. It was established that this cryptosystem does not require the transmission of the encrypted signal

but instead the impulses will carry the information needed for synchronization and for retrieving the message signal. Thus the security of transmission is increased and the time-frame congestion problem, discussed in the literature, is also solved. Several other impulsive cryptosystems are also proposed to accommodate more solutions to several security issues and to illustrate the different properties of impulsive synchronization.

Finally, extending the applications of impulsive synchronization to employ spatiotemporal chaotic systems, generated by partial differential equations, is addressed. Several possible models implementing this approach are suggested in this thesis and few questions are raised towards possible future research work in this area.

Acknowledgements

I would like to thank my supervisors, Dr. X. Z. Liu and Dr. X. Shen, for their guidance and help to finish this thesis, as well as the Ontario Graduate Scholarship for their generous financial support in the form of a postgraduate scholarship. I would also like to acknowledge all the useful comments and suggestions of the members of my examination committee, including Dr. P. Yu, Dr. S. A. Campbell, Dr. G. B. Agnew and Dr. E. R. Vrscay, which have improved the quality of this thesis.

Now regarding the people who were acting behind the scenes, I would like to begin with my parents. Dad and mom, your tremendous love, care and support were absolutely overwhelming and the sole reason for me to get to this point. You have given me all what I needed and you were very generous in doing so. Words cannot describe how grateful I am to you and how much I appreciate all what you have given me. You have done everything possible to bring up this family in an excellent environment and worked hard to make us happy. We are all proud of what you have achieved and we wish we would be able to meet your expectations. You deserve everything good that this life could offer. Thank you and love you.

For the rest of my family, including my brothers, Aiman, Eyad and Iyas, and my sister-in-laws, Sabine, Nadja and Julianne, you were truly amazing and extremely supportive. You were (and still are) my role-models. I learned a lot from you and I continue to learn more every day. I am very proud of what you have achieved in your lives and of what you are right now. Thank you for everything and for being by my side whenever I needed you. You guys are the best.

For the third generation: Kathrin, Daniel, Alex and Lena, you are the present and the future. Your are the extension of the love this family has and even beyond. Thank you for just being with us and for enriching our lives with love and happiness.

For the love of my life, Karin, thank you very much for being incredibly supportive and very loving person. You have encouraged me through good times as well as through bad times. Without you, finishing this thesis would have been impossible. Living in Waterloo was a very unpleasant experience, but meeting you here made this experience absolutely worthwhile and joyful. The time we spent together in Waterloo and in many other places, are unforgettable moments. I will never forget the amount of time and money you spend to be with me or to support me. Thank you for everything and I wish one day I could be of equal support to you.

Finally, I would like to thank all my friends for making this particular journey of my life in Waterloo a bearable one. Your friendship is invaluable to me. I thank everyone of you for the joyful and happy moments we spend together. These memories will stay in my mind forever.

Contents

List of Tables

List of Figures

Chapter 1

Introduction

Secure communication and *chaos* form the foundations of what is so called chaos-based secure communication schemes. The properties of systems generating chaos, such as their unpredictability behaviour in the absence of knowing the initial conditions, led many mathematicians and engineers to integrate chaos generating systems with secure communication, in general, and to *cryptography*, in particular.

When speaking about *conventional cryptography*, we mean cryptosystems which work on discrete values and in discrete time. This involves classical cryptography as well as all modern systems being in practical use nowadays. The crucial points in *chaotic cryptography*, however, are continuous-value information and the usage of continuous-value systems which may operate in continuous or discrete time. To emphasize its difference to conventional cryptography, we shall use the term *continuous-value cryptography* synonymously with chaotic encryption or chaotic cryptography. In our understanding, it is just a necessity to utilize non-linearities and to force the system dynamics into a chaotic operation to fulfill basic cryptographical requirements in the continuous-value case.

Since its ancient beginnings, cryptographical methods have been almost exclusively applied to discrete-value information. These methods range from the so called Caesar cipher, to the well known Vigenère Cipher, up to the modern encryption algorithms like data encryption standard (DES) or the asymmetrical algorithm by Rivest, Shamir and Adelman (RSA). A comprehensive survey on these, and many more conventional ciphers, can be found in [96]. The development of cryptographical methods became a modern science which formed the basis of all encryption systems in use nowadays.

Despite the strong relevance of the discrete-value systems, there have been attempts to apply cryptographical methods to continuous-value information. Early investigations, that were mainly inspired by increasing research on chaotic systems, can be found in [16–19, 22–24, 88, 89]. In these papers, autonomous continuous-time chaotic systems were used as pseudo-random number generators and pioneering works on chaos synchronization led to a new branch of applications; namely, chaos-based secure communication.

In the next section, we shall present the structure of any network, or internet, and the security requirements needed to make any network safe from hackers or intruders. In Section 1.2, an introduction to important mathematical concepts such as asymptotic stability, Lagrange stability and, most importantly, continuous-time chaos, will be provided to facilitate the understanding of the rest of the thesis. Then, in Section 1.3, an introduction to impulsive systems and their structures, together with some stability theory associated with it, which is available in the literature, will be presented. This theory will be very crucial in the development of impulsive synchronization, a concept heavily used in this thesis.

1.1 Motivations

The requirements of information security within an organization have undergone major changes in the last several decades. Before the widespread use of data processing equipment, the security of information felt to be valuable to an organization was provided primarily by physical and administrative means. An example of the former is the use of rugged filing cabinets with a combination lock for storing sensitive documents. An example of the latter is personnel screening procedures used during hiring precesses.

However, with the introduction of the computer, the need and emphasis on automated tools for protecting information became evident. This is especially the case for shared systems, such as time-sharing systems, and the need is even more acute for systems that can be accessed over a public telephone network, data network, or internet. The generic name for the collection of tools designed to protect data and to thwart hackers is *computer security*.

The second major change, that gave birth to a new generation of security requirements, is the introduction of distributed systems and the use of networks and communication facilities for carrying data between terminal user and computer and between computer and computer. Network security measures are needed to protect data during their transmission. In fact, the term network security is somewhat misleading, because virtually all businesses, governments

and academic organizations interconnect their data processing equipment with a collection of interconnected networks. Such a collection is often referred to as an internet, and the term internet security is used.

There are no clear boundaries between different forms of information security. But in order to assess the security needs of an organization effectively and to evaluate and choose various security products and policies, the manager responsible for security must determine some systematic way of defining the requirements that correspond to the needs of the organization. In other words, there is a general platform that determines the concepts and the methods applied to information security, but, depending on the specifics and the objectives of a given organization, these methods or mechanisms differ from one to another. To characterize the general platform that describes any secure system, we give the following classifications of security services.

- Confidentiality: Confidentiality is the protection of transmitted data from *passive attacks*. By passive attacks we mean those ones which are in the nature of eavesdropping on, or monitoring of, transmissions. The broadest service protects all user data transmitted between two users over a period of time. For example, if a virtual circuit is set up between two systems, this broad protection would prevent the release of any user data transmitted over the virtual circuit. Narrower forms of this service can also be defined, including the protection of a single message or even specific fields within a message. These refinements are less useful than the broad approach and may even be more complex and expensive to implement. The other aspect of confidentiality is the protection of traffic flow from analysis. This requires that an attacker not be able to observe the source and destination, frequency, length, or other characteristics of the traffic on a communications facility.

- Authentication: The authentication service is concerned with assuring that a communication is authentic. In the case of a single message, such as a warning or an alarm signal, the function of the authentication service is to assure the recipient that the message is from the source that it claims to be from. In the case of an ongoing interaction, such as the connection of a terminal to a host, two aspects are involved. First, at the time of connection initiation, the service assures that the two entities are authentic (in other words, that each is the entity which it claims to be). Second, the service must assure that the connection is not interfered with in such away that a third party can masquerade as one of the two legitimate parties for the purposes of unauthorized transmission or reception.

- Integrity: As with confidentiality, integrity can apply to a stream of messages, a single

message, or a selected field within a message. Definitely, the most useful and straightforward approach is total stream protection. A connection-oriented integrity service, the one that deals with a stream of messages, assures that messages are received as sent, with no duplication, insertion, modification, reordering, or replays. The destruction of data is also covered under this service. Thus the connection-oriented integrity service addresses both message stream modification and denial of service. On the other hand, a connectionless integrity service, the one that deals with individual messages only without regard to any larger context, generally provides protection against message modification only. If a violation of integrity is detected, then the service may simply report this violation. In this case, some other portion of software or human intervention is required to recover from the violation.

- Non-Repudiation: Non-Repudiation prevents either the sender or the receiver of a message from denying the transmission. Thus when a message is sent, the receiver can prove that the message was in fact sent by the alleged sender. Similarly, when a message is received, the sender can prove that the message was in fact received by the alleged receiver.

- Access control: In the context of network security, access control is the ability to limit and control the access to host systems and applications via communication links. To achieve this control, each entity trying to gain access must first be identified, or authenticated, so that access rights can be tailored to the individual.

- Availability: A variety of attacks can result in the loss of or reduction in availability. Some of these attacks are amenable to automated countermeasures, such as authentication and encryption, whereas others require some sort of physical action to prevent or recover from loss of availability of elements of a distributed system.

There is no single mechanism that will provide all the services just listed. Instead, there are a variety of mechanisms that come into play. However, we can note at this point that there is one particular element that underlies most of the security mechanisms in use: *cryptographic techniques*. Encryption or encryption-like transformation of information are the most common means of providing security. These techniques establish an important field in secure communication called *cryptography*, which is defined to be the study of sending messages in a secret or hidden form, so that only those people authorized to receive the message will be able to read it (*Crypto* is derived from the Greek word which means *hidden*). *Cryptanalysis*, on the other hand,

is the science of breaking cryptographic writings. Cryptography and cryptanalysis are collectively referred to as *cryptology*.

Let us build up a typical cryptographic model to further illustrate the above definition. The basic idea is that a message is to be transferred from one party to another across some sort of internet. The two parties, who are the principals in this transition, must cooperate for the exchange to take place. A logical information channel is established by defining a route through the internet from source to destination and by the cooperative use of communication protocols by the two principals. Security aspects come into play when it is necessary or desirable to protect the information transmission from an opponent who may present a threat to confidentiality, authenticity and so on. All the techniques for providing security have two essential components. The first component is a security-related transformation on the information to be sent. Examples include the encryption of message, which scrambles the message so that it is unreadable by the opponent, and the addition of a code based on the contents of the message, which can be used to verify the identity of the sender. Whereas for the second component, we require that some secret information shared by the two principals and, it is hoped, unknown to the opponent. An example is an encryption key used in conjunction with the transformation to scramble the message before transmission and unscramble it upon reception. We should mention here that, when designing this kind of model, a trusted third party may be needed to achieve secure transmission. For example, a third party may be responsible for distributing the secret information to the two principals while keeping it from any attacker, or a third party may be needed to arbitrate disputes between the two principals concerning the authenticity of a message transmission. This general model shows that there are four basic tasks in designing a particular security service:

1. Design an algorithm for performing the security-related transformation. The algorithm should be such that an attacker cannot defeat its purpose.

2. Generate the secret information to be used with the algorithm.

3. Develop methods for the distribution and sharing of the secret information.

4. Specify a protocol to be used by the two principals that makes use of the security algorithm and the secret information to achieve a particular security service.

It is clear from the above design that the complexity and the secrecy of the keys used for encryption-decryption purposes, play a major role in the security of the model just described. They are used as tools to complement the security-related transformation in encoding messages,

and therefore they have to be generated as *randomly* as possible. In other words, the key generators must be unpredictable *random* generators in order to add more uncertainty into the cryptosystem and thus make it less vulnerable. The following two criteria are used to validate that a generator or a source is random.

- Uniform distribution: in the sense that the outcomes of the generator should be uniform; that is, the frequency of each of the outcomes should be approximately the same.
- Independence: meaning that one outcome is not influenced by the previous one.

We would like to adopt these two criteria in the design of random generators employed as sources of encryption keys used in a given cryptosystem.

Due to the importance of randomness in cryptography, recently the use of chaos for secure communication has become much more interesting field, since chaotic signals are broadband, noise-like and difficult to predict. In fact, objects exhibiting chaotic behaviour would follow unpredictable patterns which would be considered a good source of randomness needed for a strong cryptosystem; they are hoped to be good mask or key signals for private communication. Therefore in the last ten years many cryptosystems based on chaos phenomenon have been proposed. Some of them use continuous-time chaos (a system of ordinary differential equations, ODE's) and others use discrete-time chaos (iterating chaotic maps). The continuous case has been applied mainly to secure communication where continuous signals (e.g., voice signals) are encrypted and transfered within a given network; however, the discrete chaotic systems are applied on secret key cryptosystems that lie within the category of block and stream ciphers. The pivotal issue of this thesis is to try to apply chaos theory with its different aspects, such as synchronization, to the study and development of cryptography.

The idea of *synchronized oscillations* is usually associated with the frequency and phase locking of oscillations in various generators of periodic signals. This phenomenon, known since the 17^{th} century, plays a very important role both in physics as well as in engineering. The synchronization of radio-generators is crucial for the operation of modern radio-devices [101]. It is widely used for the frequency stabilization of powerful generators such as klystron and magnetron generators [101]. In industrial engineering, synchronization is important for minimizing stress due to multiple sources of vibrations [101]. Many mechanical mechanisms powered by multiple vibrators, such as transporters, separators, grinders and mixers, are based on the principle of synchronization [101]. Nowadays, synchronization of longitudinal cavity modes in lasers receives considerable

attention as one of the most effective mechanisms for producing ultra-short pulses for fibre-optics communications [101].

Such a wide interest in the phenomenon of synchronization has supported a very intensive research directed towards the development of the theory of synchronization of periodic oscillations. The first serious steps in this direction were taken by Van der Pol in 1927 and by Andronov and Vitt in 1930 who analyzed the synchronization of oscillations in triode generators. As a result of the efforts of physicists and engineers over the last few decades, many aspects of the synchronization of periodic oscillations is well understood now. At the same time, it has been realized that in many physical, biological and chemical systems and technical devices, the regime of periodic oscillations can be replaced by a chaotic behaviour and still observe synchronization. In 1983, Fujisaka and Yamada published the first paper discussing the synchronization of chaos. In that paper, the authors considered a system of diffusively coupled identical chaotic oscillators and demonstrated that when the coupling is sufficiently strong, all elements exhibit identical chaotic oscillations. They developed a procedure for linear stability analysis for the synchronized chaotic oscillations which was a very important step. The problem of synchronized chaotic oscillations in diffusive media composed of coupled chaotic oscillators, was also studied by Pikovskii in 1984. This work motivated Carroll and Pecora to use synchronization to control the behaviour of chaotic systems and employ this phenomenon in designing chaos-based communication security schemes which implement synchronization for decryption purposes, as well shall see in Chapter 2.

In this thesis, we shall be interested in examining and analyzing the use of continuous-time chaos in secure communication using different synchronization approaches. Chief among them is the method of impulsive control which uses samples of the state variables to synchronize two chaotic systems. This synchronization method may give an efficient way to deal with systems which cannot endure continuous disturbances (i.e., control input) unlike other methods suggested in controlling continuous-time chaos. Its sensitivity to attacks and insensitivity to noise present in public channels, make this method quite powerful and more promising to be used in designing chaos-based secure communication systems with the aid of conventional cryptographic schemes. We shall further investigate this synchronization approach by analyzing it using the concept of Lagrange stability. Since Lagrange stability is a weaker condition than asymptotic stability and that it reflects the desired synchronization behaviour, we derive, in this thesis, sufficient conditions for Lagrange stability. These conditions, which are weaker than the ones discussed in the literature for asymptotic stability, reflect the types of requirements needed for chaos synchronization using impulsive methods. Furthermore, due to the fact that deigning identical chaotic systems in prac-

tice is impossible, the concept of robustness becomes very crucial in impulsive synchronization. In this thesis, we establish theoretically how robust this method is towards parameter mismatch between the chaotic systems involved. We also compare the robustness performance of this method with the method of Carroll-Pecora synchronization described in the literature. We show that impulsive synchronization is more robust than the Carroll-Pecora synchronization. We then address the issue of delay in impulsive synchronization with and without continuous driving and establish how robust impulsive synchronization is towards bounded delays. Sufficient conditions are obtained to reflect the needed requirements for robustness towards delay and estimates on the upper bounds on the delay terms are derived using these sufficient conditions. The theory developed considers the general case when the delay terms and the impulses are time varying, which has not been investigated previously in the literature. We generalize the theory of impulsive control and synchronization to include spatiotemporal chaos generated by spatially extended systems such as partial differential equations. The Kuramoto-Sivashinsky equation and the Grey-Scott models are used as examples of partial differential equations generating spatiotemporal chaos for impulsive control and synchronization. We derive the sufficient conditions that guarantee the impulsive control and synchronization of the above mentioned models. All of these results are further investigated numerically by simulating the results and by analyzing the Lyapunov exponents of the synchronization errors to verify the theoretical results. The structure of the impulses, using the Dirac delta function, is used to study these systems numerically. Eventually, we check how these models can be implemented in designing communication security schemes based on impulsive synchronization. We propose a new scheme called the induced-message cryptosystem which adds more security to the impulsive methods available in the literature and solves the problem of time-frame-congestion which is persistent in these cryptosystems.

This thesis can be summarized as follows. In the remaining of this chapter, we shall introduce the concepts of Lagrange stability, equi-attractivity in the large, continuous-time chaos and the theory of impulsive differential equations needed for the development of the thesis. In Chapter 2, the robustness of impulsive synchronization is investigated and sufficient conditions for certain types of impulsive systems to be equi-Lagrange stable are obtained. Furthermore, Lyapunov exponent analysis is provided to confirm the theoretical results. Then in Chapter 3, the delay factor in impulsive synchronization is considered and its robustness, in the presence of delay in the impulses as well as in the differential system, is established. In Chapter 4, extending the theory of impulsive control and impulsive synchronization to spatiotemporal chaotic systems generated by partial differential equations, is discussed and sufficient conditions for the equi-attractivity in the

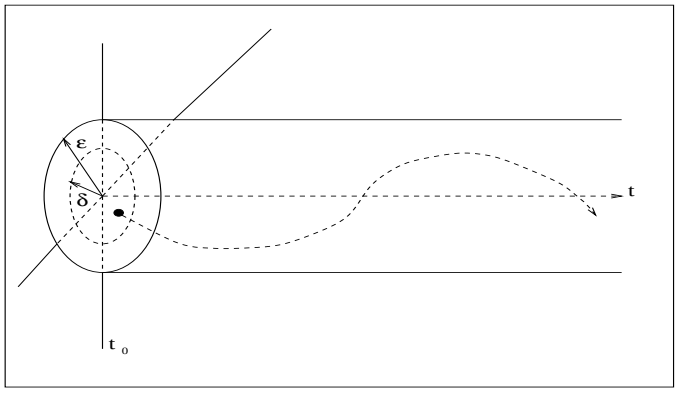

Figure 1.1: Trajectory of a stable solution.

large property for both cases are obtained. Moreover, Lyapunov exponent analysis is provided to confirm the theoretical results once more. Applying the theory of impulsive synchronization, with all of its aspects and theory developed in this thesis, to secure communication, is done in Chapter 5 and numerical simulations to reflect on its performance are also given. Finally, some concluding remarks and discussion regarding future research work are presented in Chapter 6.

1.2 Mathematical Preliminaries

In this section, we shall consider some important definitions and notations that will be useful in this thesis as it will become evident in the subsequent chapters.

Suppose that we have a continuous-time non-linear system given by

$$\dot{\mathbf{x}} = \mathbf{f}(t, \mathbf{x}), \tag{1.1}$$

where $\mathbf{x}(t) = (x_1(t), x_2(t), \ldots, x_n(t))^T$ are the state variables of the system and $\mathbf{f}$ is an n-dimensional continuous-time non-linear map. Let $\mathbf{x} = \mathbf{0}$ be the trivial solution (equilibrium point) of equation (1.1), i.e., $\mathbf{f}(t, \mathbf{0}) = \mathbf{0}$. In addition, for $(t_0, \mathbf{x}_0) \in \mathbb{R}_+ \times \mathbb{R}^n$, assume that $\mathbf{x}(t) = \boldsymbol{\phi}(t, t_0, \mathbf{x}_0)$ is a solution to equation (1.1) through $(t_0, \mathbf{x}_0)$. Then we have the following definitions.

Definition 1.2.1 *The trivial solution of (1.1) is said to be* stable *if for every $\epsilon > 0$ and any $t_0 \in \mathbb{R}_+$, there exists a $\delta(\epsilon, t_0) > 0$ such that $||\mathbf{x}(t)|| < \epsilon$, for all $t > t_0$, whenever $||\mathbf{x}_0|| < \delta(\epsilon, t_0)$.*

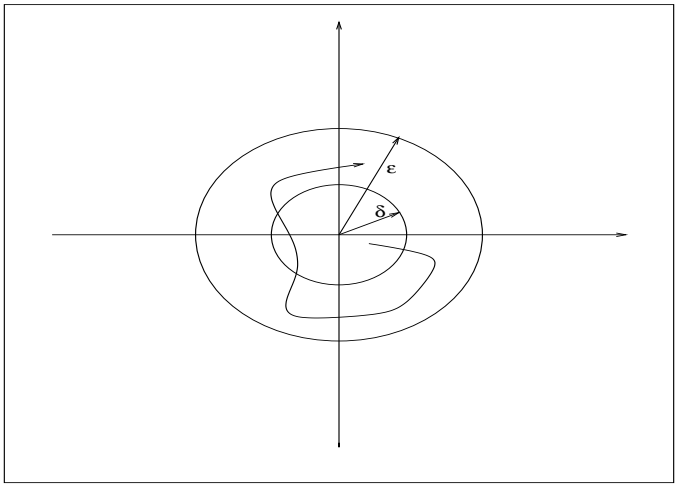

Figure 1.2: Trajectory of a uniformly stable solution.

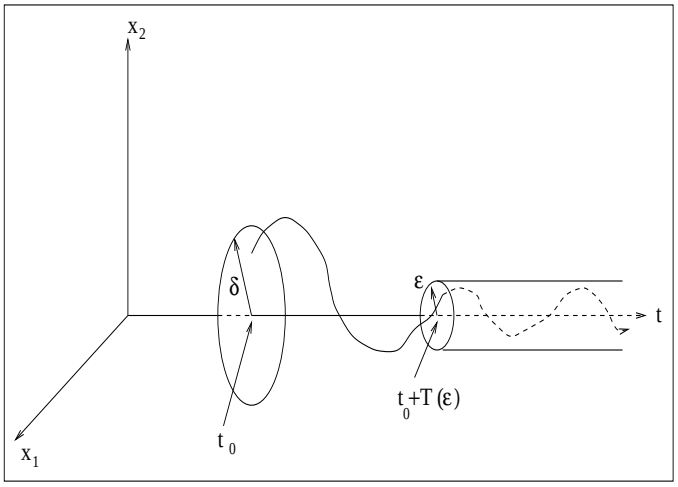

Figure 1.3: Trajectory of a uniformly asymptotically stable solution.

Definition 1.2.2 *The trivial solution of (1.1) is said to be* uniformly stable *if δ in Definition 1.2.1 satisfies $\delta(\epsilon, t_0) = \delta(\epsilon)$, i.e., δ is independent of t_0.*

Definition 1.2.3 *The trivial solution of (1.1) is said to be* asymptotically stable *if*

- *it is stable, and*
- *for every $t_0 \geq 0$, there exists an $\eta(t_0) > 0$ such that*

$$\lim_{t \to \infty} \mathbf{x}(t) = \mathbf{0},$$

whenever $||\mathbf{x}_0|| < \eta(t_0)$.

The set of all $\mathbf{x}_0 \in \mathbb{R}^n$ such that $\mathbf{x}(t) \longrightarrow \mathbf{0}$ as $t \longrightarrow \infty$, for some $t_0 \geq 0$, is called the *basin of attraction* (or the *domain of attraction*) of the trivial solution, $\mathbf{x} = \mathbf{0}$, of (1.1).

Definition 1.2.4 *The trivial solution of (1.1) is said to be* uniformly asymptotically stable *if*

- *it is uniformly stable, and*
- *there exists a δ_0 such that for every $\epsilon > 0$ and for any $t_0 \in \mathbb{R}_+$, there exists a $T(\epsilon) > 0$, independent of t_0, such that*

$$||\mathbf{x}(t)|| < \epsilon, \text{ for all } t \geq t_0 + T(\epsilon),$$

whenever $||\mathbf{x}_0|| < \delta_0$.

A geometrical interpretation of stability, uniform stability and uniform asymptotic stability notions are given in Figures 1.1, 1.2 and 1.3, respectively. They show typical behaviours of three different solution trajectories according to the type of stability they possess. As for asymptotic stability, geometrically speaking, solution trajectories would approach the trivial solution as $t \longrightarrow \infty$.

We introduce now three definitions that are necessary to illustrate the concept of *synchronization*, a special feature that certain continuous-time non-linear systems would possess. These definitions are:

Definition 1.2.5 *System (1.1) is said to be* equi-bounded *if for every $\alpha > 0$ and $t_0 \in \mathbb{R}_+$, there exists a $\beta = \beta(t_0, \alpha) > 0$, continuous in t_0, such that $||\mathbf{x}(t)|| < \beta$, for all $t \geq t_0$, whenever $||\mathbf{x}_0|| < \alpha$.*

Definition 1.2.6 *System (1.1) is said to be* uniformly bounded *if β in Definition 1.2.5 satisfies $\beta(t_0, \alpha) = \beta(\alpha)$, i.e., β is independent of t_0.*

Definition 1.2.7 *System (1.1) is said to be* equi-attractive in the large *if for every $\epsilon > 0$, $\alpha > 0$ and $t_0 \in \mathbb{R}_+$, there exists a $T = T(t_0, \epsilon, \alpha) > 0$ such that $||\mathbf{x}(t)|| < \epsilon$, for all $t \geq t_0 + T$, whenever $||\mathbf{x}_0|| < \alpha$.*

Definition 1.2.8 *System (1.1) is said to be* uniformly attractive in the large *if T in Definition 1.2.7 satisfies $T(t_0, \epsilon, \alpha) = T(\epsilon, \alpha)$, i.e., T is independent of t_0.*

Definition 1.2.9 *System (1.1) is said to be* equi-Lagrange stable *if it is equi-bounded and equi-attractive in the large.*

Definition 1.2.10 *System (1.1) is said to be* uniformly Lagrange stable *if it is uniformly bounded and uniformly attractive in the large.*

There is a special class of functions that is quite important in the study of stability features of well-behaved autonomous systems given by

$$\dot{\mathbf{x}} = \mathbf{f}(\mathbf{x}), \tag{1.2}$$

where $\mathbf{f}(\mathbf{0}) = \mathbf{0}$. This class of functions provide us with sufficient conditions needed to prove that the trivial solution of (1.2) possesses certain stability properties as illustrated in the following theorem.

Theorem 1.2.1 *Let S be an open subset of $\mathbb{R}^n$ containing the trivial solution of (1.2), and let $\mathbf{x}(t)$ be a solution to (1.2). Let $V : S \longrightarrow \mathbb{R}$ be a continuously differentiable function, such that*

$$V(\mathbf{0}) = 0 \quad \text{and} \quad V(\mathbf{x}) > 0 \quad \text{in} \quad S\backslash\{\mathbf{0}\} \tag{1.3}$$

and

$$\dot{V}(\mathbf{x}) := \nabla V(\mathbf{x}) \cdot \mathbf{f}(\mathbf{x}) \leq 0 \quad \text{in} \quad S. \tag{1.4}$$

Then the trivial solution of (1.2) is stable. Moreover, if

$$\dot{V}(\mathbf{x}) < 0 \quad \text{in} \quad S\backslash\{\mathbf{0}\},$$

then the trivial solution of (1.2) is asymptotically stable.

Thus the task of proving the stability or the asymptotic stability of the trivial solution of (1.2), reduces to finding a continuously differentiable function V satisfying the conditions in Theorem 1.2.1. Actually, the class of continuously differentiable functions, whose elements satisfy conditions (1.3) and (1.4), is called the *class of Lyapunov functions* (in fact, this class can be extended to non-autonomous systems, but we shall not present them here because we seek not to overload the readers with unnecessary definitions; for further details, see [57] and [77]).

Another important task that we would like to investigate is to give an estimate on the rate of convergence of a nearby trajectory $\widetilde{\mathbf{x}}$ to the true trajectory $\mathbf{x}$ (e.g., during *synchronization*). It should be noted that the estimate is essentially for small differences $\mathbf{e} := \mathbf{x} - \widetilde{\mathbf{x}}$, but, in practice, it appears to work well in many systems for differences on the attractor size (see [89]). This will probably depend on the shape of the basin of attraction of the system $\widetilde{\mathbf{x}}$, as well as for the general flow of the system from the starting point to the true trajectory $\mathbf{x}$. Both of these could cause the system to *wind around* in phase space before getting near the true trajectory. Thus caution must be taken when using the convergence rates for large $||\mathbf{e}||$. To estimate the actual convergence rates, we want to get an estimate on the average convergence rates and their associated directions. This translates into finding quantities called *Lyapunov exponents* and their associated eigenvectors (note that we shall introduce the definitions here and leave the illustration of the correlation of these concepts with convergence in the coming sections). In order to define these quantities, we denote by $Z(t)$ the solution of the equation $\dot{Z}(t) = J_{\mathbf{x}}\mathbf{f}(t, \mathbf{x})Z(t)$, where $J_{\mathbf{x}}\mathbf{f}$ is the Jacobian matrix of $\mathbf{f}$ at $\mathbf{x} = \mathbf{0}$ and $Z(t_0)$ is the identity matrix ($Z(t)$ is often referred to as the *state transition matrix* or the *principal matrix solution*).

Definition 1.2.11 *Let $a_1(t), a_2(t), \ldots, a_n(t)$ be the eigenvalues of $Z(t)$. The* Lyapunov exponents *of (1.2), starting at $\mathbf{x}_0$, are given by*

$$\lambda_i := \lim_{t\to\infty} \frac{1}{t} \ln |a_i(t)|, \quad i = 1, 2, \ldots, n,$$

whenever the limit exists.

The above definitions are used intensively in the theory of chaos, the theory of impulsive systems and in several problem formulations described in this thesis. They will be referred to whenever it is necessary.

We turn our attention now to the concept of *chaos*. The word *chaos* is familiar in everyday speech. It normally means a lack of order or predictability. For example, one says that the weather is chaotic, or that rising particles of smoke are chaotic, or the stock market is chaotic. It is the lack

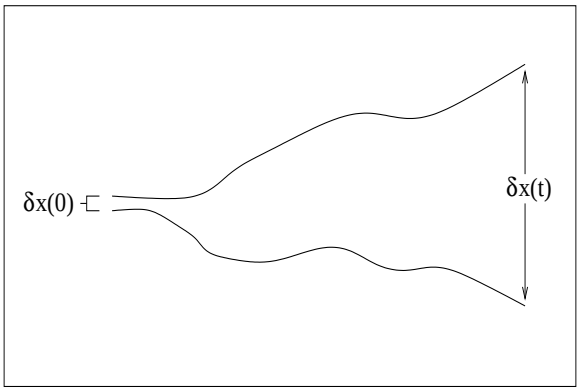

Figure 1.4: Effect of a small change in initial conditions.

of predictability that lies behind the mathematical notion of chaos. Chaotic systems comprise the transition between solvable and near-solvable systems and those that are completely stochastic or random. They are the most recent to be investigated by scientists and mathematicians because they are the least susceptible to study using the tools of mathematical analysis. In order to give a more rigorous mathematical definition for the terminology chaos, we distinguish between two types of chaos that will be defined and explained separately:

1. Continuous-time chaos.

2. Discrete-time chaos.

Continuous-time chaotic systems are non-linear deterministic dynamical systems which can exhibit erratic and irregular behaviour. Its bounded steady-state behaviour is not an equilibrium point, not periodic and not quasi-periodic. A very common representation of these systems is that of a system of n-simultaneous first order ODE's given by equation (1.1). We let, as before, $\mathbf{x}(t)$ be the solution of (1.1) with the initial condition $(t_0, \mathbf{x}_0)$. If we slightly change the position of the initial point, $\mathbf{x}(t_0) \longrightarrow \mathbf{x}'(t_0) = \mathbf{x}(t_0) + \delta\mathbf{x}(t_0)$, the point at time t will also be changed (see Figure 1.4). Generally speaking, from the continuity of solutions of an ODE with respect to initial conditions, one expects that if $\delta\mathbf{x}(t_0)$ is small, $\delta\mathbf{x}(t)$ is also small. To the contrary, what may happen is that, when the time becomes large, the small initial distance grows anyway and it may grow exponentially fast: $\delta\mathbf{x}(t) \sim \delta\mathbf{x}(t_0)\exp(\lambda t)$, where $\lambda > 0$ is the largest Lyapunov exponent which measures the mean rate of divergence of the orbits (see Definition 1.2.11 and [92]).

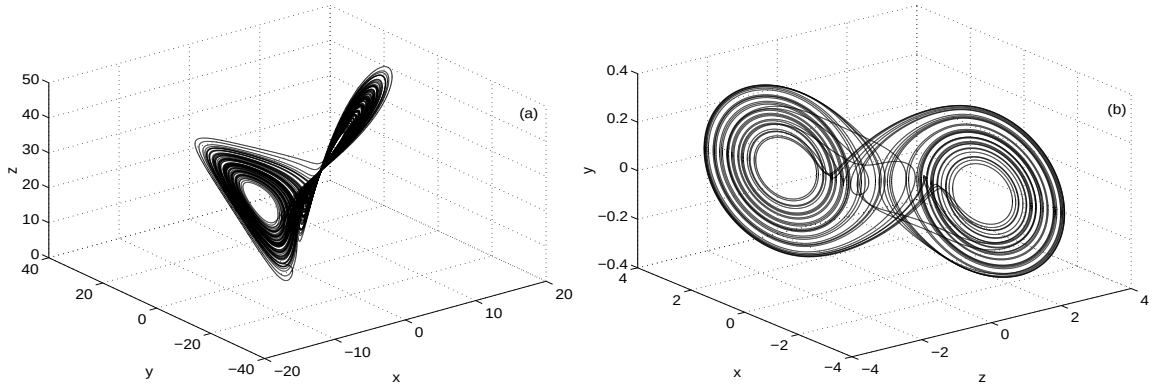

Figure 1.5: (a) Trajectory of Lorenz system. (b) Trajectory of Chua's oscillator.

Therefore sensitive dependence on initial conditions and possessing positive Lyapunov exponents are associated with each other. In this case, the motion, although purely deterministic, has those stochastic features referred to as chaos. In fact, in all those cases in which the initial state is given with limited precision, we may observe a situation where trajectories emerge from the *same* initial point. Thus, even though there is a deterministic situation from a mathematical point of view (the uniqueness theorem for ODE's is not in question), nevertheless the exponential growth of errors makes the time evolution self-independent from its past history and then non-deterministic in any practical sense.

The limiting trajectory of the dissipative chaotic systems are attracted to a region in state space which forms a set having fractional dimension and zero volume. These sets are not simple geometrical objects like a circle or a torus; in fact, it is not even a manifold [22, 37, 63]. Solution trajectories in this limiting set are locally unstable, yet remain bounded within some region of the system's state space [22]. These sets are termed *strange attractors* because they exhibit the following properties [92].

1. Sensitive dependence on initial conditions: i.e., system (1.1) possesses at least one positive Lyapunov exponent.

2. Attractivity: In the sense that for every open set $\mathcal{V}$ containing the strange attractor, the solution trajectories of (1.1) starting in $\mathcal{U}$ will converge to $\mathcal{V}$ after a given time t. In other words, for every $\epsilon > 0$, for every $\alpha > 0$ and for every $t_0 \in \mathbb{R}_+$, there exists a $T = T(t_0, \epsilon, \alpha) > 0$ such that $d(\mathbf{x}, \mathcal{V}) < \epsilon$, for all $t > t_0 + T$, whenever $d(\mathbf{x}_0, \mathcal{V}) < \alpha$, where $d(\mathbf{x}, \mathcal{V}) :=$

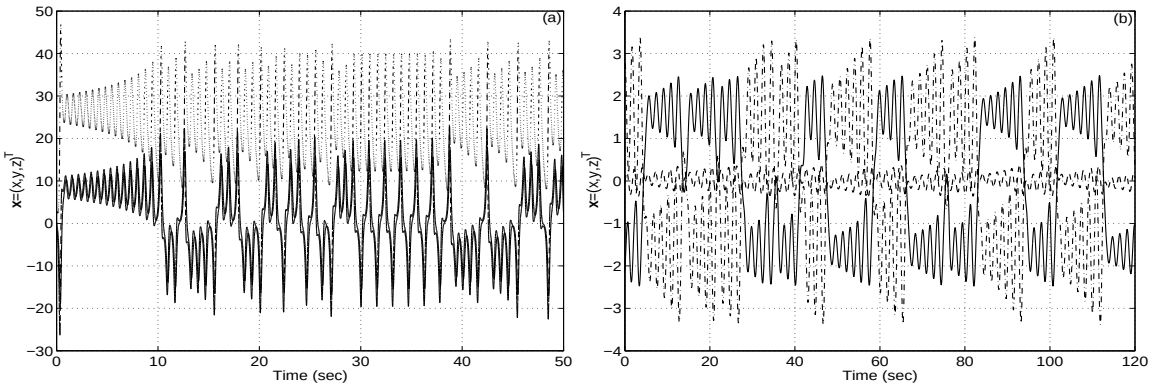

Figure 1.6: (a) Time propagation of the Lorenz system. (b) Time propagation of Chua's oscillator.

$$\min_{\mathbf{y}\in\mathcal{V}} ||\mathbf{x}-\mathbf{y}||.$$

3. Invariance with respect to (1.1): In the sense that solutions starting in the strange attractors, remain there for all future time.

4. Irreducibility: In the sense that these sets do not consist of a number of disjoint invariant pieces, some of which may not be attracting.

Considering the facts that at least one Lyapunov exponent of a chaotic system must be positive, that one Lyapunov exponent of any limit set other than an equilibrium point must be zero and that the sum of the Lyapunov exponents of an attractor must be negative, it follows that a strange attractor must have at least three Lyapunov exponents. Hence chaos cannot occur in a first or second order autonomous continuous-time systems or in a first order non-autonomous continuous-time systems [84]. In the three dimensional case, the only possibility for chaos to occur is when we have the Lyapunov exponents to be $\lambda_1 > 0$, $\lambda_2 = 0$ and $\lambda_3 < 0$. In addition, since contraction must outweigh expansion, a further condition on a three dimensional chaos is $\lambda_3 < -\lambda_1$ [84]. This type of chaos is termed *low-dimensional chaos*.

Examples of systems that exhibit low-dimensional chaotic behaviour are:

1. The *Lorenz system*, given by

$$\begin{aligned} \frac{dx}{dt} &= -\sigma x + \sigma y \\ \frac{dy}{dt} &= rx - y - xz \\ \frac{dz}{dt} &= xy - bz, \end{aligned} \tag{1.5}$$

   where σ, r and b are positive constants.

2. The *Chua's oscillator*, given by

$$\begin{aligned} \frac{dx}{dt} &= \alpha(y - x - f(x)) \\ \frac{dy}{dt} &= x - y + z \\ \frac{dz}{dt} &= -\beta y - \gamma z, \end{aligned} \tag{1.6}$$

   where α, β, γ are positive constants and $f(x) = bx + \frac{1}{2}(a-b)(|x+1| - |x-1|)$, $a < b < 0$.

3. *Rössler system*, given by

$$\begin{aligned} \frac{dx}{dt} &= p + x(z - c) \\ \frac{dy}{dt} &= -(x + z) \\ \frac{dz}{dt} &= y + az, \end{aligned} \tag{1.7}$$

   where a, p and c are positive constants.

Notice that the trajectories of the first two systems (Lorenz system and Chua's oscillator), as shown in Figure 1.5, lie inside a bounded but locally unstable regions with two wells being the strange attractors mentioned earlier. Furthermore, the time propagation of the solution trajectories of these two chaotic systems are also shown in Figure 1.6.

Now concerning fourth order systems, there are three possibilities to consider regarding chaos [84].

- $\lambda_1 > 0$, $\lambda_2 = 0$ and $\lambda_4 \leq \lambda_3 < 0$.
- $\lambda_1 \geq \lambda_2 > 0$, $\lambda_3 = 0$ and $\lambda_4 < 0$. This type of chaos was termed *hyperchaos* by Rössler.
- $\lambda_1 > 0$, $\lambda_2 = \lambda_3 = 0$ and $\lambda_4 < 0$. This corresponds to a chaotic two-torus which, according to Parker et al., [84], has not been observed.

Examples of systems that exhibit hyperchaotic behaviour are:

1. The *high dimensional Chua's oscillator*, given by

$$\begin{aligned} \frac{dx_1}{dt} &= \alpha_1(f(x_3 - x_1) - x_2) \\ \frac{dx_2}{dt} &= x_1 + (\delta - \epsilon)x_2 \\ \frac{dx_3}{dt} &= -\beta_1(f(x_3 - x_1) + x_4) \\ \frac{dx_4}{dt} &= \gamma_1 x_3 - \epsilon x_4, \end{aligned} \tag{1.8}$$

   where α_1, β_1, γ_1, δ, ϵ are positive constants and $f(u)$ is as defined before in Chua's oscillator.

2. The *high dimensional Rössler system*, given by

$$\begin{aligned} \frac{dx_1}{dt} &= -x_2 - x_3 \\ \frac{dx_2}{dt} &= x_1 + \eta x_2 + x_4 \\ \frac{dx_3}{dt} &= x_1 x_3 + \theta \\ \frac{dx_4}{dt} &= -\nu x_3 + \zeta x_4, \end{aligned} \tag{1.9}$$

   where η, θ, ν, ζ are positive constants.

3. The *hysteresis chaos generator*, given by

$$\begin{aligned} \frac{dx_1}{dt} &= -x_3 - x_4 \\ \frac{dx_2}{dt} &= 2\gamma_2\delta_2 x_2 + \gamma_3 x_3 \\ \frac{dx_3}{dt} &= \rho(x_1 - x_2) \\ \frac{dx_4}{dt} &= \frac{1}{\epsilon_1}(x_1 - g(x_4)), \end{aligned} \tag{1.10}$$

where γ_2, γ_3, δ_2, ρ, ϵ_1 are positive constants and

$$g(x_4) = \begin{cases} x_4 + (1+\eta_1) & \text{if} \quad x_4 \leq -\eta_1 \\ -\dfrac{1}{\eta_1}x_4 & \text{if} \quad -\eta_1 < x_4 < \eta_1 \\ x_4 - (1+\eta_1) & \text{if} \quad x_4 \geq \eta_1, \end{cases}$$

where η_1 is also a positive constant.

In Section 3.3, we shall show the projections of the strange attractor of a system that resembles (1.8), in three dimensional spaces, and a plot of its time propagation.

Now for the discrete-time chaos, its theory lies outside the scope of this thesis, but we shall present here a few of its properties for the sake of illustrating different aspects of chaos. In this case, similar features to those we have seen for the continuous-time chaos will carry over to the discrete case, although they follow different formulation. This formulation is expressed in terms of difference equations defined by a continuous mapping $\mathbf{F} : S \longrightarrow S$, where S is a closed and bounded subset of $\mathbb{R}^m$, given by

$$\mathbf{x}_{n+1} = \mathbf{F}(\mathbf{x}_n, \boldsymbol{\alpha}),\ n = 0, 1, 2, \ldots,$$

where again $\mathbf{x}_n = (x_{n1}, x_{n2}, \ldots, x_{nm})^T$ are the state variables and $\boldsymbol{\alpha} = (\alpha_1, \alpha_2, \ldots, \alpha_l)^T$ is a set of parameters. i.e., we are considering the $(n+1)^{\text{st}}$ iterate of a given point, $\mathbf{x}_0$, in S and constructing the sequence $\{\mathbf{x}_i\}_{i=0}^{\infty}$ (orbit). Notice that the map $\mathbf{F}$ might possess a fixed point $\mathbf{x}^*$ such that $\mathbf{x}^* = \mathbf{F}(\mathbf{x}^*, \boldsymbol{\alpha})$, a periodic point $\mathbf{p}$ of period n such that $\mathbf{p} = \mathbf{F}^{[n]}(\mathbf{p}, \boldsymbol{\alpha})$ and, in

addition, $\mathbf{p}, \mathbf{F}(\mathbf{p}, \boldsymbol{\alpha}), \ldots, \mathbf{F}^{[n-1]}(\mathbf{p}, \boldsymbol{\alpha})$ are all distinct, or an eventually periodic point $\mathbf{p}^*$ whose i^{th} iterate, $F^{[i]}(\mathbf{p}^*)$, for some $i > 1$, is periodic (these terminologies are analogous to those given in the continuous case). The extension of Lyapunov exponents, defined for the continuous case, to the discrete case, lead us to formulate other types of quantities, called *Lyapunov numbers*. These numbers, when evaluated at fixed points, periodic points, etc., describe the amount of contraction or expansion of the orbit $\{\mathbf{x}_i\}_{i=0}^{\infty}$ per iteration in all possible eigendirections.

The behaviour of the orbit $\{\mathbf{x}_i\}_{i=0}^{\infty}$ depends entirely on the behaviour of the map $\mathbf{F}$. Thus, in order for the map $\mathbf{F}$ to exhibit chaotic behaviour, it has to possess certain properties very much similar to those explained for the continuous case. These properties define discrete-time chaos [38], and can be summarized as follows.

1. Sensitive dependence on parameters: If a parameter (the shape of $\mathbf{F}$) varies slightly, then two orbits obtained from repeated iterations of the chaotic map, starting from the same initial point, eventually become quite different.

2. Sensitive dependence on initial points: If an initial point $\mathbf{x}_0$ varies slightly, the two orbits obtained from repeated iterations of the chaotic map with the same parameters eventually become quite different.

3. $\mathbf{F}$ has positive Lyapunov exponents at each point in its domain which is not eventually periodic.

These features imply that if the parameters and the exact initial point are kept unknown, then it is impossible to predict the path of the chaotic orbit.

Let us consider the *tent* function as an example of one-dimensional chaotic map. The tent function $F_\alpha : [0,1] \to [0,1]$, for $0 < \alpha < 1$, is given by

$$x_{k+1} = F_\alpha(x_k, \alpha) = \begin{cases} x_k/\alpha & \text{if} \quad 0 \le x_k \le \alpha \\ \\ (x_k - 1)/(\alpha - 1) & \text{if} \quad \alpha < x_k \le 1. \end{cases} \tag{1.11}$$

It has been established in [37] that this map possesses the following three important properties: (a) it is chaotic, (b) it has dense set of periodic points (i.e., any non-empty open interval $J \subset [0,1]$ will always contain at least one periodic point), and (c) it is transitive (i.e., for any pair of non-empty open interval $J_1, J_2 \subset [0,1]$, there is a positive integer n such that $F_\alpha^{[n]}(J_1) \cap J_2 \neq \phi$, where ϕ is the non-empty set). Therefore, by applying the definition of strong chaos, the three properties make the tent map F_α strongly chaotic over the interval $[0,1]$.

We shall see in the next chapters the important role continuous-time chaotic systems play in developing synchronization theory and in building secure communication schemes.

1.3 Impulsive Systems

Many evolution processes are characterized by the fact that at certain moments of time they experience a change of state abruptly. These processes are subject to short-term perturbations whose duration is negligible in comparison with the duration of the process. Consequently, it is natural to assume that these perturbations act instantaneously, that is, in the form of impulses. It is known, for example, that many biological phenomena involving thresholds, bursting rhythm models in medicine and biology, optimal control models in economics, population dynamics [71], space navigation [74], chaos control [72, 112, 113, 117], etc., do exhibit impulsive effects. Thus impulsive differential equations, that is, differential equations involving impulse effects, appear as a natural description of observed evolution phenomena of several real world problems.

The mathematical description of these impulsive systems of differential equations, modeling evolutionary processes that are subject to impulsive effects, consists of a system of ordinary differential equations together with a system of difference equations that define the impulsive actions. These difference equations are given by

$$\Delta \mathbf{x}(t) = \mathbf{I}(t, \mathbf{x}(t)), \tag{1.12}$$

where $\Delta \mathbf{x}(t) = \mathbf{x}(t^+) - \mathbf{x}(t^-)$. Here and elsewhere throughout this thesis, we use the abbreviated notation $\mathbf{x}(t^+) = \lim_{\tau \to t^+} \mathbf{x}(\tau)$ and $\mathbf{x}(t^-) = \lim_{\tau \to t^-} \mathbf{x}(\tau)$ to refer to the right-hand and left-hand limits, respectively. It is assumed that equation (1.12), which describes the instantaneous changes of state, or impulses, is satisfied when a particular spatiotemporal relation, given by $h(t, \mathbf{x}(t)) = 0$, is satisfied. Let $\mathcal{M} := \{(t, \mathbf{x}(t)) \in \mathbb{R}_+ \times \mathbb{R}^n : h(t, \mathbf{x}(t)) = 0\}$ denotes the hypersurface of the equation $h(t, \mathbf{x}(t)) = 0$ in $\mathbb{R}_+ \times \mathbb{R}^n$. Let $\mathcal{A} : \mathcal{M} \to \mathbb{R}_+ \times \mathbb{R}^n$, where $\mathcal{A}(t, \mathbf{x}(t)) := (t, x(t) + \mathbf{I}(t, \mathbf{x}(t)))$, denote the function which defines the impulsive action. It should be noted that we require $\mathbf{x}(t) + \mathbf{I}(t, \mathbf{x}(t)) \in \mathbb{R}^n$, for $(t, \mathbf{x}(t)) \in \mathbb{R}_+ \times \mathbb{R}^n$. Thus, according to this set up, the combination of equations (1.1) and (1.12) lead us to the the following impulsive differential equation, given by

$$\begin{cases} \dot{\mathbf{x}}(t) = \mathbf{f}(t, \mathbf{x}(t)), & h(t, \mathbf{x}(t)) \neq 0 \\ \\ \Delta \mathbf{x}(t) = \mathbf{I}(t, \mathbf{x}(t)), & h(t, \mathbf{x}(t)) = 0 \end{cases} \tag{1.13}$$

This means that for as long as we have $h(t, \mathbf{x}(t)) \neq 0$, then the evolution of the state is governed by the ordinary differential equation (1.1). However, whenever $h(t, \mathbf{x}(t)) = 0$, the state undergoes an impulse and instantly changes by some amount given by $\mathbf{I}(t, \mathbf{x}(t))$ according to equation (1.12). This causes a jump discontinuity in the solution. Following this impulsive action, and assuming $\mathbf{h}(t, \mathbf{x}(t))$ is non-zero for some time thereafter, the solution will continue to evolve according to (1.1) until it undergoes an impulse once more.

We shall now define the notion of solutions to system (1.13) as follows.

Definition 1.3.1 *A function* $\mathbf{x} : (t_0, \tilde{\sigma}) \to \mathbb{R}^n$, *where* $0 \leq t_0 < \tilde{\sigma} \leq \infty$ *is called a* solution *of system (1.13) if the following conditions are satisfied:*

(i) $(t, \mathbf{x}(t)) \in \mathbb{R}_+ \times \mathbb{R}^n$, *for* $t \in (t_0, \tilde{\sigma})$;

(ii) $\mathbf{x}(t_0^+) = \lim_{t \to t_0^+} \mathbf{x}(t)$ *exists and* $(t_0, \mathbf{x}(t_0^+)) \in \mathbb{R}_+ \times \mathbb{R}^n$;

(iii) for each $t \in (t_0, \tilde{\sigma})$, *if* $h(t, \mathbf{x}(t)) \neq 0$ *then* $\mathbf{x}$ *is continuously differentiable at* t *and satisfies* $\dot{\mathbf{x}}(t) = \mathbf{f}(t, \mathbf{x}(t))$;

(iv) the set $\mathcal{T} := \{t \in (t_0, \tilde{\sigma}) : h(t, \mathbf{x}(t)) = 0\}$ *of instants of impulsive effect (moments of impulse) is finite (possibly empty) or consists of a countable increasing sequence of points with limit* $\tilde{\sigma}$; *and*

(v) if $t \in \mathcal{T}$ *then* $\mathbf{x}(t^-)$ *exists and* $\mathbf{x}(t^-) = \mathbf{x}(t)$, *for* $t \neq t_0$ *and* $\mathbf{x}(t^+)$ *exists and* $\mathbf{x}(t^+) = \mathbf{x}(t) + \mathbf{I}(t, \mathbf{x}(t))$, *for* $t \neq \tilde{\sigma}$.

If $\mathbf{x}(t)$ is a solution of (1.13), then we call the solution curve in $\mathbb{R}_+ \times \mathbb{R}^n$, described by the points $(t, \mathbf{x}(t))$, the integral curve associated with $\mathbf{x}(t)$. Clearly these solutions curves are either continuous or piecewise continuous with simple jump discontinuities.

The arbitrary nature of the relation $h(t, \mathbf{x}(t)) = 0$ makes the study of system (1.13) extremely difficult. It is therefore common to focus on a particular type of relation. The set of points $(t, \mathbf{x}) \in \mathbb{R}_+ \times \mathbb{R}^n$, for which $h(t, \mathbf{x}) = 0$, will be assumed to consist of a sequence of hypersurfaces of the form $t = \tau_k(\mathbf{x})$, where $\tau_k \in C(\mathbb{R}^n, \mathbb{R}_+)$, for $k = 1, 2, \ldots$ and $0 = \tau_1(\mathbf{x}) < \tau_2(\mathbf{x}) < \tau_3(\mathbf{x}) < \ldots$ with $\lim_{k \to \infty} \tau_k(\mathbf{x}) = \infty$, for each $\mathbf{x} \in \mathbb{R}^n$. This system is then written as

$$\left\{ \begin{array}{ll} \dot{\mathbf{x}}(t) = \mathbf{f}(t, \mathbf{x}(t)), & t \neq \tau_k(\mathbf{x}(t)) \\ \\ \Delta \mathbf{x}(t) = \mathbf{I}(t, \mathbf{x}(t)), & t = \tau_k(\mathbf{x}(t)) \end{array} \right\}, \; k = 1, 2, \ldots . \tag{1.14}$$

When the functions τ_k depend on the state, then system (1.14) is said to have impulses at variable times. This is reflected in the fact that different solution trajectories will tend to undergo impulses at different times. If the functions τ_k are all constant, then (1.14) is said to be a system having impulses at fixed times. In this case all solution trajectories of the state variables undergo the impulsive action, described by the function $\mathbf{I}$ in equation (1.14), at the same exact times. In other words, the impulsive differential system will be given by

$$\left\{ \begin{array}{ll} \dot{\mathbf{x}}(t) = \mathbf{f}(t, \mathbf{x}(t)), & t \neq \tau_k \\ \\ \Delta\mathbf{x}(t) = \mathbf{I}(t, \mathbf{x}(t)), & t = \tau_k \end{array} \right\}, \; k = 1, 2, \ldots. \tag{1.15}$$

The question of existence of solutions of system (1.14) is a non-trivial one when impulses occur at variable times. Even the precise notion of what a solution is, must be carefully stated. It is fairly clear that solutions should be piecewise continuous and, in fact, piecewise continuously differentiable (or piecewise absolutely continuous if considering generalized types of solutions). A solution will undergo simple jump discontinuities when it intersects impulse hypersurfaces $t = \tau_k(\mathbf{x}(t))$, $k = 1, 2, \ldots$.

It is common practice to assume that the solutions of (1.14) (and hence solutions of (1.15)) are left continuous, as described by item (v) in Definition 1.3.1 [7, 63, 64]. This is also intuitively appealing since one can think of a solution as approaching and actually reaching a hypersurface before being mapped to some new point. Thus under this assumption of left continuity, the initial condition for system (1.14) is typically given by

$$\mathbf{x}(t_0^+) = \mathbf{x}_0, \tag{1.16}$$

which is a slight modification of the usual way of expressing initial conditions for ordinary differential equations, i.e., $\mathbf{x}(t_0) = \mathbf{x}_0$ (see Definition 1.3.1 (ii)). In fact, the two latter expressions for initial conditions become equivalent when $t_0 \neq \tau_k(\mathbf{x}_0)$, for all $k = 1, 2, \ldots$. Condition (1.16) emphasizes the fact that we do not consider a solution to instantly undergo an impulse at the initial time t_0. We shall denote solutions to system (1.14) satisfying (1.16) by $\mathbf{x}(t) = \mathbf{x}(t, t_0, \mathbf{x}_0)$.

Even after focusing on a particular class of relations $h(t, \mathbf{x}(t)) = 0$ given by these impulse hypersurfaces, described in system (1.14), impulsive differential equations still exhibit some unusual behaviour. Solutions, depending on how they are defined, could undergo an infinite number of impulses in a finite amount of time unless some additional restrictions on the functions τ_k are imposed. Furthermore, solutions may not exist after reaching one of the impulse hypersurfaces.

They may also intercept the same hypersurface $t = \tau_k(\mathbf{x}(t))$ more than once or not at all or even intercept it after intercepting a subsequent hypersurface $t = \tau_i(\mathbf{x}(t))$, for some $i > k$. The repeated intersection of the same hypersurface by a solution is commonly known as a pulse or beating phenomenon and conditions are often sought to guarantee that it does not happen.

Another problem associated with system (1.14) is: the usual notions of continuous dependence and stability of solutions tend to break down since neighbouring solutions tend to undergo jump discontinuities at slightly different times. When impulses occur at fixed times, as in system (1.15), then much of the theory of ordinary differential equations can be directly carried over to the study of these impulsive differential equations.

In this thesis, we will restrict ourselves to impulsive differential equations whose impulses occur at fixed times, i.e., to those impulsive systems described by (1.15). In this case, it should be mentioned that if the function $\mathbf{I}$ is defined so that $\mathbf{x} + \mathbf{I}(\tau_k, \mathbf{x})$ is not a one to one function in $\mathbf{x}$, then it is possible that two different solutions could merge following the impulsive action at time $t = \tau_k$. This merging, which is also known as confluence, of solutions cannot happen in ordinary differential equations when $\mathbf{f}$ is sufficiently smooth. Note also that, in this situation, if one were to try to extend a solution for system (1.14) backwards in time, then non-unique solutions would result. In fact, if $\mathbf{x} + \mathbf{I}(t, \mathbf{x})$ were not also surjective function, then backward continuation of solutions would be impossible. It is therefore more fruitful to consider only the forward continuation of solutions.

We shall now state a theorem that displays the conditions which govern the existence and uniqueness of solutions to system (1.15) with the presence of the initial condition (1.16) [63].

Theorem 1.3.1 *Let $\Omega \subset \mathbb{R}^n$. If the function $\mathbf{f}$, described in equation (1.15), is continuous on $(\tau_k, \tau_{k+1}] \times \Omega$ and $\lim_{(t,\mathbf{y})\to(\tau_k^+,\mathbf{x})} \mathbf{f}(t, \mathbf{y})$ exists, for $\mathbf{x} \in \Omega$, $k = 1, 2, \ldots$, then solutions to system (1.15) together with the condition (1.16) exist locally. Moreover, if $\mathbf{f}$ is continuous on $\mathbb{R}_+ \times \Omega$ and locally Lipschitz with respect to $\mathbf{x}$ in $\mathbb{R}_+ \times \mathbb{R}^n$, then solutions of equation (1.15) satisfying (1.16) are unique.*

Most of the impulsive differential equations we will be dealing with in this thesis, resemble the initial value impulsive differential system given by equations (1.15) and (1.16). Therefore it will be assumed, when dealing with these systems, that the conditions of Theorem 1.3.1 are satisfied and thus a unique solution exists.

The importance of the theory of impulsive differential equations in developing a framework for controlling chaos through impulsive synchronization will become evident in Chapter 2. Therefore

we shall, in the remaining of this section, introduce some of the impulsive models and the theory associated with it which is available in the literature. In this theory, the asymptotic stability of solutions of impulsive models are investigated and, for special cases, sufficient conditions on the parameters of these systems are obtained to guarantee asymptotic stability properties. However, by considering Definitions 1.2.3 and 1.2.9, we could see very clearly that the equi-Lagrange stability of solutions of impulsive systems is a weaker property which requires weaker conditions than asymptotic stability. Moreover, we shall see later that synchronization will require only equi-Lagrange stability of solutions. Hence we shall improve the results stated in this section and we shall provide an extension of this work in Chapter 2.

Let us begin our discussion by introducing the following classes of functions and definitions.

$$\begin{aligned}
\mathcal{K}_0 &:= \{g \in C[\mathbb{R}_+, \mathbb{R}_+] : g(s) > 0 \text{ if } s > 0 \text{ and } g(0) = 0\},\\
\mathcal{K} &:= \{g \in \mathcal{K}_0 : g(s) \text{ is strictly increasing in } s\},\\
\mathcal{KR} &:= \{g \in \mathcal{K} : \lim_{s\to\infty} g(s) = \infty\},\\
\mathcal{PC} &:= \{p : \mathbb{R}_+ \to \mathbb{R}_+ : p(t) \in C((\tau_k, \tau_{k+1}]) \text{ and } p(\tau_k^+) \text{ exists},\\
&\qquad k = 1, 2, \ldots\},\\
S_r &:= \{\mathbf{x} \in \mathbb{R}^n : ||\mathbf{x}|| \leq r\},\\
S^c(M) &:= \{\mathbf{x} \in \mathbb{R}^n : ||\mathbf{x}|| \geq M\},\\
S^c(M)^0 &:= \{\mathbf{x} \in \mathbb{R}^n : ||\mathbf{x}|| > M\},
\end{aligned}$$

where $r > 0$ and $M \geq 0$.

Definition 1.3.2 *Let $V : \mathbb{R}_+ \times S^c(M) \longrightarrow \mathbb{R}_+$, then V is said to belong to class $\nu_0(M)$ if*

- *V is continuous in $(\tau_k, \tau_{k+1}] \times S^c(M)$ and, for each $\mathbf{x} \in \mathbb{R}^n$,*

$$\lim_{(t,\mathbf{y})\to(\tau_k^+,\mathbf{x})} V(t, \mathbf{y}) = V(\tau_k^+, \mathbf{x})$$

  exists, $k = 1, 2, \ldots,$;

- *V is locally Lipschitz in $\mathbf{x}$.*

The class ν_0 will represent the class of Lyapunov functions which will be used in studying the stability theory of impulsive systems.

Definition 1.3.3 *Let $M \geq 0$ and $V \in \nu_0(M)$. Define the* upper right derivative *of $V(t, \mathbf{x})$ with respect to the continuous portion of system (1.15), for $(t, \mathbf{x}) \in \mathbb{R}_+ \times S^c(M)^0$ and $t \neq \tau_k$,*

$k = 1, 2, \ldots,$ *by*

$$D^+V(t,\mathbf{x}) := \lim_{\delta \to 0^+} \sup \frac{1}{\delta} \left[V(t+\delta, \mathbf{x} + \delta \mathbf{f}(t,\mathbf{x})) - V(t,\mathbf{x}) \right].$$

It is clear that Definition 1.3.3 will automatically reduce to the usual notion of derivative if the function $V(t,\mathbf{x})$ is differentiable on $\mathbb{R}_+ \times \mathbb{R}^n$. i.e.,

$$D^+V(t,\mathbf{x}) = \frac{\partial}{\partial t} V(t,\mathbf{x}) + \frac{\partial}{\partial \mathbf{x}} V(t,\mathbf{x}) \cdot \mathbf{f}(t,\mathbf{x}).$$

Definition 1.3.4 *Let $V \in \nu_0(0)$ and assume that*

$$\left\{ \begin{array}{ll} D^+V(t,\mathbf{x}) \leq g[t, V(t,\mathbf{x})], & t \neq \tau_k \\ \\ V[t, \mathbf{x} + \mathbf{I}(t,\mathbf{x})] \leq \psi_k[V(t,\mathbf{x})], & t = \tau_k \end{array} \right\}, \; k = 1, 2, \ldots,$$

where $g : \mathbb{R}_+ \times \mathbb{R}_+ \longrightarrow \mathbb{R}$ is continuous and $\psi_k : \mathbb{R}_+ \longrightarrow \mathbb{R}_+$ is non-decreasing. Then the system

$$\left\{ \begin{array}{ll} \dot{w} = g(t,w), & t \neq \tau_k \\ \\ w(\tau_k^+) = \psi_k[w(\tau_k)] & k = 1, 2, \ldots \\ \\ w(t_0^+) = w_0 \geq 0, \end{array} \right. \tag{1.17}$$

is called the comparison system of system (1.15).

It should be noted that in the rest of the argument to follow, it is assumed that $\mathbf{f}(t,\mathbf{0}) = \mathbf{I}(t,\mathbf{0}) = \mathbf{0}$ and $g(t,0) = 0$.

Now using the above definitions, we are ready to state some important results regarding the stability properties of the trivial solution of system (1.15) (for detailed proofs, see [63] and [114–116]).

Theorem 1.3.2 *Assume that*

1. *for $V : \mathbb{R}_+ \times S_r \longrightarrow \mathbb{R}_+$, $V \in \nu_0(0)$, we have*

$$D^+V(t,\mathbf{x}) \leq g(t, V(t,\mathbf{x})), \; t \neq \tau_k, \; k = 1, 2, \ldots;$$

2. *there exists an $r_0 > 0$ such that for all $\mathbf{x} \in S_{r_0}$, we have $\mathbf{x} + \mathbf{I}(t,\mathbf{x}) \in S_r$ and $V[t, \mathbf{x} + \mathbf{I}(t,\mathbf{x})] \leq \psi_k[V(t,\mathbf{x})]$, for $t = \tau_k$, $k = 1, 2, \ldots$.*

3. *there exist functions* $\alpha, \beta \in \mathcal{K}$ *such that* $\beta(||\mathbf{x}||) \leq V(t, \mathbf{x}) \leq \alpha(||\mathbf{x}||)$ *on* $\mathbb{R}_+ \times S_r$.

Then the stability properties of the comparison system (1.17) imply the stability properties of the corresponding impulsive system (1.15).

Since the comparison system is easier to work with, the stability theory of impulsive systems, given by (1.15), will become simpler to investigate. This will be quite clear in the next result where the different stability properties of the trivial solution of the comparison system and their required conditions will imply, as in Theorem 1.3.2, the stability properties of the trivial solution of the corresponding impulsive system.

Corollary 1.3.1 *We have three different cases to consider.*

1. *Suppose that* $g(t, w) = 0$, $\psi_k(w) = d_k w$, *for all* $k = 1, 2, \ldots$, *are admissible in Theorem 1.3.2. Then the trivial solution,* $\mathbf{x} = \mathbf{0}$, *of system (1.15) is uniformly stable provided that*

$$\prod_{k=1}^{\infty} d_k < \infty.$$

2. *Suppose that* $g(t, w) = \lambda'(t)w$, $\lambda \in C^1[\mathbb{R}_+, \mathbb{R}_+]$, $\psi_k(w) = d_k w$, *where* $d_k \geq 0$, *for all* $k = 1, 2, \ldots$, *are admissible in Theorem 1.3.2. Then the trivial solution,* $\mathbf{x} = \mathbf{0}$, *of system (1.15) is stable provided that*

$$\lambda'(t) \geq 0 \tag{1.18}$$

and

$$\lambda(\tau_{k+1}) + \ln d_k \leq \lambda(\tau_k),$$

for all $k = 1, 2, \ldots$.

3. *Suppose that the functions in 2. are also admissible in Theorem 1.3.2. Then the trivial solution,* $\mathbf{x} = \mathbf{0}$, *of system (1.15) is asymptotically stable provided that equation (1.18) is satisfied and*

$$\lambda(\tau_{k+1}) + \ln \xi d_k \leq \lambda(\tau_k),$$

for all $k = 1, 2, \ldots$, *where* $\xi > 1$.

Yang and Chua in [114–116, 120, 122] applied the above results to impulsively control the dynamics of a certain kind of non-linear systems, given by

$$\begin{cases} \dot{\mathbf{x}} = A\mathbf{x} + \mathbf{\Phi}(\mathbf{x}), & t \neq \tau_k \\ \\ \Delta\mathbf{x}|_{t=\tau_k} = B\mathbf{x}, & k = 1, 2, \ldots. \end{cases} \tag{1.19}$$

In particular, they applied the third case of Corollary 1.3.1 to obtain sufficient conditions for system (1.19) to be asymptotically stable, as illustrated in the following corollary.

Corollary 1.3.2 *Let Γ be an $n \times n$ symmetric and positive definite matrix with $\lambda_1, \lambda_2 > 0$ being the smallest and the largest eigenvalues of Γ, respectively. Moreover, let*

$$Q = \Gamma A + A^T \Gamma,$$

with λ_3 being the largest eigenvalue of $\Gamma^{-1}Q$, and let $\mathbf{\Phi}(\mathbf{x})$ be a continuous mapping which satisfies Lipschitz condition at $\mathbf{0}$, i.e., $||\mathbf{\Phi}(\mathbf{x})|| \leq L||\mathbf{x}||$, for some positive constant L. Finally, suppose that λ_4 is the largest eigenvalue of the matrix $\Gamma^{-1}(I+B)\Gamma(I+B)$, where B is a symmetric matrix satisfying $||I+B|| \leq 1$. Then the trivial solution of system (1.19) is asymptotically stable provided that

$$\left(\lambda_3 + 2L\sqrt{\frac{\lambda_2}{\lambda_1}}\right)(\tau_{k+1} - \tau_k) \leq -\ln(\xi\lambda_4), \quad \xi > 1 \tag{1.20}$$

and

$$\lambda_3 + 2L\sqrt{\frac{\lambda_2}{\lambda_1}} \geq 0.$$

Let us take the Chua's oscillator, defined by system (1.6), as an example to explain Corollary 1.3.2. In this case, we have $\mathbf{\Phi}(\mathbf{x}) = (-\alpha f(x), 0, 0)^T$, where $f(x) = bx + 1/2(a-b)(|x+1| - |x-1|)$, and $||\mathbf{\Phi}(\mathbf{x})|| \leq |\alpha a|\ ||\mathbf{x}||$. Suppose that Γ is a 3×3 identity matrix and q is the largest eigenvalue of $(A + A^T)$. Moreover, suppose that B is a symmetric matrix satisfying $||I + B|| \leq 1$, and let d denote the largest eigenvalue of $(I + B^T)(I + B)$. Thus, if the impulses are equidistant, with period $\Delta = \tau_{k+1} - \tau_k$, for all $k = 1, 2, \ldots$, then, by inequality (1.20), the trivial solution of Chua's oscillator will be asymptotically stable provided that

$$0 \leq q + 2|\alpha a| \leq -\frac{1}{\Delta}\ln(\xi d), \tag{1.21}$$

where $\xi > 1$. Inequality (1.21) gives an upper bound on Δ; namely,

$$\Delta_{\max} = \left|\frac{\ln(\xi d)}{q + 2|\alpha a|}\right|, \text{ as } \xi \longrightarrow 1^+, \tag{1.22}$$

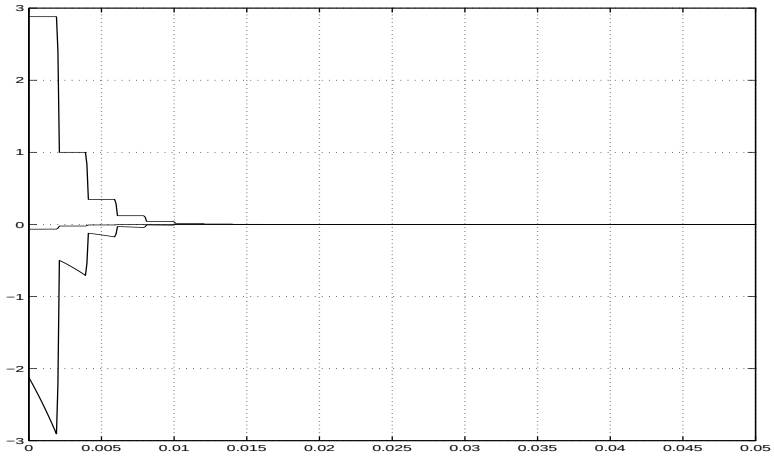

Figure 1.7: Stable simulation results for the case $B = \text{diag}(-1.5, -1, -1)$.

which is a sufficient condition, but not necessary, for the trivial solution to be asymptotically stable. It should be noted that, in [122], the same approach, mentioned above, was applied to the Lorenz system and conditions similar to (1.21) and (1.22) were obtained.

In order to illustrate Corollary 1.3.2, we present two different simulation results which correspond to two different values for the matrix B. The parameters of Chua's oscillator are chosen to be $\alpha = 15$, $\beta = 20$, $\gamma = 0.5$, $a = -120/7$, $b = -75/7$ and the initial condition is taken to be $(x(0), y(0), z(0))^T = (-2.121304, -0.06617, 2.88109)^T$. Hence the largest eigenvalue of $(A + A^T)$ will be given by $q = 20.16218$. A fourth-order Runge-Kutta method with step size 10^{-5} is used in the following simulations. We start first with a strong impulsive control model by choosing the matrix $B = \text{diag}(-1.5, -1, -1)$. Thus, by considering condition (1.21), we may choose the period of the impulses to be $\Delta = 0.002$. Figure 1.7 shows stable results, where we could see that the system asymptotically approaches the origin with a settling time of about 0.05. As a second choice for the matrix B (weak impulsive control model), we let $B = \text{diag}(-1, -0.1, -0.1)$. In this case, we may select the following value for $\Delta = 3 \times 10^{-4}$. In Figure 1.8, the control system asymptotically approaches the origin with a settling time of about 0.05.

In Theorem 1.3.2 and Corollary 1.3.1, it was assumed that $\psi_k : \mathbb{R}_+ \longrightarrow \mathbb{R}_+$, $k = 1, 2, \ldots$, are non-decreasing functions which is a strong condition that can be weakened for certain kind of impulsive systems. For example, it was realized that if the function $g(t, V(t, \mathbf{x})) = p(t)c(V(t, \mathbf{x}))$, where $p \in \mathcal{PC}$ and $c \in \mathcal{K}$, then the non-decreasing behaviour of ψ_k, $k = 1, 2, \ldots$, is no longer required to achieve the stability or asymptotic stability of the trivial solution of (1.15) [65, 71].

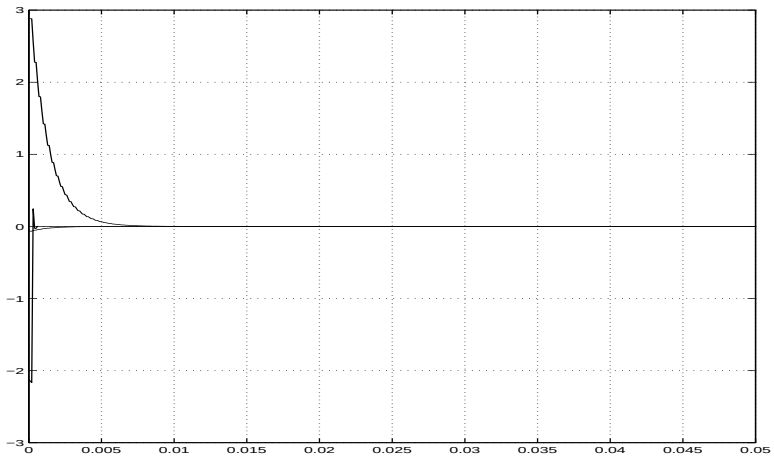

Figure 1.8: Stable simulation results for the case $B = \text{diag}(-1, -0.1, -0.1)$.

Instead, a weaker condition is required to be satisfied as explained in the following theorem.

Theorem 1.3.3 *Assume that*
1) *there exist* r *and* r_0, *with* $0 < r_0 < r$, *such that if* $\mathbf{x} \in S_{r_0}$, *it implies that* $\mathbf{x} + \mathbf{I}(t, \mathbf{x}) \in S_r$, *for all* $t = \tau_k$, $k = 1, 2, \ldots$;
2) $\beta(||\mathbf{x}||) \leq V(t, \mathbf{x}) \leq \alpha(||\mathbf{x}||)$ *on* $\mathbb{R}_+ \times S_r$, *where* $\alpha, \beta \in \mathcal{K}$, *and there exists* $\Psi_k \in \mathcal{K}_0$ *such that*

$$V(\tau_k^+, \mathbf{x} + \mathbf{I}(\tau_k, \mathbf{x})) \leq \Psi_k(V(\tau_k, \mathbf{x})), \quad k = 1, 2, \ldots;$$

3) *there exist* $c \in \mathcal{K}$ *and* $p \in \mathcal{PC}$ *such that*

$$D^+V(t, \mathbf{x}) \leq p(t)c(V(t, \mathbf{x})), \quad \mathbf{x} \in S_r, \quad t \neq \tau_k;$$

4) *there exists a constant* $\sigma > 0$ *such that for all* $z \in (0, \sigma)$, *we have*

$$\int_{\tau_k}^{\tau_{k+1}} p(s)ds + \int_{z}^{\Psi_k(z)} \frac{ds}{c(s)} \leq -\gamma_k,$$

for some constant γ_k *and* $k = 1, 2, \ldots$.
Then the trivial solution of system (1.15) is stable if $\gamma_k \geq 0$, *for all* $k = 1, 2, \ldots$, *and asymptotically stable if, in addition,* $\sum_{k=1}^{\infty} \gamma_k = \infty$.

Actually replacing conditions 3) and 4) of Theorem 1.3.3 by these two conditions
3′) there exist functions $c \in \mathcal{K}$ and $\pi \in \mathcal{PC}$ such that

$$D^+V(t,\mathbf{x}) \leq -\pi(t)c(V(t,\mathbf{x})), \quad \mathbf{x} \in S_r, \quad t \neq \tau_k;$$

4′) there exists a constant $\sigma > 0$ such that for all $z \in (0,\sigma)$, we have

$$-\int_{\tau_{k-1}}^{\tau_k} \pi(s)ds + \int_{z}^{\Psi_k(z)} \frac{ds}{c(s)} \leq -\gamma_k,$$

for some constant γ_k and $k = 1, 2, \ldots$, will also give the same conclusion as in Theorem 1.3.3; namely, the trivial solution of (1.15) is stable if $\gamma_k \geq 0$, for $k = 1, 2, \ldots$, and it is asymptotically stable if, in addition, $\sum_{k=1}^{\infty} \gamma_k = \infty$.

The latter results motivate us to weaken the conditions that guarantee the asymptotic stability of the trivial solution of system (1.15), stated in Theorem 1.3.3, and replace it by a weaker property, namely, equi-Lagrange stability, as illustrated before. In oder to do so, we shall present one theorem which deals with equi-boundedness properties of equation (1.15) [8, 73], then prove another theorem which gives the conditions under which the solutions of that equation are equi-Lagrange stable. These two theorems will be useful in the study of impulsive control needed for the next chapter.

Theorem 1.3.4 *The solutions of system (1.15) are uniformly bounded if*

(T1.1) $V \in \nu_0(M)$, *for some* $M \geq 0$, *and there exist functions* $a, b \in \mathcal{KR}$ *such that* $b(||\mathbf{x}||) \leq V(t,\mathbf{x}) \leq a(||\mathbf{x}||)$, $(t,\mathbf{x}) \in \mathbb{R}_+ \times S^c(M)$;

(T1.2) there exist functions $p \in \mathcal{PC}$ *and* $c_k \in \mathcal{K}_0$ *such that*

$$D^+V(t,\mathbf{x}) \leq p(t)c_k(V(t,\mathbf{x})), \ (t,\mathbf{x}) \in (\tau_k, \tau_{k+1}) \times S^c(M)^0, \tag{1.23}$$

for $k = 1, 2, \ldots$;

(T1.3) there exists a constant $N \geq 0$ *such that if* $||\mathbf{x}(\tau_k)|| \leq M$, *then* $||\mathbf{x} + \mathbf{I}(\tau_k, \mathbf{x})|| \leq N$, *for* $k = 1, 2, \ldots$;

(T1.4) there exist functions $\Psi \in \mathcal{KR}$ *and* $\Psi_k \in \mathcal{K}_0$ *such that* $\Psi(s) \leq \Psi_k(s) \leq s$, $s \in \mathbb{R}_+$, *and*

$$V(\tau_k^+, \mathbf{x} + \mathbf{I}(\tau_k, \mathbf{x})) \leq \Psi_k(V(\tau_k, \mathbf{x})), \tag{1.24}$$

whenever $(\tau_k, \mathbf{x}), (\tau_k, \mathbf{x} + \mathbf{I}(\tau_k, \mathbf{x})) \in \mathbb{R}_+ \times S^c(M)^0$, *for* $k = 1, 2, \ldots$;

(T1.5) there exist constants $\lambda > 0$ *and* $\gamma_k \geq 0$ *such that*

$$\int_{\tau_k}^{\tau_{k+1}} p(s)ds + \int_{y}^{\Psi_k(y)} \frac{ds}{c_k(s)} \leq -\gamma_k, \tag{1.25}$$

where $y \geq \lambda$, $k = 1, 2, \ldots$.

The next result is on equi-Lagrange stability.

Theorem 1.3.5 *The solutions of system (1.15) are equi-Lagrange stable if*

(T2.1) system (1.15) is equi-bounded;

(T2.2) condition (T1.2) holds for $V \in \nu_0(0)$ *with inequality (1.23) being true for all* $(t, \mathbf{x}) \in \mathbb{R}_+ \times \mathbb{R}^n$;

(T2.3) there exist functions $\Psi_k \in \mathcal{K}_0$ *such that inequality (1.24) holds, for all* $(\tau_k, \mathbf{x}) \in \mathbb{R}_+ \times \mathbb{R}^n$ *and for all* $k = 1, 2, \ldots$;

(T2.4) there exist a constant $\rho > 0$ *and functions* $C_k \in \mathcal{K}$ *such that* $C_k(s) \leq c_k(s)$, *for all* $s \in \mathbb{R}_+$ *and for all* $k = 1, 2, \ldots$, *and for any given fixed* $s \in \mathbb{R}_+$, $\inf_k C_k(s) > \rho$;

(T2.5) inequality (1.25) holds, for all $y > 0$, *and* $\sum_{k=1}^{\infty} \gamma_k = \infty$.

Proof: To prove equi-Lagrange stability, we need to show that system (1.15) is equi-attractive in the large in view of assumption (T2.1). For simplicity, we set $m(t) := V(t, \mathbf{x}(t))$, where $\mathbf{x}(t) = \mathbf{x}(t, t_0, \mathbf{x}_0)$ is any solution of (1.15) such that $\mathbf{x}(t_0^+) = \mathbf{x}_0$. Since system (1.15) is equi-bounded, the solution $\mathbf{x}(t) = \mathbf{x}(t, t_0, \mathbf{x}_0)$ of (1.15) exists on $[t_0, \infty)$, for all $\mathbf{x}_0 \in \mathbb{R}^n$. Since $V \in \nu_0(0)$, we have $D^+m(t) = D^+V(t, \mathbf{x}(t))$. By inequalities (1.23) and (1.24), we have

$$\begin{cases} D^+m(t) & \leq & p(t)c_k(m(t)),\ t \neq \tau_k \\ m(\tau_k^+) & \leq & \Psi_k(m(\tau_k)),\ k = 1, 2, \ldots. \end{cases} \tag{1.26}$$

Using (1.26), we obtain

$$\int_{m(\tau_k^+)}^{m(t)} \frac{ds}{c_k(s)} \leq \int_{\tau_k}^{t} p(s)ds \leq \int_{\tau_k}^{\tau_{k+1}} p(s)ds,\ t \in (\tau_k, \tau_{k+1}], \tag{1.27}$$

and

$$\int_{m(\tau_k)}^{m(\tau_k^+)} \frac{ds}{c_k(s)} \leq \int_{m(\tau_k)}^{\Psi_k(m(\tau_k))} \frac{ds}{c_k(s)}. \tag{1.28}$$

Adding (1.27) and (1.28), we get, in view of (1.25),

$$\int_{m(\tau_k)}^{m(t)} \frac{ds}{c_k(s)} \leq \int_{\tau_k}^{\tau_{k+1}} p(s)ds + \int_{m(\tau_k)}^{\Psi_k(m(\tau_k))} \frac{ds}{c_k(s)} \leq -\gamma_k. \tag{1.29}$$

With inequality (1.29), we conclude that $m(t) \leq m(\tau_k)$, for all $t \in (\tau_k, \tau_{k+1}]$, i.e., $m(\tau_{k+1}) \leq m(\tau_k)$. This means that the sequence $\{m(\tau_k)\}_{k=1}^{\infty}$ is non-increasing. Furthermore, since the sequence is bounded from below, it follows that the sequence possesses a limit, say $\mathcal{L} \geq 0$, as k approaches infinity. We shall prove that $\mathcal{L} = 0$. Let us assume $\mathcal{L} > 0$ and try to reach a contradiction. Using the fact that $c_k \in \mathcal{K}_0$, $C_k \in \mathcal{K}$, $C_k(s) \leq c_k(s)$, for all $s \in \mathbb{R}_+$, and $m(\tau_k) \geq m(\tau_{k+1})$, for all $k = 1, 2, \ldots$, we obtain

$$\int_{m(\tau_k)}^{m(\tau_{k+1})} \frac{C_k(\mathcal{L})}{c_k(s)} ds \geq m(\tau_{k+1}) - m(\tau_k),$$

for all $k = 1, 2, \ldots$. Thus for $n > 1$, we obtain

$$\begin{aligned} m(\tau_{n+1}) - m(\tau_1) &= m(\tau_{n+1}) - m(\tau_n) + m(\tau_n) - \ldots + m(\tau_2) - m(\tau_1) \\ &\leq \int_{m(\tau_n)}^{m(\tau_{n+1})} \frac{C_n(\mathcal{L})}{c_n(s)} ds + \ldots + \int_{m(\tau_1)}^{m(\tau_2)} \frac{C_1(\mathcal{L})}{c_1(s)} ds \\ &\leq -\gamma_n C_n(\mathcal{L}) - \gamma_{n-1} C_{n-1}(\mathcal{L}) - \ldots - \gamma_1 C_1(\mathcal{L}) \\ &= -\sum_{k=1}^{n} \gamma_k C_k(\mathcal{L}). \end{aligned}$$

This implies, by conditions (T2.4) and (T2.5), that

$$m(\tau_{n+1}) \leq m(\tau_1) - \rho \sum_{k=1}^{n} \gamma_k \longrightarrow -\infty$$

as $n \to \infty$, which is a contradiction. Therefore, we must have $\mathcal{L} = 0$, as we claimed. On the other hand, $m(t) \leq m(\tau_k)$, for all $t \in (\tau_k, \tau_{k+1}]$ and for all $k = 1, 2, \ldots$. Thus

$$\lim_{t \to \infty} m(t) = 0.$$

It follows that

$$\lim_{t\to\infty} ||\mathbf{x}(t)|| = \lim_{t\to\infty} b(||\mathbf{x}(t)||) = \lim_{t\to\infty} m(t) = 0,$$

i.e., system (1.15) is equi-attractive in the large and hence it is equi-Lagrange stable, as required.□

Theorems 1.3.4 and 1.3.5 give sufficient conditions on the equi-boundedness and equi-Lagrange stability of solutions for equation (1.15). In the next chapter, we shall use these results as tools to investigate the boundedness and Lagrange stability properties of particular impulsive systems which will mimic the structure of error systems between impulsively synchronized chaotic systems.

Chapter 2

Chaos Synchronization

Although the term synchronization seems to be quite regular when applied to periodic oscillations, the combination *synchronized chaotic oscillations* may sound quite mysterious. Indeed, there is an essential difference between the synchronization of periodic oscillations and synchronization of chaos. In the former case the oscillations do not have intrinsic instability which is one of the signatures of chaos. In systems oscillating chaotically, we have seen that infinitesimally nearby initial conditions trigger quite distinct evolutions. Considering this, it may appear that it is quite pointless to try to synchronize chaotic oscillations in any sense. Yet, as we shall see in this chapter, one may outline a whole class of systems which can exhibit synchronization of chaos in a very narrow sense, namely, identical synchronized chaotic oscillations.

This chapter summarizes the most important general information on this kind of synchronization and introduces the concept of impulsive synchronization. We shall limit our explanations to the case of so called *forced synchronization* of chaos which is observed in systems consisting of an autonomous chaotic driving system whose signal (or samples of its signal) serves as an input for the response system.

In Section 2.1 we shall discuss the problem of forced synchronization and some methods for its analysis in the general form which already exist in the literature. An explanation of the terminologies used for the description of synchronized chaos leading to the idea of impulsive synchronization will be provided. Then in Section 2.2, we derive sufficient conditions needed to guarantee accurate impulsive synchronization, by implementing Lagrange stability, and study the robustness of this approach towards parameter mismatch between the chaotic systems involved. In Section 2.3, the Lyapunov exponents of the error dynamics between impulsively synchronized

chaotic systems are studied and evaluated to confirm the theoretical results obtained in Section 2.2.

2.1 Synchronization

Considering the different types of chaotic systems, we wonder whether it is possible to find mechanisms for externally influencing the functioning of chaotic systems and, on the other hand, how one can explain and possibly use, for other purposes, the amazing ability of performing useful tasks such as signal processing out of cooperation of a multiple number of chaotic systems. These questions and many more may be answered through illustrating the concept of forced synchronization. We therefore describe in this section the linking of two chaotic systems with a common signal or signals (or even samples of signals) using different approaches that have been proposed so far in the literature. Each method will be investigated thoroughly and an example will be provided for each one of them.

There are two different types of forced synchronization that are discussed and explained with some illustrative examples in this section:

1. Synchronization through remote replication or Carroll-Pecora synchronization.

2. Impulsive synchronization.

Both of these forced synchronization methods consist of two dynamical systems; one of which generates the driving signals and is called the *drive system* (or driving system) and the other is driven by these signals and is called *response system* (or driven system). We shall see, in Chapter 5, the importance of these two types of forced synchronization methods in the study of cryptography and secure communication, especially impulsive synchronization that has been developed very recently. We shall explain both terminologies in detail after we introduce the following definition of synchronization in the general sense.

Definition 2.1.1 *Suppose that* $\mathbf{x}(t)$ *and* $\widetilde{\mathbf{x}}(t)$ *represent the solution trajectories of a continuous-time dynamical system, given by equation (1.1), and suppose that* $\mathbf{e} := \mathbf{x} - \widetilde{\mathbf{x}}$ *represents the error dynamics. Then* $\mathbf{x}$ *and* $\widetilde{\mathbf{x}}$ *are said to* synchronize *if the error dynamics,* $\mathbf{e}$, *is equi-Lagrange stable, i.e.,*

$$\lim_{t\to\infty} \mathbf{e}(t) = \mathbf{0}.$$

Moreover, we say that $\mathbf{x}$ *and* $\widetilde{\mathbf{x}}$ *have the property of* generalized synchronization *if a functional relation exists between them and the synchronized manifold defined with this functional relation behaves as an attractor.*

Notice that the value of β, in Definition 1.2.5, can be quite large, allowing the error dynamics between synchronized chaotic systems to have initially large values (called the *transient region*). However, the existence of T, in Definition 1.2.7, guarantees that the error will converge to zero eventually.

We see clearly from Definition 2.1.1 that synchronization of two (not necessarily identical) dynamical systems means that the trajectories of one of the two systems will converge to the same values of the other and will remain in step with each other, which makes synchronization appear to be structurally stable. Unfortunately, the capability of these two chaotic non-linear systems to oscillate in coherent and synchronized way is still not obvious. Yet, in [19, 88, 89], the method of remote replication or Carroll-Pecora (mentioned earlier), which is based on decomposing a system into at least two subsystems: a drive system and stable response subsystems that synchronize when coupled with a common drive signal, was obtained. This method may be summarized in the following manner. We shall consider an autonomous n-dimensional dynamical system given by

$$\dot{\mathbf{u}} = \mathbf{f}(\mathbf{u}). \tag{2.1}$$

System (2.1) can be arbitrarily decomposed into two subsystems, $\mathbf{u} = (\mathbf{v}, \mathbf{w})^T$, such that

$$\dot{\mathbf{v}} = \mathbf{g}(\mathbf{v}, \mathbf{w}), \quad \dot{\mathbf{w}} = \mathbf{h}(\mathbf{v}, \mathbf{w}), \tag{2.2}$$

where $\mathbf{v} = (u_1, \ldots, u_m)^T$, $\mathbf{g} = (f_1, \ldots, f_m)^T$, $\mathbf{w} = (u_{m+1}, \ldots, u_n)^T$ and $\mathbf{h} = (f_{m+1}, \ldots, f_n)^T$. We create a new subsystem $\mathbf{w}'$, called the response, identical to the $\mathbf{w}$ subsystem, but the set of variables $\mathbf{v}$ are substituted for the corresponding $\mathbf{v}'$ in the function $\mathbf{h}$. Then we augment equation (2.2) with this new system, to obtain

$$\dot{\mathbf{v}} = \mathbf{g}(\mathbf{v}, \mathbf{w}), \quad \dot{\mathbf{w}} = \mathbf{h}(\mathbf{v}, \mathbf{w}), \quad \dot{\mathbf{w}}' = \mathbf{h}(\mathbf{v}, \mathbf{w}'). \tag{2.3}$$

We now examine the difference $\mathbf{e} = \mathbf{w} - \mathbf{w}'$. The subsystem components $\mathbf{w}$ and $\mathbf{w}'$ will synchronize only if $\mathbf{e} \longrightarrow \mathbf{0}$ as $t \longrightarrow \infty$. In the infinitesimal limit, this leads to the linear variational expansion for the subsystem, given by

$$\dot{\mathbf{e}} = \dot{\mathbf{w}} - \dot{\mathbf{w}}' = \mathbf{h}(\mathbf{v}, \mathbf{w}) - \mathbf{h}(\mathbf{v}, \mathbf{w}') = J_{\mathbf{w}}\mathbf{h}(\mathbf{v}(t), \mathbf{w}(t))\mathbf{e} + \mathcal{O}(||\mathbf{e}||^2), \tag{2.4}$$

where $J_{\mathbf{w}}\mathbf{h}$ is the Jacobian of the $\mathbf{w}$ subsystem vector field with respect to $\mathbf{w}$ only. The behaviour of equation (2.4), or its matrix version, depends on the Lyapunov exponents of the $\mathbf{w}$ subsystem, which are referred to as *sub-Lyapunov exponents* or *conditional Lyapunov exponents*. In [88,89], it has been realized that the necessary and sufficient conditions for the trivial solution of (2.4) to be asymptotically stable, depends on the sign of these sub-Lyapunov exponents. This dependence is expressed in the following theorem.

Theorem 2.1.1 *The trivial solution of the non-linear non-stationary system, given by (2.4), is asymptotically stable if and only if the sub-Lyapunov exponents of the* $\mathbf{w}$ *subsystem are all negative.*

The negativity of the sub-Lyapunov exponents for the $\mathbf{w}$ subsystem is obviously a necessary condition for the asymptotic stability of the trivial solution, but since $\lim_{||\mathbf{e}||\to 0} \mathcal{O}(||\mathbf{e}||^2)/||\mathbf{e}|| = 0$ and $J_{\mathbf{w}}\mathbf{h}$ is bounded, the negativity condition is also sufficient condition because of the *Fundamental Linear Stability Theorem* (see [57,77,89]). Hence the $\mathbf{w}$ and $\mathbf{w}'$ subsystems will synchronize after a transient period. One more thing we should mention is that the theorem says nothing about the set of initial conditions in $\mathbf{w}'$ which will synchronize with $\mathbf{w}$. In fact, the effect of these set of points of initial conditions is dramatic, especially with cascaded systems, and will be investigated later in this section

A natural question to ask is: how will the synchronization be affected by the differences in parameters that exist in both $\mathbf{w}$ and $\mathbf{w}'$ subsystems which are found in real life and practical applications (e.g., in circuit design). In [88,89], this question was studied analytically and numerically as follows. We shall begin as above and examine the equation of motion for $\mathbf{e}(t) = \mathbf{w}(t) - \mathbf{w}'(t)$. Letting $\boldsymbol{\mu}$ and $\boldsymbol{\mu}'$ stand for the vector of parameters in the $\mathbf{w}$ and $\mathbf{w}'$ subsystems, respectively, and recalling the equations in (2.3), we get

$$\begin{aligned}
\dot{\mathbf{e}} &= \mathbf{h}(\mathbf{v},\mathbf{w},\boldsymbol{\mu}) - \mathbf{h}(\mathbf{v},\mathbf{w}',\boldsymbol{\mu}') \\
&= \mathbf{h}(\mathbf{v},\mathbf{w},\boldsymbol{\mu}) - \mathbf{h}(\mathbf{v},\mathbf{w},\boldsymbol{\mu}') + \mathbf{h}(\mathbf{v},\mathbf{w},\boldsymbol{\mu}') - \mathbf{h}(\mathbf{v},\mathbf{w}',\boldsymbol{\mu}') \\
&= \mathbf{h}(\mathbf{v},\mathbf{w},\boldsymbol{\mu}) - \mathbf{h}(\mathbf{v},\mathbf{w},\boldsymbol{\mu}') + J_{\mathbf{w}}\mathbf{h}\mathbf{e} + \mathcal{O}(\mathbf{v},\mathbf{w}').
\end{aligned}$$

Due to the extra terms $\mathbf{h}(\mathbf{v},\mathbf{w},\boldsymbol{\mu})$ and $\mathbf{h}(\mathbf{v},\mathbf{w},\boldsymbol{\mu}')$, the asymptotic stability of the trivial solution is not guaranteed anymore (i.e., Theorem (2.1.1) is not applicable). We can get an estimate on $\mathbf{e}$ by assuming that $||\mathbf{e}(0)|| << 1$; that is, we are letting the systems have nearly identical initial

conditions. By ignoring the term $\mathcal{O}(\mathbf{v}, \mathbf{w}')$, for times less than $t_1 > 0$, we get

$$\dot{\mathbf{e}} = \mathbf{h}(\mathbf{v}, \mathbf{w}, \boldsymbol{\mu}) - \mathbf{h}(\mathbf{v}, \mathbf{w}, \boldsymbol{\mu}') + J_{\mathbf{w}}\mathbf{h}\mathbf{e},$$

whose approximate solution is given by

$$\mathbf{e}(t) = Z(t)\mathbf{e}(0) + \int_0^t Z(t-\tau)\mathbf{B}(\tau)d\tau,$$

where $Z(t)$ is, as before, the state transition matrix which satisfies $\dot{Z} = J_{\mathbf{w}}\mathbf{h}(\mathbf{v}, \mathbf{w})Z$, and $\mathbf{B} = \mathbf{h}(\mathbf{v}, \mathbf{w}, \boldsymbol{\mu}) - \mathbf{h}(\mathbf{v}, \mathbf{w}, \boldsymbol{\mu}')$, $t \leq t_1$. We can now show that $\mathbf{e}$ may be bounded. In general, denoting the largest negative sub-Lyapunov exponent of the $\mathbf{w}$ subsystem by $-c_2$, then there will exist a $c_1 > 0$ (for further details, see [15]), such that

$$||Z(t)|| \leq c_1 \exp(-c_2 t).$$

Thus if $\mathbf{B}(t)$ is bounded by a positive constant b_1 (as it will be for most situations), we obtain

$$||\mathbf{e}|| \leq c_1 \exp(-c_2 t) + \frac{c_1 b_1}{c_2}(1 - \exp(-c_2 t)).$$

Notice that if our assumption about $\mathcal{O}(\mathbf{v}, \mathbf{w}')$ holds for long enough time, then letting t approach infinity, we get $||\mathbf{e}|| \leq c_1 b_1 / c_2$. Hence $\mathbf{e}$ will remain bounded and small provided that the differences in parameters are not large and $\mathcal{O}(\mathbf{v}, \mathbf{w}')$ is small enough. i.e., with small enough parameter differences, the actual response trajectory will remain near its drive counterpart (remain nearly synchronized). This is maybe better understood by taking a one-dimensional drive and response systems as an example (this example is given in [15], but it is slightly modified here). A small variation $e = w - w'$ and $\Delta\boldsymbol{\mu} = \boldsymbol{\mu} - \boldsymbol{\mu}'$, will give

$$\dot{e} \approx h_w e + [\frac{\partial h}{\partial \boldsymbol{\mu}}] \cdot \Delta\boldsymbol{\mu}, \tag{2.5}$$

where $[\frac{\partial h}{\partial \boldsymbol{\mu}}]$ is the gradient vector of h with respect to $\boldsymbol{\mu}$. Roughly, if h_w is constant in time and $[\frac{\partial h}{\partial \boldsymbol{\mu}}]$ is a constant vector in time, then (2.5) becomes a linear first order ODE whose solution is given by

$$e(t) = \left[e(0) + \frac{1}{h_w}[\frac{\partial h}{\partial \boldsymbol{\mu}}]\Delta\boldsymbol{\mu}\right] \exp(h_w t) - \frac{1}{h_w}[\frac{\partial h}{\partial \boldsymbol{\mu}}]\Delta\boldsymbol{\mu}.$$

Thus if $h_w < 0$, the difference between w and w' will level off at some constant value. For multi-dimensional case, it was realized numerically, in [88, 89], that such behaviour extends even if the difference in parameters are rather large [10%-20%]. It was suggested in [18] how to overcome this parameter difference in designing circuits by using cascaded systems. We shall describe later in this section cascaded systems and their applications.

Let us work now directly on a specific system called the Lorenz system, given by equation (1.5), in order to apply the above results and investigate the applications (for additional details, see [23, 24, 89]). It was established in [89] that Lorenz system is decomposable into two stable response subsystems (x_1, z_1) and (y_2, z_2). However, it was observed that the response subsystem (x_3, y_3) is unstable. These subsystems are given by the following equations.

- The (x_1, z_1) subsystem is given by

$$\begin{aligned} \dot{x}_1 &= \sigma(y - x_1) \\ \dot{z}_1 &= x_1 y - b z_1. \end{aligned}$$

- The (y_2, z_2) subsystem is given by

$$\begin{aligned} \dot{y}_2 &= rx - y_2 - x z_2 \\ \dot{z}_2 &= x y_2 - b z_2. \end{aligned}$$

- The (x_3, y_3) subsystem is given by

$$\begin{aligned} \dot{x}_3 &= \sigma(y_3 - x_3) \\ \dot{y}_3 &= r x_3 - y_3 - x_3 z. \end{aligned}$$

Notice that the dynamics of the Lorenz system is independent of all of the response subsystems given above. Therefore the Lorenz system is called the drive system, whereas the (x_1, z_1), (y_2, z_2) and (x_3, y_3) subsystems are called the response (or driven) subsystems, because they are driven by the driving signals y, x and z, respectively.

Let us examine each subsystem separately for stability issues. We start first with the (x_1, z_1) subsystem. Notice that the Jacobian matrix of (x_1, z_1) subsystem is given by

$$\begin{pmatrix} -\sigma & 0 \\ y & -b \end{pmatrix},$$

whose eigenvalues are $-\sigma$ and $-b$ which are strictly negative. Therefore

$$|x_1 - x| \longrightarrow 0 \text{ and } |z_1 - z| \longrightarrow 0 \text{ as, } \ t \longrightarrow \infty.$$

Moreover, it was established numerically [23] that the Lyapunov exponents of the (y_2, z_2) subsystem are negative and they both have the same value -2.5. Thus as above, we have

$$|y_2 - y| \longrightarrow 0 \text{ and } |z_2 - z| \longrightarrow 0, \ \text{ as } t \longrightarrow \infty.$$

However, it was discovered [89] that the last subsystem (x_3, y_3) has a slightly positive sub-Lyapunov exponent given by 7.89×10^{-3}. Therefore, x_3 and y_3 will not converge to x and y, respectively. Yet, in the subsequent sections, a very important method called *impulsive synchronization* may be integrated with the above method to achieve convergence; this convergence is enforced by applying impulses at instances whose time periods will satisfy certain conditions, as it will be explained later.

Thus, using the Carroll-Pecora synchronization, the two subsystems (x_1, z_1) and (y_2, z_2) converged to the corresponding components of the original Lorenz system (x, z) and (y, z), respectively. Suppose now that one subsystem is used to generate the full dimensional response system, then the question that we might ask is will this new system synchronize with the original one (the driving system)? In other words, if the subsystem (y_2, z_2) is used to generate the third component x_2 through the equation $\dot{x}_2 = -\sigma x_2 + \sigma y_2$, then can one conclude that the 3-dimensional response system (x_2, y_2, z_2) will converge to the original system (x, y, z)? The answer to this question depends entirely on the subsystem chosen and on the stability properties of the trivial solution of the error dynamics between the driving and response systems. We shall discuss two different ways to answer this question: one of them uses the method of Lyapunov functions which motivates a new analytical way of analyzing synchronization, and the other uses the method of cascaded systems which depends on manipulating the sub-Lyapunov exponents. We begin by illustrating the first approach in the following manner. We shall take the Lorenz system and its (y_2, z_2) subsystem as an example. But before we do that, it should be mentioned that the Lorenz system can be slightly modified, for reasons related to circuit design (for further details, see [22–24]), by applying the substitution

$$u = \frac{x}{10}, \ v = \frac{y}{10} \text{ and } w = \frac{z}{20}.$$

Hence, using the above substitution, the Lorenz system becomes

$$\begin{aligned} \dot{u} &= \sigma(v-u) \\ \dot{v} &= ru - v - 20uw \\ \dot{w} &= 5uv - bw. \end{aligned} \tag{2.6}$$

Employing u as the driving signal, i.e., using the (v_2, w_2) as a response subsystem, the full dimensional response system will be given by

$$\begin{aligned} \dot{u}_r &= \sigma(v_r - u_r) \\ \dot{v}_r &= ru - v_r - 20uw_r \\ \dot{w}_r &= 5uv_r - bw_r. \end{aligned} \tag{2.7}$$

By equations (2.6) and (2.7), the error dynamics $\mathbf{e} = \mathbf{u} - \mathbf{u}_r$, in this case, will be given by

$$\begin{aligned} \dot{e}_1 &= \sigma(e_2 - e_1) \\ \dot{e}_2 &= -e_2 - 20u(t)e_3 \\ \dot{e}_3 &= 5u(t)e_2 - be_3. \end{aligned} \tag{2.8}$$

The trivial solution of system (2.8) is asymptotically stable, since the derivative of the Lyapunov function, given by

$$V(\mathbf{e}) = \frac{1}{2\sigma}e_1^2 + \frac{1}{2}e_2^2 + 2e_3^2,$$

is strictly negative and is given by $\dot{V}(\mathbf{e}) = -(e_1 - \frac{1}{2}e_2)^2 - \frac{3}{4}e_2^2 - 4be_3^2$. Therefore

$$\lim_{t\to\infty} \mathbf{e}(t) = 0,$$

which is the desired property of synchronizing the response system with the driving system.

As an alternative approach to the method described above and an immediate extension of the Carroll-Pecora synchronization, another method, called synchronization using cascaded systems, was proposed in [18] which is considered more advantageous compared with the former approach.

This new method utilizes a chaotic system that possesses at least two stable subsystems (e.g., Lorenz system, as shown earlier). In this current method, we proceed one step further with synchronized chaotic systems. This is done as follows. We begin, as before, by using an autonomous non-linear dynamical system that may be divided into several parts

$$\begin{aligned} \dot{u} &= f(u,v,w) \\ \dot{v} &= g(u,v,w) \\ \dot{w} &= h(u,v,w). \end{aligned}$$

The dynamical variables $(u,v,w)^T$ can be thought of as scalars for simplicity, although the following argument can be generalized to vector variables. Suppose now that we have a new set of equations corresponding to the response system which is driven by the signal u:

$$\begin{aligned} \dot{v}' &= g(u,v',w') \\ \dot{w}' &= h(u,v',w'). \end{aligned} \tag{2.9}$$

By Theorem 2.1.1, if all the sub-Lyapunov exponents of the response system, given by (2.9), are negative, then after an initial transient region, $v'(t)$ will converge to $v(t)$ and $w'(t)$ will converge to $w(t)$, as explained earlier. We then reproduce an additional subsystem driven by v' and expressed in the following equations (see Figure 2.1).

$$\begin{aligned} \dot{u}'' &= f(u'',v',w''), \\ \dot{w}'' &= h(u'',v',w''). \end{aligned} \tag{2.10}$$

Once more, if this new response subsystem (2.10) has negative sub-Lyapunov exponents, then it will synchronize with the drive system, provided that the initial conditions belong to the same basin of attraction (for more details, see [18]). Thus the negativity of the sub-Lyapunov exponents is no longer a guarantee that the chaotic trajectories of the drive and the response systems will synchronize if they start from initial conditions that belong to different attractors, such as *one-well* two chaotic attractors. Actually, in the case of *two-well* chaotic attractor, the synchronization will not be as good, since after the chaotic waveform shifts from one well to the other, it spends some time in an unstable region causing a large error in synchronization. While

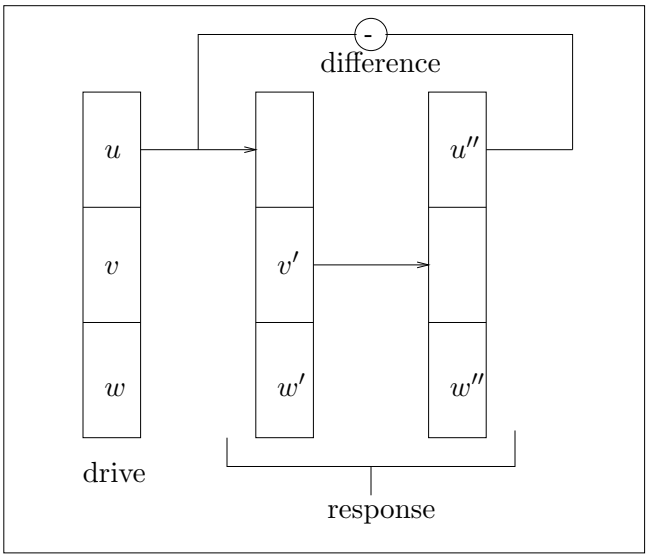

Figure 2.1: Block diagram of a cascaded system.

the chaotic waveform is in this unstable region, the time dependent conditional sub-Lyapunov exponents (calculated during this unstable period) for the response system are not all less than zero. However, the time averaged conditional sub-Lyapunov exponents for the entire response attractor are still less than zero. Parameter mismatch is another obstacle that will cause the response (u'', w'') to diverge from the drive system in the unstable region. In [18], these problems were noticed to give cascaded-system method certain properties that are very important. These properties are: we are able to reproduce all signals from one drive signal, we are able to use the pair of response subsystems as an attractor recognition device for chaotic attractors and finally we are able to use the synchronized subsystems, with the aid of *return maps*, to find the value of a parameter in the drive system and follow changes in that parameter in its magnitude and sign.

It should be mentioned that the authors of [18] and [119] obtained an estimate on how the approach to synchronization scales with time. This estimate was found out to be given by

$$e_1 = u - u'' \sim e^{\lambda_1 t}\Delta u(0) + \frac{B\Delta v(0)e^{\lambda_1 t}}{\lambda_2 - \lambda_1}\left[e^{(\lambda_2-\lambda_1)t} - 1\right], \tag{2.11}$$

where λ_1 is the largest (least negative) sub-Lyapunov exponent of the (u, w) subsystem, λ_2 is the largest (least negative) sub-Lyapunov exponent of the (v, w) subsystem and B is an upper bound on $\partial f/\partial y$. Clearly there are three regimes of scaling behaviour for equation (2.11). When

$\lambda_2 << \lambda_1$, we have $\Delta u(t) \sim e^{\lambda_1 t}$; that is, the first response follows fast enough that only the second response synchronization rate is important. When $\lambda_2 = \lambda_1$, we have $\Delta u(t) \sim e^{\lambda_1 t}$ again, but with a different amplitude. Now when $\lambda_2 >> \lambda_1$, $\Delta u(t) \sim e^{\lambda_2 t}$; that is, the first response $(v' \longrightarrow v)$ is the slow link in the cascade chain [18].

From the above discussion, we see clearly how useful this method is, in identifying attractors and finding system parameters which are considered the major tasks of this approach.

Another synchronization technique, which is useful for synchronizing hyperchaotic systems, was proposed in [33–35] and first motivated by the work in [90]. This technique does not require the computation of the Lyapunov exponents or the initial conditions belonging to the same basin of attraction. Moreover, it guarantees synchronization of a wide class of hyperchaotic systems via a scalar signal only. The synchronization method is based on a control theory result related to the idea of making the response system a linear observer for the state of the drive system, hence the name *observer design synchronization*. In order to illustrate how this method works, we shall consider the synchronization of two identical n-dimensional chaotic systems, given by

$$\dot{\mathbf{u}} = A\mathbf{u} + \mathbf{b}f(\mathbf{u}) + \mathbf{c} \tag{2.12}$$

and

$$\dot{\mathbf{u}}' = A\mathbf{u}' + \mathbf{b}f(\mathbf{u}') + \mathbf{c} + \mathbf{g}(s(\mathbf{u}) - s(\mathbf{u}')), \tag{2.13}$$

where A is an $n \times n$ matrix, $\mathbf{b} \in \mathbb{R}^{n\times 1}$, $f, s : \mathbb{R}^n \to \mathbb{R}$ and $\mathbf{g} : \mathbb{R}^n \to \mathbb{R}^n$. System (2.12) represents the drive system and system (2.13) represents the response system with $s(u)$ being the scalar synchronization signal. The low-dimensional chaotic and hyperchaotic systems, stated in the previous chapter, can be all written in the form given by equation (2.12). If $s(\mathbf{u})$ is given by

$$s(\mathbf{u}) = f(\mathbf{u}) + \mathbf{k}\mathbf{u},$$

where $\mathbf{k} = (k_1, k_2, \ldots, k_n) \in \mathbb{R}^{1\times n}$, and $\mathbf{g}$ is given by

$$\mathbf{g}(s(\mathbf{u}) - s(\mathbf{u}')) = \mathbf{b}(s(\mathbf{u}) - s(\mathbf{u}')),$$

then the error dynamics between the drive and response systems will be given by

$$\begin{aligned} \dot{\mathbf{e}} &= A\mathbf{u} + \mathbf{b}f(\mathbf{u}) + \mathbf{c} - A\mathbf{u}' - \mathbf{b}f(\mathbf{u}') - \mathbf{c} - \mathbf{b}(s(\mathbf{u}) - s(\mathbf{u}')) \\ &= A\mathbf{e} - \mathbf{b}\mathbf{k}\mathbf{e}. \end{aligned}$$

Let $v = -\mathbf{ke}$ and choose a proper coordinate transformation $\mathbf{e} = [T_1\ T_2]\overline{\mathbf{e}}$ such that the columns of T_1 form a set of basis vectors for the controllable state subspace and the columns of T_2 are orthogonal to these [57]. Since $T := [T_1\ T_2]$ is an orthogonal matrix, i.e., $T^{-1} = T^T$, then the error dynamics $\mathbf{e}$ can be transformed into to the following Kalman controllable canonical form [57]:

$$\begin{aligned}\begin{pmatrix} \dot{\overline{\mathbf{e}}}_c \\ \dot{\overline{\mathbf{e}}}_{nc} \end{pmatrix} &= \begin{pmatrix} T_1^T A T_1 & T_1^T A T_2 \\ O & T_2^T A T_2 \end{pmatrix} \begin{pmatrix} \overline{\mathbf{e}}_c \\ \overline{\mathbf{e}}_{nc} \end{pmatrix} + \begin{pmatrix} T_1^T \mathbf{b} \\ \mathbf{0} \end{pmatrix} v \\ &= \begin{pmatrix} \overline{A}_c & \overline{A}_{12} \\ O & \overline{A}_{nc} \end{pmatrix} \begin{pmatrix} \overline{\mathbf{e}}_c \\ \overline{\mathbf{e}}_{nc} \end{pmatrix} + \begin{pmatrix} \overline{\mathbf{b}}_c \\ \mathbf{0} \end{pmatrix} v,\end{aligned}$$

where O is the zero matrix of appropriate dimension, $\overline{A}_c := T_1^T A T_1$, $\overline{A}_{12} := T_1^T A T_2$, $\overline{A}_{nc} := T_2^T A T_2$ and $\overline{\mathbf{b}}_c := T_1^T \mathbf{b}$. Obviously the eigenvalues of $\overline{A}_c$ are controllable. In other words, its eigenvalues can be placed anywhere in the complex plane by proper state feedback controller $v = -\mathbf{ke}$. However, the eigenvalues of $\overline{A}_{nc}$ are uncontrollable, i.e., they are not affected by the introduction of any state feedback controller. Therefore it was realized in [33–35] that a necessary and sufficient condition to globally asymptotically stabilize the error dynamics $\mathbf{e}$ is that the eigenvalues of $\overline{A}_{nc}$ must lie in the left half of the complex plane and an appropriate choice for the vector $\mathbf{k}$ should be made to ensure that the eigenvalues of $\overline{A}_c$ will also lie in the left half of the complex plane.

To demonstrate the above observer design method for synchronization, we shall take a numerical example employing the high dimensional Rössler system, given by equation (1.9). Let $\eta = 0.25$, $\theta = 3$, $\nu = 0.5$ and $\zeta = 0.05$. In this case, by driving the response system $\mathbf{u}'$ with the signal $s(\mathbf{u}) = u_1 u_3 + \sum_{j=1}^{4} k_i u_j$, as explained above, the error dynamics $\mathbf{e}$ will be given by

$$\begin{bmatrix} \dot{e}_1 \\ \dot{e}_2 \\ \dot{e}_3 \\ \dot{e}_4 \end{bmatrix} = \left(\begin{bmatrix} 0 & -1 & -1 & 0 \\ 1 & 0.25 & 0 & 1 \\ 0 & 0 & 0 & 0 \\ 0 & 0 & -0.5 & 0.05 \end{bmatrix} - \begin{bmatrix} 0 \\ 0 \\ 1 \\ 0 \end{bmatrix} [k_1\ k_2\ k_3\ k_4] \right) \begin{bmatrix} e_1 \\ e_2 \\ e_3 \\ e_4 \end{bmatrix}. \tag{2.14}$$

Since the controllability matrix of system (2.14) is full rank [57], we may conclude, by applying the above discussion, that there exists a gain vector $\mathbf{k}$ such that the drive system $\mathbf{u}$ becomes a global observer of the response system $\mathbf{u}'$. This means that $\mathbf{u}' \to \mathbf{u}$, as $t \to \infty$, for any initial state. Taking $\mathbf{k} = (-3.3712, -0.9561, 4.3, -5.8126)$, the eigenvalues of system (2.14) can be placed at -1 and thus the error dynamics can be driven to zero as shown in Figure 2.2 (A Runge-Kutta

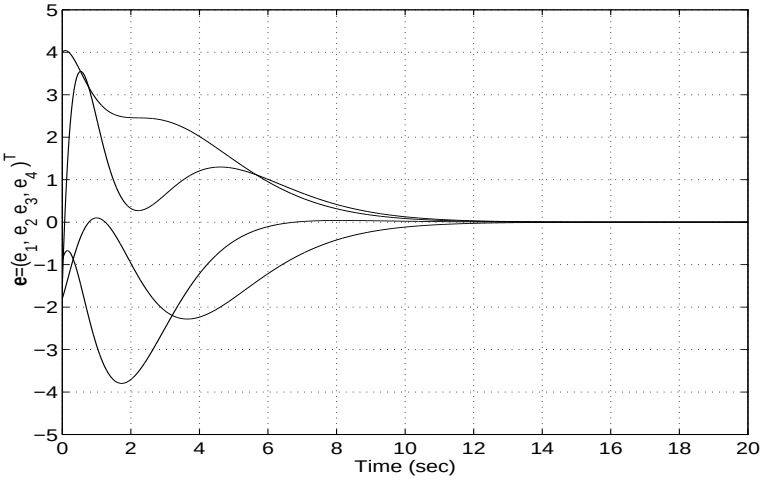

Figure 2.2: The components of the error dynamics $\mathbf{e}$, given by equation (2.14), approaching zero.

method with an integration step-size equal to 0.0001 is applied to obtain the simulation in Figure 2.2).

Recently a new synchronization method, called impulsive synchronization, which is based on the theory of impulsive control and first reported in [1, 97], has been developed. The method allows synchronization of two or more chaotic systems using only small impulses [102, 114–116]. These impulses are samples of state variables (or functions of state variables) of the drive system at discrete instances. The impulses are called synchronization impulses, and they drive the response system discretely at these instances. The equi-attractivity in the large of the error dynamics between the drive and the response chaotic systems is achieved, thus reaching the synchronization mode between the two systems. We shall now explain in detail how this method works by first discussing the model introduced in [97].

Suppose that we have two identical chaotic systems; a driving system $\mathbf{x} = (\mathbf{u}, \mathbf{w})^T$, where $\mathbf{u} = (x_1, x_2, \ldots, x_m)^T$ and $\mathbf{w} = (x_{m+1}, x_{m+2}, \ldots, x_n)^T$, satisfying

$$\dot{\mathbf{u}} = \mathbf{F}_{\mathbf{u}}(\mathbf{u}, \mathbf{w}), \quad \dot{\mathbf{w}} = \mathbf{F}_{\mathbf{w}}(\mathbf{u}, \mathbf{w}), \tag{2.15}$$

and a driven system $\mathbf{x}' = (\mathbf{u}', \mathbf{w}')^T$ satisfying

$$\dot{\mathbf{u}}' = \mathbf{F}_{\mathbf{u}}(\mathbf{u}', \mathbf{w}') + \delta_{\Delta}(t)(\mathbf{u} - \mathbf{u}'), \quad \dot{\mathbf{w}}' = \mathbf{F}_{\mathbf{w}}(\mathbf{u}', \mathbf{w}'), \tag{2.16}$$

where

$$\delta_{\Delta}(t) = \sum_{k=0}^{\infty} \delta(t - k\Delta), \tag{2.17}$$

and $\delta(t - k\Delta)$ is the delta Dirac function given by $\delta(t - k\Delta) = \lim_{T \to 0} \delta_T(t - k\Delta)$, where

$$\delta_T(t - k\Delta) = \begin{cases} 0, & t < k\Delta \\ \\ \dfrac{1}{T}, & k\Delta \leq t \leq k\Delta + T \\ \\ 0, & t > k\Delta + T. \end{cases}$$

From the above model, we can see that the solution trajectory of $\mathbf{u}'$, defined by equation (2.16), will oscillate freely and unforcedly except for the equidistant moments $\tau_k = k\Delta$, when $\mathbf{u}'(\tau_k)$ is forced to a new value $\mathbf{u}(\tau_k)$, for $k = 1, 2, \ldots$. The above representation of impulsive systems, described by equations (2.15) and (2.16), are identical to the impulsive system given by equation (1.15). However, this current representation is useful for numerical purposes when trying to obtain simulations for solution trajectories.

The next theorem [88, 97] gives the conditions that would guarantee the synchronization of the driving system $\mathbf{x}$ and the response system $\mathbf{x}'$, i.e., $\lim_{t \to \infty} \mathbf{e}(t) = \lim_{t \to \infty} [\mathbf{x}(t) - \mathbf{x}'(t)] = 0$.

Theorem 2.1.2 *Consider system (2.15). Assume that* $\dot{\mathbf{w}} = \mathbf{F}_{\mathbf{w}}(\mathbf{u}, \mathbf{w})$ *is asymptotically stable when driven by* $\mathbf{u}(t)$ *and for initial conditions* $\mathbf{w}_0 \in S \subset \mathbb{R}^{n-m}$. *Then there exists a value* Δ_H *such that for all* $\Delta < \Delta_H$, *impulsive (sporadic) driving of a copy of (2.15), given by (2.16), results in synchronization between (2.15) and (2.16). In other words,* $||\mathbf{x} - \mathbf{x}'|| \longrightarrow 0$, *when* $t \longrightarrow \infty$.

The above result gives no information or an estimate on the value of Δ_H, (the maximum duration between two impulses permissible) but it guarantees the existence of such value. However, when dealing with chaotic systems, whose structures resemble those described by equation (1.19), will be a different story. In this case, a special method proposed in [114–116] will allow us to obtain an estimate on the value of Δ_H by deriving it analytically in a manner similar to the one given in Corollary (1.3.2). We illustrate this manner in the following example that employs Chua's oscillator as the chaotic system. Consider the Chua's oscillator, given by equation (1.6), as a

driving system. The response system is given by

$$\begin{aligned}\frac{dx'}{dt} &= \alpha(y' - x' - f(x')) \\ \frac{dy'}{dt} &= x' - y' + z' \\ \frac{dz'}{dt} &= -\beta y' - \gamma z',\end{aligned}$$

where $t \neq \tau_k$, $k = 1, 2, \ldots$, and the impulses are given by

$$\Delta \mathbf{x}'|_{t=\tau_k} = -B\mathbf{e}(\tau_k),$$

where B is a 3×3 symmetric matrix and $\mathbf{e} = \mathbf{x} - \mathbf{x}'$ is the synchronization error. Thus if we let

$$A = \begin{pmatrix} -\alpha & \alpha & 0 \\ 1 & -1 & 1 \\ 0 & -\beta & -\gamma \end{pmatrix}, \quad \mathbf{\Psi}(\mathbf{x}, \mathbf{x}') = \begin{pmatrix} -\alpha f(x) + \alpha f(x') \\ 0 \\ 0 \end{pmatrix},$$

then it follows that

$$\begin{cases} \dfrac{d\mathbf{e}}{dt} = A\mathbf{e} + \mathbf{\Psi}(\mathbf{x}, \mathbf{x}'), \quad t \neq \tau_k \\ \Delta \mathbf{e}|_{t=\tau_k} = B\mathbf{e}, \quad k = 1, 2, \ldots. \end{cases} \tag{2.18}$$

Notice that $||\mathbf{\Psi}(\mathbf{x}, \mathbf{x}')|| \leq |\alpha a|\ ||\mathbf{e}||$. Therefore, by Corollary 1.3.2, the following result guarantees the asymptotic stability of the equilibrium point $(0, 0, 0)^T$ of the error dynamics and it even gives an estimate on the region of attraction of the point $(0, 0, 0)^T$.

Corollary 2.1.1 *Let d be the largest eigenvalue of $(I + B^T)(I + B)$, where B is a symmetric matrix, and q be the largest eigenvalue of $(A + A^T)$. Assume that $||I + B|| \leq 1$ and that the impulses are equidistant, i.e., $\tau_{k+1} - \tau_k = \Delta$, $\forall k = 1, 2, \ldots$. If*

$$0 \leq q + 2|\alpha a| \leq -\frac{1}{\Delta} \ln(\xi d), \quad \xi > 1, \tag{2.19}$$

then the impulsive synchronization of the two Chua's oscillators is asymptotically stable. In other words, the error dynamics (2.18) is asymptotically stable.

Corollary 2.1.1 implies that imposing condition (2.19) on the locations of τ_k, for all $k = 1, 2, \ldots$, will guarantee that $\lim_{t\to\infty} \mathbf{e}(t) = 0$.

In the above discussion, it was assumed that the impulses are equidistant, i.e., $\Delta_k = \Delta$, for $k = 1, 2, \ldots$. The sufficient conditions obtained for synchronization depend on that factor completely. However, in [70], the equidistant-impulses assumption is relaxed and a new set of sufficient conditions for asymptotic stability of the error dynamics (2.18), with time-varying impulses, are obtained. The next theorem shows the set of sufficient conditions needed for the impulsive synchronization of two Chua's oscillators by applying time-varying impulses [70].

Theorem 2.1.3 *Let d be the largest eigenvalue of $(I + B^T)(I + B)$, where B is a symmetric matrix, and q be the largest eigenvalue of $(A + A^T)$. Assume that $||I + B|| \leq 1$ and that the impulses satisfy the relation*

$$\tau_{2k+1} - \tau_{2k} \leq \epsilon(\tau_{2k} - \tau_{2k-1}),$$

where ϵ is some positive constant and $k = 1, 2, \ldots$. Then the impulsive synchronization of two Chua's oscillators, given by equation (2.18), is asymptotically stable if

$$0 \leq q + 2|\alpha a| \leq -\frac{1}{(1+\epsilon)\Delta_1} \ln(\xi d), \quad \xi > 1, \tag{2.20}$$

where

$$\Delta_1 = \sup_k \{\tau_{2k} - \tau_{2k-1}\} < \infty.$$

Comparing conditions (2.19) and (2.20), we see how applying time-varying impulses changes the type of conditions needed to achieve the asymptotic stability of system (2.18). It should be noted, however, that in the latter choice for the impulses, Δ_1 represents the supremum duration between two impulses which means that condition (2.20) does not require a smaller upper bound on the impulse duration permissible without affecting synchronization.

The whole theory of impulsive synchronization we have presented so far seeks one particular objective, namely, asymptotic stability of the error dynamics between the chaotic systems involved, although this scenario is not needed. We shall develop in the next section a new approach which leads to a weaker objective: equi-Lagrange stability that achieves our main goal; namely, synchronization.

2.2 Sufficient Conditions for Impulsive Synchronization

In this section, we shall apply Theorems 1.3.4 and 1.3.5 to an impulsive system and employ the results obtained for impulsive synchronization purposes. We begin by considering the following impulsive system.

$$\begin{cases} \dot{\mathbf{x}} &= A(t)\mathbf{x} + \mathbf{\Phi}(t,\mathbf{x}) + \mathbf{g}(\mathbf{u}(t)),\ t \neq \tau_k \\ \Delta\mathbf{x} &= B_k\mathbf{x},\ t = \tau_k,\ k = 1,2,\ldots, \end{cases} \tag{2.21}$$

where $A(t) = (a_{ij}(t))$ is an $n \times n$ continuous functional matrix, $\mathbf{\Phi}$ and $\mathbf{g}$ are continuous non-linear maps satisfying $||\mathbf{\Phi}(t,\mathbf{x})|| \leq L_1||\mathbf{x}||$ and $||\mathbf{g}(\mathbf{u}(t))|| \leq L_2||\mathbf{u}(t)||$, for some constants $L_1, L_2 > 0$, $\mathbf{u}(t)$ is an arbitrary bounded control function and B_k are $n \times n$ constant matrices, for all $k = 1,2,\ldots$.

Theorem 2.2.1 *Solutions to system (2.21) are uniformly bounded if the largest eigenvalue of $(I + B_k^T)(I + B_k)$, denoted by λ_k, satisfies*

$$\lambda_k \leq \exp(-2\alpha_k), \tag{2.22}$$

for all $k = 1,2,\ldots$ and if $||\mathbf{x}(\tau_k)||, ||\mathbf{x}(\tau_k) + B_k\mathbf{x}(\tau_k)|| > M$, for some $M \geq 0$, where $\alpha_k := (1/2)[\gamma_k + \ell_k\Delta_{k+1}] + \delta$, $\gamma_k \geq 0$ are constants and $\{\gamma_k\}_{k=1}^{\infty}$ has an upper bound, $0 < \delta \leq \inf_k(\gamma_k + \ell_k\Delta_{k+1})$, $\Delta_k = \tau_k - \tau_{k-1} > r > 0$, for all $k = 2,3,\ldots,$ and

$$\ell_k = \sup_{t\in(\tau_k,\tau_{k+1}]} p(t),$$

$$p(t) = \max_{t\in\mathbb{R}_+}\{f(t) + 2L_1, 2L_2||\mathbf{u}(t)||\}$$

and

$$f(t) = \max_{1\leq i\leq n}\left\{|q_{ii}(t)| + \frac{1}{2}\sum_{\substack{l=1\\ l\neq i}}^{n}|q_{il}(t)| + \frac{1}{2}\sum_{\substack{j=1\\ j\neq i}}^{n}|q_{ji}(t)|\right\},$$

where $q_{ij} := a_{ij} + a_{ji}$. Moreover, if $\gamma_k = 1/k$, for all $k = 1,2,\ldots$ and $\mathbf{g}(\mathbf{u}(t)) = \mathbf{0}$, then system (2.21) is uniformly Lagrange stable.

Proof: We shall first prove that system (2.21) is uniformly bounded by achieving the conditions of Theorem 1.3.4. Let $\mathcal{B} := \sup_k(\alpha_k)$, $M := (\exp(\mathcal{B}) - \exp(\delta))/(\exp(\delta) - 1) > 0$, and $V(t,\mathbf{x}) := V(\mathbf{x}) = \mathbf{x}^T\mathbf{x} = ||\mathbf{x}||^2$. Choose $b(||\mathbf{x}||) = a(||\mathbf{x}||) = ||\mathbf{x}||^2$. The upper right derivative of V is given by

$$D^+V(\mathbf{x}) = \mathbf{x}^TQ(t)\mathbf{x} + [\mathbf{x}^T\mathbf{\Phi}(t,\mathbf{x}) + \mathbf{\Phi}(t,\mathbf{x})^T\mathbf{x}] + [\mathbf{x}^T\mathbf{g}(\mathbf{u}(t)) + \mathbf{g}(\mathbf{u}(t))^T\mathbf{x}],$$

where $Q(t) = (q_{ij}(t)) := A(t)^T + A(t)$ is a symmetric matrix. Notice that

$$\begin{aligned}
\mathbf{x}^T Q(t)\mathbf{x} &= \sum_{i,j=1}^{n} q_{ij}(t)x_i x_j = \sum_{i=1}^{n} q_{ii}(t)x_i^2 + \sum_{i=1}^{n}\sum_{\substack{j=1\\ i\neq j}}^{n} q_{ij}(t)x_i x_j \\
&\leq \sum_{i=1}^{n} |q_{ii}(t)|x_i^2 + \sum_{i=1}^{n}\sum_{\substack{j=1\\ i\neq j}}^{n} |q_{ij}(t)||x_i x_j| \\
&\leq \sum_{i=1}^{n} |q_{ii}(t)|x_i^2 + \sum_{\substack{i,j=1\\ i\neq j}}^{n} \frac{|q_{ij}(t)|}{2}\left[x_i^2 + x_j^2\right] \\
&= \sum_{i=1}^{n}\left[|q_{ii}(t)| + \frac{1}{2}\sum_{\substack{j=1\\ j\neq i}}^{n}|q_{ij}(t)|\right]x_i^2 + \frac{1}{2}\sum_{j=1}^{n}\left[\sum_{\substack{i=1\\ i\neq j}}^{n}|q_{ij}(t)|\right]x_j^2 \\
&= \sum_{i=1}^{n}\left\{|q_{ii}(t)| + \frac{1}{2}\sum_{\substack{l=1\\ l\neq i}}^{n}|q_{il}(t)| + \frac{1}{2}\sum_{\substack{j=1\\ j\neq i}}^{n}|q_{ji}(t)|\right\}x_i^2 \\
&\leq \max_{1\leq i\leq n}\left\{|q_{ii}(t)| + \frac{1}{2}\sum_{\substack{l=1\\ l\neq i}}^{n}|q_{il}(t)| + \frac{1}{2}\sum_{\substack{j=1\\ j\neq i}}^{n}|q_{ji}(t)|\right\}\sum_{i=1}^{n} x_i^2 \\
&= f(t)\ \mathbf{x}^T\mathbf{x},
\end{aligned}$$

for all $t \geq 0$. Moreover, $\mathbf{x}^T\mathbf{\Phi}(t,\mathbf{x}) + \mathbf{\Phi}(t,\mathbf{x})^T\mathbf{x} \leq 2L_1\mathbf{x}^T\mathbf{x}$ and $\mathbf{g}(\mathbf{u}(t))^T\mathbf{x} + \mathbf{x}^T\mathbf{g}(\mathbf{u}(t)) \leq 2L_2||\mathbf{u}(t)||(\mathbf{x}^T\mathbf{x})^{1/2}$. This implies that

$$\begin{aligned}
D^+V(\mathbf{x}) &\leq f(t)\mathbf{x}^T\mathbf{x} + 2L_1\mathbf{x}^T\mathbf{x} + 2L_2||\mathbf{u}(t)||(\mathbf{x}^T\mathbf{x})^{1/2} \\
&= [f(t) + 2L_1]\,V(\mathbf{x}) + 2L_2||\mathbf{u}(t)||(V(\mathbf{x}))^{1/2} \\
&\leq \max_{t\in\mathbb{R}_+}\{f(t) + 2L_1, 2L_2||\mathbf{u}(t)||\}\left\{V(\mathbf{x}) + V(\mathbf{x})^{1/2}\right\} \\
&= p(t)c(V(\mathbf{x})),
\end{aligned}$$

where $c(s) := s + s^{1/2}$. Clearly $p \in \mathcal{PC}$ and $c \in \mathcal{K}$. Thus conditions (T1.1) and (T1.2) are satisfied over $\mathbb{R}_+ \times \mathbb{R}^n$. Now if $||\mathbf{x}(\tau_k)|| \leq M$, then, by inequality (2.22), we have

$$||\mathbf{x}(\tau_k) + B_k\mathbf{x}(\tau_k)|| \leq ||I + B_k||\ ||\mathbf{x}(\tau_k)|| \leq \exp(-\alpha_k)M < \exp(-\delta)M =: N,$$

for $k = 1, 2, \ldots$, and thus condition (T1.3) is also satisfied. Define the mapping $\Psi_k(s)$ as follows:

$$\Psi_k(s) := \exp(-2\alpha_k)s, \text{ for all } s \geq 0. \tag{2.23}$$

Clearly $\Psi_k(s) \leq s$, for all $s \geq 0$, and $\Psi_k(s) \geq (1/2)\exp(-2\mathcal{B})s =: \Psi(s)$, for all $s \geq 0$. i.e., $\Psi(s) \leq \Psi_k(s) \leq s$. Furthermore, by inequality (2.22), for $||\mathbf{x}(\tau_k) + B_k\mathbf{x}(\tau_k)|| > M$, we have, for $k = 1, 2, \ldots,$

$$\begin{aligned} V(\mathbf{x}(\tau_k) + B_k\mathbf{x}(\tau_k)) &= (\mathbf{x}(\tau_k) + B_k\mathbf{x}(\tau_k))^T(\mathbf{x}(\tau_k) + B_k\mathbf{x}(\tau_k)) \\ &= \mathbf{x}(\tau_k)^T(I + B_k^T)(I + B_k)\mathbf{x}(\tau_k) \\ &\leq \lambda_k\mathbf{x}(\tau_k)^T\mathbf{x}(\tau_k) \\ &\leq \exp(-2\alpha_k)||\mathbf{x}(\tau_k)||^2 \\ &= \Psi_k(V(\mathbf{x}(\tau_k))). \end{aligned}$$

This implies that condition (T1.4) is satisfied. In addition,

$$\int \frac{ds}{s + s^{1/2}} = 2\ln(1 + s^{1/2}). \tag{2.24}$$

It follows that, for $k = 1, 2, \ldots,$

$$\begin{aligned} \int_{\tau_k}^{\tau_{k+1}} p(s)ds + \int_{y}^{\Psi_k(y)} \frac{ds}{s + s^{1/2}} &= \ell_k\Delta_{k+1} + 2\ln\left[\frac{1 + \Psi_k^{1/2}(y)}{1 + y^{1/2}}\right] \\ &= \ell_k\Delta_{k+1} + 2\ln\left[\frac{1 + \exp(-\alpha_k)y^{1/2}}{1 + y^{1/2}}\right] \\ &= -\gamma_k - 2\delta + 2\ln\left[\frac{\exp(\alpha_k) + y^{1/2}}{1 + y^{1/2}}\right]. \end{aligned}$$

Notice that $\exp(\alpha_k) \leq \exp(\mathcal{B})$ and the function

$$h(y) := \ln\left[\frac{\exp(\mathcal{B}) + y^{1/2}}{1 + y^{1/2}}\right]$$

is a decreasing function of y, for all $y \geq 0$. This implies, for $y > \lambda := M^2$, that

$$\begin{aligned} \int_{\tau_k}^{\tau_{k+1}} p(s)ds + \int_{y}^{\Psi_k(y)} \frac{ds}{s + s^{1/2}} &\leq -\gamma_k - 2\delta + 2h(M^2) \\ &= -\gamma_k - 2\delta + 2\ln\left[\frac{\exp(\delta)(\exp(\mathcal{B}) - 1)}{\exp(\mathcal{B}) - 1}\right] \\ &= -\gamma_k - 2\delta + 2\delta = -\gamma_k, \end{aligned}$$

for every $y \geq \lambda := M^2$. Thus condition (T1.5) is satisfied. We therefore conclude that system (2.21) is uniformly bounded as desired. It remains to show, with the choices of $\gamma_k = 1/k$, for all

$k = 1, 2 \ldots$, and $\mathbf{g}(\mathbf{u}(t)) = \mathbf{0}$, that system (2.21) is uniformly Lagrange stable. This is done by applying Theorem 1.3.5 as follows. The upper right derivative of $V(\mathbf{x})$, in this case, satisfies

$$\begin{aligned} D^+V(\mathbf{x}) &\leq [f(t) + 2L_1]||\mathbf{x}||^2 \\ &= \widetilde{p}(t)\widetilde{c}(V(\mathbf{x})), \end{aligned}$$

where $\widetilde{p}(t) := f(t)+2L_1$ and $\widetilde{c}(s) := s$. Thus, by employing the mapping $\Psi_k(s)$, defined by (2.23), for all $k = 1, 2, \ldots$, we conclude that conditions (T2.1), (T2.2), (T2.3) and (T2.4) are all satisfied. Moreover, for $k = 1, 2, \ldots$,

$$\int_{\tau_k}^{\tau_{k+1}} \widetilde{p}(s)ds + \int_{y}^{\Psi_k(y)} \frac{ds}{\widetilde{c}(s)} \leq \ell_k \Delta_{k+1} + \ln\Big[\frac{\Psi_k(y)}{y}\Big] < -\gamma_k,$$

for all $y > 0$. Therefore condition (T2.5) is also satisfied. This implies, by Theorem 1.3.5, that system (2.21) is uniformly Lagrange stable. □

It should be mentioned that, in the proof of Theorem 2.2.1, we may conclude that the smaller the $||\mathbf{g}(\mathbf{u}(t))||$, the smaller the upper bound on $||\mathbf{x}(t)||$, for all $t \geq t_0 + T$, for some $T > 0$. This is due to the fact that when $||\mathbf{g}(\mathbf{u}(t))|| = \mathcal{O}(\epsilon)$, for some $0 < \epsilon << 1$, then $c(s) = s + \epsilon s^{1/2}$, i.e., $s^{1/2}$ becomes significantly smaller than s. This implies that inequality (1.25) will enforce a very small upper bound on the solutions of (2.21) starting from time $t_0 + T$.

We now demonstrate how equi-Lagrange stability is an integral factor in illustrating the robustness of impulsive synchronization between two non-identical chaotic systems by formulating the following example.

Consider the driving system given by this Lorenz chaotic system

$$\dot{\mathbf{x}} = \begin{pmatrix} -\sigma & \sigma & 0 \\ r & -1 & 0 \\ 0 & 0 & -b \end{pmatrix} \mathbf{x} + \begin{pmatrix} 0 \\ -xz \\ 0 \end{pmatrix} + \begin{pmatrix} 0 \\ 0 \\ xy \end{pmatrix}. \tag{2.25}$$

The response system is a non-identical Lorenz chaotic system which is driven by the signal $-xz$ and is given by

$$\begin{cases} \dot{\mathbf{u}} = \begin{pmatrix} -\sigma & \sigma & 0 \\ r & -1 & 0 \\ 0 & 0 & -b \end{pmatrix} \mathbf{u} + \begin{pmatrix} 0 \\ -xz \\ 0 \end{pmatrix} + \begin{pmatrix} -\mu u \\ -\nu v \\ uv \end{pmatrix}, \quad t \neq \tau_k \\ \Delta\mathbf{u} = -B_k\mathbf{e}, \quad t = \tau_k, \ \forall\ k = 1, 2, \ldots, \end{cases} \tag{2.26}$$

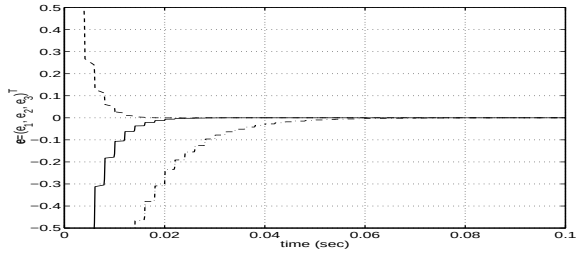

Figure 2.3: Error dynamics $\mathbf{e}$ with $\mu = \nu = 0$ and $B_k = -\text{diag}(0.02, 0.06, 0.01)$.

where $\mu, \nu \geq 0$ are constants and $\mathbf{e} = \mathbf{x} - \mathbf{u}$. It follows, by systems (2.25) and (2.26) that the error dynamics is give by

$$\begin{cases} \dot{\mathbf{e}} = \begin{pmatrix} -\sigma & \sigma & 0 \\ r & -1 & 0 \\ 0 & 0 & -b \end{pmatrix} \mathbf{e} + \begin{pmatrix} 0 \\ 0 \\ xy - uv \end{pmatrix} + \begin{pmatrix} \mu u \\ \nu v \\ 0 \end{pmatrix}, \quad t \neq \tau_k \\ \Delta \mathbf{e} = B_k \mathbf{e}, \quad t = \tau_k, \ \forall\, k = 1, 2, \ldots. \end{cases} \tag{2.27}$$

Letting

$$A = \begin{pmatrix} -\sigma & \sigma & 0 \\ r & -1 & 0 \\ 0 & 0 & -b \end{pmatrix} \tag{2.28}$$

and taking $V(\mathbf{e}) := \mathbf{e}^T \mathbf{e}$, we obtain

$$D^+ V(\mathbf{e}) \quad = \quad \mathbf{e}^T Q \mathbf{e} + 2(xy - uv)e_3 + [(\mu u, \nu v, 0)\mathbf{e} + \mathbf{e}^T (\mu u, \nu v, 0)^T],$$

where $Q := A^T + A$. Let d be the largest eigenvalue of Q and $L = \max(\mu, \nu)$. Notice that

$$\begin{aligned} 2(xy - uv)e_3 &\leq 2|xy - uv||e_3| \\ &\leq 2[|x||y - v| + |v||x - u|]|e_3| \\ &\leq 2|x||e_2 e_3| + 2|v||e_1 e_3| + e_3^2 \\ &\leq |x|(e_2^2 + e_3^2) + |v|(e_1^2 + e_3^2) + e_3^2 \\ &\leq (|x| + |v| + 1)||\mathbf{e}||^2. \end{aligned}$$

Thus

$$\begin{aligned} D^+ V(\mathbf{e}) &\leq (d + |x| + |v| + 1)\mathbf{e}^T \mathbf{e} + 2L\sqrt{u^2 + v^2}\ (\mathbf{e}^T \mathbf{e})^{1/2} \\ &\leq \max_{t \in \mathbb{R}_+} \left\{ (d + |x| + |v| + 1), 2L\sqrt{u(t)^2 + v(t)^2} \right\} [V(\mathbf{e}) + V(\mathbf{e})^{1/2}]. \end{aligned}$$

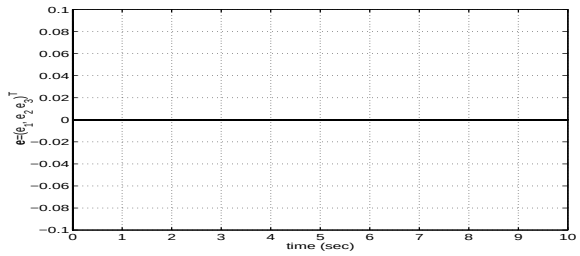

Figure 2.4: Error dynamics $\mathbf{e}$ with $\mu = \nu = 0.01$ and $B_k = -\text{diag}(0.5, 0.33, 0.2)$.

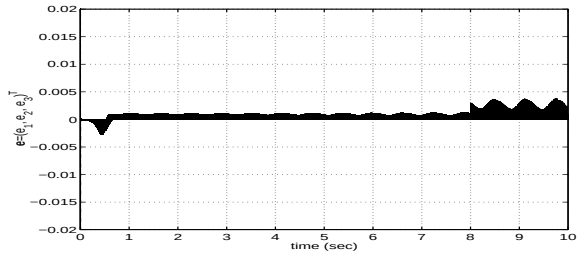

Figure 2.5: Error dynamics $\mathbf{e}$ with $\mu = \nu = 1$ and $B_k = -\text{diag}(0.5, 0.6, 0.2)$.

Let $p(t) = \max_{t\in\mathbb{R}_+}\left\{(d + |x| + |v| + 1), 2\sqrt{u(t)^2 + v(t)^2}\right\}$ and $c(s) = s + s^{1/2}$. We may conclude, by imposing the conditions of Theorem 2.2.1 on the matrices B_k, for all $k = 1, 2, \ldots$, that the error dynamics, described by system (2.27), is uniformly bounded. Furthermore, choosing $\gamma_k = 1/k$, for all $k = 1, 2, \ldots$, and letting $\mu = \nu = 0$, we can also conclude that system (2.27) is uniformly Lagrange stable. Note that if μ and ν are chosen such that $0 \leq \mu, \nu << 1$, then impulsive synchronization shows very robust results as illustrated in the following examples. In these numerical examples, a fourth order Runge-Kutta method with step size 10^{-5} is used.

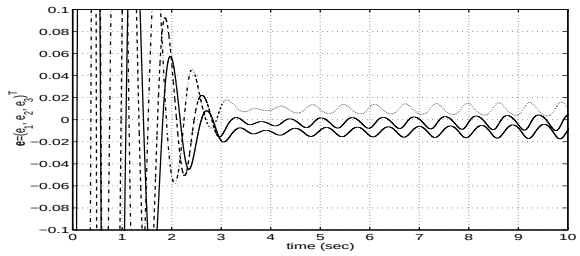

Figure 2.6: Error dynamics $\mathbf{e}$ with $\mu = \nu = 0.01$ by implementing the continuous driving method proposed in [22–24].

Moreover, we choose the values of the parameters and the initial conditions to be $\sigma = 10$, $r = 28$, $b = 8/3$, $\Delta_k = \Delta = 0.002$, $(x_0, y_0, z_0) = (1.12, -1, 0.5)$ and $(u_0, v_0, w_0) = (2.7, -2.1, 2.502)$. Thus starting with the first and simplest case when $\mu = \nu = 0$ and $B_k = B = -\text{diag}(0.02, 0.06, 0.01)$, we obtain Figure 2.3 which shows how the error dynamics components reach zero in a small finite time given by 0.1 (for the remaining of this section, the first component of the error dynamics is represented by a solid curve, the second component is represented by a dashed curve and the third component is represented by a dashed-dotted curve). In the second example, we take $\mu = \nu = 0.01$ and $B_k = B = -\text{diag}(0.5, 0.33, 0.2)$. The impulsive synchronization, in this case, is achieved as shown in Figure 2.4. We can see from the above examples that impulsive synchronization exhibits a very robust behaviour towards parameter mismatch. In fact, with relatively large differences in parameters, the performance of this model is still acceptable. For example, in the case when $\mu = \nu = 1$, the simulation of this model is shown in Figure 2.5, where the error is of the order of 0.003 starting from the time $t = 8$ seconds (it is even smaller for time $t < 8$ seconds). This promising behaviour indicates that in practice, the condition $\mu, \nu << 1$ can be relaxed and still reach desirable results. In comparison with the method of continuous driving, discussed in the previous section and proposed by Cuomo and Oppenheim in [22–24], this robust behaviour fails completely as shown clearly in Figure 2.6, where the error is of the order of 0.02 for $\mu = \nu = 0.01$.

We shall now extend the above work and Theorem 2.21 to study the dynamics of another type of impulsive systems. This new type will have a very important role in building a chaos-based secure-communication scheme which will be proposed in Chapter 5.

Let us consider the following second order impulsive system which depends on $\widetilde{\mathbf{x}}$ and $\dot{\widetilde{\mathbf{x}}}$, simultaneously:

$$\begin{cases} \ddot{\widetilde{\mathbf{x}}} &= \widetilde{A}\dot{\widetilde{\mathbf{x}}} + \widetilde{\mathbf{\Phi}}(t, \widetilde{\mathbf{x}}, \dot{\widetilde{\mathbf{x}}}) + \widetilde{\mathbf{g}}(\dot{\widetilde{\mathbf{x}}}, \mathbf{u}(t)),\ t \neq \tau_k \\ \Delta\widetilde{\mathbf{x}} &= D_k\widetilde{\mathbf{x}},\ t = \tau_k,\ \ k = 1, 2, \ldots \\ \Delta\dot{\widetilde{\mathbf{x}}} &= \widetilde{D}_k\dot{\widetilde{\mathbf{x}}},\ t = \tau_k,\ \ k = 1, 2, \ldots, \end{cases} \tag{2.29}$$

where $\widetilde{A}$ is an $n \times n$ constant matrix, $\widetilde{\mathbf{\Phi}}$ and $\widetilde{\mathbf{g}}$ are continuous non-linear maps satisfying

$$\dot{\widetilde{\mathbf{x}}}^T\widetilde{\mathbf{\Phi}}(t, \widetilde{\mathbf{x}}, \dot{\widetilde{\mathbf{x}}}) \leq L_1\left[||\widetilde{\mathbf{x}}||^2 + ||\dot{\widetilde{\mathbf{x}}}||^2\right]$$

and $||\widetilde{\mathbf{g}}(\dot{\widetilde{\mathbf{x}}}, \mathbf{u}(t))|| \leq L_2||\dot{\widetilde{\mathbf{x}}}|| + L_3$, for some constant $L_2 > 0$ and $L_3 \geq 0$, $\mathbf{u}(t)$ is an arbitrary control function satisfying $||\mathbf{u}(t)|| \leq K$, for some $K \geq 0$, and D_k and $\widetilde{D}_k$ are $n \times n$ constant matrices, for all $k = 1, 2, \ldots$. Set $\mathbf{x}_1 = \widetilde{\mathbf{x}}$, $\mathbf{x}_2 = \dot{\widetilde{\mathbf{x}}}$, and let $\mathbf{x} = (\mathbf{x}_1, \mathbf{x}_2)^T$,

$$A := \begin{pmatrix} 0 & I \\ 0 & \widetilde{A} \end{pmatrix},\ B_k := \begin{pmatrix} D_k & 0 \\ 0 & \widetilde{D}_k \end{pmatrix}$$

be block matrices, where I is the identity matrix,

$$\mathbf{\Phi}(t,\mathbf{x}) := \begin{pmatrix} 0 \\ \widetilde{\mathbf{\Phi}}(t,\mathbf{x}) \end{pmatrix} \text{ and } \mathbf{g}(\mathbf{x},\mathbf{u}(t)) := \begin{pmatrix} 0 \\ \widetilde{\mathbf{g}}(\mathbf{x}_2,\mathbf{u}(t)) \end{pmatrix}.$$

Then system (2.29) becomes

$$\begin{cases} \dot{\mathbf{x}} &= A\mathbf{x} + \mathbf{\Phi}(t,\mathbf{x}) + \mathbf{g}(\mathbf{x},\mathbf{u}(t)),\ t \neq \tau_k \\ \Delta\mathbf{x} &= B_k\mathbf{x},\ t = \tau_k,\ k = 1,2,\ldots. \end{cases} \tag{2.30}$$

We shall investigate the equi-boundedness and equi-Lagrange stability of solutions of system (2.29) using system (2.30).

Theorem 2.2.2 *System (2.30) is uniformly bounded if the largest eigenvalue of* $(I+B_k^T)(I+B_k)$, *denoted by* λ_k, *satisfies*

$$\lambda_k \leq \exp(-2\alpha_k), \tag{2.31}$$

for all $k = 1,2,\ldots$ *and if* $||\mathbf{x}(\tau_k)||, ||\mathbf{x}(\tau_k) + B_k\mathbf{x}(\tau_k)|| > M$, *for some* $M \geq 0$, *where* $\alpha_k := (1/2)[\gamma_k + \ell\Delta_{k+1}] + \delta$, $\gamma_k \geq 0$ *are constants and* $\{\gamma_k\}_{k=1}^{\infty}$ *has an upper bound,* $0 < \delta << \inf_k(\gamma_k + \ell\Delta_{k+1})$, $\Delta_k := \tau_k - \tau_{k-1} > r > 0$, *for all* $k = 2,3,\ldots,$ *and*

$$\ell := |d| + 2L_1 + 2L_2 + 2L_3,$$

where d *is the largest eigenvalue of* $Q := A + A^T$. *Moreover, if* $\gamma_k = 1/k$, *for all* $k = 1,2,\ldots,$ *and* $L_3 = 0$, *then system (2.30) is uniformly Lagrange stable.*

Proof: To prove equi-boundedness property, we shall check all the conditions stated in Theorem 1.3.4. Let $\mathcal{B} := \sup_k(\alpha_k)$, $M := (\exp(\mathcal{B}) - \exp(\delta))/(\exp(\delta) - 1) > 0$ and $V(t,\mathbf{x}) := V(\mathbf{x}) = \mathbf{x}^T\mathbf{x} = ||\mathbf{x}||^2$. Choose $b(||\mathbf{x}||) = a(||\mathbf{x}||) = ||\mathbf{x}||^2$. The upper right derivative of V is given by

$$\begin{aligned} D^+V(\mathbf{x}) &= \dot{\mathbf{x}}^T\mathbf{x} + \mathbf{x}^T\dot{\mathbf{x}} \\ &= \mathbf{x}^TQ\mathbf{x} + 2\mathbf{\Phi}(t,\mathbf{x})^T\mathbf{x} + 2\mathbf{g}(\mathbf{x},\mathbf{u}(t))^T\mathbf{x} \\ &\leq d||\mathbf{x}||^2 + 2L_1||\mathbf{x}||^2 + 2L_2||\mathbf{x}||^2 + 2L_3||\mathbf{x}|| \\ &= (d + 2L_1 + 2L_2)||\mathbf{x}||^2 + 2L_3||\mathbf{x}|| \\ &\leq (|d| + 2L_1 + 2L_2 + 2L_3)(V(\mathbf{x}) + V(\mathbf{x})^{1/2}) \\ &= p(t)c(V(\mathbf{x})), \end{aligned} \tag{2.32}$$

where $p(t) := |d| + 2L_1 + 2L_2 + 2L_3$ and $c(s) := s + s^{1/2}$. Clearly $p \in \mathcal{PC}$ and $c \in \mathcal{K}$. Thus conditions (T1.1) and (T1.2) are satisfied over $\mathbb{R}_+ \times \mathbb{R}^n$. If $||\mathbf{x}(\tau_k)|| \leq M$, $k = 1,2,\ldots,$ then, by

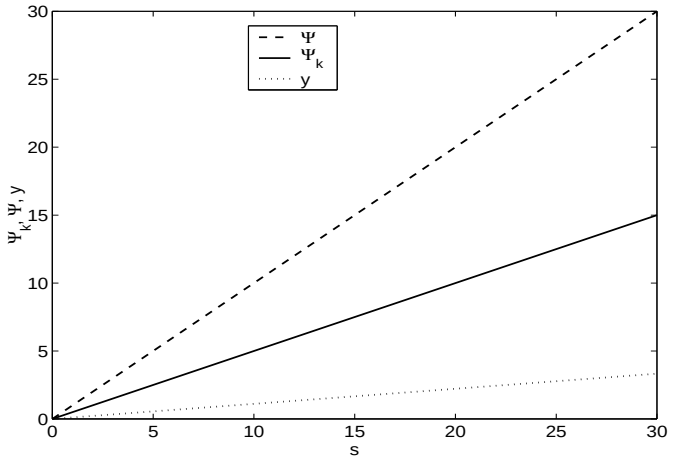

Figure 2.7: Typical sketch of the mapping $\Psi_k(s)$.

inequality (2.31), we have

$$||\mathbf{x}(\tau_k) + B_k\mathbf{x}(\tau_k)|| \leq ||I + B_k||\ ||\mathbf{x}(\tau_k)|| \leq \exp(-\alpha_k)M < \exp(-\delta)M := N,$$

for $k = 1, 2, \ldots$, and thus condition (T1.3) is also satisfied. Define the mapping $\Psi_k(s)$, for all $k = 1, 2, \ldots$, as follows:

$$\Psi_k(s) := \exp(-2\alpha_k)s, \text{ for all } s \geq 0. \tag{2.33}$$

Clearly $\Psi_k(s) \leq s$, for all $s \geq 0$, and $\Psi_k(s) \geq (1/2)\exp(-2\mathcal{B})s =: \Psi(s)$, for all $s \geq 0$. i.e., $\Psi(s) \leq \Psi_k(s) \leq s$. Figure 2.7 shows a typical sketch of the mapping $\Psi_k(s)$ lying between the two lines y $= s$ and $\Psi(s)$. Furthermore, by inequality (2.31), for $||\mathbf{x}(\tau_k) + B_k\mathbf{x}(\tau_k)|| > M$, for $k = 1, 2, \ldots$, we have

$$\begin{aligned} V(\mathbf{x}(\tau_k) + B_k\mathbf{x}(\tau_k)) &= (\mathbf{x}(\tau_k) + B_k\mathbf{x}(\tau_k))^T(\mathbf{x}(\tau_k) + B_k\mathbf{x}(\tau_k)) \\ &= \mathbf{x}(\tau_k)^T(I + B_k^T)(I + B_k)\mathbf{x}(\tau_k) \\ &\leq \lambda_k\mathbf{x}(\tau_k)^T\mathbf{x}(\tau_k) \\ &\leq \exp(-2\alpha_k)||\mathbf{x}(\tau_k)||^2 \\ &= \Psi_k(V(\mathbf{x}(\tau_k))). \end{aligned}$$

This implies that condition (T1.4) is satisfied. In addition, by equation (2.24), we have for $k = 1, 2, \ldots,$

$$\begin{aligned}\int_{\tau_k}^{\tau_{k+1}} p(s)ds + \int_{y}^{\Psi_k(y)} \frac{ds}{s + s^{1/2}} &= \ell\Delta_{k+1} + 2\ln\left[\frac{1 + \Psi_k^{1/2}(y)}{1 + y^{1/2}}\right] \\ &= \ell\Delta_{k+1} + 2\ln\left[\frac{1 + \exp(-\alpha_k)y^{1/2}}{1 + y^{1/2}}\right] \\ &= -\gamma_k - 2\delta + 2\ln\left[\frac{\exp(\alpha_k) + y^{1/2}}{1 + y^{1/2}}\right].\end{aligned}$$

Notice that $\exp(\alpha_k) \leq \exp(\mathcal{B})$, for all $k = 1, 2, \ldots,$ and the function

$$h(y) := \ln\left[\frac{\exp(\mathcal{B}) + y^{1/2}}{1 + y^{1/2}}\right]$$

is a decreasing function of y, for all $y \geq 0$. This implies, for $y \geq \lambda := M^2$ and $k = 1, 2, \ldots,$ that

$$\begin{aligned}\int_{\tau_k}^{\tau_{k+1}} p(s)ds + \int_{y}^{\Psi_k(y)} \frac{ds}{s + s^{1/2}} &\leq -\gamma_k - 2\delta + 2h(M^2) \\ &= -\gamma_k - 2\delta + 2\ln\left[\frac{\exp(\delta)(\exp(\mathcal{B}) - 1)}{\exp(\mathcal{B}) - 1}\right] \\ &= -\gamma_k - 2\delta + 2\delta = -\gamma_k\end{aligned}$$

Thus condition (T1.5) is satisfied. We therefore conclude that the system (2.30) is uniformly bounded as desired. It remains to show, with the choice of $\gamma_k = 1/k$, for all $k = 1, 2, \ldots,$ and $L_3 = 0$, that system (2.30) is uniformly Lagrange stable. This is done by applying Theorem 1.3.5 as follows. We first consider the upper right derivative of $V(\mathbf{x})$

$$\begin{aligned}D^+V(\mathbf{x}) &\leq (|d| + 2L_1 + 2L_2)||\mathbf{x}||^2 \\ &= \widetilde{p}(t)\widetilde{c}(V(\mathbf{x})),\end{aligned}$$

where $\widetilde{p}(t) := |d| + 2L_1 + 2L_2$ and $\widetilde{c}(s) := s$. Thus, by employing the mapping Ψ_k, defined by (2.33), for all $k = 1, 2, \ldots,$ we conclude that conditions (T2.1), (T2.2), (T2.3) and (T2.4) are all satisfied. Moreover, for $k = 1, 2, \ldots,$

$$\int_{\tau_k}^{\tau_{k+1}} \widetilde{p}(s)ds + \int_{y}^{\Psi_k(y)} \frac{ds}{\widetilde{c}(s)} \leq \ell\Delta_{k+1} + \ln\left[\frac{\Psi_k(y)}{y}\right] < -\gamma_k,$$

for all $y > 0$. Therefore condition (T2.5) is also satisfied, since $\sum_{k=1}^{\infty}(1/k) = \infty$. This means that, by Theorem 1.3.5, solutions to system (2.30) are uniformly Lagrange stable, as required. □

If we return now to system (2.29), Theorem 2.2.2 implies that $\lim_{t\to\infty} \widetilde{\mathbf{x}}(t) = \lim_{t\to\infty} \dot{\widetilde{\mathbf{x}}}(t) = \mathbf{0}$. In other words, if the conditions of Theorem 2.2.2 are satisfied, then the solutions to system (2.29) are uniformly Lagrange stable. This important result will be applied considerably in the discussion of Chapter 5. For now, we shall illustrate the above Theorem by considering an example consisting of one pair of Lorenz chaotic systems and one pair of their derivatives. The uniform Lagrange stability of the two error dynamics associated with those two pairs will be discussed and established by employing Theorem 2.2.2.

Once more, we consider the Lorenz system as our driving system in the equation $\dot{\mathbf{x}} = \mathbf{f}(\mathbf{x}, m(t), a)$, i.e.,

$$\dot{\mathbf{x}} = A\mathbf{x} + \begin{pmatrix} 0 \\ -x(z + am(t)) \\ xy \end{pmatrix}, \tag{2.34}$$

where A is given by (2.28), $m(t) \in C^1([0,\infty))$ satisfies $|m(t)| \le K_1$ and $|\dot{m}(t)| \le K_2$, for some $K_1, K_2 > 0$, and $a = 0$ or 1. The second driving system is the derivative of the Lorenz chaotic system given by (2.34), for $a = 1$, and is expressed by

$$\ddot{\mathbf{x}} = A\dot{\mathbf{x}} + \begin{pmatrix} 0 \\ -\dot{x}z - x\dot{z} \\ \dot{x}y + x\dot{y} \end{pmatrix} + \begin{pmatrix} 0 \\ -\dot{x}m(t) - x\dot{m}(t) \\ 0 \end{pmatrix}. \tag{2.35}$$

Let the first response Lorenz chaotic system be

$$\begin{cases} \dot{\mathbf{u}} &= A\mathbf{u} + \begin{pmatrix} 0 \\ -uw \\ uv \end{pmatrix},\ t \neq \tau_k \\ \Delta\mathbf{u} &= -B_k\mathbf{e},\ t = \tau_k,\ k = 1, 2, \ldots, \end{cases} \tag{2.36}$$

where B_k are $n \times n$ constant matrices, for all $k = 1, 2, \ldots$, and $\mathbf{e} = \mathbf{x} - \mathbf{u}$ with $a = 0$. The second response system is the derivative of the first response system, and is given by

$$\begin{cases} \ddot{\overline{\mathbf{u}}} &= A\dot{\overline{\mathbf{u}}} + \begin{pmatrix} 0 \\ -\dot{\overline{u}}w - u\dot{\overline{w}} \\ \dot{\overline{u}}v + u\dot{\overline{v}} \end{pmatrix} + q\begin{pmatrix} 0 \\ -\dot{\overline{u}}m(t) - u\dot{m}(t) \\ 0 \end{pmatrix},\ t \neq \tau_k \\ \Delta\dot{\overline{\mathbf{u}}} &= -B_k\dot{\overline{\mathbf{e}}},\ t = \tau_k,\ k = 1, 2, \ldots, \end{cases} \tag{2.37}$$

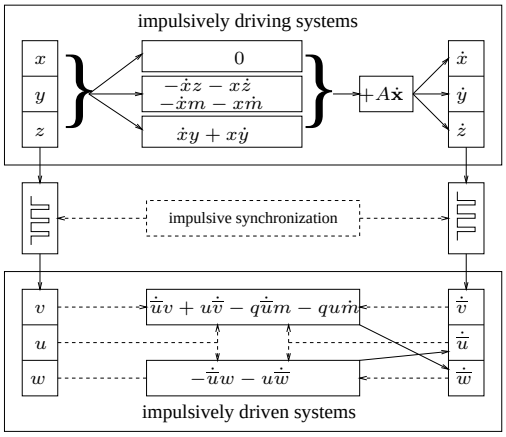

Figure 2.8: Impulsive synchronization of two Lorenz chaotic systems.

where $q = 0$ or 1, $\dot{\mathbf{e}} = \dot{\mathbf{x}} - \dot{\bar{\mathbf{u}}}$, x, y, z, u, v and w are the chaotic signals. The above set up shown in Figure 2.8 can be described as follows. x, y and z, produced by the Lorenz chaotic system (2.34), with $a = 1$, are used to completely generate the derivative system (2.35). System (2.36), however, is driven impulsively by system (2.34), with $a = 0$, while system (2.37) is driven impulsively by system (2.35), and continuously by the chaotic signals u, v and w from system (2.36).

With equations (2.34)-(2.37), the error dynamics $\mathbf{e}$, for $a = 0$, and $\dot{\mathbf{e}}$ can be expressed as follows:

$$\begin{cases} \dot{\mathbf{e}} &= A\mathbf{e} + \begin{pmatrix} 0 \\ -xz + uw \\ xy - uv \end{pmatrix}, \ t \neq \tau_k \\ \Delta\mathbf{e} &= B_k\mathbf{e}, \ t = \tau_k, \ k = 1, 2, \ldots \end{cases} \tag{2.38}$$

and

$$\begin{cases} \ddot{\mathbf{e}} = A\dot{\mathbf{e}} + \begin{pmatrix} 0 \\ -\dot{x}z + \dot{\bar{u}}w - x\dot{z} + u\dot{\bar{w}} \\ \dot{x}y - \dot{\bar{u}}v + x\dot{y} - u\dot{\bar{v}} \end{pmatrix} - \begin{pmatrix} 0 \\ (\dot{x} - q\dot{\bar{u}})m + (x - qu)\dot{m} \\ 0 \end{pmatrix}, \ t \neq \tau_k \\ \Delta\dot{\mathbf{e}} = B_k\dot{\mathbf{e}}, \ t = \tau_k, \ k = 1, 2, \ldots. \end{cases} \tag{2.39}$$

Notice that the error dynamics $\mathbf{e}$, given by system (2.38) is uniformly Lagrange stable provided that the matrices B_k, for all $k = 1, 2, \ldots$, are chosen to satisfy the conditions of Theorem 2.2.2, where $\mathbf{g}(\mathbf{x}, \mathbf{u}(t)) = \mathbf{0}$, i.e., $\lim_{t\to\infty} \mathbf{e}(t) = \mathbf{0}$. We have already shown in Figure 2.3 how the error

dynamics $\mathbf{e}$ in terms of its three components e_1, e_2 and e_3 converge to zero. It was also shown that this method of synchronization is robust towards parameter mismatch.

We shall now prove that system $\dot{\widetilde{\mathbf{e}}}$ is uniformly Lagrange stable, which is to prove that system (2.39) satisfies all the conditions described by Theorem 2.2.2. Let $\widetilde{\mathbf{e}} = (\mathbf{e}, \dot{\overline{\mathbf{e}}})^T$ and choose $V(\widetilde{\mathbf{e}}) := \widetilde{\mathbf{e}}^T\widetilde{\mathbf{e}}$, then

$$\begin{aligned}
D^+V(\widetilde{\mathbf{e}}) &= \dot{\widetilde{\mathbf{e}}}^T\widetilde{\mathbf{e}} + \widetilde{\mathbf{e}}^T\dot{\widetilde{\mathbf{e}}} \\
&= (\dot{\mathbf{e}}^T, \ddot{\overline{\mathbf{e}}}^T)(\mathbf{e}, \dot{\overline{\mathbf{e}}})^T + (\mathbf{e}^T, \dot{\overline{\mathbf{e}}}^T)(\dot{\mathbf{e}}, \ddot{\overline{\mathbf{e}}})^T \\
&= \dot{\mathbf{e}}^T\mathbf{e} + \ddot{\overline{\mathbf{e}}}^T\dot{\overline{\mathbf{e}}} + \mathbf{e}^T\dot{\mathbf{e}} + \dot{\overline{\mathbf{e}}}^T\ddot{\overline{\mathbf{e}}} \\
&\leq 2L||\mathbf{e}||^2 + \dot{\overline{\mathbf{e}}}^T(A^T + A)\dot{\overline{\mathbf{e}}} - 2[(\dot{x}z - \dot{\overline{u}}w) + (x\dot{z} - u\dot{\overline{w}})]\dot{\overline{e}}_2 + \\
&\quad 2[(\dot{x}y - \dot{\overline{u}}v) + (x\dot{y} - u\dot{\overline{v}})]\dot{\overline{e}}_3 - 2[(\dot{x} - q\dot{\overline{u}})m + (x - qu)\dot{m}]\dot{\overline{e}}_2,
\end{aligned}$$

where $\dot{\mathbf{e}}^T\mathbf{e} \leq L||\mathbf{e}||^2$, for some $L > 0$, which follows from system (2.38). Note that $\dot{\overline{\mathbf{e}}}^T(A^T + A)\dot{\overline{\mathbf{e}}} \leq d\,\dot{\overline{\mathbf{e}}}^T\dot{\overline{\mathbf{e}}}$, where d is the largest eigenvalue of $A^T + A$,

$$\begin{aligned}
[(\dot{x}z - \dot{\overline{u}}w) + (x\dot{z} - u\dot{\overline{w}})]\dot{\overline{e}}_2 &\leq |(\dot{x}z - \dot{\overline{u}}w) + (x\dot{z} - u\dot{\overline{w}})||\dot{\overline{e}}|_2 \\
&= |\dot{x}(z - w) + w(\dot{x} - \dot{\overline{u}}) + x(\dot{z} - \dot{\overline{w}}) + \dot{\overline{w}}(x - u)|\ |\dot{\overline{e}}_2| \\
&= |\dot{x}e_3 + w\dot{\overline{e}}_1 + x\dot{\overline{e}}_3 + \dot{\overline{w}}e_1|\ |\dot{\overline{e}}_2| \\
&\leq |\dot{x}|\ |e_3\dot{\overline{e}}_2| + |w|\ |\dot{\overline{e}}_1\dot{\overline{e}}_2| + |x|\ |\dot{\overline{e}}_3\dot{\overline{e}}_2| + |\dot{\overline{w}}|\ |e_1\dot{\overline{e}}_2| \\
&\leq |\dot{x}|\ ||\mathbf{e}||\ ||\dot{\overline{\mathbf{e}}}|| + \frac{1}{2}|w|\ ||\dot{\overline{\mathbf{e}}}||^2 + \frac{1}{2}|x|\ ||\dot{\overline{\mathbf{e}}}||^2 + |\dot{\overline{w}}|\ ||\mathbf{e}||\ ||\dot{\overline{\mathbf{e}}}|| \\
&\leq \frac{1}{2}(|\dot{x}| + |w| + |x| + |\dot{\overline{w}}|)||\widetilde{\mathbf{e}}||^2,
\end{aligned}$$

$$\begin{aligned}
[(\dot{x}y - \dot{\overline{u}}v) + (x\dot{y} - u\dot{\overline{v}})]\dot{\overline{e}}_3 &\leq |(\dot{x}y - \dot{\overline{u}}v) + (x\dot{y} - u\dot{\overline{v}})|\ |\dot{\overline{e}}_3| \\
&= |\dot{x}(y - v) + v(\dot{x} - \dot{\overline{u}}) + x(\dot{y} - \dot{\overline{v}}) + \dot{\overline{v}}(x - u)|\ |\dot{\overline{e}}_3| \\
&= |\dot{x}e_2 + v\dot{\overline{e}}_1 + x\dot{\overline{e}}_2 + \dot{\overline{v}}e_1|\ |\dot{\overline{e}}_3| \\
&\leq |\dot{x}|\ |e_2\dot{\overline{e}}_3| + |v|\ |\dot{\overline{e}}_1\dot{\overline{e}}_3| + |x|\ |\dot{\overline{e}}_2\dot{\overline{e}}_3| + |\dot{\overline{v}}|\ |e_1\dot{\overline{e}}_3| \\
&\leq |\dot{x}|\ ||\mathbf{e}||\ ||\dot{\overline{\mathbf{e}}}|| + \frac{1}{2}|v|\ ||\dot{\overline{\mathbf{e}}}||^2 + \frac{1}{2}|x|\ ||\dot{\overline{\mathbf{e}}}||^2 + |\dot{\overline{v}}|\ ||\mathbf{e}||\ ||\dot{\overline{\mathbf{e}}}|| \\
&\leq \frac{1}{2}(|\dot{x}| + |v| + |x| + |\dot{\overline{v}}|)||\widetilde{\mathbf{e}}||^2
\end{aligned}$$

and

$$\begin{aligned}
[(\dot{x} - q\dot{\overline{u}})m + (x - qu)\dot{m}]\dot{\overline{e}}_2 &\leq |(\dot{x} - q\dot{\overline{u}})m + (x - qu)\dot{m}||\dot{\overline{\mathbf{e}}}|| \\
&\leq \Big[K_1|\dot{x} - q\dot{\overline{u}}| + K_2|x - qu|\Big]||\widetilde{\mathbf{e}}||.
\end{aligned}$$

Thus we may conclude that

$$\begin{aligned} D^+V(\widetilde{\mathbf{e}}) &\leq \Big[2L + d + 2|x| + 2|\dot{x}| + |v| + |w| + |\dot{\overline{v}}| + |\dot{\overline{w}}|\Big]||\widetilde{\mathbf{e}}||^2 + \\ &\quad \Big[2K_1|\dot{x} - q\dot{\overline{u}}| + 2K_2|x - qu|\Big]||\widetilde{\mathbf{e}}|| \\ &\leq \Big\{2L + d + 2|x| + 2|\dot{x}| + |v| + |w| + |\dot{\overline{v}}| + |\dot{\overline{w}}| + \\ &\quad 2K_1|\dot{x} - q\dot{\overline{u}}| + 2K_2|x - qu|\Big\}\Big[V(\widetilde{\mathbf{e}}) + V(\widetilde{\mathbf{e}})^{1/2}\Big]. \end{aligned}$$

Thus if the impulses of system (2.39) are chosen to satisfy inequality (2.31), then, for $q = 0$ and 1, it can be concluded that system (2.39) is uniformly bounded. Furthermore, if we let $q = 1$, then the upper right derivative of $V(\widetilde{\mathbf{e}})$ will satisfy

$$D^+V(\widetilde{\mathbf{e}}) \leq \Big[2L + d + 2|x| + 2|\dot{x}| + |v| + |w| + |\dot{\overline{v}}| + |\dot{\overline{w}}| + 2K_1 + 2K_2\Big]V(\widetilde{\mathbf{e}}).$$

This implies, by choosing $\gamma_k = 1/k$, for all $k = 1, 2, \ldots$, and applying Theorem 2.2.2, that solutions to system (2.39) are also uniformly Lagrange stable, as desired. It should be mentioned that if $m(t)$ decays exponentially in time, then, due to the properties of exponential functions, the convergence of $\dot{\widetilde{\mathbf{e}}}$ to zero becomes faster.

The following numerical examples are used to explain how uniform Lagrange stability may be achieved by applying Theorem 2.2.2 and by employing the system described in Figure 2.8. The parameters in the examples are $B_k = B = -\text{diag}(0.5, 0.6, 0.2)$, the period of the impulses $\Delta_k = \Delta = 0.002$, the initial conditions $(x_0, y_0, z_0) = (3.07, -2.37, 0.88)$, $(u_0, v_0, w_0) = (1.46, -1.87, 0.5)$ and $(\dot{\overline{u}}_0, \dot{\overline{v}}_0, \dot{\overline{w}}_0) = (3.9,\ 0.74, -1.62)$. In the following two examples a fourth-order Runge-Kutta method with step size 10^{-5} is used. In the first example, $m(t)$ is taken to be with small upper bound and small frequency, whereas in the second example, $m(t)$ is taken to be with large upper bound and large frequency. The two choices are considered in order to show the performance of the system described in Figure 2.8. For the first example, let $m(t) = 2\exp(-10t)\sin(4t)$. As shown in Figure 2.9, the system converges to zero in 1.35 seconds. Note that the largest eigenvalue of B is 0.6, and it possesses all the required properties given in Theorem 2.2.2. For the second example, let $m(t) = 20\exp(-10t)\sin(50t)$, which possesses a relatively large amplitude and high frequency for short time t. Figure 2.10 shows that the uniform Lagrange stability is still achieved and the performance of the model is as desired. The conditions of Theorem 2.2.2 are satisfied by both the matrix B and system (2.39).

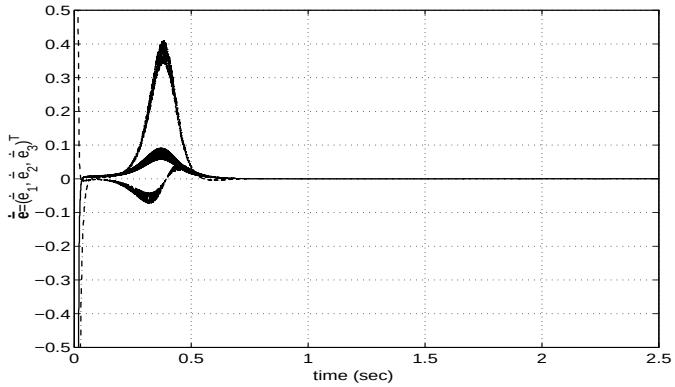

Figure 2.9: Uniform Lagrange stability of system (2.39), for $m(t) = 2\exp(-10t)\sin(4t)$.

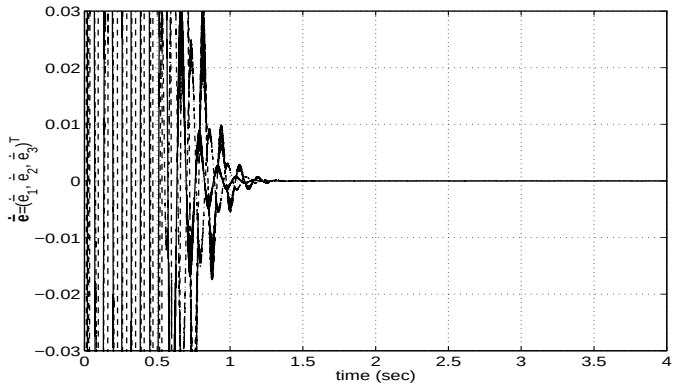

Figure 2.10: Uniform Lagrange stability of system (2.39), for $m(t) = 20\exp(-10t)\sin(50t)$.

2.3 Lyapunov Exponent Analysis

We have developed in the previous section a scheme for impulsively synchronizing chaotic systems. This was done by applying analytical methods which generate sufficient conditions on the impulses and on the parameters of the system. Enforcing these conditions guarantees equi-Lagrange stability (or uniform Lagrange stability) of the error dynamics between the chaotic systems involved in the model. It remains to investigate how this method behaves when we analyze the model numerically. In other words, we need to check the Lyapunov exponents of the models developed in the previous section and see if the results are consistent with the theoretical results we have already obtained in Theorems 2.2.1 and 2.2.2. Due to the fact that impulsive systems have a unique character represented by jump discontinuities at the moments of impulse, the classical approach of finding Lyapunov exponents of the error dynamics is not very applicable in this case. We shall apply a method proposed by Itoh et al., in [44] to study the dynamics of the synchronization error systems described by equations (2.38) and (2.39). Let us first explain the steps of this technique.

Recall that, in the previous models, we only considered the impulsive synchronization of two chaotic systems with unidirectional-coupling. i.e., one chaotic system was impulsively driving the other but not vice versa. In a uni-coupled synchronization scheme, we transmit the impulses sampled from one state variable of the driving system to the response system (driven system). To avoid clutter, and without loss of generality, we study the case when impulse samples are equidistant. Let P and Q denote the period and the width of the impulse samples, respectively. Note that P and Q must satisfy $Q << P$ and the area enclosed by the impulse is equal to 1 (see Figure 2.11). This structure for the sequence of impulses reflects the properties of the function $\delta_{\Delta}(t)$, defined by equation (2.17), which impulsively controls the general behaviour of the synchronization error system. This motivates us to split this error system into two dynamical models: one which corresponds to the period given by Q and the other which corresponds to the period given by $P - Q$. The error dynamics we are interested in, is the one which resembles equation (2.30), i.e., the impulses applied are of linear nature and represented by the set of matrices B_k, $k = 0, 1, \ldots$. In fact, in the following argument, we shall assume that the set of matrices $B_k = B$, $k = 0, 1, \ldots$, where B is a block diagonal matrix whose diagonal block elements are the $\ell \times \ell$ negative identity matrix, $-I$, and the $m \times m$ zero matrix, O, where $n = \ell + m$. In

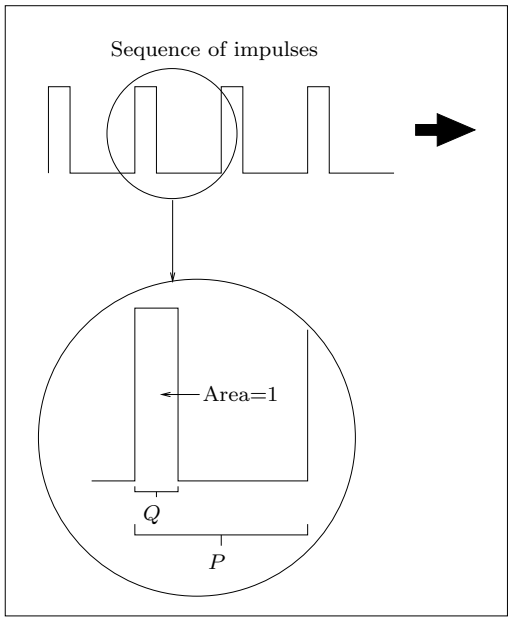

Figure 2.11: A scheme showing the structure of the impulses.

other words,

$$B_k = B = \begin{pmatrix} -I & O \\ O & O \end{pmatrix}.$$

Consider the following general form of a continuous dynamical system whose state variables can be grouped into two parts corresponding to the dimensions of the negative identity matrix $-I$ and the zero matrix O in B; namely, $\mathbf{x}(t)$ and $\mathbf{y}(t)$, where

$$\begin{cases} \dot{\mathbf{x}} &= \mathbf{f}(\mathbf{x}, \mathbf{y}) \\ \dot{\mathbf{y}} &= \mathbf{g}(\mathbf{x}, \mathbf{y}), \end{cases} \tag{2.40}$$

where $\mathbf{x} = (x_1, x_2, \ldots, x_l)^T \in \mathbb{R}^l$, $\mathbf{y} = (y_1, y_2, \ldots, y_m)^T \in \mathbb{R}^m$ and $\mathbf{f}$, $\mathbf{g}$ are smooth maps. Let us assume that samples of the state variable $\mathbf{x}(t)$ are sent to the response system. During the time interval when the k^{th} impulse is applied to the response system, we have

$$\begin{aligned} \mathbf{x}'(\tau_k^+) &= \mathbf{x}'(\tau_k) + I\mathbf{x}(\tau_k) - I\mathbf{x}'(\tau_k) \\ &= (I - I)\mathbf{x}'(\tau_k) + I\mathbf{x}(\tau_k) = \mathbf{x}(\tau_k), \end{aligned}$$

where $(\mathbf{x}'(t), \mathbf{y}'(t))^T$ is the response system. This implies that, for $t \in [kP, kP+Q)$, $k = 0, 1, \ldots$, the response system can be written as

$$\text{Response system A} \begin{cases} \mathbf{x}' &= \mathbf{x} \\ \dot{\mathbf{y}}' &= \mathbf{g}(\mathbf{x}, \mathbf{y}'). \end{cases} \tag{2.41}$$

During the time interval when the k^{th} impulse is not applied to the driven system; namely, for $t \in [kP+Q, (k+1)P)$, $k = 0, 1, \ldots$, the response system, in this case, can be written as

$$\text{Response system B} \begin{cases} \dot{\mathbf{x}}' &= \mathbf{f}(\mathbf{x}', \mathbf{y}') \\ \dot{\mathbf{y}}' &= \mathbf{g}(\mathbf{x}', \mathbf{y}'). \end{cases} \tag{2.42}$$

Therefore, by equations (2.41) and (2.42), the synchronization error systems are given by

$$\text{for response system A} \begin{cases} \mathbf{x} - \mathbf{x}' &= \mathbf{0} \\ \dot{\mathbf{y}} - \dot{\mathbf{y}}' &= \mathbf{g}(\mathbf{x}, \mathbf{y}) - \mathbf{g}(\mathbf{x}, \mathbf{y}'), \end{cases} \tag{2.43}$$

and

$$\text{for response system B} \begin{cases} \dot{\mathbf{x}} - \dot{\mathbf{x}}' &= \mathbf{f}(\mathbf{x}, \mathbf{y}) - \mathbf{f}(\mathbf{x}', \mathbf{y}') \\ \dot{\mathbf{y}} - \dot{\mathbf{y}}' &= \mathbf{g}(\mathbf{x}, \mathbf{y}) - \mathbf{g}(\mathbf{x}', \mathbf{y}'), \end{cases} \tag{2.44}$$

respectively. If the synchronization errors $\mathbf{X} := \mathbf{x} - \mathbf{x}'$ and $\mathbf{Y} := \mathbf{y} - \mathbf{y}'$ are sufficiently small, then the synchronization error systems (2.43) and (2.44) can be approximated by the variational systems

$$\dot{\mathbf{Y}} = J_{\mathbf{y}}\mathbf{g}(\mathbf{x}, \mathbf{y})\mathbf{Y} \tag{2.45}$$

and

$$\begin{pmatrix} \dot{\mathbf{X}} \\ \dot{\mathbf{Y}} \end{pmatrix} = \begin{pmatrix} J_{\mathbf{x}}\mathbf{f}(\mathbf{x}, \mathbf{y}) & J_{\mathbf{y}}\mathbf{f}(\mathbf{x}, \mathbf{y}) \\ J_{\mathbf{x}}\mathbf{g}(\mathbf{x}, \mathbf{y}) & J_{\mathbf{y}}\mathbf{g}(\mathbf{x}, \mathbf{y}) \end{pmatrix} \begin{pmatrix} \mathbf{X} \\ \mathbf{Y} \end{pmatrix}, \tag{2.46}$$

respectively, where again $J_{\mathbf{x}}\mathbf{f}(\mathbf{x}, \mathbf{y})$ and $J_{\mathbf{y}}\mathbf{f}(\mathbf{x}, \mathbf{y})$ are the Jacobian matrices of $\mathbf{f}$ with respect to $\mathbf{x}$ and $\mathbf{y}$, respectively, and $J_{\mathbf{x}}\mathbf{g}(\mathbf{x}, \mathbf{y})$ and $J_{\mathbf{y}}\mathbf{g}(\mathbf{x}, \mathbf{y})$ are the Jacobian matrices of $\mathbf{g}$ with respect to $\mathbf{x}$ and $\mathbf{y}$, respectively.

Let us now define $||\mathbf{E}(t)||$ as

$$||\mathbf{E}(t)|| := \sqrt{\mathbf{X}(t)^T\mathbf{X}(t) + \mathbf{Y}(t)^T\mathbf{Y}(t)}.$$

It follows that, for some $n \in \mathbb{Z}_+$,

$$\begin{aligned}\frac{||\mathbf{E}(nP)||}{||\mathbf{E}(0)||} &= \frac{||\mathbf{E}(Q)||}{||\mathbf{E}(0)||}\frac{||\mathbf{E}(P)||}{||\mathbf{E}(Q)||}\frac{||\mathbf{E}(P+Q)||}{||\mathbf{E}(P)||}\frac{||\mathbf{E}(2P)||}{||\mathbf{E}(P+Q)||}\cdots \\ &\quad \frac{||\mathbf{E}((n-1)P+Q)||}{||\mathbf{E}((n-1)P)||}\frac{||\mathbf{E}(nP)||}{||\mathbf{E}((n-1)P+Q)||} \\ &= \left[\frac{||\mathbf{E}(Q)||}{||\mathbf{E}(0)||}\frac{||\mathbf{E}(P+Q)||}{||\mathbf{E}(P)||}\cdots\frac{||\mathbf{E}((n-1)P+Q)||}{||\mathbf{E}((n-1)P)||}\right] \\ &\quad \times\left[\frac{||\mathbf{E}(P)||}{||\mathbf{E}(Q)||}\frac{||\mathbf{E}(2P)||}{||\mathbf{E}(P+Q)||}\cdots\frac{||\mathbf{E}(nP)||}{||\mathbf{E}((n-1)P+Q)||}\right].\end{aligned}$$

This implies that

$$\begin{aligned}\ln\left(\frac{||\mathbf{E}(nP)||}{||\mathbf{E}(0)||}\right) &= nQ\left[\frac{1}{nQ}\sum_{j=0}^{n-1}\ln\left(\frac{||\mathbf{E}(jP+Q)||}{||\mathbf{E}(jP)||}\right)\right] \\ &\quad +n(P-Q)\left[\frac{1}{n(P-Q)}\sum_{j=0}^{n-1}\ln\left(\frac{||\mathbf{E}((j+1)P)||}{||\mathbf{E}(jP+Q)||}\right)\right].\end{aligned} \tag{2.47}$$

Let μ and λ be the largest Lyapunov exponents of the systems (2.45) and (2.46), respectively. Assuming that P and Q are sufficiently small and n is sufficiently large in (2.47), we have

$$\begin{aligned}\ln\left(\frac{||\mathbf{E}(nP)||}{||\mathbf{E}(0)||}\right) &\approx nQ\mu + n(P-Q)\lambda \\ &= n(\mu-\lambda)Q + nP\lambda.\end{aligned}$$

Hence

$$||\mathbf{E}(nP)|| \approx \exp\left(n(\mu-\lambda)Q + nP\lambda\right)||\mathbf{E}(0)||.$$

Therefore if the inequality

$$D := (\mu-\lambda)Q + \lambda P < 0 \tag{2.48}$$

is satisfied, then we may conclude that

$$\ln\left(\frac{||\mathbf{E}(nP)||}{||\mathbf{E}(0)||}\right) \to 0, \qquad n \to \infty,$$

from which we know that the driving and the response systems are impulsively synchronized.

Equation (2.48) can explain the following observations:

- The accuracy of synchronization depends on both the period and the width of synchronization impulses.
- The minimum impulse width for synchronization increases as the impulse period increases.

In fact, we can get a numerical estimate on the maximum length for the period P if the length of the impulse Q is known. This can be done by solving for P from inequality (2.48) (in other words, we need $P < (\lambda - \mu/\lambda)Q$). Clearly we were able to provide another method to generate an estimate on the impulse period $\Delta = P$ for synchronization.

We shall now examine inequality (2.48) by considering the model we discussed in the previous section and described by equations (2.38) and (2.39). In that model, we employed the Lorenz system as being our chaos generating system. We shall take several numerical examples to illustrate our previous arguments. We begin by analyzing equation (2.38). As a first scenario, we suppose that samples of the state variable y are used to drive the state variable v, of the response system, at the discrete moments τ_k, $k = 0, 1, \ldots$ (here $\ell = 1$ and $m = 2$). Using our previous notations and discussion, the response system A_1, for $t \in [kP, kP + Q)$, $k = 0, 1, \ldots$, is given by

$$\begin{cases} v = y \\ \begin{pmatrix} \dot{u} \\ \dot{w} \end{pmatrix} = \begin{pmatrix} -\sigma u + \sigma y \\ uy - bw \end{pmatrix}. \end{cases}$$

Thus the error dynamics between the drive and response systems is given by

$$\begin{cases} e_2 = 0 \\ \begin{pmatrix} \dot{e}_1 \\ \dot{e}_3 \end{pmatrix} = \begin{pmatrix} -\sigma e_1 \\ ye_1 - be_3 \end{pmatrix} = \begin{pmatrix} -\sigma & 0 \\ y & -b \end{pmatrix} \begin{pmatrix} e_1 \\ e_3 \end{pmatrix}. \end{cases}$$

Notice the the second equation in the error dynamics is linear differential equation whose eigenvalues are given by $-\sigma$ and $-b$. Since eigenvalues and Lyapunov exponents become identical for linear systems, we may conclude immediately that the largest Lyapunov exponent in this model is $\mu = \max(-\sigma, -b)$. It follows that if $\sigma = 10$ and $b = 8/3$ (using the same values considered in the previous section), we obtain $\mu = -8/3$. The situation changes if we take instead samples of the

state variable x as our driving signal. In this case, the response system A_2, for $t \in [kP, kP+Q)$, $k = 0, 1, \ldots$, is given by

$$\begin{cases} x & = & u \\ \\ \begin{pmatrix} \dot{v} \\ \dot{w} \end{pmatrix} & = & \begin{pmatrix} rx - v - xw \\ xv - bw \end{pmatrix}. \end{cases}$$

This implies that the error dynamics between the drive and response systems is given by

$$\begin{cases} e_1 & = & 0 \\ \\ \begin{pmatrix} \dot{e}_2 \\ \dot{e}_3 \end{pmatrix} & = & \begin{pmatrix} -e_2 - xe_3 \\ xe_2 - be_3 \end{pmatrix} = \begin{pmatrix} -1 & -x \\ x & -b \end{pmatrix} \begin{pmatrix} e_2 \\ e_3 \end{pmatrix}. \end{cases}$$

Again the resulting model, describing the synchronization error, is a linear system except that its eigenvalues are functions of t. This makes finding the Lyapunov exponents, using the latter approach, not feasible. Therefore, we evaluate the largest Lyapunov exponents of the above model numerically by using Matlab coding, which reveals that $\mu = -2.668$.

Considering both scenarios, A_1 and A_2, described above, the corresponding response system B outside the impulse duration, i.e., for $t \in [kP+Q, (k+1)P)$, for $k = 0, 1, \ldots$, is given by

$$\dot{\mathbf{u}} = A\mathbf{u} + \begin{pmatrix} 0 \\ -uw \\ uv \end{pmatrix}$$

and the error dynamics is given by

$$\dot{\mathbf{e}} = A\mathbf{e} + \begin{pmatrix} 0 \\ -xz + uw \\ xy - uv \end{pmatrix}.$$

Thus, using once more Matlab coding, the largest Lyapunov exponent of the synchronization error is $\lambda = 0.907$. With these values, one can determine an upper bound on P once an impulse width Q is chosen.

We shall now apply the same analysis we just discussed to the next system; namely, (2.39), where, for simplicity, we shall take $m(t) = 0$. The coming derivations, however, can still be done for other choices of $m(t)$ such as those taken in the previous section. There are three different

scenarios that we need to analyze. In the first one, we shall take samples of the state variables x and $\dot{x}$ as our driving signals. In this case, the response system A_1', for $t \in [kP, kP+Q)$, $k = 0, 1, \ldots$, will be given by

$$\left\{ \begin{array}{rcl} \dot{\overline{u}} & = & \dot{x} \\ \\ \left(\begin{array}{c} \dot{\overline{v}} \\ \dot{\overline{w}} \end{array} \right) & = & \left(\begin{array}{c} r\dot{x} - \dot{\overline{v}} - \dot{x}w - x\dot{\overline{w}} \\ -b\dot{\overline{w}} + \dot{x}v + x\dot{\overline{v}} \end{array} \right), \end{array} \right.$$

where it is known that $u = x$, for $t \in [kP, kP+Q)$, $k = 0, 1, \ldots$. Hence the synchronization error between the drive and response systems is given by

$$\left\{ \begin{array}{rcl} \dot{\overline{e}}_1 & = & 0 \\ \\ \left(\begin{array}{c} \dot{\overline{e}}_2 \\ \dot{\overline{e}}_3 \end{array} \right) & = & \left(\begin{array}{c} -\dot{\overline{e}}_2 - \dot{x}e_3 - x\dot{\overline{e}}_3 \\ -b\dot{\overline{e}}_3 + \dot{x}e_2 + x\dot{\overline{e}}_2 \end{array} \right) = \left(\begin{array}{c} -\dot{\overline{e}}_2 + (\sigma x - \sigma y)e_3 - x\dot{\overline{e}}_3 \\ -b\dot{\overline{e}}_3 - (\sigma x - \sigma y)e_2 + x\dot{\overline{e}}_2 \end{array} \right), \end{array} \right.$$

where it is known that $e_1 = 0$, for $t \in [kP, kP+Q)$, $k = 0, 1, \ldots$. The resulting error system is a linear one and its largest Lyapunov exponent is given by $\mu = -1.607$. Similarly, when we take the driving impulses to be samples of the state variables x and $\dot{y}$, the response system A_2', for $t \in [kP, kP+Q)$, $k = 0, 1, \ldots$, will be given by

$$\left\{ \begin{array}{rcl} \dot{\overline{v}} & = & \dot{y} \\ \\ \left(\begin{array}{c} \dot{\overline{u}} \\ \dot{\overline{w}} \end{array} \right) & = & \left(\begin{array}{c} -\sigma\dot{\overline{u}} + \sigma\dot{y} \\ -b\dot{\overline{w}} + \dot{\overline{u}}v + x\dot{y} \end{array} \right), \end{array} \right.$$

where, again, $u = x$, for $t \in [kP, kP+Q)$, $k = 0, 1, \ldots$. Hence the synchronization error between the drive and response systems is given by

$$\left\{ \begin{array}{rcl} \dot{\overline{e}}_2 & = & 0 \\ \\ \left(\begin{array}{c} \dot{\overline{e}}_1 \\ \dot{\overline{e}}_3 \end{array} \right) & = & \left(\begin{array}{c} -\sigma\dot{\overline{e}}_1 \\ -b\dot{\overline{e}}_3 + \dot{x}e_2 + v\dot{\overline{e}}_1 \end{array} \right) = \left(\begin{array}{c} -\sigma\dot{\overline{e}}_1 \\ -b\dot{\overline{e}}_3 - (\sigma x - \sigma y)e_2 + v\dot{\overline{e}}_1 \end{array} \right), \end{array} \right.$$

where $e_2 = 0$, for $t \in [kP, kP+Q)$, $k = 0, 1, \ldots$. The largest Lyapunov exponent associated with this new error dynamics is $\mu = -1.764$. Finally, the last scenario we shall discuss, is when the

state variables y and $\dot{y}$ are taken to be the generators of the driving impulses. Taking $v = y$, for $t \in [kP, kP + Q)$, $k = 0, 1, \ldots$, the response system A'_3, on the same interval, will be given by

$$\begin{cases} \dot{\overline{v}} & = & \dot{y} \\ \\ \begin{pmatrix} \ddot{\overline{u}} \\ \ddot{\overline{w}} \end{pmatrix} & = & \begin{pmatrix} -\sigma\dot{\overline{u}} + \sigma\dot{y} \\ -b\dot{\overline{w}} + \dot{\overline{u}}y + u\dot{y} \end{pmatrix}, \end{cases}$$

and the synchronization error between the drive and response systems will given by

$$\begin{cases} \dot{\overline{e}}_2 & = & 0 \\ \\ \begin{pmatrix} \ddot{\overline{e}}_1 \\ \ddot{\overline{e}}_3 \end{pmatrix} & = & \begin{pmatrix} -\sigma\dot{\overline{e}}_1 \\ -b\dot{\overline{e}}_3 + \dot{y}e_1 + y\dot{\overline{e}}_1 \end{pmatrix} = \begin{pmatrix} -\sigma\dot{\overline{e}}_1 \\ -b\dot{\overline{e}}_3 + (rx - y - xz)e_1 + y\dot{\overline{e}}_1 \end{pmatrix}, \end{cases}$$

where we have taken $e_2 = 0$. Calculating the largest Lyapunov exponent of the latter synchronization error reveals that $\mu = -2.5106$. It still remains to calculate the largest Lyapunov exponent of the error dynamics when the impulses are not applied, i.e., when $t \in [kP + Q, (k + 1)P)$, for all $k = 0, 1, \ldots$. The response system B' outside the impulses will be given by

$$\ddot{\overline{\mathbf{u}}} = \begin{pmatrix} -\sigma\dot{\overline{u}} + \sigma\dot{\overline{v}} \\ r\dot{\overline{u}} - \dot{\overline{v}} - \dot{\overline{u}}w - u\dot{\overline{w}} \\ -b\dot{\overline{w}} + \dot{\overline{u}}v + u\dot{\overline{v}} \end{pmatrix}$$

and the error dynamics will be given by

$$\begin{aligned} \ddot{\overline{\mathbf{e}}} &= \begin{pmatrix} -\sigma\dot{\overline{e}}_1 + \sigma\dot{\overline{e}}_2 \\ r\dot{\overline{e}}_1 - \dot{\overline{e}}_2 - \dot{x}z + \dot{\overline{u}}w - x\dot{z} + u\dot{\overline{w}} \\ -b\dot{\overline{e}}_3 + \dot{x}y - \dot{\overline{u}}v + x\dot{y} - u\dot{\overline{v}} \end{pmatrix} \\ \\ &= \begin{pmatrix} -\sigma\dot{\overline{e}}_1 + \sigma\dot{\overline{e}}_2 \\ (r - w)\dot{\overline{e}}_1 - \dot{\overline{e}}_2 - u\dot{\overline{e}}_3 + \sigma(x - y)e_3 + (bz - xy)e_1 \\ v\dot{\overline{e}}_1 + u\dot{\overline{e}}_2 - b\dot{\overline{e}}_3 - \sigma(x - y)e_2 + (rx - y - xz)e_1 \end{pmatrix}. \end{aligned}$$

The largest Lyapunov exponent of the error dynamics, in this case, is given by $\lambda = 0.9751$. This indicates, as before that once the width of the impulse is chosen, an upper bound on the length of the impulse period $\Delta = P$ can be determined for this case as well.

We see clearly that the discussion in this section indicates that the numerical results obtained by finding the Lyapunov exponents, are consistent with the theoretical results obtained in Section 2.2. We shall see later in Chapter 4 that a modification of this method will be also used in studying the Lyapunov exponents of the error dynamics between impulsively synchronized spatiotemporal chaotic systems generated by non-linear partial differential equations.

Chapter 3

Delayed Impulsive Systems

Ordinary differential equations are sometimes inadequate as models of certain physical processes and therefore, in such cases, one or more generalizations of equation (1.1) is necessary. Two properties inherent in system (1.1) are that it satisfies the principle of *causality*, meaning that the future state of the system depends exclusively on the present state and not on past (or future) states and that the evolution of the state is continuous. However, in many processes, including physical, chemical, economic, biological and control systems (one of which is impulsive control), time delay factor is a fundamental issue. The rate of change of the state, $\dot{\mathbf{x}}(t)$, may depend on historical values of the state at times $t+s$, where $s \leq 0$, in addition to the present state values. In other words, it may be unreasonable to assume that the causality principle applies to the system. In fact, strictly speaking, the causality principle does not apply to most real systems. Instead, it is an approximation to how the true system behaves. When time delays are negligible, then they can often be ignored in mathematical models, leading us to simple equations like (1.1). When time delays are an important feature of a process, then one is led to consider delay differential equations, also known as *retarded functional differential equations*. In many processes, including physical, chemical, economic, biological and control systems, time delays are important factor. For example, in reactors and mixing tanks, in reality, a certain time is needed for the mixing of liquids in the vessels to take place. This time lag will generate models which will be described by delayed differential equations. It should be mentioned that some phenomena might even possess large enough time lags [63]. For example, the delay that arises in the description of the process of cellulose cooking is about 3 min., and the delay in the description of the limestone drying process in rotating furnaces reaches several tens of minutes.

Impulsive differential equations, described by equations (1.14) and (1.15), are no exceptions to what has been said regarding time delay and equation (1.1). In fact, we shall see, in this chapter, that a more accurate description of every impulsive differential equation will definitely involve time delay at least in the impulses. This follows from the fact that applying the impulses at a given exact moment t_i, for some $i = 1, 2, \ldots$, is practically impossible, since a time delay between sampling the impulse and applying it, will occur. This will become evident when we discuss the robustness of impulsive synchronization towards time delay, which will, in this case, also include transmission delay.

In Chapter 5, we shall see the importance of investigating the robustness of impulsive synchronization in the presence of two types of delay; namely, *sampling delay* and *transmission delay*. There are several attempts in the literature to study the existence, uniqueness, boundedness and stability of solutions for a specific type of delayed impulsive systems using the notion of Lyapunov functionals and Lyapunov functions [9, 10]. Whereas in [36], the asymptotic stability of singularly perturbed delayed impulsive systems with uncertainty from non-linear perturbations was explored. In this chapter, we address the stability issue of impulsive systems and impulsive synchronization with the presence of delay. We shall establish the sufficient conditions under which the chaotic systems will synchronize in the presence of delay in the impulses and in the differential system. We would like to study the influence of delay on the general behaviour of synchronization and its relationship with the other parameters of the system in order to maintain the equi-attractivity property of the error dynamics. In other words, we shall explore how far the synchronization process can endure the maximum amount of delay without losing its equi-attractivity properties. This will certainly describe the robustness of impulsive synchronization towards delay in the impulses and in the differential system itself. The sufficient conditions obtained relate the delay terms with systems' parameters and guarantee the convergence of solutions of the error dynamics to zero, which is the desired property in synchronizing chaotic systems.

This chapter is organized as follows. In the next section, we shall introduce several important definitions, which are similar to those definitions presented in Section 1.2 but incorporating delay, then we shall state some results regarding the existence and uniqueness of delayed impulsive systems. In Section 3.2, we shall investigate the stability properties of impulsive synchronization with the response of linear delayed impulses only. Whereas, in Section 3.3, we extend these results to study the stability of impulsive synchronization (which will also include continuous driving) which possesses delay in the differential system as well as in the impulses. This will be done by exploring the sufficient conditions which guarantee the equi-attractivity properties of delayed

impulsive systems whose structure resemble those describing the synchronization error in both cases.

3.1 Introduction

We have discussed in the previous chapter how two identical chaotic systems could synchronize impulsively by driving the response system with samples of the state variables of the drive system at the discrete moments t_i, $i = 1, 2, \ldots$. We obtained sufficient conditions on the impulses in terms of the different parameters of the chaotic systems involved so that this synchronization technique would work. i.e., the uniform Lagrange stability (or just the uniform attractivity in the large property, since chaotic systems are already uniformly bounded) of the synchronization error is achieved upon satisfying the sufficient conditions of Theorem 2.2.1. It still remains to investigate the robustness of this method with the presence of delay. In order to do so, we need to distinguish between two different situations.

1. The response system is driven impulsively only by the drive system. i.e., the impulses are the only values transmitted for synchronization.

2. The response system is driven impulsively and continuously simultaneously. In other words, the impulses together with a continuous signal, consisting of a combination of the state variables of the drive system, are transmitted to achieve synchronization.

The purpose of making the above classification will become evident when discussing the design of communication security schemes in Chapter 5. In fact, we shall see how delay arise in each case described in the classification above and how it plays an important role in affecting the general performance of chaos-based secure communication schemes. Figures 3.1 and 3.2 give illustrative diagrams of the two categories 1. and 2., respectively, where, in the second case, the signal $-xz$ is chosen as an example of a continuous driving signal (as in Lorenz system). Clearly, with these two types of design, the delay involved in each case will be different from the other. Actually, there are two kinds of delay involved in each case. The first kind is the *transmission delay* required for the impulses to reach the receiver end. Whereas the second type of delay is the *sampling delay* required to sample the system $\mathbf{u}(t)$ at each instance t_i and formulating the difference $\Delta\mathbf{e}(t_i) = \Delta\mathbf{x}(t_i) - \Delta\mathbf{u}(t_i)$, $i = 1, 2, \ldots$. Therefore the error dynamics between the synchronized chaotic systems will possess delay terms representing the transmission and sampling delays. However, this representation will differ between the two categories involving impulsive

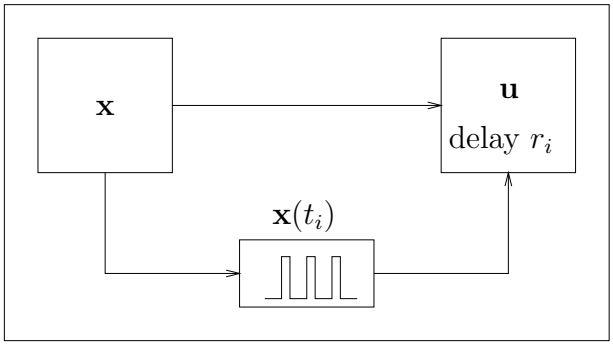

Figure 3.1: Synchronizing two identical chaotic systems impulsively only.

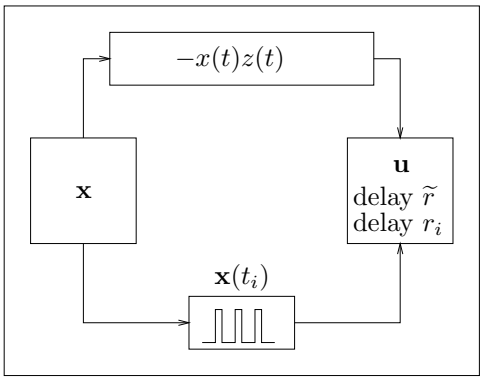

Figure 3.2: Synchronizing two identical chaotic systems impulsively and continuously by the signal $-xz$.

driving only and impulsive/continuous driving, mentioned above. We shall discuss each category separately and see what happens to the error dynamics with the presence of the delay factor.

1. Impulsive driving only: As we said earlier, only samples of the chaotic systems, at the discrete instances t_i, generated at the transmitter end (the driving system), are transmitted and installed at the receiver end (the response system). In other words, the state variables of the response system are subject to jumps at these instances, by applying linear maps, in order to make them behave in accordance with the state variables of the driving chaotic system. Due to the existence of transmission and sampling delays, it is not feasible to apply the impulses at the exact instances t_i to achieve synchronization. Instead, there will be delay, r_i, which is the maximum of the two types of delay involved in the system, in general, and involved in the impulses, in particular. i.e., the impulses will be applied at the instances $t_i + r_i$, for some $r_i > 0$, $i = 1, 2, \ldots$. We shall analyze the general dynamics of impulsive synchronization with the presence of delay in the impulses, and investigate how robust impulsive synchronization is towards delayed impulses subject to the physically reasonable assumption that delay is bounded, i.e., there exists an upper bound $r \geq r_i$, for some $r \geq 0$ and for all $i = 1, 2, \ldots$.

Let $\tau_i = t_i + r_i$, for $i = 1, 2, \ldots$. This implies that τ_i, becomes the moment of impulse and $t_i = \tau_i - r_i$. In this case, using the Lorenz chaotic attractor, Chua's oscillator or Rössler system, the general expression of the drive and response systems, whose structures resemble the structure of the above mentioned chaotic systems, are given by

$$\dot{\mathbf{x}} = A\mathbf{x} + \mathbf{\Omega}(\mathbf{x}) \tag{3.1}$$

and

$$\begin{cases} \dot{\mathbf{u}} &= A\mathbf{u} + \mathbf{\Omega}(\mathbf{u}), & t \neq \tau_i \\ \Delta\mathbf{u}(t) &= -B_i\mathbf{e}(t - r_i), & t = \tau_i,\ i = 1, 2, \ldots, \end{cases} \tag{3.2}$$

respectively, where A is an $n \times n$ constant matrix, $\mathbf{\Omega}(\mathbf{x})$ is a continuous non-linear mapping from $\mathbb{R}^3 \to \mathbb{R}^3$ and $\mathbf{e} = \mathbf{x} - \mathbf{u}$. Since the impulses depend on the values of $\mathbf{e}$ in the past time and by using systems (3.1) and (3.2), we conclude that the error dynamics is given by

$$\begin{cases} \dot{\mathbf{e}} &= A\mathbf{e} + \mathbf{\Phi}(\mathbf{x}, \mathbf{u}), & t \neq \tau_i \\ \Delta\mathbf{e}(t) &= B_i\mathbf{e}(t - r_i), & t = \tau_i,\ i = 1, 2, \ldots, \end{cases} \tag{3.3}$$

where $\mathbf{\Phi}(\mathbf{x}, \mathbf{u}) = \mathbf{\Omega}(\mathbf{x}) - \mathbf{\Omega}(\mathbf{u})$. A common property possessed by the mapping $\mathbf{\Phi}$, upon using any of the three chaotic systems we mentioned earlier, is given by $||\mathbf{\Phi}(\mathbf{x}, \mathbf{u})|| \leq L_2||\mathbf{e}||$, for some

$L_2 > 0$. In order for the two systems (3.1) and (3.2) to synchronize, the error dynamics $\mathbf{e}$, given by (3.3), must satisfy $\lim_{t\to\infty} \mathbf{e}(t) = \mathbf{0}$. We shall investigate the influence of delay in achieving this desired property and obtain conditions on the system, in general, and on the delays, in particular, to make the error dynamics $\mathbf{e}$ converge to zero.

In the next section, an arbitrary impulsive system with varying impulse intervals and linear delayed impulses is considered. Its structure resembles the error dynamics given by (3.3). The objective is to obtain a general theory regarding the convergence of solutions of that particular class of differential systems to zero, and apply the results to the model described by system (3.3).

2. Impulsive and continuous driving: In this case, the response system is driven continuously by a continuous signal constructed from the state variables of the drive system, and impulsively by the synchronizing impulses at the discrete instances t_i, $i = 1, 2, \ldots$, where the impulses are applied linearly on the chaotic response system. As before, this model will possess transmission and sampling delays. Applying the same technique used in the previous model, the impulses will include delay terms exactly in the same manner described before. However, due to the use of continuous driving in this model, the transmission delay will also appear in the differential system of the response system $\mathbf{u}$. Let us denote this type of delay, appearing in the chaotic system $\mathbf{u}$ itself, but not in the impulses, by $\widetilde{r}$. Whereas, we denote the delay appearing in the impulses by r_i, $i = 1, 2, \ldots$. As before, the moments $\tau_i = t_i - r_i$, $i = 1, 2, \ldots$, will become the moments of impulse acting on the response system. Let us consider the Lorenz chaotic system as a model for this category (actually other systems, such as Chua's oscillator and Rössler system, will also work). Hence the drive and response systems, in this case, will be given by

$$\dot{\mathbf{x}}(t) = A\mathbf{x}(t) + \mathbf{\Phi}_1(\mathbf{x}(t)) + \mathbf{\Phi}_2(\mathbf{x}(t)) \tag{3.4}$$

and

$$\begin{cases} \dot{\mathbf{u}}(t) & = A\mathbf{u}(t) + \mathbf{\Phi}_1(\mathbf{x}(t-\widetilde{r})) + \mathbf{\Phi}_2(\mathbf{u}(t)),\ t \neq \tau_i \\ \Delta\mathbf{u}(t) & = -B_i\mathbf{e}(t-r_i),\ t = \tau_i,\ i = 1, 2, \ldots, \end{cases} \tag{3.5}$$

respectively, where A is defined by (2.28), $\mathbf{\Phi}_1(\mathbf{x}) = (0, -xz, 0)^T$, $\mathbf{\Phi}_2(\mathbf{x}) = (0, 0, xy)^T$ and $\mathbf{e} = \mathbf{x} - \mathbf{u}$ is the error dynamics. Notice that according to this model, the system at the receiver end is driven continuously by the signal $-xz$ and by the impulses. From (3.4) and (3.5) the error dynamics $\mathbf{e}$ is given by

$$\begin{cases} \dot{\mathbf{e}}(t) & = A\mathbf{e}(t) + \mathbf{\Psi}_1(\mathbf{x}(t), \mathbf{x}(t-\widetilde{r})) + \mathbf{\Psi}_2(\mathbf{x}(t), \mathbf{u}(t)),\ t \neq \tau_i \\ \Delta\mathbf{e}(t) & = B_i\mathbf{e}(t-r_i),\ t = \tau_i,\ i = 1, 2, \ldots, \end{cases} \tag{3.6}$$

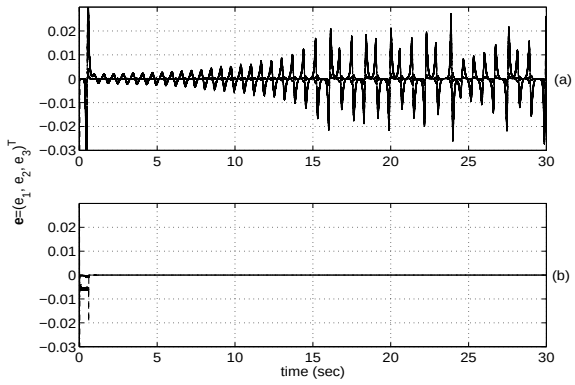

Figure 3.3: Error dynamics for (a) system (3.6); (b) system (3.7).

where $\mathbf{\Psi}_1(\mathbf{x}(t), \mathbf{x}(t-\widetilde{r})) = \mathbf{\Phi}_1(\mathbf{x}(t)) - \mathbf{\Phi}_1(\mathbf{x}(t-\widetilde{r}))$ and $\mathbf{\Psi}_2(\mathbf{x}(t), \mathbf{u}(t)) = \mathbf{\Phi}_2(\mathbf{x}(t)) - \mathbf{\Phi}_2(\mathbf{u}(t))$. Let $\sigma = 10$, $\rho = 28$, $b = 8/3$, $B_i = B = -\text{diag}(0.5,\ 0.6, 0.2)$, $\Delta := \Delta_{i+1} = \tau_{i+1} - \tau_i = 0.002$, and $r_i = \widetilde{r} = 0.001$, for all $i = 1, 2, \ldots$. By applying the Runge-Kutta integration method with an integration step-size given by 0.0001, to integrate system (3.6), identical synchronization cannot be achieved, although the magnitude of the delay is fairly small, as shown in Figure 3.3 (a). In fact, choosing different matrices B_i, $i = 1, 2, \ldots$, does not improve the synchronization results. The reason for such behaviour is that the two terms $\mathbf{\Phi}_1(\mathbf{x}(t))$ and $\mathbf{\Phi}_1(\mathbf{x}(t-\widetilde{r}))$ no longer eliminate each other. Thus the magnitude of the error between them will not approach zero, since $\mathbf{x}$ is a chaotic signal. Therefore it is necessary to construct a new response system that can synchronize with the chaotic attractor. By adding the two terms $\mathbf{\Phi}_1(\mathbf{u}(t))$ and $-\mathbf{\Phi}_1(\mathbf{u}(t-\widetilde{r}))$ in (3.5), we obtain

$$\begin{cases} \dot{\mathbf{u}}(t) &= A\mathbf{u}(t) + \mathbf{\Phi}_1(\mathbf{u}(t)) + \mathbf{\Phi}_1(\mathbf{x}(t-\widetilde{r})) - \mathbf{\Phi}_1(\mathbf{u}(t-\widetilde{r})) + \mathbf{\Phi}_2(\mathbf{u}(t)),\ t \neq \tau_i \\ \Delta\mathbf{u}(t) &= -B_i\mathbf{e}(t-r_i),\ t = \tau_i,\ i = 1, 2, \ldots. \end{cases} \tag{3.7}$$

The latter operation of adding two more terms is feasible because these two terms are generated using the response system and are totally independent of the drive system. Upon the addition of these two terms and by applying systems (3.4) and (3.7), the error dynamics will be given by

$$\begin{cases} \dot{\mathbf{e}}(t) &= A\mathbf{e}(t) + \mathbf{\Psi}_1(\mathbf{x}(t), \mathbf{u}(t)) + \mathbf{\Psi}_1(\mathbf{x}(t-\widetilde{r}), \mathbf{u}(t-\widetilde{r})) + \mathbf{\Psi}_2(\mathbf{x}(t), \mathbf{u}(t)),\ t \neq \tau_i \\ \Delta\mathbf{e}(t) &= B_i\mathbf{e}(t-r_i),\ t = \tau_i,\ i = 1, 2, \ldots. \end{cases} \tag{3.8}$$

The simulation of the error dynamics, given by (3.8), using the same values given above except for the delay terms, where we have chosen $r_i = 0.002$, $i = 1, 2, \ldots$, and $\widetilde{r} = 0.6$, shows identical

synchronization (see Figure 3.3 (b)). Notice that the model in (3.8) possesses the following important property:

$$||\mathbf{\Psi}_m(\mathbf{x},\mathbf{u})|| \leq \overline{L}_m||\mathbf{x}-\mathbf{u}|| = \overline{L}_m||\mathbf{e}||,$$

where $m = 1, 2$ and $\overline{L}_1$ and $\overline{L}_2$ are two positive constants. The latter inequality will be used in the theory developed for a certain kind of delayed impulsive differential equations with delayed impulses.

We shall analyze in Section 3.3 the dynamics of system (3.8) and find the conditions under which the equi-attractivity in the large property of the synchronization error may be achieved. This will be done by considering an arbitrary impulsive system whose structure resembles the system described by (3.8) and attempt to derive the conditions which guarantee convergence of solutions to zero (i.e., to achieve the equi-attractivity in the large property of the solutions).

3.2 Impulsive Control and Synchronization with Linear Delayed Impulses

Consider the impulsive system

$$\left\{\begin{array}{rcll} \dot{\mathbf{x}} & = & A\mathbf{x}+\mathbf{\Phi}(\mathbf{x}), & t \neq \tau_i \\ \Delta\mathbf{x}(t) & = & B_i\mathbf{x}(t-r_i), & t=\tau_i, \\ \mathbf{x}(t) & = & \boldsymbol{\phi}(t-t_0), & \end{array}\right\} \begin{array}{c} t > t_0 \\ \\ t_0 - r \leq t \leq t_0, \end{array} \tag{3.9}$$

where A is an $n\times n$ constant matrix, $\Delta\mathbf{x}(\tau_i) = \mathbf{x}(\tau_i^+)-\mathbf{x}(\tau_i^-)$, $\mathbf{x}(\tau_i^+) = \lim_{t\to\tau_i^+}\mathbf{x}(t)$, the moments of impulse satisfy $t_0 < \tau_1 < \tau_2 < \ldots < \tau_i < \ldots$ and $\lim_{i\to\infty}\tau_i = \infty$, $\boldsymbol{\phi}(t-t_0)$ is an arbitrary differentiable initial function defined over $[t_0-r, t_0]$, r_i are the delay constants, for all $i = 1, 2, \ldots,$ and $r := \max_i(r_i) \geq 0$. Let k, k_i, $i = 1, 2, \ldots,$ be a set of non-negative integers chosen in such a way that $t_0 < \tau_{i-k} < \tau_i - r \leq \tau_{i-k+1}$ and $t_0 < \tau_{i-k_i} < \tau_i - r_i \leq \tau_{i-k_i+1}$, where $1 \leq k_i, k \leq i$ and τ_0 is defined to be some point satisfying $t_0 < \tau_0 < \tau_1$ (τ_0 does not represent a moment of impulse). It should be mentioned that the subscript i in k_i is a label only, where k_i reflects the number of backward steps that corresponds to the delay r_i at the i^{th} impulse. Assume that $\mathbf{\Phi}(\mathbf{x})$ is a continuous non-linear map satisfying $||\mathbf{\Phi}(\mathbf{x})|| \leq L_2||\mathbf{x}||$, for some $L_2 > 0$, and B_i are $n \times n$ constant matrices satisfying $||B_i|| := \sqrt{\lambda_{\max}(B_i^TB_i)} < L_1$, for all $i = 1, 2, \ldots,$ and for some $L_1 > 0$ ($\lambda_{\max}(B^TB)$ is the largest eigenvalue of B^TB). This guarantees that, for each $(t_0, \boldsymbol{\phi}) \in \mathbb{R}_+ \times C([-r, 0], \mathbb{R}^n)$, there exists a local solution of (3.9) satisfying the initial condition

$\mathbf{x}(t) = \boldsymbol{\phi}(t-t_0)$, for $t_0 - r \leq t \leq t_0$ [9,10]. Let $\mathbf{x}(t) := \mathbf{x}(t, t_0, \boldsymbol{\phi})$ be any solution of (3.9) satisfying $\mathbf{x}(t) = \boldsymbol{\phi}(t - t_0)$, for $t_0 - r \leq t \leq t_0$, and $\mathbf{x}(t)$ be left continuous at each $\tau_i > t_0$ in the interval of existence, i.e., $\mathbf{x}(\tau_i^-) = \mathbf{x}(\tau_i)$, $i = 1, 2, \ldots$. Using the above set up, we define the impulse interval Δ_i by $\Delta_i := \tau_i - \tau_{i-1}$, and the quantities δ_{i-k_i+1}, by $\delta_{i-k_i+1} := r_i - (\tau_i - \tau_{i-k_i+1})$, where $0 \leq \delta_{i-k_i+1} < \Delta_{i-k_i+1}$, $i = 1, 2, \ldots$. These terms, together with the following definitions, will be very necessary to state the main results of this section. It should be mentioned that the following definitions are generalizations of previously defined terms, except that they incorporate delay.

Definition 3.2.1 *Given the delay constant r, we equip the linear space $C([-r, 0], \mathbb{R}^n)$ with the norm $||\cdot||_r$ defined by $||\boldsymbol{\phi}||_r = \sup_{-r \leq s \leq 0} ||\boldsymbol{\phi}(s)||$.*

Definition 3.2.2 *Let $M \geq 0$ and $V \in \nu_0(M)$, and consider the following delayed impulsive system, given by*

$$\begin{aligned} \dot{\mathbf{x}} &= \mathbf{f}(t, \mathbf{x}_t),\ t \neq \tau_i \\ \Delta\mathbf{x} &= \mathbf{I}(t, \mathbf{x}_t),\ t = \tau_i,\ i = 1, 2, \ldots, \end{aligned} \tag{3.10}$$

where $\mathbf{x}_t = \mathbf{x}_t(s) = \mathbf{x}(t + s)$, for $-r \leq s \leq 0$. The upper right derivative *of $V(t, \mathbf{x})$ with respect to the continuous portion of the system (3.10), for $(t, \mathbf{x}) \in \mathbb{R}_+ \times S^c(M)^0$ and $t \neq \tau_i$, by*

$$D^+V(t, \mathbf{x}) := \lim_{\delta \to 0^+} \sup \frac{1}{\delta} \left[V(t + \delta, \mathbf{x} + \delta \mathbf{f}(t, \mathbf{x}_t)) - V(t, \mathbf{x}) \right].$$

Definition 3.2.3 *Solutions of the impulsive system (3.9) are said to be*

(S1) equi-attractive in the large *if for each $\epsilon > 0$, $\alpha > 0$ and $t_0 \in \mathbb{R}_+$, there exists a number $T := T(t_0, \epsilon, \alpha) > 0$ such that $||\boldsymbol{\phi}||_r < \alpha$ implies $||\mathbf{x}(t)|| < \epsilon$, for $t \geq t_0 + T$;*

(S2) uniformly attractive in the large *if T in (S1) is independent of t_0.*

From the definition of equi-attractivity in the large, it can been seen that the solutions of system (3.9), which possess this property, will converge to zero no matter how large $||\boldsymbol{\phi}||_r$ is, i.e., $\lim_{t \to \infty} \mathbf{x}(t) = \mathbf{0}$. Moreover, the properties (S1) and (S2) in Definition 3.2.3 become identical for autonomous systems. Therefore the term uniform is dropped. Furthermore, equi-attractivity in the large will be able to reflect the desired behaviour of impulsive synchronization of the two chaotic systems (3.1) and (3.2), by driving the error dynamics (3.3) to zero. Finally, it should be noted that the definitions mentioned above, will also apply to the impulsive system we shall use in the next section. Therefore these definitions will be automatically used in the next section and no confusion should arise when applying them.

We shall prove now the following lemma.

Lemma 3.2.1 *Suppose that* $\mathbf{f}(t) = (f_1(t), f_2(t), \ldots, f_m(t))^T$, *where* $f_s(t) \in C[a,b]$, $s = 1, 2, \ldots, m$, *and* a, b *are constants. If* $||\cdot||$ *is the Euclidean norm, then*

$$||\int_a^b \mathbf{f}(t)dt||^2 \leq (b-a)\int_a^b ||\mathbf{f}(t)||^2 dt, \tag{3.11}$$

where the integration in the left hand side represents a componentwise integration.

Proof: By applying the Schwarz-Hölder inequality for integrals [30], we obtain

$$\begin{aligned} ||\int_a^b \mathbf{f}(t)dt||^2 &= \sum_{s=1}^m \left[\int_a^b f_s(t)dt\right]^2 \\ &\leq \sum_{s=1}^m \left[\left(\int_a^b 1^2 dt\right)^{1/2}\left(\int_a^b f_s(t)^2 dt\right)^{1/2}\right]^2 \\ &= (b-a)\int_a^b \sum_{s=1}^m f_s(t)^2 dt = (b-a)\int_a^b ||\mathbf{f}(t)||^2 dt, \end{aligned}$$

as required. □

Lemma 3.2.1 will be useful in the following derivations. By applying Taylor's Theorem, Taylor's Remainder Theorem and system (3.9), we obtain

$$\begin{aligned} \mathbf{x}(\tau_i - r_i) &= \mathbf{x}(\tau_{i-k_i+1} - \delta_{i-k_i+1}) = \mathbf{x}(\tau_{i-k_i+1}) - \delta_{i-k_i+1}\dot{\mathbf{x}}(t) \\ &= \mathbf{x}(\tau_{i-k_i+1}) - \delta_{i-k_i+1}A\mathbf{x}(t) - \delta_{i-k_i+1}\mathbf{\Phi}(\mathbf{x}(t)), \end{aligned}$$

for small δ_{i-k_i+1}, $0 \leq \delta_{i-k_i+1} < \Delta_{i-k_i+1}$, and for some $t \in (\tau_{i-k_i+1} - \delta_{i-k_i+1}, \tau_{i-k_i+1}) \subset (\tau_{i-k_i}, \tau_{i-k_i+1})$, $i = 1, 2, \ldots$. Thus

$$\begin{aligned} ||\mathbf{x}(\tau_i) - \mathbf{x}(\tau_i - r_i)|| &= ||\mathbf{x}(\tau_i) - \mathbf{x}(\tau_{i-k_i+1} - \delta_{i-k_i+1})|| \\ &\leq ||\mathbf{x}(\tau_i) - \mathbf{x}(\tau_{i-k_i+1})|| + \delta_{i-k_i+1}(||A|| + L_2)||\mathbf{x}(t)||, \end{aligned} \tag{3.12}$$

for some $t \in (\tau_{i-k_i+1} - \delta_{i-k_i+1}, \tau_{i-k_i+1})$ and for $i = 1, 2, \ldots$. Furthermore, according to the Fundamental Theorem of Calculus, we have, for all $i = 1, 2, \ldots$,

$$\mathbf{x}(\tau_i) - \mathbf{x}(\tau_{i-1}^+) = \int_{\tau_{i-1}^+}^{\tau_i} \dot{\mathbf{x}}(t)dt.$$

It follows from system (3.9) and inequality (3.11) that

$$\begin{aligned} ||\mathbf{x}(\tau_i) - \mathbf{x}(\tau_{i-1}^+)||^2 &= ||\int_{\tau_{i-1}^+}^{\tau_i} \dot{\mathbf{x}}(t)dt||^2 \leq \Delta_i \int_{\tau_{i-1}^+}^{\tau_i} ||\dot{\mathbf{x}}(t)||^2 dt \\ &\leq \Delta_i(||A|| + L_2)^2 \int_{\tau_{i-1}^+}^{\tau_i} ||\mathbf{x}(t)||^2 dt, \end{aligned} \tag{3.13}$$

for $i = 1, 2, \ldots$. The importance of inequalities (3.12) and (3.13) will eventually become evident in the proof of the next theorem.

Notice that system (3.9) has varying impulse durations and varying delay terms corresponding to each impulse. We shall state in the next theorem the sufficient conditions under which system (3.9) is equi-attractive in the large, then, in Theorem 3.2.2, we shall develop the same conditions for the same system but with equidistant impulses and having a maximum constant delay term in all of the impulses.

Theorem 3.2.1 *Let $2\widetilde{\lambda}$ be the largest eigenvalue of $A^T + A$, $\Delta_i \leq \Delta$ for some $\Delta > 0$,*

$$\mathcal{K}_i := e^{a\Delta_i}||I + B_i||, \tag{3.14}$$

$$\mathcal{F}_i^{(j)} := \Delta_j e^{a\Delta_j}||B_i||(||A|| + L_2), \;\; i - k_i + 2 \leq j \leq i, \;\; k_i > 1, \tag{3.15}$$

$$\mathcal{E}_i^{(j)} := e^{a\delta_{j-k_j+1}}||B_i||||B_j||, \;\; i - k_i + 1 \leq j \leq i - 1, \;\; k_i > 1 \tag{3.16}$$

and

$$\mathcal{L}_i := \delta_{i-k_i+1} e^{a\Delta_{i-k_i+1}}||B_i||(||A|| + L_2), \tag{3.17}$$

$i = 1, 2, \ldots,$ where $a := \widetilde{\lambda} + L_2$ and I is the identity matrix with the appropriate dimension. Let J_i be the $(i - p_i) \times (i - p_i)$ matrix (where $p_i = \max(0, q_i)$ and $q_i = \min(i - k_i, i - 1 - k_{i-1}, i - 2 - k_{i-2}, \ldots, i - k_i + 1 - k_{i-k_i+1})$, given by

$$\begin{cases} J_i := (\mathcal{K}_i + \mathcal{L}_i), \text{ if } i = 1 \text{ or } k_i = 1 \text{ (i.e., } p_i = i - k_i), \text{ for some } i = 2, 3, \ldots, \text{ or} \\ \\ J_i := \begin{pmatrix} 0 & 1 & 0 & \cdots & 0 & 0 \\ 0 & 0 & 1 & \cdots & 0 & 0 \\ 0 & 0 & 0 & \cdots & 0 & 0 \\ \vdots & \vdots & \vdots & \ddots & \vdots & \vdots \\ 0 & 0 & 0 & \cdots & 0 & 1 \\ \alpha_i^{(1)} & \alpha_i^{(2)} & \alpha_i^{(3)} & \cdots & \alpha_i^{(i-p_i-1)} & \alpha_i^{(i-p_i)} \end{pmatrix}, \text{ if } k_i > 1, \text{ for some } i = 2, 3, \ldots, \end{cases} \tag{3.18}$$

where

$$\begin{aligned}
\alpha_i^{(j)} &:= \sum_{S_{i,j}} \mathcal{E}_i^{(S_{i,j})}, \qquad 1 \le j \le i - k_i - p_i, \\
\alpha_i^{(i-k_i-p_i+1)} &:= \mathcal{L}_i + \sum_{S_{i,i-k_i-p_i+1}} \mathcal{E}_i^{(S_{i,i-k_i-p_i+1})}, \\
\alpha_i^{(j)} &:= \mathcal{F}_i^{(j+p_i)} + \sum_{S_{i,j}} \mathcal{E}_i^{(S_{i,j})}, \qquad i - k_i - p_i + 2 \le j \le i - p_i - 1, \\
\alpha_i^{(i-p_i)} &:= \mathcal{K}_i + \mathcal{F}_i^{(i)}
\end{aligned}$$

(the bounds on the set of integers $S_{i,j}$, which could be empty, depend on the impulse i and the entry j which both depend on the delay terms r_i, for all i such that $k_i > 1$). Then system (3.9) is equi-attractive in the large if each eigenvalue, $\lambda^{(i)}$, of J_i satisfies $|\lambda^{(i)}| \le \gamma$, where $0 \le \gamma < 1$, $i = 1, 2, \ldots$ (i.e., the matrix J_i can define a contraction linear mapping).

Remark 3.1: When $k_i > 1$, the structure of the matrices J_i and the values of the parameters $\alpha_i^{(j)}$, for some $i = 2, 3, \ldots$ and $j = 1, 2, \ldots, i - p_i$, will become clearer in the following proof. Actually there is no general formulation to describe all of these quantities (the matrices and the parameters) since they change at every impulse i. A simpler and clearer version of this theorem will be stated in Theorem 3.2.2.

Proof: We shall use the Euclidean norm as a Lyapunov function to prove this theorem. According to Definition 3.2.2, we have

$$\begin{aligned}
D^+ \left[||\mathbf{x}||\right] &= \frac{1}{2}(\mathbf{x}^T\mathbf{x})^{-1/2}\left[\dot{\mathbf{x}}^T\mathbf{x} + \mathbf{x}^T\dot{\mathbf{x}}\right] \\
&= \frac{1}{2||\mathbf{x}||}\left[\mathbf{x}^T(A^T + A)\mathbf{x} + 2\mathbf{\Phi}(\mathbf{x})^T\mathbf{x}\right] \\
&\le \frac{1}{2||\mathbf{x}||}(2\widetilde{\lambda} + 2L_2)||\mathbf{x}||^2 \\
&= a||\mathbf{x}||. \qquad (3.19)
\end{aligned}$$

Thus, by (3.19), we have, for every $t \in (\tau_{i-1}, \tau_i]$ and for every $i = 1, 2, \ldots,$

$$\int_{||\mathbf{x}(\tau_{i-1}^+)||}^{||\mathbf{x}(t)||} \frac{D^+ [||\mathbf{x}||]}{||\mathbf{x}||} \leq \int_{\tau_{i-1}}^{t} a dt.$$

Hence, for every $t \in (\tau_{i-1}, \tau_i]$, $i = 1, 2, \ldots,$ we have

$$||\mathbf{x}(t)|| \quad \leq \quad e^{a(t-\tau_{i-1})}||\mathbf{x}(\tau_{i-1}^+)|| \leq e^{a\Delta_i}||\mathbf{x}(\tau_{i-1}^+)||. \tag{3.20}$$

Let us first consider the case when $i = 1$. We have by inequalities (3.12) and (3.20), for some $t^* \in (\tau_1 - r_1, \tau_1)$,

$$\begin{aligned}
||\mathbf{x}(\tau_1^+)|| &= ||\mathbf{x}(\tau_1) + B_1\mathbf{x}(\tau_1 - r_1)|| \\
&= ||\mathbf{x}(\tau_1) + B_1\mathbf{x}(\tau_1) - B_1\mathbf{x}(\tau_1) + B_1\mathbf{x}(\tau_1 - r_1)|| \\
&\leq ||I + B_1||||\mathbf{x}(\tau_1)|| + ||B_1||||\mathbf{x}(\tau_1) - \mathbf{x}(\tau_1 - r_1)|| \\
&\leq e^{a\Delta_1}||I + B_1||||\mathbf{x}(\tau_0^+)|| + r_1||B_1||(||A|| + L_2)||\mathbf{x}(t^*)|| \\
&\leq e^{a\Delta_1}||I + B_1||||\mathbf{x}(\tau_0^+)|| + r_1 e^{a\Delta_1}||B_1||(||A|| + L_2)||\mathbf{x}(\tau_0^+)||,
\end{aligned}$$

since $\tau_0 < \tau_1 - r_1$ (recall that $\mathbf{x}(\tau_0^+) = \mathbf{x}(\tau_0)$). Thus

$$||\mathbf{x}(\tau_1^+)|| \leq (\mathcal{K}_1 + \mathcal{L}_1)||\mathbf{x}(\tau_0^+)||. \tag{3.21}$$

Similarly, if $k_i = 1$, for some $i = 2, 3, \ldots,$ we may also conclude that

$$||\mathbf{x}(\tau_i^+)|| \leq (\mathcal{K}_i + \mathcal{L}_i)||\mathbf{x}(\tau_{i-1}^+)||. \tag{3.22}$$

However, if $k_i > 1$, for some $i = 2, 3, \ldots$, we have, by applying system (3.9), Schwarz inequality and inequalities (3.12) and (3.20), for some $t \in (\tau_{i-k_i+1} - \delta_{i-k_i+1}, \tau_{i-k_i+1})$, $0 \leq \delta_{i-k_i+1} < \Delta_{i-k_i+1}$,

$$\begin{aligned}
||\mathbf{x}(\tau_i^+)|| &= ||\mathbf{x}(\tau_i) + B_i\mathbf{x}(\tau_i - r_i)|| \\
&= ||\mathbf{x}(\tau_i) + B_i\mathbf{x}(\tau_i) - B_i\mathbf{x}(\tau_i) + B_i\mathbf{x}(\tau_i - r_i)|| \\
&\leq ||I + B_i||||\mathbf{x}(\tau_i)|| + ||B_i||||\mathbf{x}(\tau_i) - \mathbf{x}(\tau_i - r_i)|| \\
&\leq e^{a\Delta_i}||I + B_i||||\mathbf{x}(\tau_{i-1}^+)|| + ||B_i||||\mathbf{x}(\tau_i) - \mathbf{x}(\tau_{i-k_i+1})|| \\
&\quad +\delta_{i-k_i+1}||B_i||(||A|| + L_2)||\mathbf{x}(t)|| \\
&\leq e^{a\Delta_i}||I + B_i||||\mathbf{x}(\tau_{i-1}^+)|| + ||B_i||||\mathbf{x}(\tau_i) - \mathbf{x}(\tau_{i-k_i+1})|| \\
&\quad +\delta_{i-k_i+1}e^{a\Delta_{i-k_i+1}}||B_i||(||A|| + L_2)||\mathbf{x}(\tau_{i-k_i}^+)||.
\end{aligned} \tag{3.23}$$

Moreover, if $k_i > 1$, for some $i = 2, 3, \ldots$, we have

$$\begin{aligned}
||\mathbf{x}(\tau_i) - \mathbf{x}(\tau_{i-k_i+1})|| &= ||\mathbf{x}(\tau_i) + [-\mathbf{x}(\tau_{i-1}) + \mathbf{x}(\tau_{i-1})] + \ldots \\
&\quad +[-\mathbf{x}(\tau_{i-k_i+2}) + \mathbf{x}(\tau_{i-k_i+2})] - \mathbf{x}(\tau_{i-k_i+1})|| \\
&\leq ||\mathbf{x}(\tau_i) - \mathbf{x}(\tau_{i-1})|| + \ldots + ||\mathbf{x}(\tau_{i-k_i+2}) - \mathbf{x}(\tau_{i-k_i+1})|| \\
&= ||\mathbf{x}(\tau_i) - \mathbf{x}(\tau_{i-1}^+) + \mathbf{x}(\tau_{i-1}^+) - \mathbf{x}(\tau_{i-1})|| + \ldots \\
&\quad +||\mathbf{x}(\tau_{i-k_i+2}) - \mathbf{x}(\tau_{i-k_i+1}^+) + \mathbf{x}(\tau_{i-k_i+1}^+) - \mathbf{x}(\tau_{i-k_i+1})|| \\
&\leq ||\mathbf{x}(\tau_i) - \mathbf{x}(\tau_{i-1}^+)|| + ||\Delta\mathbf{x}(\tau_{i-1})|| + \ldots \\
&\quad +||\mathbf{x}(\tau_{i-k_i+2}) - \mathbf{x}(\tau_{i-k_i+1}^+)|| + ||\Delta\mathbf{x}(\tau_{i-k_i+1})|| \\
&\leq \sum_{j=i-k_i+2}^{i} ||\mathbf{x}(\tau_j) - \mathbf{x}(\tau_{j-1}^+)|| + \sum_{j=i-k_i+1}^{i-1} ||B_j||||\mathbf{x}(\tau_j - r_j)||.
\end{aligned}$$

Thus, by inequalities (3.13) and (3.20), we have

$$\begin{aligned}
||\mathbf{x}(\tau_i) - \mathbf{x}(\tau_{i-k_i+1})|| &\leq \sum_{j=i-k_i+2}^{i} \Delta_j^{1/2}(||A|| + L_2) \left\{ \int_{\tau_{j-1}^+}^{\tau_j} ||\mathbf{x}(t)||^2 dt \right\}^{1/2} \\
&\quad + \sum_{j=i-k_i+1}^{i-1} ||B_j||||\mathbf{x}(\tau_{j-k_j+1} - \delta_{j-k_j+1})|| \\
&\leq \sum_{j=i-k_i+2}^{i} \Delta_j^{1/2}(||A|| + L_2) \left\{ \int_{\tau_{j-1}^+}^{\tau_j} e^{2a\Delta_j} ||\mathbf{x}(\tau_{j-1}^+)||^2 dt \right\}^{1/2} \\
&\quad + \sum_{j=i-k_i+1}^{i-1} e^{a\delta_{j-k_j+1}} ||B_j||||\mathbf{x}(\tau_{j-k_j}^+)|| \\
&= \sum_{j=i-k_i+2}^{i} \Delta_j e^{a\Delta_j}(||A|| + L_2)||\mathbf{x}(\tau_{j-1}^+)|| \\
&\quad + \sum_{j=i-k_i+1}^{i-1} e^{a\delta_{j-k_j+1}} ||B_j||||\mathbf{x}(\tau_{j-k_j}^+)||.
\end{aligned}$$

Therefore the latter inequality, together with inequality (3.23) and equations (3.14), (3.15), (3.16) and (3.17), imply, for all i such that $k_i > 1$, that

$$||\mathbf{x}(\tau_i^+)|| \leq \mathcal{K}_i||\mathbf{x}(\tau_{i-1}^+)|| + \sum_{j=i-k_i+2}^{i} \mathcal{F}_i^{(j)}||\mathbf{x}(\tau_{j-1}^+)|| + \sum_{j=i-k_i+1}^{i-1} \mathcal{E}_i^{(j)}||\mathbf{x}(\tau_{j-k_j}^+)|| + \mathcal{L}_i||\mathbf{x}(\tau_{i-k_i}^+)||. \quad (3.24)$$

Since $q_i = \min(i - k_i, i - 1 - k_{i-1}, \ldots, i - k_i + 1 - k_{i-k_i+1})$ and $p_i = \max(0, q_i)$, we may define the quantities $v_1(p_i) := ||\mathbf{x}(\tau_{p_i}^+)||$, $v_2(p_i) := ||\mathbf{x}(\tau_{p_i+1}^+)||$, $\ldots$, $v_{i-p_i}(p_i) := ||\mathbf{x}(\tau_{i-1}^+)||$. It follows that

$$v_j(p_i + 1) = ||\mathbf{x}(\tau_{p_i+j}^+)|| = v_{j+1}(p_i), \quad (3.25)$$

where $1 \leq j \leq i - p_i$. Now, with the consideration of inequality (3.24) and equation (3.25), we have

$$\begin{aligned} v_{i-p_i}(p_i+1) &= v_{i-p_i+1}(p_i) = ||\mathbf{x}(\tau_i^+)|| \\ &\leq \mathcal{K}_i v_{i-p_i}(p_i) + \sum_{j=i-k_i+2}^{i} \mathcal{F}_i^{(j)} v_{j-p_i}(p_i) \\ &\quad + \sum_{i-k_i+1}^{i-1} \mathcal{E}_i^{(j)} v_{j+1-k_j-p_i}(p_i) + \mathcal{L}_i v_{i-k_i-p_i+1}(p_i). \end{aligned}$$

Let $\mathbf{v}(p_i) := (v_1(p_i), v_2(p_i), \ldots, v_{i-p_i}(p_i))^T$. Then, by equation (3.18), the system of difference inequalities obtained above, including inequalities (3.21) and (3.22), can be written in a vector form as

$$\mathbf{v}(p_i + 1) \leq J_i \mathbf{v}(p_i), \tag{3.26}$$

for all $i = 1, 2, \ldots$, with the convention that the same inequality holds between the corresponding components. Thus if each eigenvalue, $\lambda^{(i)}$, of J_i, $i = 1, 2, \ldots$, satisfies $|\lambda^{(i)}| \leq \gamma$, $0 \leq \gamma < 1$, then, by (3.26), it follows that $\lim_{s\to\infty} \mathbf{v}(p_i + s) = \mathbf{0}$, since $k_i < k$. On the other hand, $v_{i-p_i}(p_i + s) = ||\mathbf{x}(\tau_{i+s-1}^+)||$, for $i = 1, 2, \ldots$. Therefore if we let $\ell = i + s - 1$, we can conclude that

$$\lim_{\ell\to\infty} ||\mathbf{x}(\tau_\ell^+)|| = \lim_{s\to\infty} ||\mathbf{x}(\tau_{i+s-1}^+)|| = \lim_{s\to\infty} v_{i-p_i}(p_i + s) = 0.$$

Moreover, from inequality (3.20), we can further conclude that, for every $t \in (\tau_{i-1}, \tau_i]$ and $i = 1, 2, \ldots$,

$$||\mathbf{x}(t)|| \leq e^{a\Delta_i} ||\mathbf{x}(\tau_{i-1}^+)|| \leq e^{a\Delta} ||\mathbf{x}(\tau_{i-1}^+)|| \to 0,$$

as $i \to \infty$. In other words $||\mathbf{x}(t)|| \to 0$, as $t \to \infty$. Thus solutions to system (3.9) are equi-attractive in the large, as required. □

The complexity of Theorem 3.2.1 reduces drastically when considering impulsive systems with equidistant impulses and with maximum constant delay in the driving impulses. In other words, we shall now consider the impulsive system, given by

$$\left\{ \begin{array}{rcll} \dot{\mathbf{x}} &=& A\mathbf{x} + \mathbf{\Phi}(\mathbf{x}), & t \neq \tau_i \\ \Delta\mathbf{x}(t) &=& B_i\mathbf{x}(t-r), & t = \tau_i, \\ \mathbf{x}(t) &=& \boldsymbol{\phi}(t - t_0), & \end{array} \right\} \begin{array}{c} t > t_0 \\ \\ t_0 - r \leq t \leq t_0, \end{array} \tag{3.27}$$

where $\tau_{i+1} - \tau_i = \Delta$ and $r_i = r$, for all $i = 1, 2, \ldots$. The delay parameter r represents the maximum delay that system (3.27) can endure without losing its equi-attractivity in the large

property. In this case, $k_i = k$ and $\delta_i = \delta$, for all $i = 1, 2, \ldots$. Therefore, using the above set up, we may obtain the following theorem.

Theorem 3.2.2 *Let $2\widetilde{\lambda}$ be the largest eigenvalue of $A^T + A$, $\Delta_i = \Delta$, for some $\Delta > 0$,*

$$\mathcal{K}_i := e^{a\Delta}||I + B_i||, \tag{3.28}$$

$$\mathcal{F}_i^{(j)} := \Delta e^{a\Delta}||B_i||(||A|| + L_2), \;\; i - k + 2 \leq j \leq i, \;\; k > 1, \tag{3.29}$$

$$\mathcal{E}_i^{(j)} := e^{a\delta}||B_i||||B_j||, \;\; i - k + 1 \leq j \leq i - 1, \;\; k > 1 \tag{3.30}$$

and

$$\mathcal{L}_i := \delta e^{a\Delta}||B_i||(||A|| + L_2), \tag{3.31}$$

$i = 1, 2, \ldots$, where $a := \widetilde{\lambda} + L_2$ and I is the identity matrix with the appropriate dimension. Let J_i be the $(2k-1) \times (2k-1)$ matrix given by

$$\begin{cases} J_i \;\; := (\mathcal{K}_i + \mathcal{L}_i), \text{ if } k = 1, \text{ for } i = 1, 2, \ldots, \\ \\ J_i \;\; := \begin{pmatrix} 0 & 1 & 0 & \cdots & 0 & 0 \\ 0 & 0 & 1 & \cdots & 0 & 0 \\ 0 & 0 & 0 & \cdots & 0 & 0 \\ \vdots & \vdots & \vdots & \ddots & \vdots & \vdots \\ 0 & 0 & 0 & \cdots & 0 & 1 \\ \alpha_i^{(1)} & \alpha_i^{(2)} & \alpha_i^{(3)} & \cdots & \alpha_i^{(2k-2)} & \alpha_i^{(2k-1)} \end{pmatrix}, \text{ if } k > 1, \text{ for } i = 2, 3, \ldots, \end{cases} \tag{3.32}$$

where

$$\begin{aligned} \alpha_i^{(j)} &:= \mathcal{E}_i^{(i-k+j)}, \qquad 1 \leq j \leq k-1, \\ \alpha_i^{(k)} &:= \mathcal{L}_i, \\ \alpha_i^{(j)} &:= \mathcal{F}_i^{(i+j-2k+1)}, \qquad k+1 \leq j \leq 2k-2, \\ \alpha_i^{(2k-1)} &:= \mathcal{K}_i + \mathcal{F}_i^{(i)}. \end{aligned}$$

Then system (3.27) is equi-attractive in the large if each eigenvalue, $\lambda^{(i)}$, of J_i satisfies $|\lambda^{(i)}| \leq \gamma$, where $0 \leq \gamma < 1$, $i = 1, 2, \ldots$.

Proof: Using an identical approach to the proof of Theorem 3.2.1, we may reach inequalities (3.21) and (3.22), provided that $k = 1$, for all $i = 1, 2, \ldots$. However, if $k > 1$, for all $i = 2, 3, \ldots$, then inequality (3.24) becomes

$$||\mathbf{x}(\tau_i^+)|| \leq \mathcal{K}_i||\mathbf{x}(\tau_{i-1}^+)|| + \sum_{j=i-k+2}^{i} \mathcal{F}_i^{(j)}||\mathbf{x}(\tau_{j-1}^+)|| + \sum_{j=i-k+1}^{i-1} \mathcal{E}_i^{(j)}||\mathbf{x}(\tau_{j-k}^+)|| + \mathcal{L}_i||\mathbf{x}(\tau_{i-k}^+)||. \quad (3.33)$$

Thus if we choose $v_1(i-1) := ||\mathbf{x}(\tau_{i-2k+1}^+)||$, $v_2(i-1) := ||\mathbf{x}(\tau_{i-2k+2}^+)||$, $\ldots$, $v_{2k-1}(i-1) := ||\mathbf{x}(\tau_{i-1}^+)||$, for $i = 2, 3, \ldots$ and $k > 1$, we can conclude that

$$v_j(i) = ||\mathbf{x}(\tau_{i+1-2k+j}^+)|| = v_{j+1}(i-1),$$

where $1 \leq j \leq 2k-1$. Hence, by using (3.33), it follows that

$$\begin{aligned} v_{2k-1}(i) &= v_{2k}(i-1) = ||\mathbf{x}(\tau_i^+)|| \\ &\leq \mathcal{K}_i v_{2k-1}(i-1) + \sum_{j=i-k+2}^{i} \mathcal{F}_i^{(j)} v_{j-i+2k-1}(i-1) + \sum_{i-k+1}^{i-1} \mathcal{E}_i^{(j)} v_{j-i+k}(i-1) \\ &\quad + \mathcal{L}_i v_k(i-1). \end{aligned}$$

Like before, we define $\mathbf{v}(i) := (v_1(i), v_2(i), \ldots, v_{2k-1}(i))^T$. Then, by equations (3.28), (3.29), (3.30), (3.31) and (3.32), the corresponding system of difference inequalities obtained above, including inequalities (3.21) and (3.22), can be written in a vector form as

$$\mathbf{v}(i) \leq J_i \mathbf{v}(i-1), \quad (3.34)$$

for all $i = 1, 2, \ldots$, with the convention that the same inequality holds between the corresponding components. Thus, with the same reasoning as before, if each eigenvalue, $\lambda^{(i)}$, of J_i, $i = 1, 2, \ldots$, satisfies $|\lambda^{(i)}| \leq \gamma$, $0 \leq \gamma < 1$, then, by (3.34), it follows that $\lim_{i\to\infty} \mathbf{v}(i) = \mathbf{0}$. However, since $v_{2k-1}(i-1) = ||\mathbf{x}(\tau_{i-1}^+)||$, we may deduce that

$$\lim_{i\to\infty} ||\mathbf{x}(\tau_{i-1}^+)|| = \lim_{i\to\infty} v_{2k-1}(i-1) = 0.$$

Finally, by inequality (3.20) (which is satisfied by system (3.27)), we can further conclude that, for every $t \in (\tau_{i-1}, \tau_i]$, $i = 1, 2, \ldots$,

$$||\mathbf{x}(t)|| \leq e^{a\Delta}||\mathbf{x}(\tau_{i-1}^+)|| \to 0,$$

as $i \to \infty$. In other words $||\mathbf{x}(t)|| \to 0$, as $t \to \infty$. This means that system (3.27) is equi-attractive in the large, as required. □

With Theorems (3.2.1) and (3.2.2), we have the following six useful remarks.

Remark 3.2: If $k_i = 1$ (or $k = 1$), for some $i = 1, 2, \ldots$, then the matrix J_i corresponding to the i^{th} impulse will be a 1×1 matrix, given by $J_i = (\mathcal{K}_i + \mathcal{L}_i)$. However, if $k_i > 1$ (or $k > 1$), for some $i = 2, 3, \ldots$, then the eigenvalues of the matrix J_i, defined by equation (3.18) (and also by equation (3.32)), corresponding to the i^{th} impulse, are the roots of the characteristic equation, given by

$$\det(\lambda^{(i)} I - J_i) = \left(\lambda^{(i)}\right)^{i-p_i} - \sum_{j=1}^{i-p_i} \left(\lambda^{(i)}\right)^{i-p_i-j} \alpha_i^{(i-p_i+1-j)} = 0. \tag{3.35}$$

In fact, the matrix J_i is called the companion matrix of the polynomial given by the left hand side of equation (3.35). We may find the roots of this characteristic equation numerically and choose the matrices B_i in such a way that all the eigenvalues $\lambda^{(i)}$, will lie inside a circle of radius γ. The choice of k_i, $i = 2, 3, \ldots$, is determined by trial and error.

Remark 3.3: Theorems 3.2.1 and 3.2.2 indicate that if we choose some integer $K > 1$ such that the matrices J_i, for all $i \geq K$, satisfy the conditions of these theorems, whereas the matrices J_i, for $1 \leq i < K$, may not necessarily satisfy the conditions, then systems (3.9) and (3.27) will remain equi-attractive in the large regardless of what the value of $K > 1$ is.

Remark 3.4: From the structure of the matrix J_i, for $i = 1, 2, \ldots$, we conclude that the smaller the choice of the impulse duration Δ_i, (and thus Δ), the bigger the upper bound on the delay terms $r_i \leq r$, for $i = 1, 2, \ldots$. In other words, system (3.9) (and also system (3.27)) can endure larger delays in the impulses if Δ_i (and also Δ), $i = 1, 2, \ldots$, are chosen to be small enough.

Remark 3.5: From equations (3.14), (3.15), (3.16) and (3.17) (similarly from equations (3.28), (3.29), (3.30) and (3.31)), we see clearly that as the delay term r_i, $i = 1, 2, \ldots$, increases, the magnitude of the impulse, $||B_i||$, must be chosen small enough in order to achieve the equi-attractivity in the large property for system (3.9) (and system (3.27)). This is due to the fact that, for small $||B_i||$, $i = 1, 2, \ldots$, $\mathcal{F}_i^{(j)}$, $\mathcal{E}_i^{(j)}$ and $\mathcal{L}_i$ will become relatively small and $\mathcal{K}_i$ will become the more dominant term, i.e., we can reduce the influence of all the impulses preceding i^{th} impulse and increase the influence of the i^{th} impulse. However, there exists a threshold value β_i for $||B_i||$, with

a fixed value for Δ_i, $i = 1, 2, \ldots$, such that if $||B_i|| < \beta_i$ the desired property of equi-attractivity in the large will never be achieved since $\mathcal{K}_i$ will become large and consequently $|\lambda^{(i)}|$ will become greater than 1. This means that, for large enough r_i and with a fixed choice for Δ_i, $i = 1, 2, \ldots$, there will not exist a matrix B_i which can drive the solutions of system (3.9) (and system (3.27)) to zero. This phenomenon will be illustrated in the next section by an example employing two Chua's oscillators.

Remark 3.6: In the absence of delay from system (3.9), the resulting system will be given by

$$\left\{ \begin{array}{rcll} \dot{\mathbf{x}} & = & A\mathbf{x} + \mathbf{\Phi}(\mathbf{x}), & t \neq \tau_i \\ \Delta\mathbf{x}(t) & = & B_i\mathbf{x}(t), & t = \tau_i,\ i = 1, 2, \ldots, \\ \mathbf{x}(t_0^+) & = & \mathbf{x}_0, & \end{array} \right. \tag{3.36}$$

where $\mathbf{x}_0$ represents the initial condition. In other words, the delay terms r_i, $i = 1, 2, \ldots$, in system (3.9), are set to be equal to zero. In this case, we have $k_i = 0$, $\mathcal{K}_i = e^{a\Delta_i}||I + B_i||$ and $\mathcal{F}_i^{(j)} = \mathcal{E}_i^{(j)} = \mathcal{L}_i = 0$, $i = 1, 2, \ldots$. Thus the condition on the eigenvalues of J_i to lie inside a circle of radius γ reduces to the condition that $||I + B_i|| \leq e^{-a\Delta_i}\gamma$. This implies that if we choose $\gamma_i := 1/i$, for all $i = 1, 2, \ldots$, and $\epsilon := (1/2)\ln(1/\gamma)$, then we may let $||I + B_i|| \leq e^{-a\Delta_i - \gamma_i - 2\epsilon} \leq e^{-a\Delta_i}\gamma$. The latter inequality represents the condition on the matrices B_i, $i = 1, 2, \ldots$, so that system (3.36) is equi-attractive in the large, which is identical to the condition obtained in Theorem 2.2.1; namely, inequality (2.22) with $\mathbf{g}(\mathbf{u}) = \mathbf{0}$.

Remark 3.7: The conditions of Theorem 3.2.1 and Theorem 3.2.2 are sufficient conditions but not necessary. Therefore in the process of searching for impulse durations Δ_i and matrices B_i, $i = 1, 2, \ldots$, which achieve equi-attractivity in the large, we may apply Theorem 3.2.1 (or Theorem 3.2.2) to find such matrices B_i, $i = 1, 2, \ldots$. However, there might still exist other matrices B_i, $i = 1, 2, \ldots$, which will fail the conditions of Theorem 3.2.1 (or Theorem 3.2.2) and still achieve the desired equi-attractivity in the large property. In other words, B_i, $i = 1, 2, \ldots$, define a basin of attraction for the trivial solution of (3.9) (or of system (3.27)) which is smaller than the actual basin of attraction of the trivial solution. This will be illustrated in the numerical examples considered later in this section.

Several simulation examples employing a fourth order Runge-Kutta method with step size 10^{-5} will be presented. We shall show, through these numerical examples, how the simulations agree with the theory, although one might still be able to obtain synchronization with choices of B_i which may not satisfy the theory.

Let us demonstrate the applications of Theorem 3.2.2 by considering the impulsive synchronization of two Chua's oscillators. In this case, the parameters of the error dynamics $\mathbf{e}$ between the two Chua's oscillators, described by (3.3), are given by

$$A = \begin{pmatrix} -15 & 15 & 0 \\ 1 & -1 & 1 \\ 0 & -20 & -0.5 \end{pmatrix},$$

$\mathbf{\Omega}(\mathbf{x}) = \Big[(1125/7)x + (675/7)(|x+1| - |x-1|), 0, 0\Big]^T$, $\mathbf{\Phi}(\mathbf{x}, \mathbf{u}) = \mathbf{\Omega}(\mathbf{x}) - \mathbf{\Omega}(\mathbf{u})$, $t_0 = 0$ and $\boldsymbol{\phi}(t - t_0) = \boldsymbol{\phi}(t) = (-2.436, 0.345, 1.639)^T$ (a constant initial function). Hence the parameters of the system are $2\widetilde{\lambda} = 20.16218025$, $||A|| = 26.97909637$ and $||\mathbf{\Phi}(\mathbf{x}, \mathbf{u})|| \leq L_2||\mathbf{e}||$, where $L_2 = 1800/7$ (see [114–116]), i.e., $a = 267.2239473$. Suppose that the delay term $r_i = r$ is constant (i.e., $k_i = k$), $\Delta_i = \Delta = 0.002$ is also a constant and that $B_i := B = -I$, for all $i = 1, 2, \ldots$. Then, from Theorem 3.2.2 and by equation (3.35), $\mathcal{K}_i = 0$, $\mathcal{F}_i^{(j)}$ and $\mathcal{E}_i^{(j)}$ are not applicable (because $k = 1$), $\mathcal{L}_i = \mathcal{L} = re^{a\Delta}(||A|| + L_2)$ and $J_i = J = (\mathcal{L})$, for all $i = 1, 2, \ldots$. Thus the error dynamics $\mathbf{e}$ is equi-attractive in the large or, in other words, the two chaotic systems $\mathbf{x}$ and $\mathbf{u}$ will impulsively synchronize, if

$$r_i \leq r_{\max} \approx \frac{e^{-a\Delta}\gamma}{||A|| + L_2} = 0.002062469033\gamma,$$

which indicates the maximum amount of delay permissible predicted by Theorem 3.2.2. The parameter γ can be chosen to be very close to one but less than one. Let us take $\gamma := 0.999$, then

$$r_i \leq r_{\max} = 0.002060406564.$$

As mentioned earlier, if the delay is less or equal to the above value, solutions will always be equi-attractive in the large. The solutions might still remain equi-attractive in the large for slightly bigger values of $r = r_{\max}$, as indicated in Remark 3.7. But as r gets significantly bigger, the attractivity property will be lost at one point. This is shown clearly in Figure 3.4. The solid curve represents the first component e_1, of the error dynamics $\mathbf{e}$, whereas the dashed curve represents the second component e_2 and the dashed-dotted curve represents the third component e_3. We see that in (a), for $B = -I$ and $r = 0.0011$, solutions quickly converge to zero in 0.031 seconds, as we have predicted. However, in (b), we see that, for $r = 0.0021 > r_{\max}$ equi-attractivity in the large is still achieved and solutions approach zero in 3.1 seconds. Finally, if we increase r significantly beyond this value (i.e., completely outside the actual basin of attraction defined by $B = -I$), such as $r = 0.003$, solutions never approach zero, as shown in (c). This

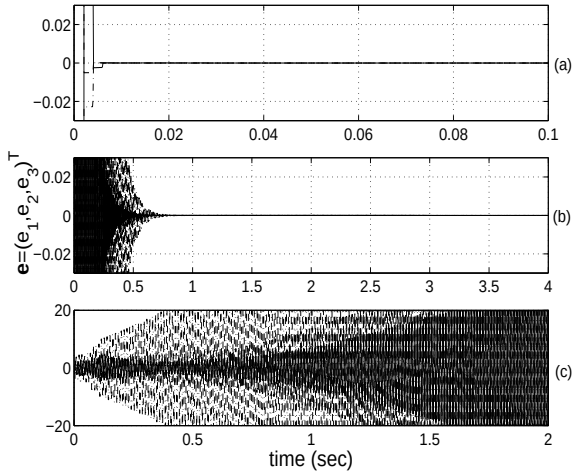

Figure 3.4: Impulsive synchronization of two Chua's oscillators with different delay values: (a) $r = 0.0011$. (b) $r = 0.0021$. (c) $r = 0.003$.

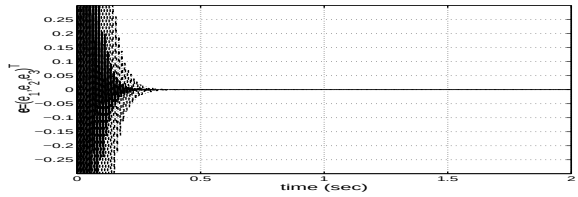

Figure 3.5: Impulsive synchronization of two Chua's oscillators with $B = -0.7I$ and $r = 0.003$.

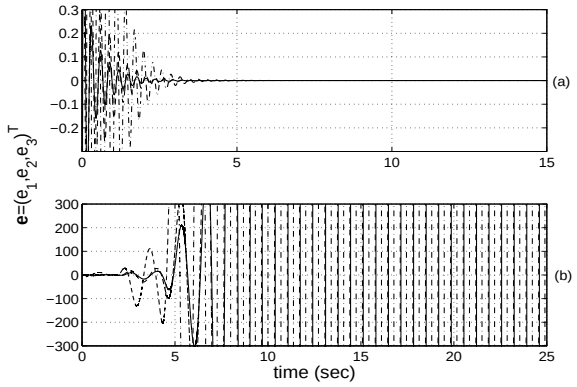

Figure 3.6: Impulsive synchronization of two Chua's oscillators with (a) $B = -0.03I$ and $r = 0.07$; (b) $B = -0.01I$ and $r = 2$.

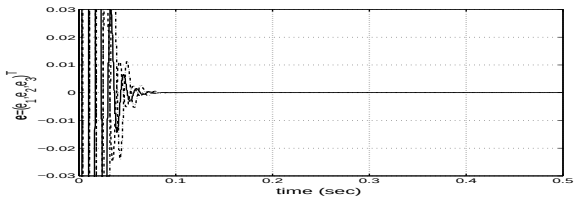

Figure 3.7: Impulsive synchronization of two Chua's oscillators with $B = -I$, $r = 0.003$ and $\Delta = 0.001$.

means that the two Chua's oscillators will never synchronize. On the other hand, if we decrease $||B_i||$ to a value less than 1, say $B = -0.7I$, and for $r = 0.003$, equi-attractivity in the large is achieved, as predicted by Theorem 3.2.2 and as shown in Figure 3.5.

When the delay term r increases to a relatively large value and Δ is kept fixed, we have to choose the matrices $B_i = B$, $i = 1, 2, \ldots$, so that $||B||$ must be small enough. For example, in Figure 3.6 (a), we see that if the delay term r is taken to be 0.07, then we must choose $||B|| = 0.03$ in order to impulsively synchronize the two Chua's oscillators. This is due, as mentioned in Remark 3.5, to the fact that we need to keep the influence of the impulses preceding the i^{th} impulse, for all $i = 1, 2, \ldots$, as small as possible. Furthermore, as we increase the delay term to a large enough value and keep Δ fixed, impulsive synchronization of the two Chua's oscillators will not be achieved no matter how small $||B||$ is. This is illustrated in Figure 3.6 (b), where we can see that for $r = 2$, the error dynamics $\mathbf{e}$ will never become equi-attractive in the large even if we select a matrix B with a very small norm (e.g., in (b), we have taken $B = -0.01I$ and $\Delta = 0.002$). This suggests that there is a lower bound for $||B||$, with Δ being fixed, such that if we choose a matrix B whose norm is below that lower bound, equi-attractivity in the large will fail to hold.

Finally, in Remark 3.4, we have indicated that Theorems 3.2.1 and 3.2.2 predict that the influence of the impulse duration Δ on the amount of delay r in the impulses, which the system can endure, is very significant. For example, reconsidering the above example where r, Δ and B are chosen to be 0.003, 0.002 and $-I$, respectively, we find out that the error dynamics is not equi-attractive in the large. However, reducing the impulse duration to $\Delta = 0.001$, shown in Figure 3.7, solutions to system (3.3) become equi-attractive in the large, as expected.

3.3 Delayed Impulsive Systems with Delayed Linear Impulses

To analyze the dynamics of the impulsive error dynamics, given by equation (3.8), which involves delay in the differential system as well as in the impulses, we shall discuss a general impulsive system which resembles system (3.8).

Consider the system

$$\left\{\begin{array}{rcl} \dot{\mathbf{x}}(t) &=& A\mathbf{x}(t) + \boldsymbol{\Psi}_1(\mathbf{x}(t)) + \boldsymbol{\Psi}_1(\mathbf{x}(t-\widetilde{r})) + \boldsymbol{\Psi}_2(\mathbf{x}(t)),\ t \neq \tau_i \\ \Delta\mathbf{x}(t) &=& B_i\mathbf{x}(t-r_i),\ t = \tau_i\ i = 1,2,\ldots, \\ \mathbf{x}(t) &=& \boldsymbol{\phi}(t-t_0),\ t_0 - \overline{r} \leq t \leq t_0, \end{array}\right\}\ t > t_0 \tag{3.37}$$

where A, $\Delta\mathbf{x}(\tau_i)$, r_i, $i = 1,2,\ldots,$ and $\boldsymbol{\phi}(t)$ are as defined before when considering system (3.9). The only difference in the new model is the presence of constant delay term $\widetilde{r}$ in the differential system. Let $\overline{r} := \max_i\{\widetilde{r}, r_i\} \geq 0$ and $\overline{k}, \widetilde{k}, k_i,\ i = 1,2,\ldots,$ be a set of non-negative integers chosen in such a way that $t_0 < \tau_{i-\overline{k}} < \tau_i - \overline{r} \leq \tau_{i-\overline{k}+1}$, $t_0 < \tau_{i-k_i} < \tau_i - r_i \leq \tau_{i-k_i+1}$ and $t_0 < \tau_{i-\widetilde{k}} < \tau_i - \widetilde{r} \leq \tau_{i-\widetilde{k}+1}$, where $1 \leq k_i + \widetilde{k} \leq i$ and τ_0 is defined to be some point satisfying $t_0 < \tau_0 < \tau_1$. Assume that $\boldsymbol{\Psi}_1$ and $\boldsymbol{\Psi}_2$ are continuous non-linear maps satisfying $||\boldsymbol{\Psi}_m(\mathbf{x})|| \leq \overline{L}_m||\mathbf{x}||$, where $m = 1$ or 2, for some $\overline{L}_1$ and $\overline{L}_2 > 0$, and B_i are, as before, $n \times n$ constant matrices satisfying $||B_i|| < L_1$, for all $i = 1,2,\ldots,$ and for some $L_1 > 0$. This guarantees that, for each $(t_0, \boldsymbol{\phi}) \in \mathbb{R}_+ \times C([-\overline{r}, 0], \mathbb{R}^n)$, there exists a local solution of (3.37) satisfying the initial condition $\mathbf{x}(t) = \boldsymbol{\phi}(t - t_0)$, for $t_0 - \overline{r} \leq t \leq t_0$ [9, 10]. Let $\mathbf{x}(t) := \mathbf{x}(t, t_0, \boldsymbol{\phi})$ be any solution of (3.37) satisfying $\mathbf{x}(t) = \boldsymbol{\phi}(t - t_0)$, for $t_0 - \overline{r} \leq t \leq t_0$, and $\mathbf{x}(t)$ be left continuous at each $\tau_i > t_0$ in the interval of existence, i.e., $\mathbf{x}(\tau_i^-) = \mathbf{x}(\tau_i)$. The definitions of the impulse durations, Δ_i, and the terms δ_i, $i = 1,2,\ldots,$ will remain the same as the we defined in Section 3.2.

Applying Taylor's Theorem, Taylor's Remainder Theorem and system (3.37) in a manner similar to the one used in the previous section, we obtain

$$\begin{aligned} \mathbf{x}(\tau_i - r_i) &= \mathbf{x}(\tau_{i-k_i+1} - \delta_{i-k_i+1}) = \mathbf{x}(\tau_{i-k_i+1}) - \delta_{i-k_i+1}\dot{\mathbf{x}}(t) \\ &= \mathbf{x}(\tau_{i-k_i+1}) - \delta_{i-k_i+1}\left[A\mathbf{x}(t) + \boldsymbol{\Psi}_1(\mathbf{x}(t)) + \boldsymbol{\Psi}_1(\mathbf{x}(t-\widetilde{r})) + \boldsymbol{\Psi}_2(\mathbf{x}(t))\right], \end{aligned}$$

for small δ_{i-k_i+1}, $0 \leq \delta_{i-k_i+1} < \Delta_{i-k_i+1}$, and for some $t \in (\tau_{i-k_i+1} - \delta_{i-k_i+1}, \tau_{i-k_i+1}) \subset (\tau_{i-k_i}, \tau_{i-k_i+1})$, $i = 1,2,\ldots.$ Since

$$||\mathbf{x}(t)|| \leq ||\mathbf{x}_t||_{\widetilde{r}} = ||\mathbf{x}(t+s)||_{\widetilde{r}} \tag{3.38}$$

for every $t \in \mathbb{R}_+$, it follows that

$$\begin{aligned} ||\mathbf{x}(\tau_i) - \mathbf{x}(\tau_i - r_i)|| &= ||\mathbf{x}(\tau_i) - \mathbf{x}(\tau_{i-k_i+1})|| + \delta_{i-k_i+1}(||A|| + \overline{L}_1 + \overline{L}_2)||\mathbf{x}(t)|| + \\ & \quad \delta_{i-k_i+1}\overline{L}_1||\mathbf{x}(t-\widetilde{r})|| \\ &\leq ||\mathbf{x}(\tau_i) - \mathbf{x}(\tau_{i-k_i+1})|| + \delta_{i-k_i+1}(||A|| + 2\overline{L}_1 + \overline{L}_2)||\mathbf{x}_t||_{\widetilde{r}}, \end{aligned} \tag{3.39}$$

for some $t \in (\tau_{i-k_i+1} - \delta_{i-k_i+1}, \tau_{i-k_i+1})$ and for $i = 1, 2, \ldots$. In addition, in a similar fashion as before, the Fundamental Theorem of Calculus implies, for all $i = 1, 2, \ldots$, that

$$\mathbf{x}(\tau_i) - \mathbf{x}(\tau_{i-1}^+) = \int_{\tau_{i-1}^+}^{\tau_i} \dot{\mathbf{x}}(t)dt.$$

It follows from inequality (3.11) and system (3.37) that

$$\begin{aligned} ||\mathbf{x}(\tau_i) - \mathbf{x}(\tau_{i-1}^+)||^2 &= ||\int_{\tau_{i-1}^+}^{\tau_i} \dot{\mathbf{x}}(t)dt||^2 \leq \Delta_i \int_{\tau_{i-1}^+}^{\tau_i} ||\dot{\mathbf{x}}(t)||^2 dt \\ &\leq \Delta_i(||A|| + \overline{L}_1 + \overline{L}_2)^2 \int_{\tau_{i-1}^+}^{\tau_i} ||\mathbf{x}(t)||^2 dt + \Delta_i \overline{L}_1^2 \int_{\tau_{i-1}^+}^{\tau_i} ||\mathbf{x}(t-\widetilde{r})||^2 dt \\ &\leq \Delta_i(||A|| + \overline{L}_1 + \overline{L}_2)^2 \int_{\tau_{i-1}^+}^{\tau_i} ||\mathbf{x}_t||_{\widetilde{r}}^2 dt + \Delta_i \overline{L}_1^2 \int_{\tau_{i-1}^+}^{\tau_i} ||\mathbf{x}_t||_{\widetilde{r}}^2 dt \\ &\leq \Delta_i \left[(||A|| + \overline{L}_1 + \overline{L}_2)^2 + \overline{L}_1^2\right] \int_{\tau_{i-1}^+}^{\tau_i} ||\mathbf{x}_t||_{\widetilde{r}}^2 dt, \end{aligned} \tag{3.40}$$

for $i = 1, 2, \ldots$.

The importance of inequalities (3.39) and (3.40) will become evident in the proof of the next theorem which will give the conditions under which system (3.37) is equi-attractive in the large.

Theorem 3.3.1 *Let $2\widetilde{\lambda}$ be the largest eigenvalue of $A^T + A$, $\Delta_i \leq \Delta$ for some $\Delta > 0$,*

$$\mathcal{K}_i' := \exp\left[\overline{a}(\tau_i - \tau_{i-1-\widetilde{k}}) + \overline{L}_1(\tau_i - \tau_{i-1-\widetilde{k}})e^{\overline{a}(\tau_i - \tau_{i-1-\widetilde{k}})}\right]||I + B_i||, \tag{3.41}$$

$$\Gamma_i^{(j)} := \Delta_j \mathcal{K}'_j ||B_i|| \left[(||A|| + \overline{L}_1 + \overline{L}_2)^2 + \overline{L}_1^2 \right]^{1/2}, \;\; i - k_i + 2 \leq j \leq i, \;\; k_i + \widetilde{k} > 1, \tag{3.42}$$

$$\Upsilon_i^{(j)} := \mathcal{G}'_j ||B_i|| ||B_j||, \;\; i - k_i + 1 \leq j \leq i - 1, \;\; k_i + \widetilde{k} > 1, \tag{3.43}$$

$$\mathcal{L}'_i := \delta_{i-k_i+1} \mathcal{G}'_i ||B_i|| (||A|| + 2\overline{L}_1 + \overline{L}_2), \tag{3.44}$$

and

$$\mathcal{G}'_i := \exp\left\{ \overline{a}(\tau_i - \tau_{i-k_i-\widetilde{k}}) + \frac{\overline{L}_1}{\overline{a}} e^{\overline{a}(\tau_i - \tau_{i-k_i-\widetilde{k}})} - \frac{\overline{L}_1}{\overline{a}} \right\}, \tag{3.45}$$

$i = 1, 2, \ldots,$ *where* $\overline{a} := \widetilde{\lambda} + \overline{L}_1 + \overline{L}_2 > 0$ *and* I *is the identity matrix with the appropriate dimension. Let* $\overline{J}_i$ *be the* $(i - \overline{p}_i) \times (i - \overline{p}_i)$ *matrix (where* $\overline{p}_i = \max(0, \overline{q}_i)$ *and* $\overline{q}_i = \min(i - k_i - \widetilde{k}, i - 1 - k_{i-1} - \widetilde{k}, i - 2 - k_{i-2} - \widetilde{k}, \ldots, i - k_i + 1 - k_{i-k_i+1} - \widetilde{k})$ *given by*

$$\begin{cases} \overline{J}_i \;\; := (\mathcal{K}'_i + \mathcal{L}'_i), \text{ if } i = 1 \text{ or } k_i + \widetilde{k} = 1 \text{ (i.e., } \overline{p}_i = i - k_i - \widetilde{k}), \text{ for some } i = 2, 3, \ldots, \text{ or} \\ \\ \overline{J}_i \;\; := \begin{pmatrix} 0 & 1 & 0 & \cdots & 0 & 0 \\ 0 & 0 & 1 & \cdots & 0 & 0 \\ 0 & 0 & 0 & \cdots & 0 & 0 \\ \vdots & \vdots & \vdots & \ddots & \vdots & \vdots \\ 0 & 0 & 0 & \cdots & 0 & 1 \\ \overline{\alpha}_i^{(1)} & \overline{\alpha}_i^{(2)} & \overline{\alpha}_i^{(3)} & \cdots & \overline{\alpha}_i^{(i-\overline{p}_i-1)} & \overline{\alpha}_i^{(i-\overline{p}_i)} \end{pmatrix}, \text{ if } k_i > 1, \text{ for some } i = 2, 3, \ldots, \end{cases} \tag{3.46}$$

where

$$\overline{\alpha}_i^{(j)} := \sum_{S_{i,j}} \Upsilon_i^{(S_{i,j})}, \qquad 1 \leq j \leq i - k_i - \widetilde{k} - \overline{p}_i,$$

$$\overline{\alpha}_i^{(i-k_i-\widetilde{k}-\overline{p}_i+1)} := \mathcal{L}'_i + \sum_{S_{i,i-k_i-\widetilde{k}-\overline{p}_i+1}} \Upsilon_i^{(S_{i,i-k_i-\widetilde{k}-\overline{p}_i+1})},$$

$$\overline{\alpha}_i^{(j)} := \Gamma_i^{(j+\overline{p}_i)} + \sum_{S_{i,j}} \Upsilon_i^{(S_{i,j})}, \qquad i - k_i - \widetilde{k} - \overline{p}_i + 2 \leq j \leq i - \widetilde{k} - \overline{p}_i - 1,$$

$$\overline{\alpha}_i^{(i-\widetilde{k}-\overline{p}_i)} := \mathcal{K}'_i + \Gamma_i^{(i)},$$

$$\overline{\alpha}_i^{(j)} := 0 \qquad i - \widetilde{k} - \overline{p}_i \leq j \leq i - \overline{p}_i$$

(the bounds on the set of integers $S_{i,j}$*, which could be empty, depend on the impulse* i *and the entry* j *which both depend on the delay terms* r_i*, for all* i *such that* $k_i + \widetilde{k} > 1$*). Then system (3.37)*

is equi-attractive in the large if each eigenvalue, $\lambda^{(i)}$, of $\overline{J}_i$ satisfies $|\lambda^{(i)}| \leq \overline{\gamma}$, where $0 \leq \overline{\gamma} < 1$, $i = 1, 2, \ldots$ (i.e., the matrix $\overline{J}_i$ can define a contraction linear mapping).

Proof: We shall prove that under the assumptions of Theorem 3.3.1, $||\mathbf{x}_t||_{\widetilde{r}} \to 0$, as $t \to \infty$. Thus, in view of inequality (3.38), we may immediately conclude that $||\mathbf{x}(t)|| \to 0$, as $t \to \infty$ which means that system (3.37) is equi-attractive in the large. By considering the Euclidean norm $||\mathbf{x}(t)|| = (\mathbf{x}^T\mathbf{x})^{1/2} \in \nu_0(0)$, as our Lyapunov function, we have

$$\begin{aligned} D^+\big[||\mathbf{x}||\big] &= \frac{1}{2}(\mathbf{x}^T\mathbf{x})^{-1/2}(\dot{\mathbf{x}}^T\mathbf{x} + \mathbf{x}^T\dot{\mathbf{x}}) \\ &= \frac{1}{2}\frac{1}{||\mathbf{x}||}\Big[\mathbf{x}^T(A^T + A)\mathbf{x} + 2\mathbf{\Psi}_1(\mathbf{x})^T\mathbf{x} + 2\mathbf{\Psi}_1(\mathbf{x}(t-\widetilde{r}))^T\mathbf{x} + 2\mathbf{\Psi}_2(\mathbf{x})^T\mathbf{x}\Big] \\ &\leq \frac{1}{2||\mathbf{x}||}\Big[2\widetilde{\lambda}||\mathbf{x}||^2 + 2\overline{L}_1||\mathbf{x}||^2 + 2\overline{L}_2||\mathbf{x}||^2 + 2||\mathbf{\Psi}_1(\mathbf{x}(t-\widetilde{r}))||||\mathbf{x}||\Big] \\ &\leq \Big(\widetilde{\lambda} + \overline{L}_1 + \overline{L}_2\Big)||\mathbf{x}|| + \overline{L}_1||\mathbf{x}(t-\widetilde{r})||. \end{aligned}$$

i.e., $D^+\big[||\mathbf{x}(t)||\big] \leq \overline{a}||\mathbf{x}(t)|| + \overline{L}_1||\mathbf{x}(t-\widetilde{r})||$, which implies that

$$D^+\big[||\mathbf{x}(t)||\big] - \overline{a}||\mathbf{x}(t)|| \leq \overline{L}_1||\mathbf{x}(t-\widetilde{r})||.$$

Multiplying both sides of the above inequality by $\exp(-\overline{a}t)$, we obtain

$$e^{-\overline{a}t}D^+\big[||\mathbf{x}(t)||\big] - \overline{a}e^{-\overline{a}t}||\mathbf{x}(t)|| \leq \overline{L}_1e^{-\overline{a}t}||\mathbf{x}(t-\widetilde{r})||.$$

This implies that

$$D^+\Big[e^{-\overline{a}t}||\mathbf{x}(t)||\Big] \leq \overline{L}_1e^{-\overline{a}t}||\mathbf{x}(t-\widetilde{r})||. \tag{3.47}$$

Therefore, for every $t \in (\tau_i - r_i, \tau_i] \subset (\tau_{i-k_i}, \tau_i]$, for every $s \in [-\widetilde{r}, 0]$ and for every $i = 1, 2, \ldots,$

we have $t+s \in (\tau_{i-k_i} - \widetilde{r}, \tau_i] \subset (\tau_{i-k_i-\widetilde{k}}, \tau_i]$, where $t - \widetilde{r} > \tau_{i-k_i-\widetilde{k}}$, and, by (3.47),

$$\int\limits_{\tau^+_{i-k_i-\widetilde{k}}}^{t+s} D^+\Big[e^{-\overline{a}\tau}||\mathbf{x}(\tau)||\Big]d\tau \le \overline{L}_1 \int\limits_{\tau^+_{i-k_i-\widetilde{k}}}^{t+s} e^{-\overline{a}\tau}||\mathbf{x}(\tau-\widetilde{r})||d\tau \quad \Longrightarrow$$

$$e^{-\overline{a}(t+s)}||\mathbf{x}(t+s)|| - e^{-\overline{a}\tau_{i-k_i-\widetilde{k}}}||\mathbf{x}(\tau^+_{i-k_i-\widetilde{k}})|| \le \overline{L}_1 \int\limits_{\tau^+_{i-k_i-\widetilde{k}}}^{t+s} e^{-\overline{a}\tau}||\mathbf{x}(\tau-\widetilde{r})||d\tau \quad \Longrightarrow$$

$$||\mathbf{x}(t+s)|| \le e^{\overline{a}(t+s-\tau_{i-k_i-\widetilde{k}})}||\mathbf{x}(\tau^+_{i-k_i-\widetilde{k}})|| + \overline{L}_1 \int\limits_{\tau^+_{i-k_i-\widetilde{k}}}^{t+s} e^{\overline{a}(t+s-\tau)}||\mathbf{x}(\tau-\widetilde{r})||d\tau \quad \Longrightarrow$$

$$||\mathbf{x}_t(s)|| \le e^{\overline{a}(t+s-\tau_{i-k_i-\widetilde{k}})}||\mathbf{x}(\tau^+_{i-k_i-\widetilde{k}})|| + \overline{L}_1 \int\limits_{\tau^+_{i-k_i-\widetilde{k}}}^{t+s} e^{\overline{a}(t+s-\tau)}||\mathbf{x}_\tau||_{\widetilde{r}}d\tau \quad \Longrightarrow$$

$$\sup_{s\in[-\widetilde{r},0]}||\mathbf{x}_t(s)|| \le \sup_{s\in[-\widetilde{r},0]}\left\{ e^{\overline{a}(t+s-\tau_{i-k_i-\widetilde{k}})}||\mathbf{x}(\tau^+_{i-k_i-\widetilde{k}})|| + \overline{L}_1 \int\limits_{\tau^+_{i-k_i-\widetilde{k}}}^{t+s} e^{\overline{a}(t+s-\tau)}||\mathbf{x}_\tau||_{\widetilde{r}}d\tau \right\}$$

$$= e^{\overline{a}(t-\tau_{i-k_i-\widetilde{k}})}||\mathbf{x}(\tau^+_{i-k_i-\widetilde{k}})|| + \overline{L}_1 \int\limits_{\tau^+_{i-k_i-\widetilde{k}}}^{t} e^{\overline{a}(t-\tau)}||\mathbf{x}_\tau||_{\widetilde{r}}d\tau$$

$$\le e^{\overline{a}(\tau_i-\tau_{i-k_i-\widetilde{k}})}||\mathbf{x}(\tau^+_{i-k_i-\widetilde{k}})|| + \overline{L}_1 \int\limits_{\tau^+_{i-k_i-\widetilde{k}}}^{t} e^{\overline{a}(t-\tau)}||\mathbf{x}_\tau||_{\widetilde{r}}d\tau.$$

Thus

$$||\mathbf{x}_t||_{\widetilde{r}} \le e^{\overline{a}(\tau_i-\tau_{i-k_i-\widetilde{k}})}||\mathbf{x}(\tau^+_{i-k_i-\widetilde{k}})|| + \overline{L}_1 \int\limits_{\tau^+_{i-k_i-\widetilde{k}}}^{t} e^{\overline{a}(t-\tau)}||\mathbf{x}_\tau||_{\widetilde{r}}d\tau.$$

Applying Gronwall's Lemma [77] and equation (3.45), we obtain

$$
\begin{aligned}
||\mathbf{x}_t||_{\widetilde{r}} &\leq e^{\overline{a}(\tau_i-\tau_{i-k_i-\widetilde{k}})}||\mathbf{x}(\tau^+_{i-k_i-\widetilde{k}})|| \exp\left[\overline{L}_1 \int\limits_{\tau^+_{i-k_i-\widetilde{k}}}^{t} e^{\overline{a}(t-\tau)}d\tau\right] \\
&= e^{\overline{a}(\tau_i-\tau_{i-k_i-\widetilde{k}})}||\mathbf{x}(\tau^+_{i-k_i-\widetilde{k}})|| \exp\left\{-\frac{\overline{L}_1}{\overline{a}}\left[1-e^{\overline{a}(t-\tau_{i-k_i-\widetilde{k}})}\right]\right\} \\
&\leq \exp\left\{\overline{a}(\tau_i-\tau_{i-k_i-\widetilde{k}}) + \frac{\overline{L}_1}{\overline{a}}e^{\overline{a}(\tau_i-\tau_{i-k_i-\widetilde{k}})} - \frac{\overline{L}_1}{\overline{a}}\right\}||\mathbf{x}(\tau^+_{i-k_i-\widetilde{k}})|| \\
&= \mathcal{G}'_i||\mathbf{x}(\tau^+_{i-k_i-\widetilde{k}})||.
\end{aligned}
$$

By inequality (3.38), it follows, for every $t \in (\tau_i - r_i, \tau_i] \subset (\tau_{i-k_i}, \tau_i]$ and $i = 1, 2, \ldots,$ that

$$
||\mathbf{x}(t)|| \leq ||\mathbf{x}_t||_{\widetilde{r}} \leq \mathcal{G}'_i||\mathbf{x}(\tau^+_{i-k_i-\widetilde{k}})||. \tag{3.48}
$$

Similarly, by inequality (3.47) and for all $t \in (\tau_{i-1}, \tau_i]$, $s \in [-\widetilde{r}, 0]$ and $i = 1, 2, \ldots,$ where $t+s \in (\tau_{i-1} - \widetilde{r}, \tau_i] \subset (\tau_{i-1-\widetilde{k}}, \tau_i]$, we have

$$
\int\limits_{\tau^+_{i-1-\widetilde{k}}}^{t+s} D^+\left[e^{-\overline{a}\tau}||\mathbf{x}(\tau)||\right]d\tau \leq \overline{L}_1 \int\limits_{\tau^+_{i-1-\widetilde{k}}}^{t+s} e^{-\overline{a}\tau}||\mathbf{x}(\tau-\widetilde{r})||d\tau \qquad \Longrightarrow
$$

$$
e^{-\overline{a}(t+s)}||\mathbf{x}(t+s)|| - e^{-\overline{a}\tau_{i-1-\widetilde{k}}}||\mathbf{x}(\tau^+_{i-1-\widetilde{k}})|| \leq \overline{L}_1 \int\limits_{\tau^+_{i-1-\widetilde{k}}}^{t+s} e^{-\overline{a}\tau}||\mathbf{x}(\tau-\widetilde{r})||d\tau \qquad \Longrightarrow
$$

$$
||\mathbf{x}_t(s)|| \leq e^{\overline{a}(t+s-\tau_{i-1-\widetilde{k}})}||\mathbf{x}(\tau^+_{i-1-\widetilde{k}})|| + \overline{L}_1 \int\limits_{\tau^+_{i-1-\widetilde{k}}}^{t+s} e^{\overline{a}(t+s-\tau)}||\mathbf{x}_\tau||_{\widetilde{r}}d\tau \qquad \Longrightarrow
$$

$$
\sup_{s\in[-\widetilde{r},0]}||\mathbf{x}_t(s)|| \leq \sup_{s\in[-\widetilde{r},0]}\left\{e^{\overline{a}(t+s-\tau_{i-1-\widetilde{k}})}||\mathbf{x}(\tau^+_{i-1-\widetilde{k}})|| + \overline{L}_1 \int\limits_{\tau^+_{i-1-\widetilde{k}}}^{t+s} e^{\overline{a}(t+s-\tau)}||\mathbf{x}_\tau||_{\widetilde{r}}d\tau\right\} \qquad \Longrightarrow
$$

$$
\begin{aligned}
||\mathbf{x}_t||_{\widetilde{r}} &\leq e^{\overline{a}(t-\tau_{i-1-\widetilde{k}})}||\mathbf{x}(\tau^+_{i-1-\widetilde{k}})|| + \overline{L}_1 \int\limits_{\tau^+_{i-1-\widetilde{k}}}^{t} e^{\overline{a}(t-\tau)}||\mathbf{x}_\tau||_{\widetilde{r}} d\tau \\
&\leq e^{\overline{a}(\tau_i-\tau_{i-1-\widetilde{k}})}||\mathbf{x}(\tau^+_{i-1-\widetilde{k}})|| + \overline{L}_1 \int\limits_{\tau^+_{i-1-\widetilde{k}}}^{t} e^{\overline{a}(\tau_i-\tau)}||\mathbf{x}_\tau||_{\widetilde{r}} d\tau \\
&\leq e^{\overline{a}(\tau_i-\tau_{i-1-\widetilde{k}})}||\mathbf{x}(\tau^+_{i-1-\widetilde{k}})|| + \overline{L}_1 e^{\overline{a}(\tau_i-\tau_{i-1-\widetilde{k}})} \int\limits_{\tau^+_{i-1-\widetilde{k}}}^{t} ||\mathbf{x}_\tau||_{\widetilde{r}} d\tau.
\end{aligned}
$$

It follows, by Gronwall's Lemma, that, for all $i = 1, 2, \ldots,$

$$
||\mathbf{x}_t||_{\widetilde{r}} \leq \exp\left[\overline{a}(\tau_i - \tau_{i-1-\widetilde{k}}) + \overline{L}_1(\tau_i - \tau_{i-1-\widetilde{k}})e^{\overline{a}(\tau_i-\tau_{i-1-\widetilde{k}})}\right]||\mathbf{x}(\tau^+_{i-1-\widetilde{k}})||.
$$

Passing to the limit as $t \to \tau_i$ and by applying inequality (3.38), the latter inequality becomes, for $i = 1, 2, \ldots,$

$$
||\mathbf{x}(\tau_i)|| \leq ||\mathbf{x}_{\tau_i}||_{\widetilde{r}} \leq \exp\left[\overline{a}(\tau_i - \tau_{i-1-\widetilde{k}}) + \overline{L}_1(\tau_i - \tau_{i-1-\widetilde{k}})e^{\overline{a}(\tau_i-\tau_{i-1-\widetilde{k}})}\right]||\mathbf{x}(\tau^+_{i-1-\widetilde{k}})||. \tag{3.49}
$$

Let us first consider the case when $i = 1$. We have, by inequalities (3.38), (3.39) and (3.48), for some $t^* \in (\tau_1 - r_1, \tau_1)$,

$$
\begin{aligned}
||\mathbf{x}(\tau_1^+)|| &= ||\mathbf{x}(\tau_1) + B_1\mathbf{x}(\tau_1 - r_1)|| \\
&\leq ||I + B_1||||\mathbf{x}(\tau_1)|| + ||B_1||||\mathbf{x}(\tau_1) - \mathbf{x}(\tau_1 - r_1)|| \\
&= e^{\overline{a}\Delta_1}||I + B_1||||\mathbf{x}(\tau_0^+)|| + r_1||B_1||(||A|| + \overline{L}_1 + \overline{L}_2)||\mathbf{x}(t^*)|| + r_1\overline{L}_1||B_1||||\mathbf{x}(t^* - \widetilde{r})|| \\
&\leq e^{\overline{a}\Delta_1}||I + B_1||||\mathbf{x}(\tau_0^+)|| + r_1||B_1||(||A|| + 2\overline{L}_1 + \overline{L}_2)||\mathbf{x}_{t^*}||_{\widetilde{r}} \\
&\leq e^{\overline{a}\Delta_1}||I + B_1||||\mathbf{x}(\tau_0^+)|| + r_1\mathcal{G}_1'||B_1||(||A|| + 2\overline{L}_1 + \overline{L}_2)||\mathbf{x}(\tau_0^+)||,
\end{aligned}
$$

since $\tau_0 < \tau_1 - r_1$ (notice again that $\mathbf{x}(\tau_0^+) = \mathbf{x}(\tau_0)$). Hence equations (3.41) and (3.43) imply that

$$
||\mathbf{x}(\tau_1^+)|| \leq (\mathcal{K}_1' + \mathcal{L}_1')||\mathbf{x}(\tau_0^+)||. \tag{3.50}
$$

Similarly, if $k_i + \widetilde{k} = 1$, for some $i = 2, 3, \ldots$, we may also conclude that

$$||\mathbf{x}(\tau_i^+)|| \leq (\mathcal{K}_i' + \mathcal{L}_i')||\mathbf{x}(\tau_{i-1}^+)||. \tag{3.51}$$

On the other hand, if $k_i > 1$, for some $i = 2, 3, \ldots$, we have, by system (3.37), equations (3.41) and (3.44) and inequalities (3.38), (3.39) and (3.49), for some $t \in (\tau_{i-k_i+1} - \delta_{i-k_i+1}, \tau_{i-k_i+1})$, $0 \leq \delta_{i-k_i+1} < \Delta_{i-k_i+1}$, the following.

$$\begin{aligned}
||\mathbf{x}(\tau_i^+)|| &= ||\mathbf{x}(\tau_i) + B_i\mathbf{x}(\tau_i - r_i)|| \\
&\leq ||I + B_i||||\mathbf{x}(\tau_i)|| + ||B_i||||\mathbf{x}(\tau_i) - \mathbf{x}(\tau_i - r_i)|| \\
&\leq ||I + B_i||||\mathbf{x}(\tau_i)|| + ||B_i|| \left[||\mathbf{x}(\tau_i) - \mathbf{x}(\tau_{i-k_i+1})|| + \delta_{i-k_i+1}(||A|| + 2\overline{L}_1 + \overline{L}_2)||\mathbf{x}_t||_{\widetilde{r}}\right] \\
&\leq ||I + B_i||||\mathbf{x}(\tau_i)|| + ||B_i||||\mathbf{x}(\tau_i) - \mathbf{x}(\tau_{i-k_i+1})||+ \\
&\quad \delta_{i-k_i+1}\mathcal{G}_i'||B_i||(||A|| + 2\overline{L}_1 + \overline{L}_2)||\mathbf{x}(\tau_{i-k_i-\widetilde{k}})|| \\
&\leq \mathcal{K}_i'||\mathbf{x}(\tau_{i-1-\widetilde{k}})|| + ||B_i||||\mathbf{x}(\tau_i) - \mathbf{x}(\tau_{i-k_i+1})|| + \mathcal{L}_i'||\mathbf{x}(\tau_{i-k_i-\widetilde{k}})||.
\end{aligned} \tag{3.52}$$

But, in the proof of Theorem 3.2.1, we proved that

$$||\mathbf{x}(\tau_i) - \mathbf{x}(\tau_{i-k_i+1})|| \leq \sum_{j=i-k_i+2}^{i} ||\mathbf{x}(\tau_j) - \mathbf{x}(\tau_{j-1}^+)|| + \sum_{j=i-k_i+1}^{i-1} ||B_j||||\mathbf{x}(\tau_j - r_j)||.$$

Therefore, by inequalities (3.40), (3.48) and (3.49), it follows that

$$\begin{aligned}
||\mathbf{x}(\tau_i) - \mathbf{x}(\tau_{i-k_i+1})|| &= \sum_{j=i-k_i+2}^{i} \Delta_j^{1/2} \left[(||A|| + \overline{L}_1 + \overline{L}_2)^2 + \overline{L}_1^2 \right]^{1/2} \left\{ \int_{\tau_{j-1}^+}^{\tau_j} ||\mathbf{x}_t||_{\widetilde{r}}^2 dt \right\}^{1/2} \\
&\quad + \sum_{j=i-k_i+1}^{i-1} ||B_j|| ||\mathbf{x}(\tau_{j-k_j+1} - \delta_{j-k_j+1})|| \\
&\leq \sum_{j=i-k_i+2}^{i} \Delta_j^{1/2} \left[(||A|| + \overline{L}_1 + \overline{L}_2)^2 + \overline{L}_1^2 \right]^{1/2} \left\{ \int_{\tau_{j-1}^+}^{\tau_j} \mathcal{K}_j' ||\mathbf{x}(\tau_{j-1-\widetilde{k}}^+)||^2 dt \right\}^{1/2} \\
&\quad + \sum_{j=i-k_i+1}^{i-1} \mathcal{G}_j' ||B_j|| ||\mathbf{x}(\tau_{j-k_j-\widetilde{k}}^+)|| \\
&= \sum_{j=i-k_i+2}^{i} \Delta_j \mathcal{K}_j' \left[(||A|| + \overline{L}_1 + \overline{L}_2)^2 + \overline{L}_1^2 \right]^{1/2} ||\mathbf{x}(\tau_{j-1}^+)|| + \\
&\quad \sum_{j=i-k_i+1}^{i-1} \mathcal{G}_j' ||B_j|| ||\mathbf{x}(\tau_{j-k_j-\widetilde{k}}^+)||.
\end{aligned}$$

Hence the latter inequality, together with inequality (3.52) and equations (3.41), (3.42), (3.43), (3.44) and (3.45), imply that, for all i such that $k_i > 1$,

$$\begin{aligned}
||\mathbf{x}(\tau_i^+)|| &\leq \mathcal{K}_i' ||\mathbf{x}(\tau_{i-1-\widetilde{k}}^+)|| + \sum_{j=i-k_i+2}^{i} \Gamma_i^{(j)} ||\mathbf{x}(\tau_{j-1-\widetilde{k}}^+)|| + \sum_{j=i-k_i+1}^{i-1} \Upsilon_i^{(j)} ||\mathbf{x}(\tau_{j-k_j-\widetilde{k}}^+)|| \\
&\quad + \mathcal{L}_i' ||\mathbf{x}(\tau_{i-k_i-\widetilde{k}}^+)||.
\end{aligned} \tag{3.53}$$

Since $\overline{q}_i = \min(i - k_i - \widetilde{k}, i - 1 - k_{i-1} - \widetilde{k}, \ldots, i - k_i + 1 - k_{i-k_i+1} - \widetilde{k})$ and $\overline{p}_i = \max(0, \overline{q}_i)$, we may, as in the proof of Theorem 3.2.1, define the quantities $v_1(\overline{p}_i) := ||\mathbf{x}(\tau_{\overline{p}_i}^+)||$, $v_2(\overline{p}_i) := ||\mathbf{x}(\tau_{\overline{p}_i+1}^+)||$, $\ldots$, $v_{i-\overline{p}_i}(\overline{p}_i) := ||\mathbf{x}(\tau_{i-1}^+)||$. It follows that

$$v_j(\overline{p}_i + 1) = ||\mathbf{x}(\tau_{\overline{p}_i+j}^+)|| = v_{j+1}(\overline{p}_i), \tag{3.54}$$

where $1 \leq j \leq i - \overline{p}_i$. Now taking inequality (3.53) and equation (3.54) into consideration, we have

$$\begin{aligned} v_{i-\overline{p}_i}(\overline{p}_i + 1) &= v_{i-\overline{p}_i+1}(\overline{p}_i) = ||\mathbf{x}(\tau_i^+)|| \\ &\leq \mathcal{K}_i' v_{i-\overline{p}_i-\widetilde{k}}(\overline{p}_i) + \sum_{j=i-k_i+2}^{i} \gamma_i^{(j)} v_{j-\overline{p}_i-\widetilde{k}}(\overline{p}_i) + \sum_{i-k_i+1}^{i-1} \Upsilon_i^{(j)} v_{j+1-k_j-\overline{p}_i-\widetilde{k}}(\overline{p}_i) + \\ &\quad \mathcal{L}_i' v_{i-k_i-\overline{p}_i+1-\widetilde{k}}(\overline{p}_i). \end{aligned}$$

Let $\mathbf{v}(\overline{p}_i) := (v_1(\overline{p}_i), v_2(\overline{p}_i), \ldots, v_{i-\overline{p}_i}(\overline{p}_i))^T$. Then, by equation (3.46), the system of difference inequalities obtained above, including inequalities (3.50) and (3.51), can be written in a vector form as

$$\mathbf{v}(\overline{p}_i + 1) \leq \overline{J}_i \mathbf{v}(\overline{p}_i), \tag{3.55}$$

for all $i = 1, 2, \ldots$, with the convention that the same inequality holds between the corresponding components. Thus if each eigenvalue, $\lambda^{(i)}$, of $\overline{J}_i$, $i = 1, 2, \ldots$, satisfies $|\lambda^{(i)}| \leq \overline{\gamma}$, $0 \leq \overline{\gamma} < 1$, then, by (3.55), it follows that $\lim_{s\to\infty} \mathbf{v}(\overline{p}_i + s) = \mathbf{0}$, since $k_i < \overline{k}$. Furthermore, $v_{i-\overline{p}_i}(\overline{p}_i + s) = ||\mathbf{x}(\tau_{i+s-1}^+)||$, for $i = 1, 2, \ldots$. Therefore if we let $\ell = i + s - 1$, we can conclude that

$$\lim_{\ell\to\infty} ||\mathbf{x}(\tau_\ell^+)|| = \lim_{s\to\infty} ||\mathbf{x}(\tau_{i+s-1}^+)|| = \lim_{s\to\infty} v_{i-\overline{p}_i}(\overline{p}_i + s) = 0.$$

Therefore, from inequality (3.48), we can further conclude that, for every $t \in (\tau_{i-\widetilde{k}}, \tau_i]$ and $i = 1, 2, \ldots$,

$$||\mathbf{x}(t)|| \leq \mathcal{G}_i' ||\mathbf{x}(\tau_{i-k_i-\widetilde{k}}^+)|| \leq \mathcal{G}' ||\mathbf{x}(\tau_{i-1}^+)|| \to 0,$$

as $i \to \infty$, where

$$\mathcal{G}' = \exp\left\{ 2\overline{k}\overline{a}\Delta + \frac{\overline{L}_1}{\overline{a}} - e^{2\overline{k}\overline{a}} \frac{\overline{L}_1}{\overline{a}} \right\}.$$

In other words $||\mathbf{x}(t)|| \to 0$, as $t \to \infty$. Thus solutions to system (3.37) are equi-attractive in the large, as required. □

With the absence of the delay term $\widetilde{r}$ from (3.37), the resulting system is an impulsive system with delayed impulses, given by system (3.9). This means that if $\widetilde{r} = 0$, then Theorem 3.3.1 will reduce to Theorem 3.2.1, except that Theorem 3.3.1 produces an estimate on the upper bound of the maximum delay that system (3.9) can endure which is smaller than the estimate Theorem 3.2.1 produces. We just mention here that Theorem 3.3.1 can be applied to system

(3.9), by comparing system (3.9) with (3.37). In this case, we have $\widetilde{r} = 0$, $\widetilde{k} = 0$, $\mathbf{\Psi}_1(\mathbf{x}) = \mathbf{0}$ and $\mathbf{\Psi}_2(\mathbf{x}) = \mathbf{\Phi}(\mathbf{x})$, which means that $L_1 = 0$ and $\overline{L}_2 = L_2$. With these values, the equi-attractivity properties of system (3.9) can be studied using the result of Theorem 3.3.1.

Remark 3.8: If $k_i + \widetilde{k} = 1$, for some $i = 1, 2, \ldots$, then the matrix $\overline{J}_i$ corresponding to this i^{th} impulse will be a 1×1 matrix given by $\overline{J}_i = (\mathcal{K}_i' + \mathcal{L}_i')$. However, if $k_i + \widetilde{k} > 1$, for some $i = 2, 3, \ldots$, then the eigenvalues of the matrix $\overline{J}_i$, defined by equation (3.46), corresponding to the i^{th} impulse, are the roots of the characteristic equation, given by

$$\det(\lambda^{(i)} I - \overline{J}_i) = \left(\lambda^{(i)}\right)^{i-\overline{p}_i} - \sum_{j=1}^{i-\overline{p}_i} \left(\lambda^{(i)}\right)^{i-\overline{p}_i-j} \overline{\alpha}_i^{(i-\overline{p}_i+1-j)} = 0, \tag{3.56}$$

which is similar to the structure of the characteristic equation given by equation (3.35). We may find the roots of this characteristic equation numerically and choose the matrices B_i, as before, in such a way that all the eigenvalues $\lambda^{(i)}$, will lie inside a circle of radius $\overline{\gamma}$. The choice of k_i, $i = 2, 3, \ldots$, is determined by trial and error.

Remark 3.9: Although, intuitively, one may think that the delay term $\widetilde{r}$ has no influence on the dynamics of the impulsive system, Theorem 3.3.1 indicates that the value of $\mathcal{G}_i'$ and the dimension of the matrix $\overline{J}_i$, for $i = 1, 2, \ldots$, will increase as the value $\widetilde{r}$ increases. Thus the upper bound on the range of values of r_i will change accordingly so that system (3.37) will remain equi-attractive in the large. We will show, through several numerical examples that when considering impulsive synchronization of hyperchaotic systems, the larger the delay term $\widetilde{r}$, the smaller the upper bound on the delay terms r_i, $i = 1, 2, \ldots$, in order to obtain identical synchronization.

Remark 3.10: The conditions of Theorem 3.3.1, as for Theorem 3.2.1, are all sufficient conditions but not necessary, i.e., system (3.37) may remain equi-attractive in the large, although one of the conditions of Theorem 3.3.1 may fail. This is also illustrated through several numerical examples employing impulsive synchronization.

We shall now present several examples to investigate impulsive synchronization of two identical four-dimensional hyperchaotic systems with the presence of delay, in order to show the applications of Theorem 3.3.1. Recently, there has been considerable attention towards hyperchaotic systems and their applications to secure communication. Since hyperchaotic systems possess more

than one positive Lyapunov exponent, unlike low-dimensional chaotic systems, it is believed that hyperchaos might be a better tool for constructing a chaos-based secure communication scheme. This topic will be discussed in detail in Chapter 5.

Hyperchaos was observed for the first time in 1986 from a real physical system - a fourth order electrical circuit [76]. This simple circuit is autonomous and contains only one non-linear element, a three-segment piecewise-linear resistor. All other elements are linear and passive, except an active resistor, which has a negative resistance. By considering the circuit parameters from [76], the dynamics can be written as

$$\begin{pmatrix} \dot{x}_1 \\ \dot{x}_2 \\ \dot{x}_3 \\ \dot{x}_4 \end{pmatrix} = \begin{pmatrix} 0 & 0 & -2 & 0 \\ 0 & 0 & 0 & -20 \\ 1 & 0 & 1 & 0 \\ 0 & 1.5 & 0 & 0 \end{pmatrix} \begin{pmatrix} x_1 \\ x_2 \\ x_3 \\ x_4 \end{pmatrix} + \begin{pmatrix} 2g(x_2 - x_1) \\ -20g(x_2 - x_1) \\ 0 \\ 0 \end{pmatrix}, \tag{3.57}$$

where x_1 and x_2 denote the voltage across the two capacitors in the circuit, whereas x_3 and x_4 denote the currents through the two inductors included in the same circuit. g is a piecewise-linear function, given by

$$g(x_2 - x_1) = 3(x_2 - x_1) - 1.6(|x_2 - x_1 + 1| - |x_2 - x_1 - 1|). \tag{3.58}$$

Let $\mathbf{\Phi}_1(\mathbf{x}) = \Big[0, -20g(x_2 - x_1), 0, 0\Big]^T$, $\mathbf{\Phi}_2(\mathbf{x}) = \Big[2g(x_2 - x_1), 0, 0, 0\Big]^T$ and

$$A = \begin{pmatrix} 0 & 0 & -2 & 0 \\ 0 & 0 & 0 & -20 \\ 1 & 0 & 1 & 0 \\ 0 & 1.5 & 0 & 0 \end{pmatrix}.$$

Then system (3.57) becomes

$$\dot{\mathbf{x}}(t) = A\mathbf{x}(t) + \mathbf{\Phi}_1(\mathbf{x}(t)) + \mathbf{\Phi}_2(\mathbf{x}(t)). \tag{3.59}$$

System (3.59) will represent the driving system in our model, whereas the response system will be given by

$$\begin{cases} \dot{\mathbf{u}}(t) &= A\mathbf{u}(t) + \mathbf{\Phi}_1(\mathbf{u}(t)) + \mathbf{\Phi}_1(\mathbf{x}(t-\widetilde{r})) - \mathbf{\Phi}_1(\mathbf{u}(t-\widetilde{r})) + \mathbf{\Phi}_2(\mathbf{u}(t)),\ t \neq \tau_i \\ \Delta\mathbf{u}(t) &= -B_i\mathbf{e}(t - r_i),\ t = \tau_i, i = 1, 2, \ldots, \end{cases} \tag{3.60}$$

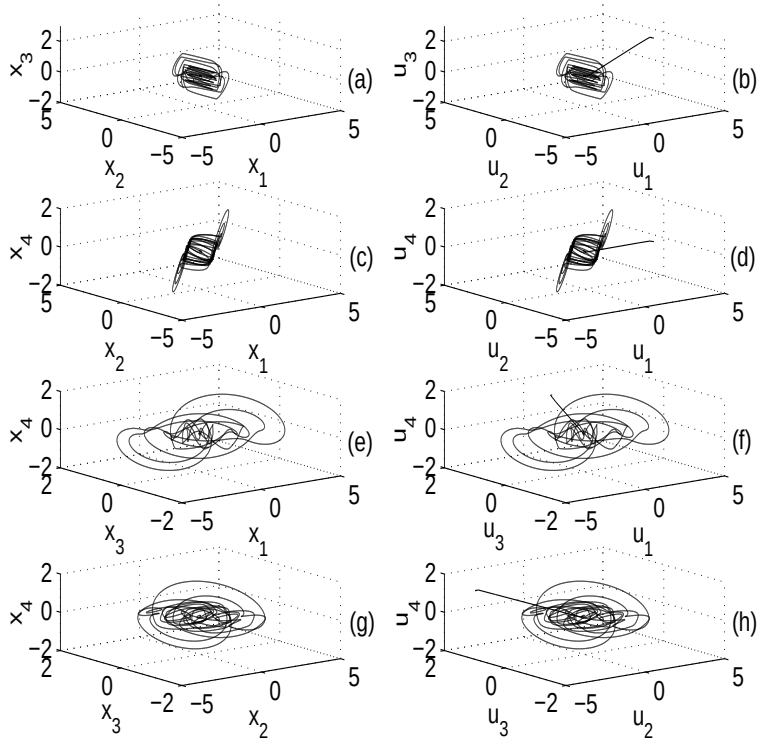

Figure 3.8: Solution trajectories of systems (3.59) and (3.60) in the state spaces (a) (x_1, x_2, x_3), (b) (u_1, u_2, u_3), (c) (x_1, x_2, x_4), (d) (u_1, u_2, u_4), (e) (x_1, x_3, x_4), (f) (u_1, u_3, u_4), (g) (x_2, x_3, x_4), (h) (u_2, u_3, u_4).

where $\mathbf{e}(t) = \mathbf{x}(t) - \mathbf{u}(t)$. This new model resembles the one given by system (3.7). In this case, system (3.60) is impulsively driven by system (3.59), using the matrices B_i , $i = 1, 2, \ldots$, and continuously driven by the signal $\mathbf{\Phi}_1(\mathbf{x}(t - \widetilde{r}))$, where $\widetilde{r}$ represents the transmission delay. The solution trajectories of system (3.59) in the state spaces (x_1, x_2, x_3), (x_1, x_2, x_4), (x_1, x_3, x_4) and (x_2, x_3, x_4), are displayed in Figure 3.8 (a), (c), (e) and (g), respectively, whereas the trajectories of the system (3.60) in the state spaces (u_1, u_2, u_3), (u_1, u_2, u_4), (u_1, u_3, u_4) and (u_2, u_3, u_4) are shown in Figure 3.8 (b), (d), (f) and (h), respectively. In addition, the time evolution of the state variables of both systems (3.59) and (3.60) are shown in Figure 3.9 (a) and (b), respectively, where the first component of each system is represented by a solid curve, the second component by a dashed curve, the third component by a dashed-dotted curve and the fourth component

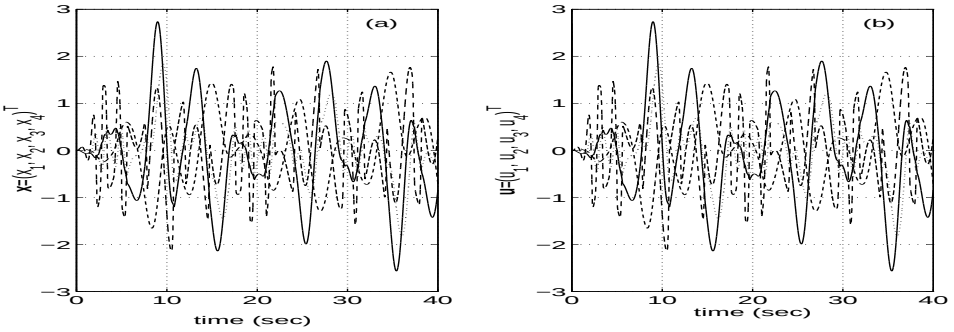

Figure 3.9: Time evolution of the state variables for (a) system (3.59); (b) system (3.60).

by a dotted curve. Notice their identical behaviour, although they start from different initial conditions. The identical behaviour is verified by considering the error system, given by

$$\left\{\begin{array}{rcl} \left.\begin{array}{rcl} \dot{\mathbf{e}}(t) &=& A\mathbf{e}(t) + \mathbf{\Psi}_1(\mathbf{x}(t),\mathbf{u}(t)) + \mathbf{\Psi}_1(\mathbf{x}(t-\widetilde{r}),\mathbf{u}(t-\widetilde{r})) \\ && +\mathbf{\Psi}_2(\mathbf{x}(t),\mathbf{u}(t)),\ t \neq \tau_i \end{array}\right\} & t > t_0 \\ \Delta\mathbf{e}(t) &=& B_i\mathbf{e}(t-r_i),\ t=\tau_i\ i=1,2,\ldots, \\ \mathbf{e}(t) &=& \boldsymbol{\phi}(t-t_0),\ t_0-\overline{r} \leq t \leq t_0, \end{array}\right. \tag{3.61}$$

where, $\mathbf{\Psi}_1(\mathbf{x},\mathbf{u}) = \mathbf{\Phi}_1(\mathbf{x}) - \mathbf{\Phi}_1(\mathbf{u})$, $\mathbf{\Psi}_2(\mathbf{x},\mathbf{u}) = \mathbf{\Phi}_2(\mathbf{x}) - \mathbf{\Phi}_2(\mathbf{u})$, $\boldsymbol{\phi}(t-t_0)$ is an initial constant function and $\overline{r} = \max_i\{r_i, \widetilde{r}\}$. Theorem 3.3.1 gives the sufficient conditions under which the error system (3.61) is equi-attractive in the large, i.e., $\mathbf{e} \to \mathbf{0}$, as $t \to 0$.

Notice that

$$\begin{array}{rcl} ||\mathbf{\Psi}_1(\mathbf{x},\mathbf{u})|| &=& ||\mathbf{\Phi}_1(\mathbf{x}) - \mathbf{\Phi}_1(\mathbf{u})|| \\ &=& 20|g(x_2-x_1) - g(x_2-x_1)| \\ &\leq& 124(|e_2| + |e_1|) \leq 124||\mathbf{e}||. \end{array}$$

Similarly, it can be checked that $||\mathbf{\Psi}_2(\mathbf{x},\mathbf{u})|| \leq 24.8||\mathbf{e}||$. With the above model, we have $||A|| = 20$, $2\widetilde{\lambda} = 18.5$, $L_1 = 248$, $L_2 = 24.8$ and $a = 282.05$. Thus applying equi-distant stabilizing impulses with $\Delta_i = \Delta = 0.002$ and $B_i = B = -I$, for all $i = 1, 2, \ldots,$ where I is the identity matrix, we obtain $\mathcal{K}_i' = 0$, $\Gamma_i^{(j)}$ and $\Upsilon_i^{(j)}$ are not applicable because $k_i + \widetilde{k} = \hat{k} = 1$,

$$\begin{array}{rcl} \mathcal{L}_i' &=& \mathcal{L}' = \exp\left[\overline{a}\hat{k}\Delta + \dfrac{\overline{L}_1}{\overline{a}}e^{\overline{a}\hat{k}\Delta} - \dfrac{\overline{L}_1}{\overline{a}}\right] r_i(||A|| + 2\overline{L}_1 + \overline{L}_2) \\ &=& 540.8\exp\left[0.5641\hat{k} + 0.0879276724e^{0.5641\hat{k}} - 0.0879276724\right] r_i \end{array}$$

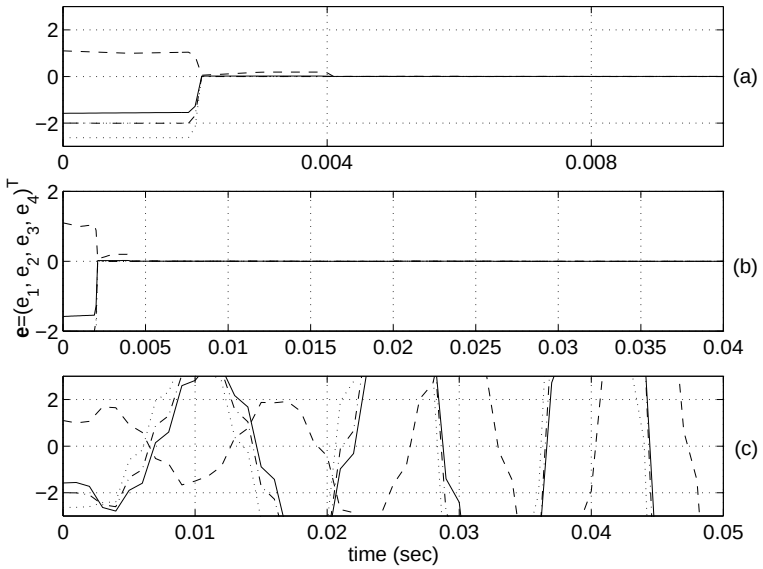

Figure 3.10: Solution trajectories of system (3.61) with the presence of delay: (a) $\widetilde{r} = 0.001$ and $\overline{r} = 0.0004$. (b) $\widetilde{r} = 0.001$ and $\overline{r} = 0.001$. (c) $\widetilde{r} = 1$ and $\overline{r} = 0.0021$.

and $J_i = J = (\mathcal{L}')$, for all $i = 1, 2, \ldots$. Therefore, according to Theorem 3.3.1 and Remark 3.8, system (3.61) is equi-attractive in the large if

$$r_i \leq r_{\max} \approx \frac{\overline{\gamma}}{540.8} \exp\Big[-0.5641\hat{k} - 0.0879276724e^{0.5641\hat{k}} + 0.0879276724\Big] \tag{3.62}$$

for all $i = 1, 2, \ldots$. It follows that the maximum delay the error system can endure in the impulses, for $\overline{\gamma} = 0.999$, is given by

$$r_i < r_{\max} = 0.0009831121,$$

for all $i = 1, 2, \ldots$. Notice that $r_{\max}$, in this case, is smaller than $\Delta = 0.002$. From (3.62), we may conclude that as $\widetilde{r} \to \infty$, then $\widetilde{k} \to \infty$ and $r_{\max} \to 0$, which reflects the nature of the relationship between the two delay terms. In general, it can be checked that as $\widetilde{r}$ increases, the upper bound on r_i, for all $i = 1, 2, \ldots$, given by $r_{\max}$, decreases.

From the above discussion, we may conclude that if the delay terms r_i, for all $i = 1, 2, \ldots$, are all bounded above by $r_{\max}$, then Theorem 3.3.1 will guarantee that system (3.61) remains equi-attractive in the large. This is reflected in the numerical simulations, employing the Runge-Kutta method, presented in Figure 3.10 (a), where the initial constant function is given by $\boldsymbol{\phi}(t - t_0) = \boldsymbol{\phi}(t) = (1.12, -1, 0.5, -0.2)^T$ $(t_0 = 0)$, the integration step-size is taken to be 0.0001

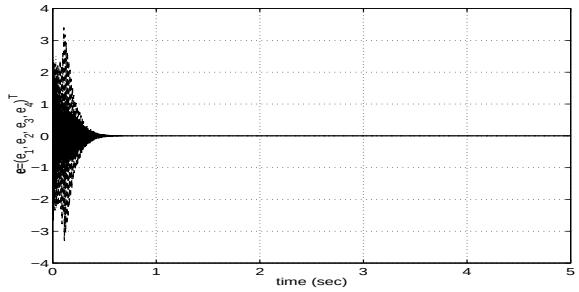

Figure 3.11: Solution trajectories of system (3.61) with $\widetilde{r} = 0$ and $\overline{r} = 0.0021$.

and the delay terms are taken to be $\widetilde{r} = 0.001$ and $r_i = \overline{r} = 0.0004$, for all $i = 1, 2, \ldots$. It can be seen that the solution curves, presented by a solid curve for $e_1(t)$, dashed curve for $e_2(t)$, dashed-dotted curve for $e_3(t)$ and dotted curve for $e_4(t)$, all converge to zero. In addition, Figure 3.10 (b) shows that the desired result of equi-attractivity in the large is still achieved, although $\widetilde{r} = 0.001$ and $r_i = 0.001 > r_{\max}$, for all $i = 1, 2, \ldots$, which indicates that the conditions of Theorem 3.3.1 are sufficient conditions but not necessary, as discussed in Remark 3.10. Finally, taking the delay term $\widetilde{r} = 1$ and $r_i = 0.0021$, for all $i = 1, 2, \ldots$, the synchronization is lost and the equi-attractivity in the large of system (3.61) fails, as shown in Figure 3.10 (c). Actually, without the presence of the delay term $\widetilde{r}$, i.e.,when $\widetilde{r} = 0$, and keeping $\overline{r} = 0.0021$, the numerical simulation shows that system (3.61) remains equi-attractive in the large, as shown in Figure 3.11. This kind of relationship between $\widetilde{r}$ and $r_{\max}$ is already expected in view of equation (3.62) and Remark 3.9.

Before we end this chapter, we shall have a few comments about Lyapunov exponents of the error dynamics between the two hyperchaotic systems employed in the previous example. The numerical method we developed in Section 2.3, which we used to analyze Lyapunov exponents of synchronization error dynamics between identical chaotic systems, will fail when dealing with delayed systems. The reason lies behind the fact that delay will force us to consider previous impulses in addition to the one at which the system is analyzed at. For example, when the time frames, P, were constructed, and the Lyapunov exponents were analyzed over the intervals $[iP, iP + Q)$ and $[iP + Q, (i + 1)P)$, for $i = 0, 1, \ldots$, the method becomes inapplicable, because the delay will imply that for the ith impulse, we also need to consider the $(i - k_i - \widetilde{k})^{\text{th}}$ impulse as well and the inequality (2.48) will not be valid anymore. This opens the door to an unresolved problem of developing a technique which will be able to accommodate delay and be able to find the Lyapunov exponents associated with it.

Chapter 4

Spatiotemporal Chaos Control and Synchronization

The study of complex phenomena in spatially extended dynamical systems, such as coupled map lattices [60, 61], coupled ordinary differential equations [59, 61] and partial differential equations [60, 61], can provide insights into the behaviour found in such diverse fields as biology, chemistry and physics. An understanding of the rich variety of modes that can be excited due to the interplay between spatial and temporal behaviour may provide a clue to phenomena like pattern formation in natural systems and turbulence. Spatially extended dynamical systems often serve as standard models for investigating the phenomena occurring in living cells, tissues, neural networks, physiological systems and ecosystems, hydrodynamics, plasma physics, lasers and chemical reaction systems. The most complicated type of dynamics encountered in spatially extended dynamical systems is spatiotemporal chaos, when the observed trajectories exhibit chaotic properties both in time and space, thus characterized by positive Lyapunov exponents [21]. One of the properties of oscillations generated by non-linear dynamical systems is their ability to be synchronized. We have discussed and analyzed this phenomenon with low dimensional chaotic and hyperchaotic dynamical systems. We shall extend this work to spatially extended systems. In particular, we shall study the synchronization of two or more non-linear partial differential equations which generate spatiotemporal chaos.

In the next section, we shall introduce several synchronization methods presented in the literature by employing two one-dimensional coupled complex Ginzburg-Landau equations (the expression "one dimensional" refers to the concept of one spatial dimension). In Section 4.2, the

concept of impulsive partial differential equations and some of the theory associated with it, such as existence, uniqueness and stability (for linear ones), will be given. Then, in Section 4.3, we shall generalize the ideas of stability theory of linear impulsive partial differential equations to non-linear equations by attempting to impulsively control the spatiotemporal chaotic Kuramoto-Sivashinsky equation. In Section 4.4, sufficient conditions to impulsively synchronize two identical chaotic systems, called Grey-Scott models, will be derived and several supportive simulation results will be presented. Finally, in the last section, we shall analyze the Lyapunov exponents of the error dynamics between the impulsively synchronized Grey-Scott models.

4.1 Introduction

So far we have only considered the synchronization of chaos in systems which had a finite number of degrees of freedom or, in other words, a finite-dimensional phase space. Therefore one important class of coupled systems was left out of our consideration. In this section, we shall discuss briefly the possibility of synchronization of fluctuations of coupled chaotic fields in spatially extended systems which form one particular class of coupled systems with an infinite number of degrees of freedom.

The phenomenon of synchronization of chaos in spatially extended systems (termed *spatiotemporal chaos*) remains quite uninvestigated. As a result, it is not very clear exactly how important this phenomenon is in physics and engineering. However, there are quite a few physical systems for which the observation of synchronization of coupled spatiotemporal chaotic fields would definitely be important.

Firstly, this would be an important step for understanding the dynamics of multi-layered natural and artificial neural networks. It has been hypothesized that a neural network must be in a chaotic state to successfully process information [99]. At the same time it is clear that information processing becomes impossible if the behaviours of different layers in the network are completely uncorrelated. Therefore, in a properly arranged chaotic neural network, the chaotic excitations in coupled neural layers must be synchronized.

Secondly, the synchronization of chaotic fields would be relevant to analysis of some physical systems where physically separated spatially extended systems interact through some mechanism. This class includes, for instance, thermal convection in multi-layered media and oscillations in long coupled Josephson junctions [99].

Lastly, the behaviour of many physical systems is described by the interaction of quite few

spatial modes. These modes may be, for example, wave packets with close frequencies but with different propagation speeds which are frequently observed in binary convection patterns and in electrohydrodynamical convection in liquid crystals, or, on the contrary, waves propagating with close speeds but having different frequencies and wave numbers, as it occurs in bi-harmonically excited gravity-capillary ripples [99]. In many cases, the behaviour of partial wave fields can be described by coupled equations for the slow amplitudes of these wave fields. Thus rather than being spatially separated, these fields are separated due to the fact that they describe the amplitudes of orthogonal modes.

Although spatially extended systems have infinitely many degrees of freedom and as such, in principle, can exhibit very complicated behaviour practically indistinguishable from noise, it is quite common that chaotic oscillations in these systems correspond to a *low dimensional* attractor. In such situations, the problem of synchronization of spatiotemporal chaos may seem no different from synchronization of chaos in systems with a small number of degrees of freedom. However, although these problems have many similarities, a clear distinction should be made. The effects of synchronization of spatiotemporal chaos, generated by spatially extended partial differential equations, can be much more dramatic. If two chaotic systems with low dimensional phase-spaces are coupled, even without synchronization, the dimension of the resulting attractor will be low. In the case of spatially extended systems, the coupling between two systems by itself may lead to excitation of many additional degrees of freedom. Thus, in contrast with what one observes in coupled finite dimensional systems, the loss of synchronization between chaotic fields may result to the onset of a regime which is characterized by a dimension much larger than the dimension of the chaotic oscillations in coupled systems. This dimension can become so high that the fluctuations in the system can be treated as noise in all practical situations. Therefore the onset of synchronization, in this case, would mark the point of transition from noise to chaos with clear consequences for the choice of methods and models used for the description of the system.

Although the general analysis of synchronization of spatiotemporal chaos is very complicated and goes beyond the scope of this thesis, the principal possibility of such synchronization can be clearly demonstrated analytically and numerically. To do this we shall consider the simplest form of spatiotemporal chaotic synchronization which is the synchronization of coupled chaotic fields which are generated by identical (apart from the coupling term) partial differential equations.

When the coupled systems are identical, it is easy to obtain the condition under which two systems can exhibit synchronized spatiotemporal chaos in the case when the coupling is of a special linear form. For simplicity, we shall discuss, as for low-dimensional chaotic and hyperchaotic

systems, the case of uni-directional coupling only. We write the equation for complex variables of the driving field in the form

$$\frac{\partial \mathbf{u}}{\partial t} = \mathbf{F}(\mathbf{u}, \mathbf{u}^*, \mathbf{r}, t) + \hat{L}\left(\frac{\partial}{\partial \mathbf{r}}\right)\mathbf{u}, \tag{4.1}$$

where $\mathbf{u}(t, \mathbf{r}) = (u_1, u_2, \ldots, u_m)^T$ is the vector of complex amplitudes for the wave fields, $\mathbf{u}^* = (|u_1|, |u_2|, \ldots, |u_m|)^T$, $\hat{L}(\partial/\partial \mathbf{r})$ is the linear operator which contains the derivatives with respect to space variables. Equation (4.1) is a general form of many non-linear PDE models which are used for studying spatiotemporal chaotic behaviour. We consider complex $\mathbf{u}$ and complex function $\mathbf{F}$ (rather than real) to keep this analysis as general as possible and so that it can be easily applied to the analysis of synchronization of chaotic wave fields with $\mathbf{u}$ being the complex amplitudes of the partial wave modes. We use $\mathbf{u}(t, \mathbf{r})$ to drive the response system which is identical to the drive system except for the coupling term

$$\frac{\partial \mathbf{v}}{\partial t} = \mathbf{F}(\mathbf{v}, \mathbf{v}^*, \mathbf{r}, t) + \hat{L}\left(\frac{\partial}{\partial \mathbf{r}}\right)\mathbf{v} - \hat{E}(\mathbf{v} - \mathbf{u}), \tag{4.2}$$

where $\mathbf{v}(t, \mathbf{r}) = (v_1, v_2, \ldots, v_m)^T$ is the vector of variables of the response fields. The matrix $\hat{E}$ describes the coupling between the drive system (4.1) and the response system (4.2). Let us assume that both systems are bounded in space and have identical boundary conditions. One can see that there is a solution of the response system (4.2) which corresponds to identical behaviour of the vectors of complex amplitudes $\mathbf{v}(t, \mathbf{r})$ and $\mathbf{u}(t, \mathbf{r})$, i.e.,

$$\mathbf{u}(t, \mathbf{r}) = \mathbf{v}(t, \mathbf{r}), \tag{4.3}$$

while both of them can be chaotic in space and in time. It should be emphasized here that the stability of this solution depends on the parameters of the coupling matrix $\hat{E}$. The above set up models two different types of synchronization, which we shall discuss now, and, in fact, can also model impulsive synchronization, which we shall discuss in Section 4.4, although we shall develop the model differently in Section 4.3.

As an example, let us consider a real coupling in the form

$$\hat{E} = \epsilon I, \tag{4.4}$$

where ϵ is a positive real scalar and I is, as usual, the identity matrix of appropriate dimensions. We shall assume that the rate of instability which is responsible for the spatiotemporal chaos in

the drive system is restricted by some limited value. This instability, in the case of spatiotemporal chaos, is characterized by the spectrum of Lyapunov exponents. Usually the spectrum is limited from above and therefore this assumption is valid. Suppose that the spectrum of Lyapunov exponents of the solution generated by the system (4.1) has values which are less than some value Λ.

Let us consider the evolution of the perturbations $\boldsymbol{\xi}(t, \mathbf{r})$ against the background of the solution of the form (4.3). If these perturbations are small, they are described by the following linearized system

$$\frac{\partial \boldsymbol{\xi}}{\partial t} = (J_{\mathbf{u}}\mathbf{F} - \epsilon I)\,\boldsymbol{\xi} + J_{\mathbf{u}^*}\mathbf{F}\boldsymbol{\xi}^* + \hat{L}\left(\frac{\partial}{\partial \mathbf{r}}\right)\boldsymbol{\xi}, \tag{4.5}$$

where $\boldsymbol{\xi} := \mathbf{v} - \mathbf{u}$ and $J_{\mathbf{u}}\mathbf{F}$, $J_{\mathbf{u}^*}\mathbf{F}$ are the Jacobian matrices calculated for a particular solution of (4.3), with respect to $\mathbf{u}$ and $\mathbf{u}^*$, respectively. We introduce a new vector field $\boldsymbol{\eta}(t, \mathbf{r})$ which is defined by the equation

$$\boldsymbol{\xi} = \boldsymbol{\eta}\exp(-\epsilon t). \tag{4.6}$$

Using (4.6), the linearized equation (4.5) can be rewritten in the form

$$\frac{\partial \boldsymbol{\eta}}{\partial t} = J_{\mathbf{u}}\mathbf{F}\boldsymbol{\eta} + J_{\mathbf{u}^*}\mathbf{F}\boldsymbol{\eta}^* + \hat{L}\left(\frac{\partial}{\partial \mathbf{r}}\right)\boldsymbol{\eta}. \tag{4.7}$$

It is easy to check that equations (4.6) and (4.7) describe the growth of small perturbations away from a particular solution $\mathbf{u}(t, \mathbf{r})$ of the drive system (4.1) in the linear approximation. As we assumed earlier, the characteristic rate at which these perturbations grow is not faster than $C\exp(\Lambda t)$, for some positive constant C. Therefore the perturbation vector ξ will decay with $t \to 0$ if the coupling factor is strong enough to suppress the instability, i.e., $\epsilon > \Lambda$.

Thus we demonstrated that a chaotic field can be synchronized to a chaotic driving field by means of dissipative coupling of a special form. The synchronous motion is linearly stable if the coupling coefficient is larger than the upper bound of the spectrum of Lyapunov exponents. When this condition is satisfied, the fields in two systems become synchronized under a proper choice of initial conditions [99].

To demonstrate the possibility of synchronization of coupled fields, we shall study numerically a system of two coupled complex Ginzburg-Landau equations for complex amplitudes $u(t, x)$ and $v(t, x)$, given by

$$\frac{\partial u}{\partial t} = u - (1 - i\beta)|u|^2 u + (1 + i\alpha)\frac{\partial^2 u}{\partial x^2} \tag{4.8}$$

$$\frac{\partial v}{\partial t} = v - (1 - i\beta)|v|^2 v + (1 + i\alpha)\frac{\partial^2 v}{\partial x^2} + \epsilon(u - v). \tag{4.9}$$

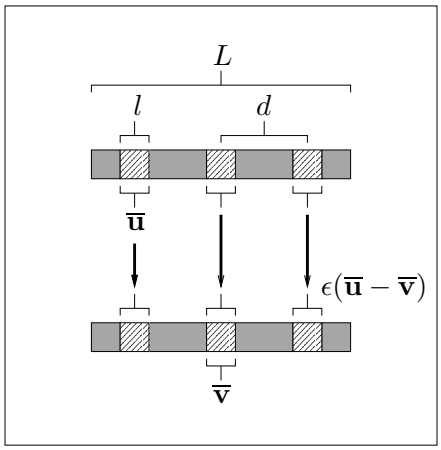

Figure 4.1: The principle of the sensor coupling scheme.

The complex Ginzburg-Landau equation is a very common model used for the description of dynamics of wave fields in non-equilibrium media close to the threshold of Hopf bifurcation.

In [99], a numerical analysis of the synchronization of systems (4.8) and (4.9) was provided. The parameters α and β were chosen to be $\alpha = \beta = 4$. At these values, $u(t, x)$ exhibited spatiotemporal amplitude chaos with Lyapunov dimension as high as $D_\lambda = 67.7$ and with the largest Lyapunov exponent equal to $\Lambda = 0.416$. It was shown, in [99], by numerical simulations, that for a coupling parameter $\epsilon > \Lambda = 0.416$, the synchronization was achieved as predicted by the analysis shown earlier. In fact, it was noticed that, by running more simulations for values of $\epsilon < \Lambda$, no synchronization between systems (4.8) and (4.9) could be achieved.

An extension of the above coupling technique was further developed in [47–49, 103] by introducing sensor coupling method. In this proposed method, a finite number of coupling signals, given in terms of local spatial averages, were used. These elements are called sensors and, for one-spatial-dimensional systems, they measure scalar time series of the form

$$\overline{\mathbf{u}}(t) = \frac{1}{l} \int_{nd-l/2}^{nd+l/2} \mathbf{u}(t, x)dx, \quad n = 1, 2, \ldots, N, \tag{4.10}$$

where N is the total number of sensor elements, d is the distance between the centers of two consecutive elements and l is the width of each sensor (see Figure 4.1).

Because of the exponential decrease of spatial correlations in extended chaotic systems, a finite number N of coupling signals that contain all the necessary information to reconstruct the

whole state in the synchronization process, is needed for this coupling technique [47]. In fact, it was realized that an equidistant arrangement of N sensors with distance $d = L/N$, turned out to be nearly optimal (for periodic boundary conditions) for this coupling scheme [49]. The coupling term chosen in [47–49, 103] was a unidirectional dissipative coupling. This method was implemented by measuring N sensor signals in the response system at the same positions as the ones in the drive system and applying the dissipative coupling term with coupling strength ϵ, given by

$$\mathbf{f}(\overline{\mathbf{u}}_n, \overline{\mathbf{v}}_n) = \begin{cases} \epsilon(\overline{\mathbf{u}}_n - \overline{\mathbf{v}}_n), & nd - \dfrac{l}{2} \leq x \leq nd + \dfrac{l}{2} \\ \\ 0, & \text{elsewhere,} \end{cases} \tag{4.11}$$

at each sensor position $n = 1, 2, \ldots, N$, respectively, as shown in Figure 4.1.

Once more, the one-dimensional complex Ginzburg-Landau equation, described by equation (4.8), was used in this model (in addition to the Kuramoto-Sivashinsky equation which will be used in the next section). The response system with the coupling factor was given by

$$\frac{\partial v}{\partial t} = v - (1 - i\beta)|v|^2 v + (1 + i\alpha)\frac{\partial^2 v}{\partial x^2} + f(\overline{u}_n, \overline{v}_n) \tag{4.12}$$

which would evolve between the sensor locations freely in time. It was established in [47,49], using numerical simulations, that, for particular values of the parameters of the systems (4.8) and (4.11) (i.e., for phase turbulence and for defect turbulence), the two systems will synchronize when the dissipative coupling factor (4.10), with an appropriate choice of the parameter ϵ, is applied. In fact, several numerical results regarding the relationship between the parameters of systems (4.8) and (4.11) and the Lyapunov dimension, D_L, of the synchronization error between them, were derived in [47, 49] (similar results are obtained for the Kuramoto-Sivashinsky equation [48, 103]). For example, it was demonstrated that $D_L \approx 0.332L$ in the case of defect turbulence ($\alpha = 1.2$ and $\beta = 2$) and $D_L \approx 0.102L$ for the case of phase turbulence ($\alpha = 0.7$ and $\beta = 2$). Furthermore, a minimal number of sensors N needed for synchronization, using different but fixed values of l and ϵ, was obtained by numerically plotting a linear curve corresponding to the relationship between N and L. Additional numerical results were also obtained when considering the relationship between the two pairs (N, l) and (L, ϵ), keeping other parameters fixed, to guarantee accurate synchronization.

Actually, there are more proposed methods of synchronization of partial differential equations, which generate spatiotemporal chaos, presented in the literature. Two of these methods are:

- Synchronizing PDE's by means of a finite number of local tiny perturbations selected by an adaptive technique [12, 13].

- Synchronizing PDE's by using an extended time-delay auto-synchronization algorithm [28].

Finally, it remains to discuss the possibility of synchronizing PDE's which generate chaos, using impulsive techniques. The work of Kocarev et al. [60, 61] motivates us to develop an impulsive method to synchronize identical non-linear PDE's and develop an analytical approach towards studying the dynamics of the synchronization error between the systems involved. We begin this study by first introducing impulsive methods to control the dynamics of spatiotemporal chaotic systems whose structures resemble the system given in (4.1). Due to the fact that there is a lack of standard set of properties that a group of PDE's would possess (i.e., different PDE's have different structural properties), we shall take specific system of PDE's to develop the theory related to impulsive control, then we shall do exactly the same concerning the theory of impulsive synchronization. In other words, we shall take the Kuramoto-Sivashinsky equation to discuss impulsive control, and the Grey-Scott model to discuss impulsive synchronization.

4.2 Impulsive Partial Differential Equations

Consider the impulsive initial boundary value problem presented by the one-dimensional (i.e., one spatial dimension) n^{th} order partial differential equation given by

$$\left\{\begin{array}{l} \left.\begin{array}{ll} \dfrac{\partial \mathbf{u}}{\partial t} = \mathbf{f}(t,x,\mathbf{u},\dfrac{\partial \mathbf{u}}{\partial x},\dfrac{\partial^2 \mathbf{u}}{\partial x^2},\ldots,\dfrac{\partial^n \mathbf{u}}{\partial x^n}), & t \neq \tau_k \\ \Delta \mathbf{u}(t,x) = Q_k \mathbf{u}(t,x), & t = \tau_k \end{array}\right\} \quad t \in \mathbb{R}_+,\ k = 1,2,\ldots \\ \mathbf{u}(0^+,x) = \mathbf{u}_0(x),\ x \in [0,L] \\ \mathbf{u}(t,0) = \mathbf{u}(t,L) = \mathbf{h}_0(t),\ \ t \in \mathbb{R}_+ \\ \dfrac{\partial \mathbf{u}}{\partial x}(t,0) = \dfrac{\partial \mathbf{u}}{\partial x}(t,L) = \mathbf{h}_1(t),\ \ t \in \mathbb{R}_+, \\ \qquad\qquad \vdots \\ \dfrac{\partial^{n_1} \mathbf{u}}{\partial x^{n_1}}(t,0) = \dfrac{\partial^{n_1} \mathbf{u}}{\partial x^{n_1}}(t,L) = \mathbf{h}_{n_1}(t),\ \ t \in \mathbb{R}_+, \end{array}\right. \tag{4.13}$$

for some n_1 such that $0 \leq n_1 < n$, where

$$\begin{aligned} \frac{\partial \mathbf{u}}{\partial t} &= (\frac{\partial u_1}{\partial t},\frac{\partial u_2}{\partial t},\ldots,\frac{\partial u_m}{\partial t})^T, \\ \frac{\partial \mathbf{u}}{\partial x} &= (\frac{\partial u_1}{\partial x},\frac{\partial u_2}{\partial x},\ldots,\frac{\partial u_m}{\partial x})^T, \\ \frac{\partial^2 \mathbf{u}}{\partial x^2} &= (\frac{\partial^2 u_1}{\partial x^2},\frac{\partial^2 u_2}{\partial x^2},\ldots,\frac{\partial^2 u_m}{\partial x^2})^T, \\ &\vdots \\ \frac{\partial^n \mathbf{u}}{\partial x^n} &= (\frac{\partial^n u_1}{\partial x^n},\frac{\partial^n u_2}{\partial x^n},\ldots,\frac{\partial^n u_m}{\partial x^n})^T, \end{aligned}$$

$\Delta \mathbf{u}(\tau_k,x) := \mathbf{u}(\tau_k^+,x) - \mathbf{u}(\tau_k^-,x)$, for all $x \in [0,L]$, $\mathbf{u}(\tau_k^+,x) = \lim_{t \to \tau_k^+} \mathbf{u}(t,x)$, for a fixed $x \in [0,L]$, and the moments of impulse satisfy $0 = \tau_1 < \tau_2 < \ldots < \tau_k < \ldots$ and $\lim_{k\to\infty} \tau_k = \infty$.

The matrices Q_k are $m \times m$ constant matrices satisfying $||Q_k|| := \sqrt{\lambda_{\max}(Q_k^T Q_k)} < L_1$, for every $k = 1, 2, \ldots$ and some $L_1 > 0$. Let $\mathbf{f} : \mathbb{R}_+ \times [0, L] \times \mathbb{R}^m \times \ldots \to \mathbb{R}^m$ be continuous on $(\tau_k, \tau_{k+1}] \times [0, L] \times \mathbb{R}^m \times \ldots \to \mathbb{R}^m$, and $\mathbf{f}(\tau_k^+, x, \mathbf{u}, \partial\mathbf{u}/\partial x, \partial^2\mathbf{u}/\partial x^2, \ldots, \partial^n\mathbf{u}/\partial x^n)$ exist for every $k = 1, 2, \ldots$. Suppose that $n = 2$ in the above model and assume that $\mathbf{f}$ satisfies Lipschitz condition with respect to $\mathbf{u}, \partial\mathbf{u}/\partial x$ and $\partial^2\mathbf{u}/\partial x^2$. Furthermore, assume that there exist functions $\mathbf{f}_1(t, \mathbf{u})$ and $\mathbf{f}_2(t, \mathbf{u})$ such that

$$\mathbf{f}_1(t, \mathbf{u}) \leq \mathbf{f}(t, x, \mathbf{u}, \mathbf{0}, \mathbf{0}) \leq \mathbf{f}_2(t, \mathbf{u}),$$

for every $(t, x, \mathbf{u}) \in [0, T] \times [0, L] \times \mathbb{R}^m$, where the inequality holds componentwise and T is a positive number, and that there exist solutions $\boldsymbol{\gamma}(t)$ and $\boldsymbol{\rho}(t)$ to the systems given by

$$\begin{cases} \dot{\boldsymbol{\gamma}}(t) &= \mathbf{f}_1(t, \boldsymbol{\gamma}),\ t \neq 0, \tau_k, T,\ 1 \leq k \leq m_1 \\ \Delta\boldsymbol{\gamma}(\tau_k) &= Q_k\boldsymbol{\gamma}(\tau_k),\ 1 \leq k \leq m_1 \\ \boldsymbol{\gamma}(0^+) &= \boldsymbol{\gamma}_0 \end{cases}$$

and

$$\begin{cases} \dot{\boldsymbol{\rho}}(t) &= \mathbf{f}_1(t, \boldsymbol{\rho}),\ t \neq 0, \tau_k, T,\ 1 \leq k \leq m_1 \\ \Delta\boldsymbol{\rho}(\tau_k) &= Q_k\boldsymbol{\rho}(\tau_k),\ 1 \leq k \leq m_1 \\ \boldsymbol{\rho}(0^+) &= \boldsymbol{\rho}_0, \end{cases}$$

respectively, where $\tau_{m_1} \leq T$. If $\boldsymbol{\rho}_0 \leq \mathbf{u}_0(x) \leq \boldsymbol{\gamma}_0$ on $[0, L]$ and if there exist functions $p \in C((0, T) \times \{0, L\}, \mathbb{R}_+)$, such that, for $i = 0, 1, \ldots, n_1$,

$$p(t, x)\boldsymbol{\rho}(t) \leq \mathbf{h}_i(t) \leq p(t, x)\boldsymbol{\gamma}(t),$$

$t \neq \tau_k$, $k = 1, 2, \ldots, m_1$, then there exists a local solution $\mathbf{u}(t, x)$ for system (4.13) satisfying

$$\boldsymbol{\rho}(t) \leq \mathbf{u}(t, x) \leq \boldsymbol{\gamma}(t)$$

provided that the original partial differential equation, in (4.13), without the impulses, has a solution [27]. For $x \in [0, L]$, let $\mathbf{u}(t, x) := \mathbf{u}(t, x, \mathbf{u}_0(x))$ be any solution of (4.13) satisfying $\mathbf{u}(0^+, x) = \mathbf{u}_0(x)$ and $\mathbf{u}(t, x)$ be left continuous at each $\tau_k > 0$, $k = 1, 2, \ldots$, in its interval of existence, i.e., $\mathbf{u}(\tau_k^-, x) = \mathbf{u}(\tau_k, x)$, for every $x \in [0, L]$.

Definition 4.2.1 *Suppose that* $\mathbf{u}(t,x) : \mathbb{R}_+ \times [0,L] \to \mathbb{R}^m$ *for some* $m > 0$, *where* $\mathbf{u}$ *is of class* $\mathcal{L}_2[0,L]$ *with respect to* x. *Then* $||\cdot||_2$ *of* $\mathbf{u}(t,x)$ *is defined by*

$$||\mathbf{u}(t,x)||_2 := \left\{ \int_0^L ||\mathbf{u}(t,x)||^2 dx \right\}^2,$$

where $||\cdot||$ *is the Euclidean norm.*

In order to study the dynamics of particular systems whose structure resemble system (4.13), we shall introduce the following classes of functions and definitions. Let
$S^c(M) := \{\mathbf{u} \in \mathbb{R}^m : ||\mathbf{u}||_2 \geq M\}$,
$S^c(M)^0 := \{\mathbf{u} \in \mathbb{R}^m : ||\mathbf{u}||_2 > M\}$,
$\nu_0(M) := \{V : \mathbb{R}_+ \times S^c(M) \to \mathbb{R}_+ : V(t,\mathbf{u}) \in C((\tau_k, \tau_{k+1}] \times S^c(M))$, locally Lipschitz in $\mathbf{u}$ and $V(\tau_k^+, \mathbf{u})$ exists for $k = 1, 2, \ldots\}$, where $M \geq 0$.

We shall now extended the definitions of the upper right derivative, equi-attractivity and uniform attractivity in the large properties that we had for ODE's to spatially extended systems represented by PDE's.

Definition 4.2.2 *Let* $M \geq 0$ *and* $V \in \nu_0(M)$. *Define the* upper right derivative *of* $V(t,\mathbf{u})$ *with respect to the continuous portion of system (4.13), for* $(t,\mathbf{u}) \in \mathbb{R}_+ \times S^c(M)^0$ *and* $t \neq \tau_k$, *by*

$$D_t^+ V(t,\mathbf{u}) := \lim_{\delta \to 0^+} \sup \frac{1}{\delta} \left[V(t+\delta, \mathbf{u} + \delta \mathbf{f}(t,x,\mathbf{u}, \frac{\partial \mathbf{u}}{\partial x}, \frac{\partial^2 \mathbf{u}}{\partial x^2}, \ldots, \frac{\partial^n \mathbf{u}}{\partial x^n})) - V(t,\mathbf{u}) \right].$$

Definition 4.2.3 *Solutions of the impulsive system (4.13) are said to be*

(S1) equi-attractive in the large *if for each* $\epsilon > 0$, $\alpha > 0$ *and* $t_0 \in \mathbb{R}_+$, *there exists a number* $T := T(t_0, \epsilon, \alpha) > 0$ *such that* $||\mathbf{u}(t_0,x)||_2 < \alpha$ *implies* $||\mathbf{u}(t,x)||_2 < \epsilon$, *for* $t \geq t_0 + T$;

(S2) uniformly attractive in the large *if* T *in (S1) is independent of* t_0.

From the definition of equi-attractivity in the large, it can been seen that the solutions of system (4.13), which possess this property, will converge to zero, with respect to the $||\cdot||_2$, no matter how large $||\mathbf{u}(t_0^+, x)||_2$ is. In other words, $\lim_{t\to\infty} ||\mathbf{u}(t,x)||_2 = 0$. Moreover, the properties (S1) and (S2) in Definition 4.2.3 become identical for autonomous systems [64], i.e., when $\mathbf{f}(t,x,\mathbf{u}, \partial\mathbf{u}/\partial x, \ldots, \partial^n\mathbf{u}/\partial x^n) = \mathbf{f}(x,\mathbf{u}, \partial\mathbf{u}/\partial x, \ldots, \partial^n\mathbf{u}/\partial x^n)$. Therefore when dealing with autonomous systems, the uniform terminology will be automatically removed.

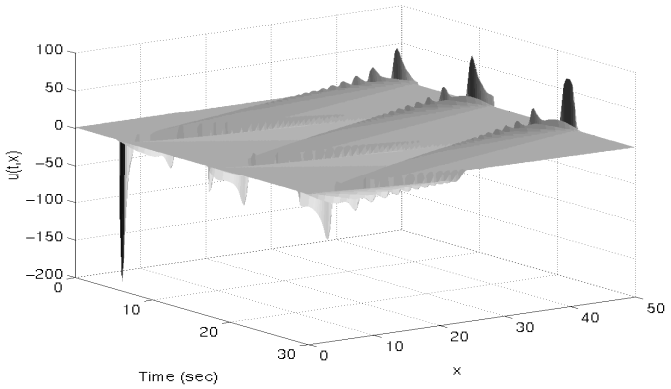

Figure 4.2: Spatiotemporal propagation of the Kuramoto-Sivashinsky equation when $L = 50$ and without the impulses.

The above definitions will be used heavily in exploring the conditions under which the solutions generated by impulsive PDE's are equi-attractive in the large.

It should be mentioned that, in [4–6], some comparison results, involving first order nonlinear PDE's, were obtained. A specific class of PDE's was chosen and comparison systems, similar to those obtained for impulsive ODE's, were designed to construct comparison results regarding asymptotic stabilities of solutions of PDE's. In other words, Bainov et al., in [4–6], were able to establish that, under certain conditions, the asymptotic stability of the comparison systems imply the asymptotic stability of the the impulsive PDE's. Unfortunately, these results do not apply to the models discussed in the coming theory, because the models discussed in the next two sections are not first order and do not satisfy many conditions required to apply the results stated in [4–6].

4.3 Impulsive Control of the K-S Equation

Consider the impulsive control of the Kuramoto-Sivashinsky equation represented by the impulsive initial boundary value problem given by

$$\left\{\begin{array}{l} \left.\begin{array}{ll} u_t + (u^2)_x + u_{xx} + u_{xxxx} = 0, & t \neq \tau_k \\ \Delta u(t,x) = -q_k u(t,x), & t = \tau_k \end{array}\right\} \quad t \in \mathbb{R}_+,\ k = 1,2,\ldots \\ u(0^+,x) = u_0(x),\ x \in [0,L] \\ u(t,0) = u(t,L) = 0,\ \ t \in \mathbb{R}_+ \\ u_x(t,0) = u_x(t,L) = 0,\ \ t \in \mathbb{R}_+, \end{array}\right. \tag{4.14}$$

where $q_k > 0$, $k = 1, 2, \ldots$, and L is the only free parameter. Equation (4.14), with the absence of the impulses, exhibits extensive chaos, which means that the Lyapunov dimension of the attractor grows linearly with the system size L [21], as shown in Figure 4.2.

The following lemma gives upper bounds on $||u(t,x)||_2$ and $||u_x(t,x)||_2$ in terms of $||u_{xx}(t,x)||_2$. These inequalities are very similar to the Poincaré inequality [75, 98].

Lemma 4.3.1 *Let $J = [0,L]$ and $u \in C^2(J)$. If $u(0) = u(L) = 0$, then*

$$||u(x)||_2 \leq \frac{L}{\pi}||u_x(x)||_2. \tag{4.15}$$

Proof: To prove this lemma, we shall apply variational methods to obtain a value for the parameter R defined by the equation

$$\frac{1}{R} = \max_{\mathcal{H}} \frac{||u(x)||_2^2}{||u_x(x)||_2^2}, \tag{4.16}$$

where $\mathcal{H} = \{u \in C^2(J) | u(0) = u(L) = 0\}$. Let $I_1 = ||u||_2^2$ and $I_2 = ||u_x||_2^2$. The optimization problem, described by equation (4.16), can be solved using the *Euler-Lagrange equations* which can be found from the equation

$$\begin{aligned} \frac{d}{d\kappa}\frac{I_1(u+\kappa\eta)}{I_2(u_x+\kappa\eta_x)}\Big|_{\kappa=0} &= \delta(\frac{I_1}{I_2}) = \frac{I_2\delta I_1 - I_1\delta I_2}{I_2^2} \\ &= \frac{1}{I_2}\left(\delta I_1 - \frac{I_1}{I_2}\Big|_{\max}\delta I_2\right) = \frac{1}{I_2}\left(\delta I_1 - \frac{1}{R}\delta I_2\right), \end{aligned}$$

where η is an arbitrary function in $\mathcal{H}$,

$$\delta I_1 = \frac{d}{d\kappa} \int_0^L (u + \kappa\eta)^2 dx \Big|_{\kappa=0} \tag{4.17}$$

and

$$\delta I_2 = \frac{d}{d\kappa} \int_0^L (u_x + \kappa\eta_x)^2 dx \Big|_{\kappa=0}. \tag{4.18}$$

Thus the solution of the optimization problem above must satisfy

$$\delta I_1 - \frac{1}{R}\delta I_2 = 0. \tag{4.19}$$

Equation (4.19) is similar to the classical approach in calculus for finding the critical points of a differentiable function by equating its first derivative (or partial derivatives) to zero in order to obtain its maximum and minimum values over a given region. Substituting equations (4.17) and (4.18) into equation (4.19), leads to

$$\int_0^L (u\eta - \frac{1}{R} u_x \eta_x) dx = 0.$$

Integrating the second term by parts, we obtain

$$\int_0^L \eta(u_{xx} + Ru) dx = 0.$$

Since η is an arbitrary function in $\mathcal{H}$, we conclude that

$$u_{xx} + Ru = 0 \quad \text{with} \quad u(0) = u(L) = 0,$$

which is a linear second order ordinary differential equation with two point boundary conditions. The general solution of the differential equation is given by

$$u(x) = C_1 \sin(R^{1/2}x) + C_2 \cos(R^{1/2}x),$$

where C_1 and C_2 are arbitrary constants to be determined. Since $u(0) = 0$, we conclude that $C_2 = 0$. Notice that $u(x) = 0$ is a trivial solution and not interesting, so we shall set $C_1 = 1$ and thus

$$u(x) = \sin(R^{1/2}x).$$

In this case, the only remaining parameter to be determined is R. Since $u(L) = 0$, it follows that $R = n^2\pi^2/L^2$, $n = \pm 1, \pm 2, \ldots$. This implies that the maximization problem, given in equation (4.16), is attained when $n = 1$ and $R = \pi^2/L^2$. In other words, due to the fact that $u \in \mathcal{H}$, we have, for every $x \in J$,

$$\frac{||u(x)||_2^2}{||u_x(x)||_2^2} \leq \frac{L^2}{\pi^2} \Longrightarrow ||u(x)||_2^2 \leq \frac{L^2}{\pi^2}||u_x(x)||_2^2,$$

as required by equation (4.15). □

The next Theorem gives the required criteria for system (4.14) to be equi-attractive in the large. It provides us with a tool towards impulsively controlling the chaotic behaviour of the Kuramoto-Sivashinsky equation by forcing the solution to converge to zero.

Theorem 4.3.1 *Let $q = \min_k q_k$ and $\Delta_{k+1} = \tau_{k+1} - \tau_k \leq \Delta$, for $k = 1, 2, \ldots$ and for some $\Delta > 0$. Then the impulsive Kuramoto-Sivashinsky equation (4.14) is equi-attractive in the large if*

$$(1 - q)^2 e^{\zeta\Delta} < 1, \tag{4.20}$$

where $\zeta = 1 - (\pi/L)^4$.

Proof: We shall prove this theorem by choosing an appropriate Lyapunov function $V(u(t, x)) \in \nu_0(0)$. Let

$$V(u(t, x)) := ||u(t, x)||_2^2 = \int_0^L u(t, x)^2 dx.$$

Then, by system (4.14) with its boundary conditions, by Definition 4.2.2 and by applying inte-

gration by parts, we obtain, for all $t \in (\tau_k, \tau_{k+1}]$, $k = 1, 2, \ldots,$

$$\begin{aligned}
D_t^+ V(u(t,x)) &= \int_0^L 2u(t,x)u_t(t,x)dx \\
&= \int_0^L \big[-4u(t,x)^2 u_x(t,x) - 2u(t,x)u_{xx}(t,x) - 2u(t,x)u_{xxxx}(t,x)\big]dx \\
&= -\frac{4}{3}u(t,x)^3\Big|_0^L - 2\int_0^L u(t,x)u_{xx}(t,x)dx - 2u(t,x)u_{xxx}(t,x)\Big|_0^L \\
&\quad +2u_x(t,x)u_{xx}(t,x)\Big|_0^L - 2\int_0^L u_{xx}(t,x)^2 dx \\
&= -2\int_0^L u(t,x)u_{xx}(t,x)dx - 2\int_0^L u_{xx}(t,x)^2 dx \\
&\leq \int_0^L u(t,x)^2 dx + \int_0^L u_{xx}(t,x)^2 dx - 2\int_0^L u_{xx}(t,x)^2 dx \\
&= ||u(t,x)||_2^2 - ||u_{xx}(t,x)||_2^2.
\end{aligned}$$

However, by Lemma 4.3.1, we have

$$||u(t,x)||_2^2 \leq L^2/\pi^2 ||u_x(t,x)||_2^2.$$

Since $u_x(t,x)$ satisfies the conditions of Lemma 4.3.1, we also have

$$||u_x(t,x)||_2^2 \leq L^2/\pi^2 ||u_{xx}(t,x)||_2^2.$$

Thus

$$D_t^+ V(u(t,x)) \leq ||u(t,x)||_2^2 - \frac{\pi^4}{L^4}||u(t,x))||_2^2 = \zeta V(u(t,x)).$$

Hence, for all $t \in (\tau_k, \tau_{k+1}]$, $k = 1, 2, \ldots$, we obtain

$$V(u(t,x)) \leq e^{\zeta(t-\tau_k)} V(u(\tau_k^+, x)), \tag{4.21}$$

and

$$V(u(\tau_{k+1},x)) \leq e^{\zeta\Delta_{k+1}} V(u(\tau_k^+, x)), \tag{4.22}$$

Moreover, according to the structure of the impulses defined in (4.14), we have, for all $x \in [0, L]$ and $k = 1, 2, \ldots$,

$$u(\tau_k^+, x) = u(\tau_k, x) - q_k u(\tau_k, x) = (1 - q_k) u(\tau_k, x) \implies$$

$$\int_0^L u(\tau_k^+, x)^2 dx = \int_0^L (1 - q_k)^2 u(\tau_k, x)^2 dx.$$

It follows that

$$V(u(\tau_k^+, x)) = (1 - q_k)^2 V(u(\tau_k, x)). \tag{4.23}$$

Hence, by using inequalities (4.22) and (4.23), we have, for every $k = 1, 2, \ldots$,

$$V(u(\tau_k^+, x)) \leq (1 - q_k)^2 e^{\zeta\Delta_{k+1}} V(u(\tau_k, x)) \leq (1 - q)^2 e^{\zeta\Delta} V(u(\tau_k, x)). \tag{4.24}$$

By inequalities (4.20) and (4.24), we can conclude that

$$\lim_{k\to\infty} V(u(\tau_k, x)) = 0.$$

Therefore, by inequality (4.21), we have, for all $t \in (\tau_k, \tau_{k+1}]$ and $k = 1, 2, \ldots$,

$$\begin{aligned} V(u(t,x)) &\leq e^{\zeta\Delta_{k+1}} V(u(\tau_k^+, x)) \\ &\leq (1 - q_k)^2 e^{\zeta\Delta_{k+1}} V(u(\tau_k, x)) \\ &\leq (1 - q)^2 e^{\zeta\Delta} V(u(\tau_k, x)) \to 0, \text{ as } k \to \infty. \end{aligned}$$

It follows that

$$\lim_{t\to\infty} V(u(t,x)) = 0.$$

In other words the solutions to the impulsive Kuramoto-Sivashinsky equation, defined by (4.14), are equi-attractive in the large. □

Remark 4.1: From Theorem 4.3.1, we see that the spatiotemporal chaotic behaviour (or when $\pi/L << 1$) of the Kuramoto-Sivashinsky equation, described by the partial differential equation in (4.14), is impulsively controlled and the solutions are driven towards the equilibrium solution $u(t,x) = 0$, achieving the desired equi-attractivity in the large property. The proof is done by reducing the problem from a PDE problem into an ODE involving the Lyapunov function $V(u(t,x)) = ||\mathbf{u}(t,x)||_2^2$ which is easier to handle.

Remark 4.2: From the proof of Theorem 4.3.1, we may conclude that if the ratio π/L is chosen to be strictly greater than 1 (by taking smaller spatial range L), the solutions of the Kuramoto-Sivashinsky equation will remain equi-attractive in the large even with the absence of the impulses. A numerical example showing this phenomenon will be given in this section. However, if $\pi/L < 1$, then the impulses are needed to stabilize the system provided that these impulses satisfy the condition stated in Theorem 4.3.1; namely, inequality (4.20).

Remark 4.3: The condition in Theorem 4.3.1 is a sufficient condition but not necessary. In other words, the impulsive partial differential equation described by system (4.14) may remain equi-attractive in the large even if inequality (4.20) is not satisfied. We shall demonstrate this result in the numerical example given in this section.

Remark 4.4: Inequality (4.20) reflects the type of relationship that exists between the magnitude of the impulses (represented by the parameter q) and the interval between two consecutive impulses (represented by the parameter Δ). Thus the larger the interval Δ_k is, the stronger the magnitude of the impulse q_k, for all $k \geq K$ for some $K \geq 1$, is required to maintain the equi-attractivity in the large property (see Figure 4.3). An estimate on the basin of attraction can be obtained by solving for Δ:

$$\Delta < \Delta_{\max} = \frac{-\ln(1-q)^2}{\zeta}, \text{ for } 0 < q < 2.$$

Remark 4.5: The Kuramoto-Sivashinsky equation is a spatiotemporal chaotic system. This means that the solutions to system (4.14) are equi-bounded solutions. Thus if the conditions of Theorem 4.3.1 are satisfied, then this indicates that the solutions of (4.14) are not just equi-attractive in the large only, but also equi-Lagrange stable.

The following numerical examples illustrate Theorem 4.3.1 and Remarks 4.1-4.4. When $L =$

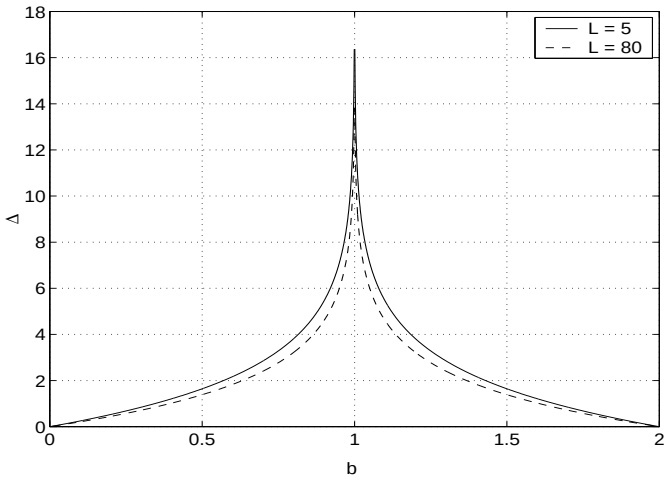

Figure 4.3: Basin of attraction of Δ with respect to q for different values of L.

50, the Kuramoto-Sivashinsky equation, given in (4.14), exhibits chaotic behaviour in both time and spatial dimensions. If we take the magnitude of the impulses to be $q_k = q = 0.4$, for all $k = 1, 2, \ldots$, then Theorem 4.3.1 indicates that the maximum impulse duration permissible to guarantee the equi-attractivity property (i.e., convergence to the equilibrium solution) is given by $\Delta_{\max} \approx 1.022$ sec. In other words, if the impulse durations satisfy $\Delta_k < \Delta_{\max}$, $k = 1, 2, \ldots$, then $\lim_{t\to\infty} ||u(t, x)||_2 = 0$. This can be shown in Figure 4.4, where the time of the convergence is approximately 0.12 sec. In this numerical simulation and the remaining ones in this section, a MacCormack's method [67, 68], with first forward differencing and then backward differencing to achieve second order accuracy, is applied. The time step size is taken to be 0.0001 sec. and the number of spatial points is taken to be 150. Moreover, in all of these simulations, the initial condition is taken to be $u_0(x) = 0$ with strong perturbations in the middle. Increasing the magnitude of the impulses to $q_k = q = 0.7$, $k = 1, 2, \ldots$, the maximum impulse duration predicted by Theorem 4.3.1 becomes $\Delta_{\max} = 2.408$ sec. Figure 4.5 shows the convergence of $||u(t, x)||_2$ to zero with impulse duration $\Delta_k = \Delta = 0.1$ sec., for $k = 1, 2, \ldots$, which is consistent with that of Theorem 4.3.1. This illustrates the type of relationship that exists between the impulse durations and the magnitude of the impulses, as mentioned in Remark 4.4. Furthermore, when applying impulses with magnitude $q_k = q = 0.2$, $k = 1, 2, \ldots$, then according to Theorem 4.3.1, $\Delta_{\max} = 0.4463$ sec. However, the impulsive control of the Kuramoto-Sivashinsky equation can still be achieved with impulse durations given by $\Delta_k = \Delta = 0.45 > \Delta_{\max}$ (see Figure 4.6).

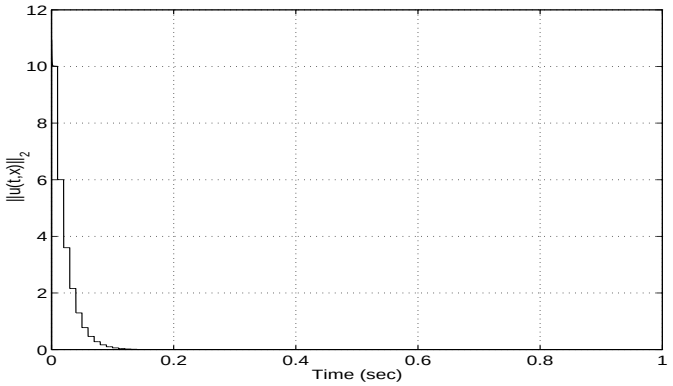

Figure 4.4: $||u(t,x)||_2$ converging to zero for $\Delta = 0.01$, $q_k = q = 0.4$ and $L = 50$.

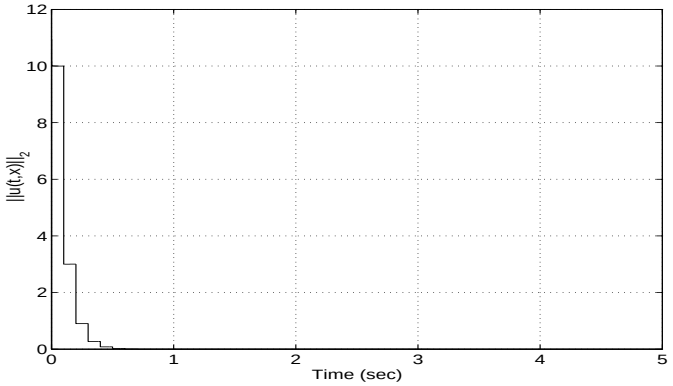

Figure 4.5: $||u(t,x)||_2$ converging to zero for $\Delta = 0.1$, $q_k = q = 0.7$ and $L = 50$.

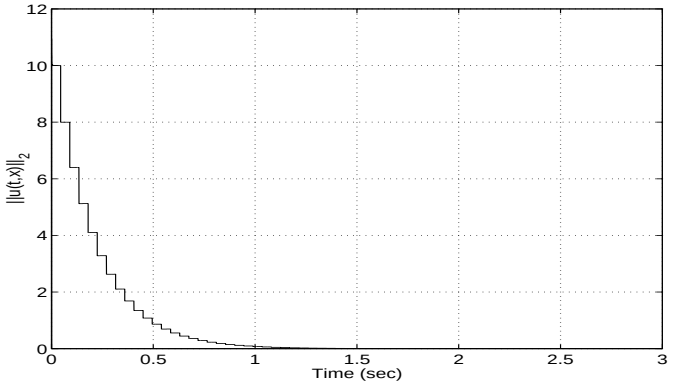

Figure 4.6: $||u(t,x)||_2$ converging to zero for $\Delta = 0.45$, $q_k = q = 0.2$ and $L = 50$.

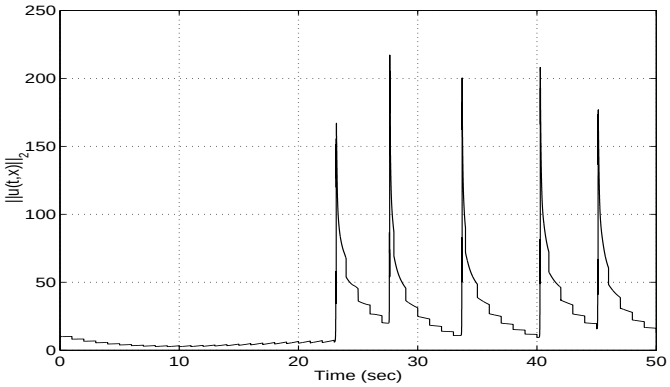

Figure 4.7: $||u(t,x)||_2$ not converging to zero for $\Delta = 1$, $q_k = q = 0.2$ and $L = 50$.

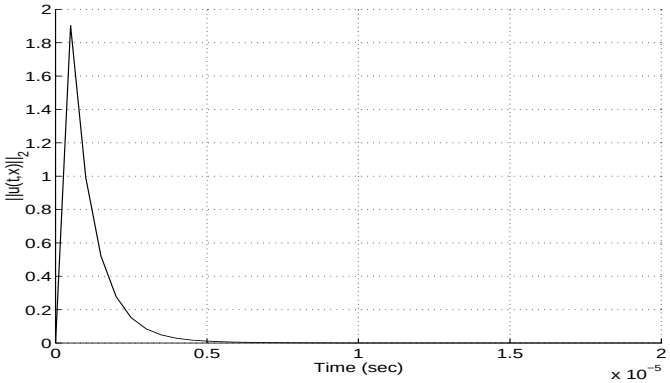

Figure 4.8: $||u(t,x)||_2$ converging to zero without the presence of impulses for $L = 2$.

This indicates that condition (4.20), in Theorem 4.3.1, is a sufficient condition but not necessary, as we discussed in Remark 4.3. In other words, the equi-attractivity property was still achieved even if the impulses lie outside the basin of attraction described by Figure 4.3. If these impulses lie drastically far from the basin of attraction, then the solutions to system (4.14) will not converge to zero, as shown in Figure 4.7, where $\Delta_k = \Delta = 1 > \Delta_{\max}$ and $q_k = q = 0.2$. Finally, we show in Figure 4.8, the convergence of the solutions of the Kuramoto-Sivashinsky equation to zero without the impulses because $L = 2$ and $(\pi/L) > 1$, as was mentioned in Remark 4.2.

4.4 Impulsive Synchronization of the Grey-Scott Model

We have been successful in using impulsive control methods to control the behaviour of the Kuramoto-Sivashinsky equation by making its solutions equi-attractive in the large, although the original PDE exhibited spatiotemporal chaotic behaviour. We will extend this work and investigate the impulsive synchronization of two identical spatiotemporal chaotic systems. The Grey-Scott model [87] will be used as the spatiotemporal chaos generator. The coming theory is definitely applicable to the synchronization of two Kuramoto-Sivashinsky equations as well as any other spatiotemporal chaotic system exhibiting the same structure.

The Grey-Scott cubic auto-catalysis model is a reaction-diffusion system which corresponds to two reactions which are both irreversible. This model exhibits mixed mode spatiotemporal chaos and is described by the following equations.

$$\begin{aligned} \frac{\partial u_1}{\partial t} &= -u_1 u_2^2 + a(1-u_1) + d_1 \bigtriangledown^2 u_1 \\ \frac{\partial u_2}{\partial t} &= u_1 u_2^2 - (a+b)u_2 + d_2 \bigtriangledown^2 u_2, \end{aligned} \tag{4.25}$$

where b is the dimensionless rate constant of the second reaction, a is the dimensionless feed rate and d_1 and d_2 are the diffusion coefficients. The system size is 2.5×2.5 and the boundary conditions are periodic. Detailed stability and bifurcation analysis of the above model is given in [87]. Figures 4.9 and 4.10 show the propagation of the solutions $u_1(t,x)$ and $u_2(t,x)$ for the one-dimensional case. A forward Euler integration of the finite difference equation, resulting from the discretization of the diffusion operator, is applied with 256 mesh points and 0.01 integration step size. The initial conditions are chosen to be $(u_{01}, u_{02})^T = (1,0)^T$ with strong perturbations in the middle and the parameters of the system are taken to be $a = 0.028$, $b = 0.053$, $d_1 = 2 \times 10^{-5}$ and $d_2 = 10^{-5}$. In the following, we shall discuss the impulsive synchronization of the one-dimensional

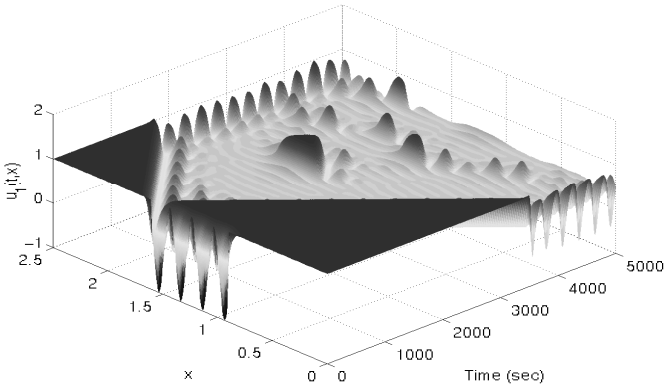

Figure 4.9: Spatiotemporal propagation of $u_1(t, x)$ in the one-dimensional case of equation (4.25).

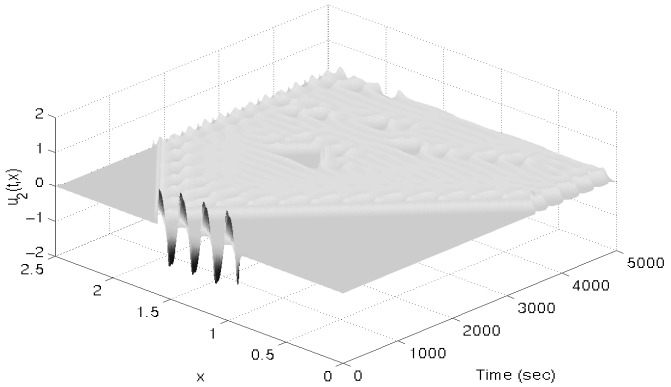

Figure 4.10: Spatiotemporal propagation of $u_2(t, x)$ in the one-dimensional case of equation (4.25).

version of system (4.25) with another identical system starting from different initial conditions. In other words, we investigate the synchronization of the chaotic signal $\mathbf{u}(t,x) = (u_1(t,x), u_2(t,x))^T$, given by

$$\text{Transmitter}: \begin{cases} \left.\begin{array}{rcl} \dfrac{\partial u_1}{\partial t} & = & -u_1u_2^2 + a(1-u_1) + d_1\dfrac{\partial^2 u_1}{\partial x^2} \\ \dfrac{\partial u_2}{\partial t} & = & u_1u_2^2 - (a+b)u_2 + d_2\dfrac{\partial^2 u_2}{\partial x^2} \end{array}\right\} \quad t \in \mathbb{R}_+ \\ \mathbf{u}(0,x) = \mathbf{u}_0(x), \quad x \in [0,L] \\ \mathbf{u}(t,0) = \mathbf{u}(t,L) = \mathbf{h}(t), \quad t \in \mathbb{R}_+, \end{cases} \tag{4.26}$$

with the chaotic signal $\mathbf{v}(t,x) = (v_1(t,x), v_2(t,x))^T$, given by

$$\text{Receiver}: \begin{cases} \left.\begin{array}{rcl} \dfrac{\partial v_1}{\partial t} & = & -v_1v_2^2 + a(1-v_1) + d_1\dfrac{\partial^2 v_1}{\partial x^2} \\ \dfrac{\partial v_2}{\partial t} & = & v_1v_2^2 - (a+b)v_2 + d_2\dfrac{\partial^2 v_2}{\partial x^2} \end{array}\right\} \quad t \neq \tau_k,\ k = 1,2,\ldots \\ \Delta\mathbf{v}(t,x) = -Q_k\mathbf{e}(t,x), \quad t = \tau_k,\ x \in [0,L], \quad k = 1,2,\ldots \\ \mathbf{v}(0^+,x) = \mathbf{v}_0(x), \quad x \in [0,L] \\ \mathbf{v}(t,0) = \mathbf{v}(t,L) = \tilde{\mathbf{h}}(t), \quad t \in \mathbb{R}_+, \end{cases} \tag{4.27}$$

where a, b, d_1 and d_2 are as defined before, $L = 2.5$ is the linear extension of the reactor tank, $\mathbf{u}_0(x)$ and $\mathbf{v}_0(x)$ are the initial conditions, $\mathbf{h}(t)$ is the periodic boundary condition for the transmitter system, $\mathbf{e}(t,x) := \mathbf{u}(t,x) - \mathbf{v}(t,x)$. Q_k are 2×2 constant matrices satisfying $||Q_k|| < L_1$, for every $k = 1,2,\ldots$ and some $L_1 > 0$. The boundary condition $\tilde{\mathbf{h}}(t)$ described at the receiver, is defined by

$$\tilde{\mathbf{h}}(t) := \mathbf{h}(t) - \mathbf{g}(t)\left\{1 + \sum_{k=1}^{\infty}\left[(||I+Q_k||^{2k} - ||I+Q_k||^{2(k-1)})H(t-\tau_k)\right]\right\}, \tag{4.28}$$

where $\mathbf{g}(t) = (g_1(t), g_2(t))^T \in C^1(\mathbb{R}_+)$, $||\mathbf{g}(t)|| \leq N$, for all $t \in \mathbb{R}_+$, I is the 2×2 identity matrix

and $H(t-\tau_k)$, $k=1,2,\ldots$, is the alternative heaviside step function, defined by

$$H(t-\tau_k)=\begin{cases} 0 & \text{if} \quad t\leq\tau_k \\ \\ 1 & \text{if} \quad t>\tau_k. \end{cases}$$

According to equations (4.26), (4.27) and (4.28), the error system $\mathbf{e}$ will be given by

$$\begin{cases} \left.\begin{array}{rcl} \dfrac{\partial e_1}{\partial t} & = & -u_1u_2^2+v_1v_2^2-ae_1+d_1\dfrac{\partial^2 e_1}{\partial x^2} \\ \\ \dfrac{\partial e_2}{\partial t} & = & u_1u_2^2-v_1v_2^2-(a+b)e_2+d_2\dfrac{\partial^2 e_2}{\partial x^2} \end{array}\right\} \quad t\neq\tau_k,\ k=1,2,\ldots \\ \\ \Delta\mathbf{e}(t,x)=Q_k\mathbf{e}(t,x),\ \ t=\tau_k,\ x\in[0,L], \qquad\qquad k=1,2,\ldots \\ \\ \mathbf{e}(0^+,x)=\mathbf{e}_0(x),\ \ x\in[0,L] \\ \\ \mathbf{e}(t,0)=\mathbf{e}(t,L)=\tilde{\mathbf{H}}(t),\ \ t\in\mathbb{R}_+, \end{cases} \tag{4.29}$$

where $\mathbf{e}_0(t):=\mathbf{u}_0(t)-\mathbf{v}_0(t)$ and

$$\tilde{\mathbf{H}}(t):=\mathbf{h}(t)-\widetilde{\mathbf{h}}(t)=\mathbf{g}(t)\left\{1+\sum_{k=1}^{\infty}\left[(||I+Q_k||^{2k}-||I+Q_k||^{2(k-1)})H(t-\tau_k)\right]\right\}.$$

Notice that if $||I+Q_k||\leq L_2<1$, for every $k=1,2,\ldots$, then

$$\lim_{t\to\infty}||\tilde{\mathbf{H}}(t)||=\lim_{t\to\infty}||\mathbf{h}(t)-\tilde{\mathbf{h}}(t)||=0.$$

This is a very important property which will be used in the upcoming theory. Furthermore, Due to the fact that $\mathbf{u}$ and $\mathbf{v}$ are both generated by spatiotemporal chaotic systems, we may conclude immediately that they are both equi-bounded. This will also be a very useful property which will be used in the proof of the next theorem. Thus, using the above description, exploring the idea of impulsive synchronization of the two systems $\mathbf{u}$ and $\mathbf{v}$, reduces to proving that the error system (4.29) is equi-attractive in the large or that $\lim_{t\to\infty}||\mathbf{e}||_2=0$.

We shall state now two lemmas ([51], Theorem 3.1, p. 45 and Corollary 2.2, p 33, respectively) and prove two other ones in order to establish several results needed for obtaining certain criteria regarding system (4.29) to be equi-attractive in the large.

Lemma 4.4.1 *Let $p(t) \neq 0$ and $r(t)$ be given functions for $t = \ell, \ell+1, \ell+2, \ldots$, for some $\ell \in \mathbb{R}_+ \cup \{0\}$. Then*

(a) The solutions of the equation $w(t+1) = p(t)w(t)$ are given by

$$w(t) = w(\ell) \prod_{s=\ell}^{t-1} p(s).$$

(b) All solutions of the equation $z(t+1) = p(t)z(t) + r(t)$ are given by

$$z(t) = w(t) \left[\sum \frac{r(t)}{Ew(t)} + C \right],$$

where $\sum$ is the indefinite sum, E is the shift operator ($Ez(t) = z(t+1)$), C is an arbitrary constant and $w(t)$ is any non-zero solution from part (a).

Lemma 4.4.2 *If $n \in \mathbb{Z}_+ \cup \{0\}$, than*

$$\sum t^n = \frac{1}{1+n} B_{n+1}(t) + C,$$

where B_n are Bernoulli polynomials [51], for all $n \in \mathbb{Z}_+ \cup \{0\}$, and C is an arbitrary constant.

Lemma 4.4.3 *Let $p(t) := q$ and $r(t) := Kt^n q^{t-1}$ in Lemma 4.4.1, for all $t = 1, 2, \ldots$ ($\ell = 1$), where $0 < q < 1$, $n \in \mathbb{Z}_+ \cup \{0\}$ and $K \in \mathbb{R}_+$. Then $\lim_{t\to\infty} z(t) = 0$.*

Proof: From Lemmas 4.4.1 and 4.4.2, we can conclude that $w(t) = q^t w(1)$ and

$$\begin{aligned}
z(t) &= w(t) \left[\sum \frac{r(t)}{Ew(t)} + C \right] \\
&= q^t w(1) \left[\sum \frac{Kt^n q^{t-1}}{q^{t+1} w(1)} + C \right] \\
&= Kq^{t-2} \left[\sum t^n + P \right] \\
&= Kq^{t-2} \left[\frac{1}{n+1} B_{n+1}(t) + P \right] \\
&= \frac{K}{1+n} B_{n+1}(t) q^{t-2} + PKq^{t-2},
\end{aligned}$$

where C is an arbitrary constant and $P = aw(1)C/K$. Notice that

$$\lim_{t\to\infty} PKq^{t-2} = 0 \quad \text{and} \quad \lim_{t\to\infty} \frac{K}{n+1} B_{n+1}(t)q^{t-2} = 0$$

(since $0 < q < 1$, B_n are Bernoulli polynomials, for all $n \in \mathbb{Z}_+ \cup \{0\}$, and because of L'Hôpital's rule applied $n+1$ times for the second limit). It follows that $\lim_{t\to\infty} z(t) = 0$. □

We can also prove that the type of function chosen for $r(t)$ in Lemma 4.4.3 satisfies

$$\lim_{t\to\infty} r(t) = \lim_{t\to\infty} Kt^n q^{t-1} = 0,$$

for all $n \in \mathbb{Z}_+ \cup \{0\}$, by applying again L'Hôpital's rule n times.

Lemma 4.4.4 *Let $f(u_1, u_2) := u_1 u_2^2$ be defined over the set $S = \{(u_1, u_2)^T \in \mathbb{R}^2 : 0 \le |u_1| \le \beta_1$ and $0 \le |u_2| \le \beta_2\}$. Then the function f satisfies Lipschitz condition on S with Lipschitz constant given by $L_0 := \beta_2\sqrt{\beta_1^2 + 4\beta_1}$. In other words, for every $(u_1, u_2)^T, (v_1, v_2)^T \in S$, we have*

$$|f(u_1, u_2) - f(v_1, v_2)| \le L_0||(u_1 - v_1, u_2 - v_2)||.$$

Proof: Since the set S is compact and convex subset of $\mathbb{R}^2$ and f has continuous partial derivatives on S, we have, by the Mean Value Theorem [40], for some $\mathbf{c} = (c_1, c_2)^T$ in the line segment joining $(u_1, u_2)^T$ and $(v_1, v_2)^T$ which lies entirely in S,

$$\begin{aligned}
|f(u_1, u_2) - f(v_1, v_2)| &= ||\nabla f(\mathbf{c}) \cdot (u_1 - v_1, u_2 - v_2)|| \\
&\le ||\nabla f(\mathbf{c})||||(u_1 - v_1, u_2 - v_2)|| \\
&= ||(c_2^2, 2c_1c_2)||||(u_1 - v_1, u_2 - v_2)|| \\
&= |c_2|\sqrt{c_2^2 + 4c_1^2}||(u_1 - v_1, u_2 - v_2)|| \\
&\le \beta_2\sqrt{\beta_2^2 + 4\beta_1^2}||(u_1 - v_1, u_2 - v_2)||,
\end{aligned}$$

as required. □

We shall now establish the following theorem which specifies the type of conditions required to guarantee the convergence of solutions of system (4.29) to zero as time approaches infinity.

Theorem 4.4.1 *Let q_k be the largest eigenvalue of $(I+Q_k)^T(I+Q_k)$ and $\Delta_{k+1} := \tau_{k+1} - \tau_k \leq \Delta$, for all $k = 1, 2, \ldots$ and for some $\Delta > 0$. In addition, let $q := \sup_k q_k$, $d = \max(d_1, d_2)$, $\widetilde{d} = \min(d_1, d_2)$,*

$$\beta_i := \max(\sup_{t\in\mathbb{R}_+} u_i(t), \sup_{t\in\mathbb{R}_+} v_i(t)),$$

$$\mathcal{E}_i := \sup_{t\in\mathbb{R}_+} \left| \frac{\partial e_i}{\partial x}(t, L) - \frac{\partial e_i}{\partial x}(t, 0) \right|,$$

for $i = 1$ and 2,

$$\beta := \beta_2 \sqrt{\beta_2^2 + 4\beta_1^2} - a,$$

$\mathcal{E} := \max(\mathcal{E}_1, \mathcal{E}_2)$ and $\mathcal{F} := 2d\mathcal{E}/\beta$. If $\tilde{\mathbf{H}}(t) = (\tilde{H}_1(t), \tilde{H}_2(t))^T$, $\tilde{H}(t) := \tilde{H}_1(t) + \tilde{H}_2(t)$ with $\mathbf{g}(t) = (0.5, 0.5)^T$, for all $t \in \mathbb{R}_+$ (i.e., $g_1(t) + g_2(t) = 1$), and

$$qe^{\beta\Delta} < 1, \tag{4.30}$$

then system (4.29) is equi-attractive in the large.

Proof: The proof of this Theorem is similar to that of Theorem 4.3.1. Choose the Lyapunov function (or energy function) to be

$$V(\mathbf{e}(t, x)) := \int_0^L \mathbf{e}^T(t, x)\mathbf{e}(t, x)dx = \int_0^L (e_1^2(t, x) + e_2^2(t, x))dx.$$

In this case, we have, by equation (4.29) and Lemma 4.4.4,

$$\begin{aligned}
D_t^+V(\mathbf{e}) &= 2\int_0^L \left(e_1\frac{\partial e_1}{\partial t}+e_2\frac{\partial e_2}{\partial t}\right)dx \\
&= 2\int_0^L \Big[-(u_1u_2^2-v_1v_2^2)e_1 - ae_1^2 + d_1e_1\frac{\partial^2 e_1}{\partial x^2} \\
&\qquad +(u_1u_2^2-v_1v_2^2)e_2-(a+b)e_2^2+d_2e_2\frac{\partial^2 e_2}{\partial x^2}\Big]dx \\
&\le 2\int_0^L \Big[|u_1u_2^2-v_1v_2^2||e_1|+|u_1u_2^2-v_1v_2^2||e_2|\Big]dx \\
&\quad +2\int_0^L \Big[-ae_1^2-(a+b)e_2^2\Big]dx + 2\int_0^L \Big[d_1e_1\frac{\partial^2 e_1}{\partial x^2}+d_2e_2\frac{\partial^2 e_2}{\partial x^2}\Big]dx \\
&\le 4\beta_2\sqrt{\beta_2^2+4\beta_1^2}\int_0^L ||\mathbf{e}||^2dx - 2\int_0^L \Big[ae_1^2+(a+b)e_2^2\Big]dx \\
&\quad +2\int_0^L \Big[d_1e_1\frac{\partial^2 e_1}{\partial x^2}+d_2e_2\frac{\partial^2 e_2}{\partial x^2}\Big]dx \\
&\le (4\beta_2\sqrt{\beta_2^2+4\beta_1^2}-a)||\mathbf{e}||_2^2 + 2\int_0^L \Big[d_1e_1\frac{\partial^2 e_1}{\partial x^2}+d_2e_2\frac{\partial^2 e_2}{\partial x^2}\Big]dx.
\end{aligned}$$

Applying integration by parts to the second term in the latter inequality, we get, for $i = 1$ and 2,

$$\int_0^L e_i\frac{\partial^2 e_i}{\partial x^2}dx = e_i\frac{\partial e_i}{\partial x}\Big|_0^L - \int_0^L \frac{\partial e_i}{\partial x}^2 dx \le \mathcal{E}_i\tilde{H}_i(t) - \int_0^L \frac{\partial e_i}{\partial x}^2 dx.$$

Thus

$$D_t^+V(\mathbf{e}) \leq (4\beta_2\sqrt{\beta_2^2+4\beta_1^2}-a)||\mathbf{e}||_2^2 + 2d_1\mathcal{E}_1\tilde{H}_1(t) + 2d_2\mathcal{E}_2\tilde{H}_2(t) - 2\widetilde{d}||\mathbf{e}_x||_2^2,$$

However, $-2\widetilde{d}||\mathbf{e}||_2^2 \leq 0$. Therefore we can conclude that

$$D_t^+V(\mathbf{e}) \leq (4\beta_2\sqrt{\beta_2^2+4\beta_1^2}-a)||\mathbf{e}||_2^2 + 2d_1\mathcal{E}_1\tilde{H}_1(t) + 2d_2\mathcal{E}_2\tilde{H}_2(t) \iff$$

$$D_t^+V(\mathbf{e}) \leq \beta||\mathbf{e}||_2^2 + 2d\mathcal{E}\tilde{H}(t) = \beta V(\mathbf{e}) + 2d\mathcal{E}\tilde{H}(t) \iff$$

$$D_t^+V(\mathbf{e}) - \beta V(\mathbf{e}) \leq 2d\mathcal{E}\tilde{H}(t).$$

By multiplying both sides of the latter inequality by $e^{-\beta t}$, we obtain

$$e^{-\beta t}D_t^+V(\mathbf{e}) - \beta e^{-\beta t}V(\mathbf{e}) \leq 2d\mathcal{E}\tilde{H}(t)e^{-\beta t} \iff$$

$$D_t^+\left[e^{-\beta t}V(\mathbf{e})\right] \leq 2d\mathcal{E}\tilde{H}(t)e^{-\beta t}.$$

It implies that, for every $t \in (\tau_k, \tau_{k+1}]$,

$$\int_{\tau_k^+}^{t} D_s^+\left[e^{-\beta s}V(\mathbf{e})\right]ds \leq -\mathcal{F}e^{-\beta t}\tilde{H}(t) + \mathcal{F}e^{-\beta\tau_k}\tilde{H}(t).$$

Hence, for $t \in (\tau_k, \tau_{k+1}]$, we have

$$V(\mathbf{e}(t,x)) = e^{\beta\Delta_{k+1}}V(\mathbf{e}(\tau_k^+,x)) + \mathcal{F}(e^{\beta\Delta_{k+1}}-1)\tilde{H}(t) \tag{4.31}$$

and

$$V(\mathbf{e}(\tau_{k+1},x)) = e^{\beta\Delta_{k+1}}V(\mathbf{e}(\tau_k^+,x)) + \mathcal{F}(e^{\beta\Delta_{k+1}}-1)\tilde{H}(t). \tag{4.32}$$

On the other hand, for every $x \in [0,L]$ and every $k = 1, 2, \ldots$, we have, by the structure of the impulses given in system (4.29),

$$\mathbf{e}(\tau_k^+,x) = (I+Q_k)\mathbf{e}(\tau_k,x) \iff$$

$$V(\mathbf{e}(\tau_k^+,x)) = \int_0^L \mathbf{e}^T(\tau_k,x)(I+Q_k)^T(I+Q_k)\mathbf{e}(\tau_k,x)dx \iff$$

$$V(\mathbf{e}(\tau_k^+,x)) \leq q_k\int_0^L \mathbf{e}^T(\tau_k,x)\mathbf{e}(\tau_k,x)dx.$$

i.e.,

$$V(\mathbf{e}(\tau_k^+, x)) \leq q_k V(\mathbf{e}(\tau_k, x)). \tag{4.33}$$

Substituting inequality (4.33) into inequalities (4.31) and (4.32), we obtain

$$V(\mathbf{e}(t,x)) = q_k e^{\beta\Delta_{k+1}} V(\mathbf{e}(\tau_k, x)) + \mathcal{F}(e^{\beta\Delta_{k+1}} - 1)\tilde{H}(t) \tag{4.34}$$

and

$$V(\mathbf{e}(\tau_{k+1}, x)) = q_k e^{\beta\Delta_{k+1}} V(\mathbf{e}(\tau_k, x)) + \mathcal{F}(e^{\beta\Delta_{k+1}} - 1)\tilde{H}(t). \tag{4.35}$$

Let $V_k := V(\mathbf{e}(\tau_k, x))$, for every $k = 1, 2, \ldots$. In this case, we have, by inequality (4.35) and for every $k = 1, 2, \ldots,$

$$\begin{aligned} V_{k+1} &\leq q_k e^{\beta\Delta_{k+1}} V_k + \mathcal{F}(e^{\beta\Delta_{k+1}} - 1)\tilde{H}(t) \\ &\leq q e^{\beta\Delta} V_k + \mathcal{F}(e^{\beta\Delta} - 1)\tilde{H}(t). \end{aligned}$$

Since $q_k < q < 1$, for every $k = 1, 2, \ldots,$ we may conclude that, for every $t \in (\tau_k, \tau_{k+1}]$,

$$\mathcal{F}(e^{\beta\Delta} - 1)\tilde{H}(t) < \mathcal{F} q^{k-1}.$$

Hence

$$V_{k+1} \leq q e^{\beta\Delta} V_k + \mathcal{F} q^{k-1}. \tag{4.36}$$

Define $\mathcal{V}_1 := V_1$ and $\mathcal{V}_{k+1} := q e^{\beta\Delta}\mathcal{V}_k + \mathcal{F} q^{k-1}$, for $k = 1, 2, \ldots$. This implies, by inequality (4.36) and induction, that $V_k \leq \mathcal{V}_k$, for all $k = 1, 2, \ldots$. However, by Lemma 4.4.3 and inequality (4.30), we have $\lim_{k\to\infty} \mathcal{V}_k = 0$. i.e., $\lim_{k\to\infty} V_k = 0$. Therefore

$$\lim_{k\to\infty} V(\mathbf{e}(\tau_k, x)) = 0,$$

which, in turn, implies that, by inequality (4.34),

$$\lim_{t\to\infty} V(\mathbf{e}(t,x)) = 0.$$

In other words, solutions to system (4.29) are equi-attractive in the large, as required. □

Remarks 4.3, 4.4 and 4.5, from the previous section characterizing the Kuramoto-Sivashinsky model, are also suitable for this model, especially Remarks 4.3 and 4.5 which reflect the fact that the conditions stated in Theorem 4.4.1 are sufficient conditions but not necessary and that the solutions of the synchronization error (4.29) is, in fact, equi-Lagrange stable, respectively. The

latter result follows from the fact that, as before, the Grey-Scott model is spatiotemporal chaotic system which implies that it is equi-bounded. This makes the error dynamics (4.29) automatically equi-bounded as well.

We shall now state some additional remarks regarding Theorem 4.4.1.

Remark 4.6: The existence of the parameters $\mathcal{E}_i$, $i = 1, 2$, indicates that the solution surfaces of the impulsive Grey-Scott model are bounded and that the frequency of the oscillations of the solution surfaces, at the boundary, is also bounded (i.e., boundary oscillations of the solution surfaces do not increase with time). This is consistent with the properties of the Grey-Scott model and the boundary conditions corresponding to it. Therefore the existence of the parameters $\mathcal{E}_1$ and $\mathcal{E}_2$ is guaranteed.

Remark 4.7: Theorem 4.4.1 can be extended to the two-dimensional Grey-Scott model described by system (4.25), although the theory is more complicated due to the use of double integrals for the evaluation of the Lyapunov functions (or energy functions).

Remark 4.8: Theorem 4.4.1 assures the existence of the matrices Q_k, $k = 1, 2, \ldots$, which will guarantee the convergence of solutions of the error system (4.29) to the equilibrium solution. Obtaining an estimate on q is done numerically upon knowing the other parameters of the system. In this case, an approximation of the basin of attraction for Δ can be obtained with this numerical value for q.

We show now several numerical simulations to confirm the results obtained in Theorem 4.4.1. The numerical method applied in these simulations is the forward Euler integration of the finite-difference equations. As in the simulations of system (4.26), the integration step size in these simulations is taken to be 0.01 sec. and the number of spatial points is taken to be 256. Moreover, the initial conditions in these simulations are taken to be $(u_{01}(x), u_{02}(x))^T = (1, 0)^T$ with strong perturbations in the middle and $(v_{01}(x), v_{02}(x))^T = (1, 0)^T$ as well but with significantly different perturbations in the middle from the transmitter system. The remaining parameters of the error system are the same as described for the simulations of system (4.26). If the impulse durations are taken to be $\Delta_k = \Delta = 0.1$ sec., for all $k = 1, 2, \ldots$, then the solutions converge to zero by choosing $Q_k = Q = -0.5I$, for all $k = 1, 2, \ldots$. Figure 4.11 shows the quick convergence of the error dynamics to zero in 0.9 sec., which is consistent with that of Theorem 4.4.1. It should be

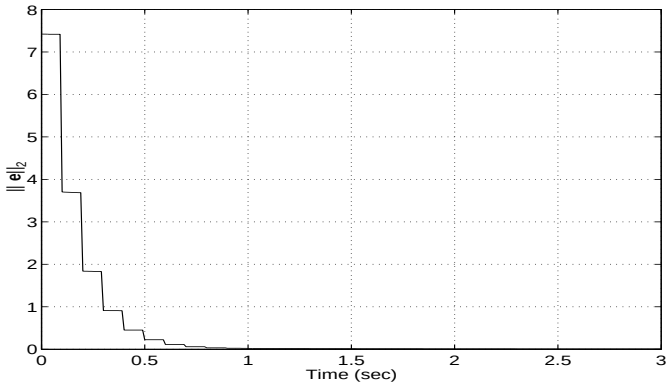

Figure 4.11: $||\mathbf{e}(t,x)||_2$ converging to zero for $\Delta = 0.1$ and $Q_k = Q = -0.5I$.

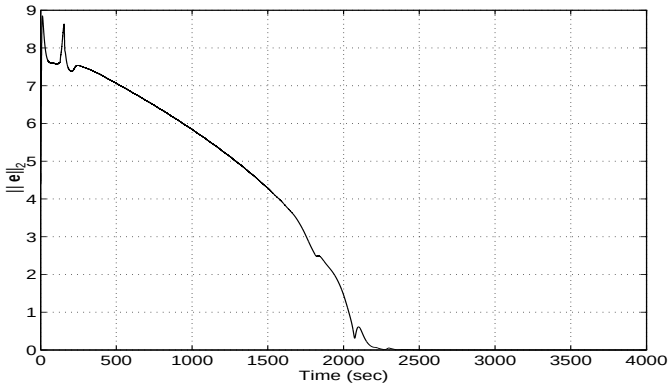

Figure 4.12: $||\mathbf{e}(t,x)||_2$ converging to zero for $\Delta = 0.1$, and $Q_k = Q = -0.5I$ with impulses applied at 32 spatial points in the direction of e_1 and e_2.

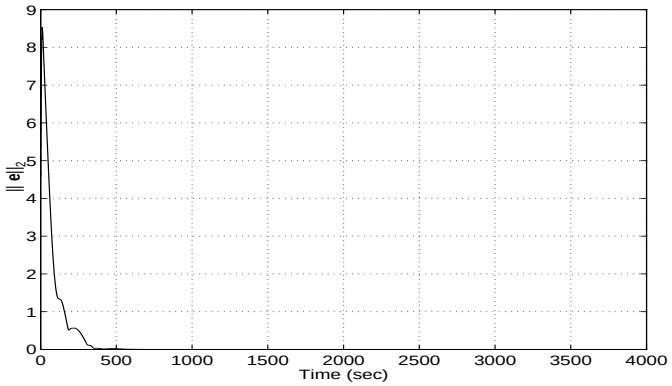

Figure 4.13: $||\mathbf{e}(t,x)||_2$ converging to zero for $\Delta = 0.1$, and $Q_k = Q = \text{diag}(0, -0.5)$ with impulses applied at 32 spatial points in the direction of e_2 only.

mentioned that with the discretization chosen above and the theoretical model represented by equation (4.29), the impulses are applied at every discrete point in the spatial direction x, at every impulsive moment τ_k, $k = 1, 2, \ldots$. In other words, in the numerical model shown here, the impulses are applied on the 256 discrete spatial points corresponding to every τ_k, $k = 1, 2, \ldots$. This explains the quick convergence of solutions to zero. However, in [60,61], it was observed (with an example) that the numerical model obtained from the discretization of systems (4.26) and (4.27) (and hence the error system (4.29)) impulsively synchronize without the need to drive all of the 256 spatial points. i.e., the synchronization of the discrete models approximating systems (4.26) and (4.27) synchronize even by driving much smaller number of points in the spatial direction for every τ_k, $k = 1, 2, \ldots$. We confirm this result by showing two different examples with the same value for Δ and Q. In the first example, we drive 32 spatial points in the e_1 and e_2 directions simultaneously, for every τ_k, $k = 1, 2, \ldots$. Figure 4.12 shows how the error system converges to zero very slowly. In fact the convergence is significantly faster if the impulses are applied at the 32 spatial points but in the e_2 direction only (i.e., $Q = \text{diag}(0, -0.5)$), as shown in Figure 4.13. This is a significant difference between the theoretical model presented earlier and the numerical model shown in the simulations. The reason for the numerical models to show convergence is that the equations obtained by discretization are coupled equations. Thus if the impulse is applied at one particular discrete point, then the neighboring points are also affected because of the coupling factor. This does not hold in the theoretical (or continuous model), because impulses are applied in a continuous manner and it is impossible to apply impulses at discrete points (since the solutions, in this case, are hypersurfaces). We shall analyze the Lyapunov exponents of the numerical examples discussed above to confirm the theoretical results obtained in this section and to provide a numerical evidence on why synchronization still occurs even with impulses not applied along the whole spatial dimension x.

4.5 Analyzing Lyapunov Exponents

In Section 2.3, we discussed a numerical method, employing Lyapunov exponents, to study the dynamics of synchronization errors between two identical Lorenz systems and their derivative systems. We shall extend this method to analyze the Lyapunov exponents of error dynamics between two identical Grey-Scott models.

We begin our discussion by first dealing with the case when we have impulsive driving along the whole spatial direction x. i.e., using the discretization we mentioned in the previous section,

where every discrete spatial point, at every moment τ_k, $k = 0, 1, \ldots$, is driven. Let us have the same set up we had in Section 2.3 where the impulsive synchronization was uni-directional and the impulses were equidistant. Moreover, let, as before, P stand for the period of the impulse and Q stand for the width of the impulse (see Figure 2.11). We shall assume, like before that samples of the state variables of the drive system are used to drive the response system at the discrete moments τ_k, $k = 0, 1, \ldots$. The set of matrices Q_k, $k = 0, 1, \ldots$, will be chosen to be

$$Q_k = \overline{Q} = \begin{pmatrix} -I & O \\ O & O \end{pmatrix},$$

where I is an $\ell \times \ell$ identity matrix and O is an $m \times m$ zero matrix ($\ell + m = n$). This suggests that we should split the drive system into two subsystems, exactly in the same manner we described in Section 2.3, i.e., we shall take $\mathbf{u} = (\mathbf{u}_1, \mathbf{u}_2)^T$, where $\mathbf{u}_1 = (u_{11}, u_{12}, \ldots, u_{1\ell})^T$ and $\mathbf{u}_2 = (u_{21}, u_{22}, \ldots, u_{2m})^T$. In this case, the general form of the driving system will be given by

$$\begin{cases} \dfrac{\partial \mathbf{u}_1}{\partial t} &= \mathbf{p}(\mathbf{u}_1, \mathbf{u}_2, \mathbf{u}_{1x}, \mathbf{u}_{2x}, \ldots) \\ \\ \dfrac{\partial \mathbf{u}_2}{\partial t} &= \mathbf{q}(\mathbf{u}_1, \mathbf{u}_2, \mathbf{u}_{1x}, \mathbf{u}_{2x}, \ldots), \end{cases} \tag{4.37}$$

where we have assumed that $\mathbf{p}$ and $\mathbf{q}$ are both independent of the time variable t and the spatial variable x, an assumption which is consistent with the the models discussed in this chapter. However, for the response system, we have two sets of time intervals to consider (exactly in the same manner discussed in Section 2.3).

- For all $x \in [0, L]$ and for $t \in [kP, kP + Q)$, $k = 0, 1, \ldots$, we have

$$\text{Response system A} \begin{cases} \mathbf{u}_1' &= \mathbf{u}_1 \\ \\ \dfrac{\partial \mathbf{u}_2'}{\partial t} &= \mathbf{q}(\mathbf{u}_1, \mathbf{u}_2', \mathbf{u}_{1x}', \mathbf{u}_{2x}', \ldots), \end{cases} \tag{4.38}$$

- For all $x \in [0, L]$ and for $t \in [kP + Q, (k + 1)P)$, $k = 0, 1, \ldots$, we have

$$\text{Response system B} \begin{cases} \dfrac{\partial \mathbf{u}_1'}{\partial t} &= \mathbf{p}(\mathbf{u}_1', \mathbf{u}_2', \mathbf{u}_{1x}', \mathbf{u}_{2x}', \ldots), \\ \\ \dfrac{\partial \mathbf{u}_2'}{\partial t} &= \mathbf{q}(\mathbf{u}_1', \mathbf{u}_2', \mathbf{u}_{1x}', \mathbf{u}_{2x}', \ldots), \end{cases} \tag{4.39}$$

It follows, from systems (4.38) and (4.39), that the synchronization error will be given by

- For response system A: with $x \in [0, L]$ and $t \in [kP, kP + Q)$, $k = 0, 1, \ldots$, we have

$$\begin{cases} \mathbf{e}_1 &= \mathbf{0} \\ \\ \dfrac{\partial \mathbf{e}_2}{\partial t} &= \mathbf{q}(\mathbf{u}_1, \mathbf{u}_2, \mathbf{u}_{1x}, \mathbf{u}_{2x}, \ldots) - \mathbf{q}(\mathbf{u}_1, \mathbf{u}'_2, \mathbf{u}'_{1x}, \mathbf{u}'_{2x}, \ldots), \end{cases} \tag{4.40}$$

- For response system B: with $x \in [0, L]$ and $t \in [kP + Q, (k + 1)P)$, $k = 0, 1, \ldots$, we have

$$\begin{cases} \dfrac{\partial \mathbf{e}_1}{\partial t} &= \mathbf{p}(\mathbf{u}_1, \mathbf{u}_2, \mathbf{u}_{1x}, \mathbf{u}_{2x}, \ldots) - \mathbf{p}(\mathbf{u}'_1, \mathbf{u}'_2, \mathbf{u}'_{1x}, \mathbf{u}'_{2x}, \ldots), \\ \\ \dfrac{\partial \mathbf{e}_2}{\partial t} &= \mathbf{q}(\mathbf{u}_1, \mathbf{u}_2, \mathbf{u}_{1x}, \mathbf{u}_{2x}, \ldots) - \mathbf{q}(\mathbf{u}'_1, \mathbf{u}'_2, \mathbf{u}'_{1x}, \mathbf{u}'_{2x}, \ldots), \end{cases} \tag{4.41}$$

Notice that systems (4.40) and (4.41) are partial differential equations. Therefore applying the same derivations presented in Section 2.3, is not feasible even with use of the norm given in Definition 4.2.1. This is due to the presence of the spatial derivatives $\mathbf{u}_{ix}, \mathbf{u}_{ixx}, \ldots$, $i = 1, 2$. Therefore in order to implement the same techniques discussed in Section 2.3, we need to apply the *numerical method of lines* for integrating partial differential equations [93]. This method is based on transforming the spatial derivatives $\mathbf{u}_{ix}, \mathbf{u}_{ixx}, \ldots$, $i = 1, 2$, into finite difference expressions (discretization). In other words, systems (4.40) and (4.41) are transformed into a system of N ordinary differential equations, where N depends on the number of spatial points in the discretization process. The new system of ODE's, which approximates the dynamics of the system of PDE's, will be used to discuss the dynamics of the synchronization error. In this case, the synchronization error, $(\mathbf{e}_1, \mathbf{e}_2)^T$, will be given by:

- For response system A: with $t \in [kP, kP + Q)$, $k = 0, 1, \ldots$, we have

$$\begin{cases} \mathbf{e}_1 &= \mathbf{0} \\ \\ \dot{\mathbf{e}}_2 &= \tilde{\mathbf{q}}(\mathbf{u}_1, \mathbf{u}_2) - \tilde{\mathbf{q}}(\mathbf{u}_1, \mathbf{u}'_2), \end{cases} \tag{4.42}$$

- For response system B: $t \in [kP + Q, (k + 1)P)$, $k = 0, 1, \ldots$, we have

$$\begin{cases} \dot{\mathbf{e}}_1 &= \tilde{\mathbf{p}}(\mathbf{u}_1, \mathbf{u}_2) - \tilde{\mathbf{p}}(\mathbf{u}'_1, \mathbf{u}'_2), \\ \\ \dot{\mathbf{e}}_2 &= \tilde{\mathbf{q}}(\mathbf{u}_1, \mathbf{u}_2) - \tilde{\mathbf{q}}(\mathbf{u}'_1, \mathbf{u}'_2), \end{cases} \tag{4.43}$$

The equations in (4.42) and (4.43) are systems of ODE's that can be approximated by the variational systems, given by

$$\dot{\mathbf{e}} = J_{\mathbf{u}_1}\tilde{\mathbf{p}}(\mathbf{u}_1, \mathbf{u}_2)\mathbf{e}_1 \tag{4.44}$$

and

$$\begin{pmatrix} \dot{\mathbf{e}}_1 \\ \dot{\mathbf{e}}_2 \end{pmatrix} = \begin{pmatrix} J_{\mathbf{u}_1}\tilde{\mathbf{p}}(\mathbf{u}_1, \mathbf{u}_2) & J_{\mathbf{u}_2}\tilde{\mathbf{p}}(\mathbf{u}_1, \mathbf{u}_2) \\ J_{\mathbf{u}_1}\tilde{\mathbf{q}}(\mathbf{u}_1, \mathbf{u}_2) & J_{\mathbf{u}_2}\tilde{\mathbf{q}}(\mathbf{u}_1, \mathbf{u}_2) \end{pmatrix} \begin{pmatrix} \mathbf{e}_1 \\ \mathbf{e}_2 \end{pmatrix}, \tag{4.45}$$

respectively, where, as before, J stands for the Jacobian matrices of the corresponding functions. Hence if we let μ and λ be the largest Lyapunov exponents of systems (4.44) and (4.45), respectively, then the derivations stated in Section 2.3 can immediately follow, and inequality (2.48); namely,

$$D := (\mu - \lambda)Q + \lambda P < 0,$$

must be satisfied to guarantee synchronization.

In order to illustrate how the numerical method of lines work and how to incorporate this with the theory of Lyapunov exponents presented in Section 2.3, we shall take the synchronization error between two identical Grey-Scott models discussed at the end of Section 4.4. Suppose that samples of the state variable u_2 are used to drive the state variable v_2 in the response system at the discrete moments τ_k, $k = 0, 1, \ldots$, for all $x \in [0, L]$ (here $\ell = m = 1$). Obviously, the response system A_1, for $x \in [0, L]$ and $t \in [kP, kP + Q)$, $k = 0, 1, \ldots$, is given by

$$\text{Response system } \mathrm{A}_1 \begin{cases} \dfrac{\partial e_1}{\partial t} &= -(a + u_2^2)e_1 + d_1\dfrac{\partial^2 e_1}{\partial x^2}. \\ \\ e_2 &= 0 \end{cases} \tag{4.46}$$

Applying the finite difference method, to discretize the last term in the first equation of (4.46), and the periodic boundary conditions, we get, for $j = 1, 2, \ldots, 255$,

$$\dot{e}_1^{(j)} = -\left[a + \left(u_2^{(j)}\right)^2\right] e_1^{(j)} + d_1\frac{e_1^{(j+1)} - 2e_1^{(j)} + e_1^{(j-1)}}{(\Delta x)^2},$$

where $\Delta x = L/256$ (here $N = 256$). The largest Lyapunov exponent of the latter model is given by $\mu = -0.80867$. To evaluate the second Lyapunov exponent λ, we need to consider the response system B, given by

$$\text{Response system B} \begin{cases} \dfrac{\partial e_1}{\partial t} &= -(u_1u_2^2 - v_1v_2^2) - ae_1 + d_1\dfrac{\partial^2 e_1}{\partial x^2} \\ \\ \dfrac{\partial e_2}{\partial t} &= u_1u_2^2 - v_1v_2^2 - (a + b)e_2 + d_2\dfrac{\partial^2 e_2}{\partial x^2}. \end{cases} \tag{4.47}$$

With the applications of the finite difference method and the periodic boundary conditions, system (4.47) becomes, for $j = 1, 2, \ldots, 255$,

$$\begin{cases} \dot{e}_1^{(j)} &= -\left[u_1^{(j)}\left(u_2^{(j)}\right)^2 - v_1^{(j)}\left(v_2^{(j)}\right)^2\right] - ae_1^{(j)} + d_1\dfrac{e_1^{(j+1)} - 2e_1^{(j)} + e_1^{(j-1)}}{(\Delta x)^2} \\ \\ \dot{e}_2^{(j)} &= u_1^{(j)}\left(u_2^{(j)}\right)^2 - v_1^{(j)}\left(v_2^{(j)}\right)^2 - (a+b)e_2^{(j)} + d_2\dfrac{e_2^{(j+1)} - 2e_2^{(j)} + e_2^{(j-1)}}{(\Delta x)^2}. \end{cases} \tag{4.48}$$

The variational equation of system (4.48) is given by

$$\begin{cases} \dot{e}_1^{(j)} &= -\left[a + \left(u_2^{(j)}\right)^2\right] e_1^{(j)} - 2u_1^{(j)}u_2(j)e_2^{(j)} + d_1\dfrac{e_1^{(j+1)} - 2e_1^{(j)} + e_1^{(j-1)}}{(\Delta x)^2} \\ \\ \dot{e}_2^{(j)} &= \left(u_2^{(j)}\right)^2 e_1^{(j)} + (2u_1^{(j)}u_2(j) - a - b)e_2^{(j)} + d_2\dfrac{e_2^{(j+1)} - 2e_2^{(j)} + e_2^{(j-1)}}{(\Delta x)^2} \end{cases} \tag{4.49}$$

The largest Lyapunov exponent of system (4.49) is given by $\lambda = 0.0023$. Using these values for μ and λ, one can give an estimate on the maximum impulse duration permissible to achieve synchronization, provided that a value for the impulse width Q is chosen.

The analysis of the case when the impulses are not applied along the whole spatial dimension x, is still very similar to the above approach. It is done by applying the method of lines first to the PDE's involved in the model, and creating a system of ODE's which will be used to find the Lyapunov exponents of the synchronization error. In the previous section, we discussed one particular example employing two identical Grey-Scott models which was motivated by the work of Kocarev et al., in [60, 61]. In that example, the spatial derivatives in the two Grey-Scott models were discretized using the finite difference method and the resulting ODE's were integrated numerically using forward Euler integration. The number of spatial points in that discrete model was 256 points for each given time step t_s, $s = 1, 2, \ldots$. The impulsive driving was done at 32 spatial points of the 256 spatial points generated from discretizing the state variable v_2. In other words, taking $K = L/32$, the values of the impulses were given by

$$v_2(\tau_k^+, \kappa K) = v_2(\tau_k, \kappa K) + \epsilon(u_2(\tau_k, \kappa K) - v_2(\tau_k, \kappa K)), \tag{4.50}$$

$k = 0, 1, \ldots$ and $\kappa = 1, 2, \ldots, 32$. In the previous section, we showed, through numerical simulations, that the norm of the error dynamics between the two Grey-Scott models approached zero when $\epsilon = -0.5$. Now suppose that the value of $\epsilon = -1$ and the method of lines is applied instead.

This means that the spatial derivatives are discretized using finite difference method and the Grey-Scott models are transformed into two systems of 2×257 ordinary differential equations. In this case, 32 equations out of each one of these two systems of ODE's will be synchronized impulsively using the impulses described by equation (4.50). These equations that synchronize are those given by

$$\dot{u}_2^{(8*\kappa)} = u_1^{(8*\kappa)} \left(u_2^{(8*\kappa)}\right)^2 - (a+b)u_2^{(8*\kappa)} + d_2 \frac{u_2^{(8*\kappa+1)} - 2u_2^{(8*\kappa)} + u_2^{(8*\kappa-1)}}{(\Delta x)^2} \tag{4.51}$$

at the transmitter end, and, by equation (4.50),

$$\begin{cases} \dot{v}_2^{(8*\kappa)} &= v_1^{(8*\kappa)} \left(v_2^{(8*\kappa)}\right)^2 - (a+b)v_2^{(8*\kappa)} + d_2 \dfrac{v_2^{(8*\kappa+1)} - 2v_2^{(8*\kappa)} + v_2^{(8*\kappa-1)}}{(\Delta x)^2} \\ \\ v_2(\tau_k^+)^{(8*\kappa)} &= v_2(\tau_k)^{(8*\kappa)} - (u_2(\tau_k)^{(8*\kappa)} - v_2(\tau_k)^{(8*\kappa)}), \end{cases} \tag{4.52}$$

for $\kappa = 1, 2, \ldots, 32$, at the receiver end. Certainly, the other equations are not impulsively synchronized. If we denote the vector $(u_1^{(8)}, u_1^{(16)}, \ldots, u_1^{(256)})$ by $\overline{\mathbf{x}}$ and the vector consisting of the remaining state variables at the transmitter end by $\overline{\mathbf{y}}$, whereas we denote the vector $(v_1^{(8)}, v_1^{(16)}, \ldots, v_1^{(256)})$ by $\overline{\mathbf{x}}'$ and the vector consisting of the remaining state variables at the receiver end by $\overline{\mathbf{y}}'$, then the theory developed in Section 2.3 is applicable. Thus a typical expression for the response system A_2, for $t \in [kP, kP+Q)$, $k = 0, 1, \ldots$, will be given by

$$\begin{cases} \overline{\mathbf{X}} &= \overline{\mathbf{x}} - \overline{\mathbf{x}}' = 0 \\ \\ \dot{\overline{\mathbf{Y}}} &= \dot{\overline{\mathbf{y}}} - \dot{\overline{\mathbf{y}}}'. \end{cases} \tag{4.53}$$

The variational equation approximating the error dynamics given by (4.53) can be evaluated and a fourth order Runge-Kutta method may be used to integrate the resulting variational equation in order to find its largest Lyapunov exponent. By applying Matlab programming, we found out that the largest Lyapunov exponent of system (4.53) is given by $\mu = -0.0242$. Unlike the latter description, when $t \in [kP + Q + (k+1)P)$, $k = 0, 1, \ldots$, (i.e., outside the impulse), the response system will be identical to the response system B obtained in the previous example. Thus the error dynamics between the ODE's at the transmitter and receiver are identical to those given by equation (4.48). This means that the value of $\lambda = 0.0023$.

Once more, knowing these values of μ and λ, one may obtain an upper bound on the maximum impulse duration permissible to achieve synchronization provided that Q, the width of the impulse, is known.

Chapter 5

Applications

Although chaos synchronization has several important applications, secure communication forms one of its most fundamentally promising applications among all others. Due to the fact that chaos exhibits pseudorandom behaviour, secure communications based on chaos have been investigated for some years, especially in the area of radio-frequency transmissions. Signal encoding and decoding are achieved using a carrier whose amplitude fluctuates chaotically and both employ different synchronization techniques some of which have been already presented in Chapter 2. Compared with conventional data encryption techniques in which the key is a pseudorandom binary number that controls the encryption algorithm, but which is slow, chaos is used as a coding key embodied directly in the structure of the carrier.

There are several methods proposed in the literature which combine chaos synchronization with communication security. Some of these methods are based on chaos masking, chaos switching, chaos modulation and impulsive related methods (called impulsive cryptosystems). We shall explain in this chapter how each method functions and give some examples to illustrates each technique. Due to the fact that impulsive cryptosystems can be combined with conventional cryptographic techniques, this makes impulsive cryptosystems very promising to build a secure cryptosystem. We shall evaluate the performance of those methods which deal with impulsive synchronization and improve on its security and its performance by proposing several modified approaches to those described in the literature.

In the next section, we shall explain, in detail, several communication security schemes, such as the methods of chaos masking, chaos switching, chaos modulation and the method based on impulsive synchronization. In Section 5.2, we shall discuss the performance of the cryptosystems

which are based on impulsive synchronization in terms of transmission and accuracy, then we shall investigate its robustness towards parameter mismatch and towards time delay leading to the construction of a newly proposed secure communication scheme called the *induced message cryptosystem*. Finally in Section 5.3, we shall extend the idea of chaos-based secure communication schemes to employ spatiotemporal chaotic systems generated by partial differential equations.

5.1 Chaos-Based Secure Communication Schemes

As one illustration of potential use of synchronized chaotic systems in communication, a group of methods were proposed in the literature concerning this matter. We shall discuss here three different methods called *chaotic masking*, *chaotic switching* and *chaotic modulation* (spread-spectrum transmission) [81, 82]). This discussion will include the description of each cryptosystem, its performance and its drawbacks. We should bear in mind that the chaotic systems employed in each of these cryptosystems may be chosen to be one of those systems described by equations (1.5), (1.6) and (1.7), or even any other system exhibiting chaotic behaviour and possessing synchronization property in the sense of Carroll-Pecora. For simplicity, we shall use the Lorenz system in the coming discussion.

We start first with the chaotic signal masking method which was proposed in [22–24]. The basic idea that underlines this method is the addition of a noise-like masking signal to the information-bearing signal $m(t)$ at the transmitter, then the masking is removed by synchronization at the receiver. This is done by using the received signal to regenerate the masking signal at the receiver and subtract it from the received signal to recover $m(t)$ (see Figure 5.1). Experimental results, done by the authors of [24], show that the ability to synchronize, using the circuit constructed and given in [22–24], is robust, i.e., is not highly sensitive to perturbations in the drive signal, and thus synchronization can be done with the use of masked signals. Even though such a property is required to achieve good synchronization results and to prevent the effect of noise contributed by the public channel connecting the transmitter and receiver, it makes the system more vulnerable to attacks, since intruders may find the information in the chaotic noise by using some adaptive filtering technique such as *blind signal separation* [110]. This problem can be avoided very easily as we shall see in the applications of impulsive systems. Although there are many possible variations, we shall consider, for example, a transmitted signal of the form $s(t) = u(t) + m(t)$. It is assumed that for masking, the power level of $m(t)$ is significantly lower than that of $u(t)$ to guarantee convergence. The dynamical system at the receiver is similar

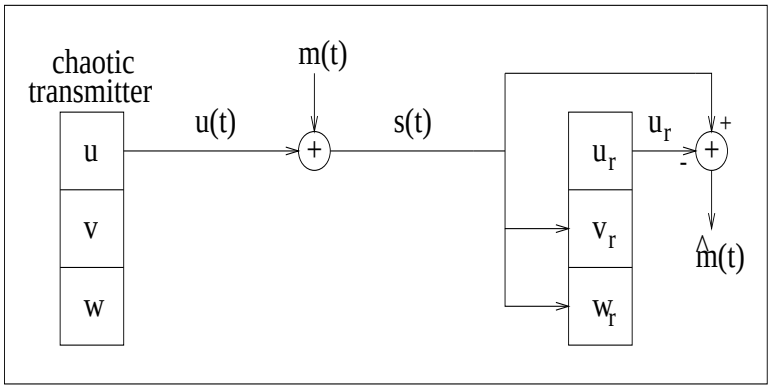

Figure 5.1: Chaotic signal masking system.

to system (2.7), with $u(t)$ replaced by $s(t)$ as a driving signal. When the receiver is synchronized with the transmitter by using $s(t)$ as a drive signal, then $u_r(t) \approx u(t)$, and consequently $m(t)$ is recovered as $\hat{m}(t) = s(t) - u_r(t)$, as illustrated in Figure 5.1. The performance of this approach was demonstrated in [22–24]. In Figure 5.2 a segment of a speech from the sentence "*He has the bluest eyes*", is used. The figure shows the original speech $m(t)$ and the recovered speech signal $\hat{m}(t)$, where these signals were low-pass filtered and down-sampled. Clearly, the speech signal was recovered and was of reasonable quality in informal listening tests.

We now demonstrate the potential use of chaotic switching in secure communication. In the previous approach (chaotic masking), a continuous information-bearing signal was encrypted by a noise-like masking signal; here we describe a quite similar cryptosystem, also proposed in [22–24], to transmit and recover a binary-valued bit streams. The basic idea of this proposed method is to modulate a transmitter coefficient with the information-bearing waveform and to transmit the chaotic drive signal. At the receiver, the coefficient modulation will produce a synchronization error between the received drive signal and the receiver's generated drive signal with an error amplitude that depends on the modulation. Using the synchronization error, the modulation can be detected (recall that the parameter modulation generated by the unavoidable difference created in designing identical circuits, can be removed, as mentioned earlier, by implementing cascaded systems; however, here we are taking an advantage of this parameter mismatch in applying it to secure communication). This modulation/detection process is illustrated in Figure 5.3. In this figure, the coefficient b of the Lorenz system of the transmitter, given by (1.5), is modulated by an

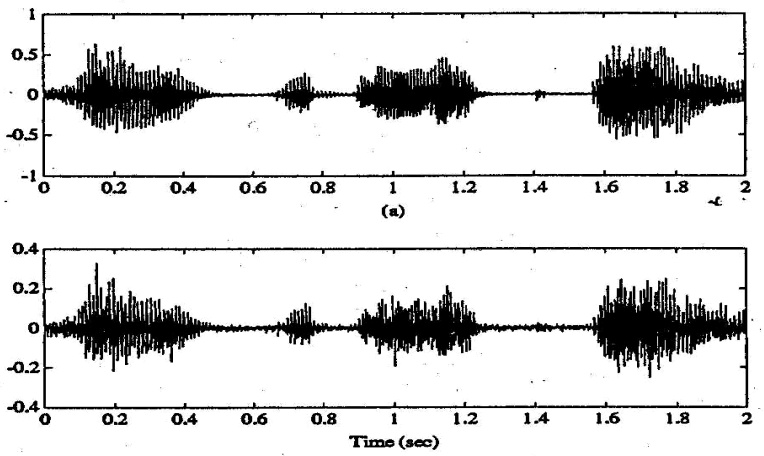

Figure 5.2: Circuit data: Speech waveform. (a) Original. (b) Recovered.

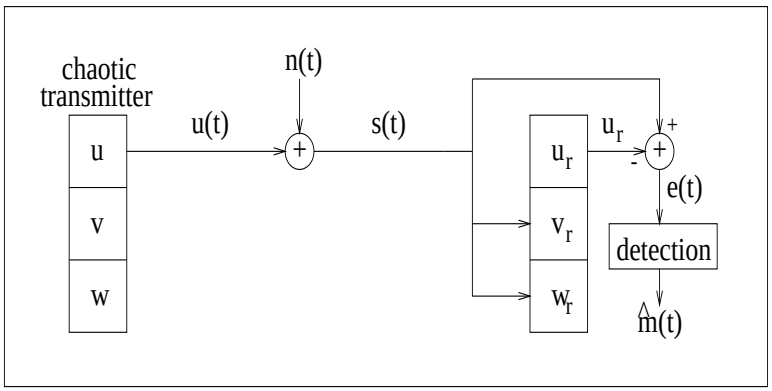

Figure 5.3: Chaotic switching communication system.

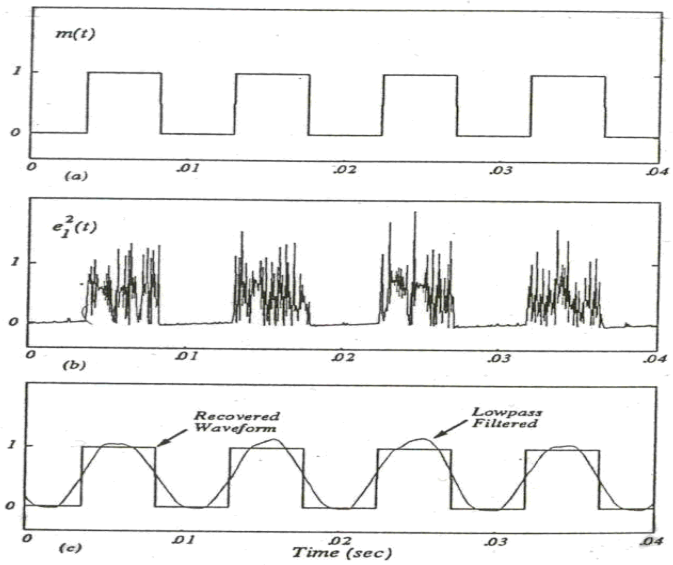

Figure 5.4: Circuit data: (a) Modulation waveform. (b) Synchronization error power. (c) Recovered waveform.

information-bearing waveform $m(t)$. The information is carried over the channel by the chaotic signal $u_m(t)$. The noisy received signal $r(t) = u_m(t) + n(t)$ serves as the driving input to the receiver. At the receiver, the modulation is detected by forming the difference between $r(t)$ and the reconstructed drive signal $u_r(t)$. If we assume that the signal-to-noise ratio (SNR) of $r(t)$ is large, the error signal $e_1(t) = r(t) - u_r(t)$ will have a small average power if no modulation is present. However, if, for example, the information-bearing waveform is a binary-valued bit stream with a "1" representing a coefficient mismatch and a "0" representing no coefficient mismatch, then $e_1(t)$ will be large in amplitude during the time period that a "1" is transmitted and small in amplitude during a "0" transmission. The synchronizing receiver can thus be viewed as a form of matched filter for the chaotic transmitter signal $u(t)$.

To illustrate this technique, we shall use a square-wave for $m(t)$ as shown in Figure 5.4(a). The square-wave produces a variation in the transmitter coefficient b with the zero-bit and one-bit coefficients corresponding to $b(0) = 4$ and $b(1) = 4.4$, respectively. Figure 5.4(b) shows the synchronization error power, $e_1(t)$, at the output of the receiver circuit. The coefficient modulation produces significant synchronization error during a "1" transmission and a very small error during a "0" transmission. Figure 5.4(c) illustrates that the square-wave modulation can be reliably recovered by low-pass filtering threshold test. The allowable data rate is, of course,

dependent on the synchronization response time of the receiver system. In [24], a low bit rate was used to illustrate the technique, but one can easily adjust to allow much faster bit rates.

Note that the ability to communicate digital bit streams using this method depend on the periodic nature of the square-wave used to demonstrate the technique. The results apply to aperiodic or random bit streams as well. In fact, in [81] and [85], Chua's oscillator was used for the process of modulation/detection of random bit streams. To explain how that was done, we use the same approach but applied on the Lorenz system for the sake of notation. In this case, the receiver will possess two almost identical chaotic systems that differ only with the value of the coefficient b, i.e., b has the value 4.4 for the first chaotic system and the value 4 for the second chaotic system. Thus in order to transmit a binary-valued bit stream, we let $b(1) = 4.4$ and $b(0) = 4$, as before. When the bit "1" is transmitted, the first system will synchronize; however, the second system will have a synchronization error. Similarly, if the bit "0" is transmitted, the second system will synchronize and the first will not. Defining the quantities $\Delta_0 := u - u_{r_0}$ and $\Delta_1 := u - u_{r_1}$, where $\mathbf{u}_{r_0} := (u_{r_0}, v_{r_0}, w_{r_0})^T$ and $\mathbf{u}_{r_1} := (u_{r_1}, v_{r_1}, w_{r_1})^T$ are the state variables of the first and the second chaotic systems, implies that the first system will synchronize if $\Delta_0 = 0$ and the second system will synchronize if $\Delta_1 = 0$. We let $b_{\text{in}}(t)$ denote the binary input signal, $s(t)$ to be the transmitter signal, a_0 to be the 40-points moving average of Δ_0, a_1 to be the 40-points moving average of Δ_1 and $\epsilon := 0.1$, then the binary output signal $b_{\text{out}}(t)$ is recovered to a very good accuracy using the following rule

$$b_{\text{out}}(t) = \begin{cases} 0, b_{\text{old}} = 0 & \text{for} \quad a_0 < \epsilon,\ a_1 > \epsilon \\ 1, b_{\text{old}} = 1 & \text{for} \quad a_0 > \epsilon,\ a_1 < \epsilon \\ b_{\text{old}} & \text{for} \quad a_0 < \epsilon,\ a_1 < \epsilon \\ 1 - b_{\text{old}} & \text{for} \quad a_0 > \epsilon,\ a_1 > \epsilon. \end{cases}$$

The experimental and numerical results were obtained in [82] and [85]. We show in Figure 5.5 some of the simulations obtained in [82] using the above approach, where we can see very clearly how the binary input signal was completely recovered by the display of the $b_{\text{out}}(t)$, using the above rule.

While the above approach is fascinating and surely warrant further investigation, it may suffer from serious drawbacks in practice. First, since two matched analogue chaotic circuits are

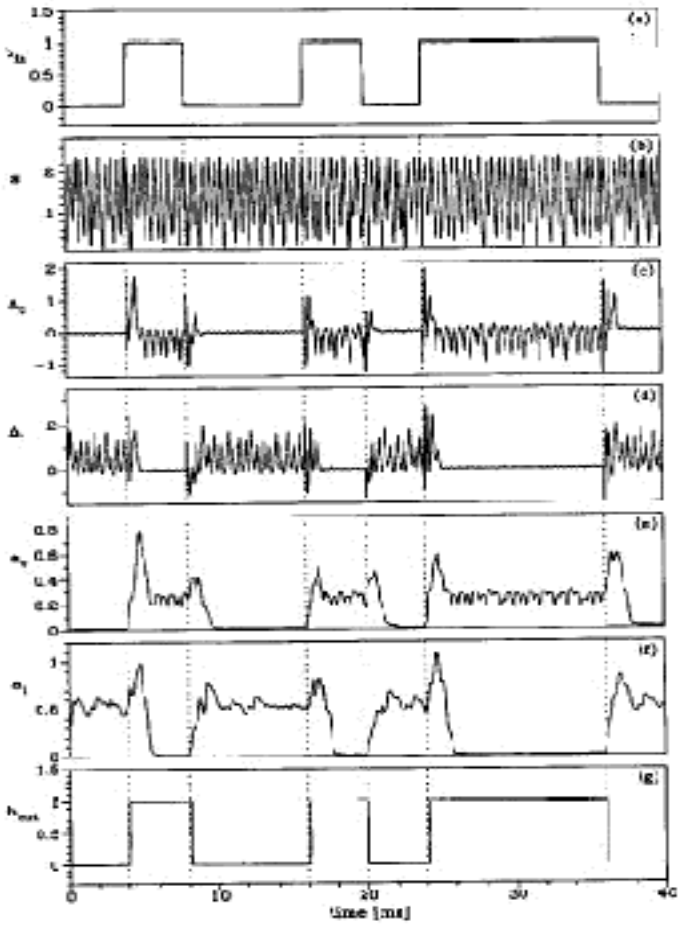

Figure 5.5: Transmission of digital signals via chaos switching: (a) Binary input signal. (b) Transmitted signal. (c) Response Δ_0. (d) Response Δ_1. (e) Average moving a_0. (f) Average moving a_1. (g) Output binary signal.

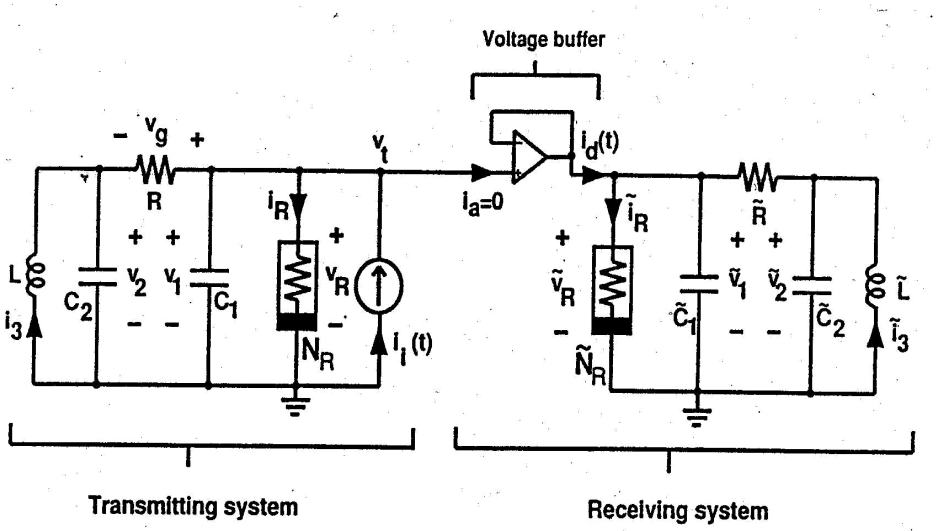

Figure 5.6: Schematic diagram of the chaotic modulating communication system.

required at remote locations, there can be serious problems with system performance unless a method of calibration is used. Second, it may be possible to distinguish one attractor from the other without locking to the chaotic signal. This can be done by performing an attack, proposed in [111], based on *short-time zero-crossing rate* (STZCR) that can recover the digital signal from the chaotic switching without locking to the chaotic signal, as desired.

We present now another method called chaotic modulation proposed in [39] and [81] that resembles the above approaches, but adds more complexity and security to the transmitted signals. The suggested idea is to multiply the information signal by a broad-spectrum, noise-like chaotic signal. By a broad-spectrum system we mean [40]: "a means of transmission in which the signal occupies a bandwidth in excess of the minimum necessary to send the information; the band spread is accomplished by means of a code which is independent of the data, and a synchronized reception with the code at the receiver is used for despreading and subsequent data recovery". For this method, we use Chua's oscillator, given in equation (1.6), as the chaotic system installed at the transmitter and the receiver, where very accurate knowledge of the parameters of the circuit, represented by Chua's oscillator, is required to generate (or synchronize to) the same chaotic signal.

We now investigate this technique in the following manner. The basic system used for communication is given in Figure 5.6. It utilizes a Chua's circuit each for the transmitting and the receiving system. In the transmitting system, an information-bearing current signal $i_i(t)$ is in-

jected into Chua's circuit, thereby modifying its dynamics. The voltage signal $v_t = v_1$ of this Chua's circuit is then transmitted. The receiving system then uses this transmitted voltage signal to obtain a detected current signal $i_d(t)$. The information we want to transmit is in the form of input information "voltage" signal $v_s(t)$ which is then coded in the injected current signal $i_i(t)$ by the invertible coding function $\mathcal{C}(.) : i_i(t) = \mathcal{C}(v_s(t))$. The detected current signal $i_d(t)$ is then decoded through $v_r(t) = \mathcal{C}^{-1}(i_d(t))$. For proper operation of the system, we want $v_r(t) \approx v_s(t)$. We also want to choose $\mathcal{C}(.)$ so that the injected signal $i_i(t)$ is such that the dynamics of the Chua's circuit and the transmitted signal v_t are still chaotic. To function as a secure communication, we also want the transmitted signal v_t to look the same regardless of the information signal v_s that is being fed into the transmitting system. The voltage across the capacitor C_1 is transmitted through the channel to the receiver circuit and is used as a forcing voltage on the second Chua's circuit capacitor $\tilde{C}_1$. Assuming that all circuit components of the transmitter and the receiver are matched exactly, and inserting a voltage buffer to separate the two subsystems, we will have $\tilde{v}_1 = v_1$. Using this condition and subtracting the circuit equations of the drive and the response, one obtains

$$\begin{aligned} i_d(t) - i_i(t) &= \frac{1}{R}(v_2 - \tilde{v}_2), \\ C_2 \frac{d(v_2 - \tilde{v}_2)}{dt} &= -\frac{1}{R}(v_2 - \tilde{v}_2) + (i_3 - \tilde{i}_3), \\ L \frac{d(i_3 - \tilde{i}_3)}{dt} &= -(v_2 - \tilde{v}_2). \end{aligned} \tag{5.1}$$

In [39], it was noticed that the last two equations of system (5.1) are the state equations of a parallel RLC circuit with positive R, L and C. This implies that the origin is globally asymptotically stable. In fact, the eigenvalues of the new system, build from the last two equations of (5.1), are given by

$$\frac{-1}{2C_2R} \pm \frac{1}{2}\sqrt{\frac{1}{C_2^2R^2} - \frac{4}{C_2L}}.$$

Thus, if these two eigenvalues are real, then they are negative, and if they are a complex conjugate pair, then they both have negative real parts. This implies, in both cases, that the origin is globally asymptotically stable and $v_2 - \tilde{v}_2 \longrightarrow 0$ as $t \longrightarrow \infty$. Thus, by the first equation of system (5.1), we have $i_d(t) \longrightarrow i_i(t)$ as $t \longrightarrow \infty$, and hence $v_r(t) \longrightarrow v_s(t)$ as $t \longrightarrow \infty$. This means that the current flowing into the second Chua's circuit must equal (maybe after some transient) the

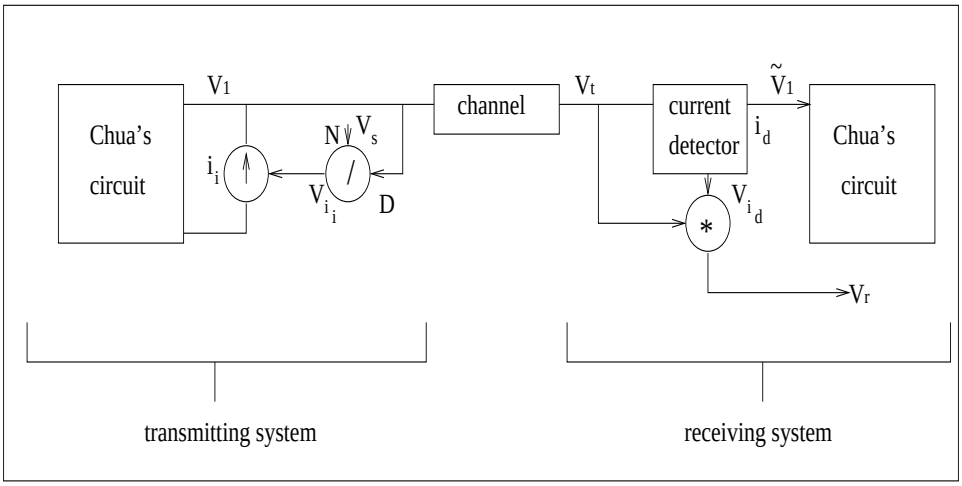

Figure 5.7: Block diagram of a chaotic modulating communication system.

current injected into the first Chua's circuit.

The laboratory implementation of such a transmission system was described in [39], where a division operation $\mathcal{C}(v_s(t)) = v_s(t)/v_1(t)$ was chosen as the coding function and multiplication operation $v_r = \mathcal{C}(v_s(t))v_1$ as the decoding one. Therefore the complexity of the transmitted signal is increased and the security of the system is enhanced, unlike the case with chaotic masking where simple addition of the chaotic signal to the transmitted one was applied. The block diagram of the implemented system is shown in Figure 5.7. This diagram could serve as a general principle of a transmission system using chaotic modulation.

In [39] and [81], it was realized that the whole range of the chaotic signal spectrum is used for hiding the information, an advantage that previous methods were lacking. Furthermore, the sensitivity of this technique to parameter variation between the transmitter and the receiver is a good feature that will increase the security of the system. Generally speaking, we would rather seek cryptosystems that must meet two outstanding criteria:

1. Security: The system must be such that an intruder cannot decode the message without access to the precise system parameter values used by the receiver and the sender. Even a slight mismatch should make recovery impossible. Further, it should be extremely difficult for the intruder to obtain the precise parameter values even if a correct message or a correct key fragment is intercepted.

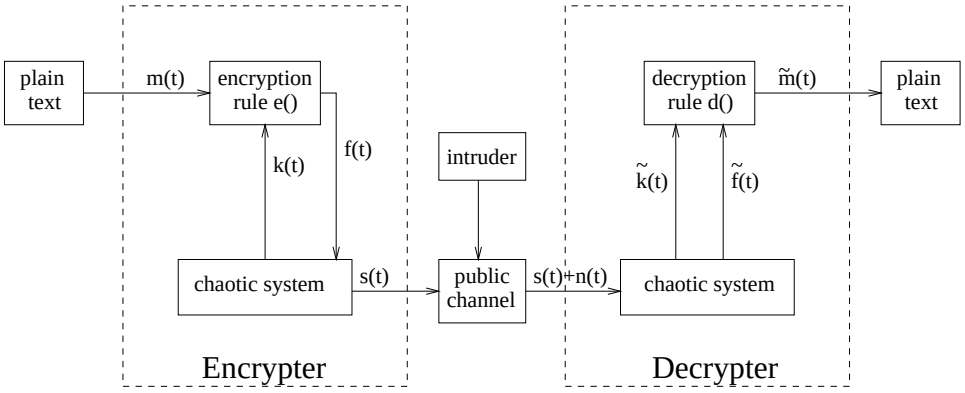

Figure 5.8: Block diagram of a chaotic cryptosystem.

2. Robustness: The system should be tolerant of additive noise in the communication channel.

These two requirements are actually rather stringent. We are essentially asking for a system with extreme sensitivity to parameter mismatch and significant insensitivity to input perturbations. Typically, chaotic systems will satisfy the first requirement, but not the second. Therefore one of our major goals in developing impulsive system technique that will be discussed later, is to achieve the second desired property, namely robustness.

The synchronization principles described above enabled us to build chaotic systems operating coherently and to use them to solve real communication problems. Understanding synchronization phenomena of simple inter-connections of chaotic oscillators enabled several interesting developments, especially with the introduction of impulsive synchronization as a technique used in certain chaos-based communication security schemes. However, the question that remains is: how would we exploit the property of impulsive synchronization to secure communication? Due to the fact that low-dimensional chaos-based secure communication systems are not sensitive enough to the modeling error of the transmitter, as we mentioned before, an intruder can recover the message signal by using an approximate model with some errors which can be easily removed by standard filtering methods. Since we shall discuss first three-dimensional systems, we may enhance the security of low-dimensional chaos-based secure communication scheme by combining conventional cryptographic schemes with chaotic systems [119]. The purpose of doing so is to increase the complexity of the transmitted signal and hence improve the sensitivity of the system to recovering and modeling errors. In this proposed method, the encrypter consists of a chaotic

system and an encryption function $e(\cdot)$, as shown in Figure 5.8. The key signal $k(t)$ is one of the state variables of the chaotic system. Another state variable $s(t)$ is the transmitted signal, which is transmitted through a public channel to the decrypter. $f(t)$ is the encrypted signal which is fed back into the chaotic system. The decrypter consists of a chaotic system and a decryption function $d(\cdot)$. The decrypter can find the key signal when the encrypter and decrypter are synchronized using the received signal $s(t) + n(t)$, where $n(t)$ is the noise added to the transmitted signal. The encrypted signal is also recovered via synchronization. Then $d(\cdot)$ is used to decrypt the encrypted signal. It should be noted that in the scheme shown in Figure 5.8, both the key signal $k(t)$ and the encrypted signal $f(t)$ are not transmitted to the decrypter.

Another goal we would like to pursue is to reduce the redundancy in the transmitted signal. To achieve this goal, impulsive synchronization offers a very promising approach. An improved version of the latter approach was proposed in [114–116], and it is illustrated here. The proposed system consists of a transmitter and a receiver, each of which (see the block diagram in Figure 5.9) possesses a chaotic system identical to the other and a conventional cryptographic scheme identical to the other. The message signal at the transmitter end is encrypted using one of the state variables of the chaotic system as a key signal and the complexity of the encrypted signal is increased by taking a linear combination of all of its components to generate the scrambled signal. The transmitted signal consists of a sequence of time frames. Every time frame is of length P seconds and it consists of two regions. As we can see from Figure 5.10, the first region of each time frame is a synchronization region of length Q seconds consisting of the synchronization impulses (which are used to synchronize both chaotic systems, as in Corollary 2.1.1). The second region is the scrambled signal region of length $P - Q$ seconds where the scrambled signal is contained. To ensure synchronization, we require $P < \Delta_{\max}$ (see Corollary 2.1.1, inequality (2.19)). These two regions are combined as shown in Figure 5.10, and transfered through a public channel. At the receiver end, the decomposition block is used to separate the synchronization region and the scrambled signal region from each other. The synchronization impulses are used to synchronize both chaotic systems and thus recover the key signal which is in turn is used to decrypt the scrambled signal.

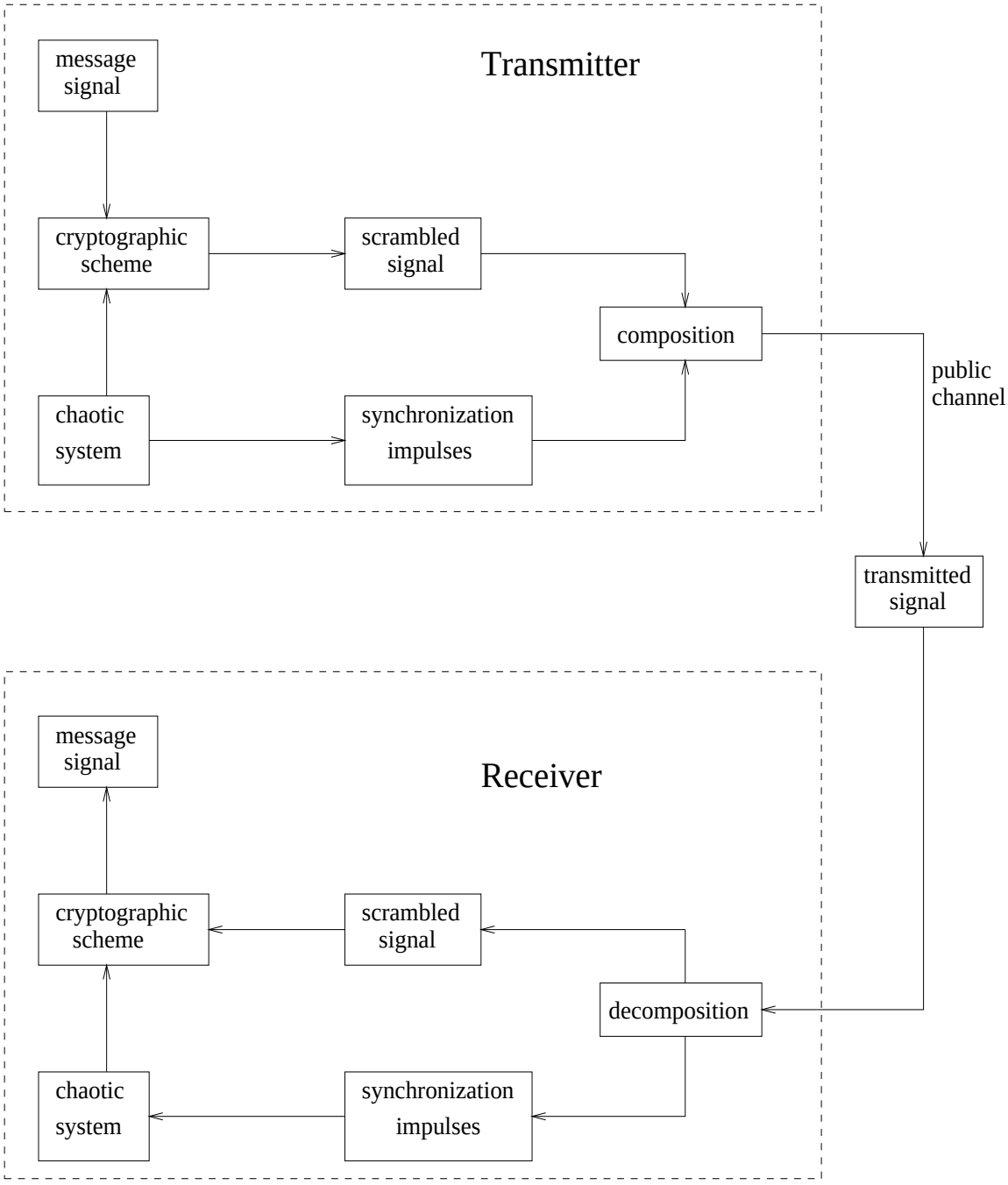

Figure 5.9: Block diagram of impulsive synchronization.

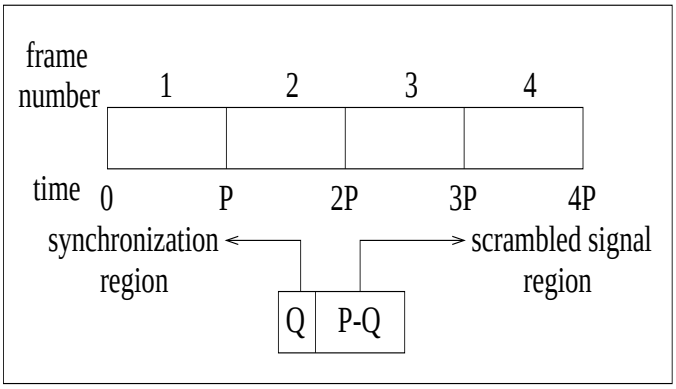

Figure 5.10: The time frames of a transmitted signal.

In order to encrypt the message signal $m(t)$, a continuous n-shift cipher, given by

$$f_1(x,k) = \begin{cases} (x+k)+2h & \text{if} \quad -2h \leq (x+k) \leq -h \\ (x+k) & \text{if} \quad -h < (x+k) < h \\ (x+k)-2h & \text{if} \quad h \leq (x+k) \leq 2h, \end{cases} \tag{5.2}$$

is used in the following manner:

$$e[m(t)] = f_1(\ldots f_1(f_1[m(t),k(t)],k(t)),\ldots,k(t)) = y(t),$$

where $k(t)$ is the key signal obtained from the chaotic system and h is chosen such that $m(t), k(t) \in [-h,h]$. It should be noted here that the map $f_1(\cdot,\cdot)$, given by equation (5.2), is implemented on continuous signals, $m(t)$ and $k(t)$, which are rescaled so that they would lie within the interval $[-h,h]$, unlike before. Obviously, to decrypt the signal $f(t)$, we apply, as before, the transformation

$$m(t) = d[f(t)] = f_1(\ldots f_1(f_1[f(t),-k(t)],-k(t)),\ldots,-k(t)).$$

Notice that, in the transmitter and the receiver, we use the same cryptographic scheme block for purposes of bidirectional communication. In bidirectional communication , every cellular phone should function both as a receiver and as a transmitter.

In the next section, we shall demonstrate the robustness of communication security schemes, which are based on impulsive synchronization, in the presence of parameter mismatch and delay.

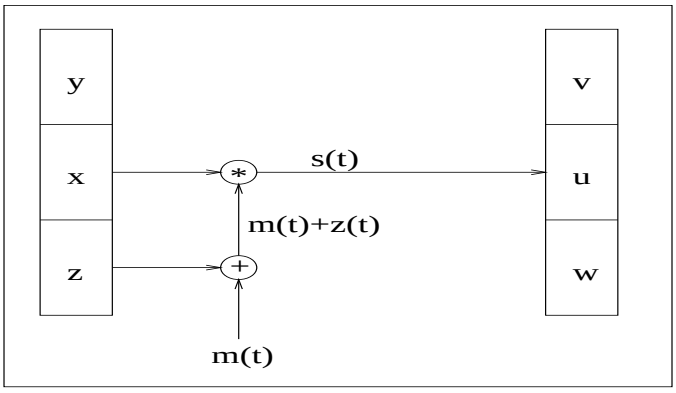

Figure 5.11: Chaotic masking-modulating of $m(t)$.

Then we shall further improve on the security of the cryptosystem proposed by Yang et al. [114–116], described above, and overcome several problems regarding its performance [41, 43–45] by proposing a modified technique for communication.

5.2 Induced-Message Cryptosystem

We are interested in investigating the robustness of communication security schemes, which are based on chaos synchronization using impulsive methods, towards parameter mismatch and delay. Due to the fact that it is physically impossible to design two identical chaotic systems and that the presence of delay in impulsive synchronization, due to transmission of signals (and impulses) and sampling delay, discussed in Chapter 3, is inevitable, we have to explore the effect of these factors on cryptosystems based on this method of synchronization. This will be done by considering a cryptographic scheme which combines masking and modulating methods with impulsive synchronization for illustrative purposes. The proposed cryptosystem contains two chaotic systems $\mathbf{x}$ and $\mathbf{u}$, not necessarily identical, which are used to mask-modulate and unmask the message signal $m(t)$, respectively. As shown in Figure 5.11, one chaotic system $\mathbf{x} = (x, y, z)^T$ is at the transmitter end and the other $\mathbf{u} = (u, v, w)^T$ is at the receiver end. The masking-modulating process of $m(t)$ is done through two operations: addition and multiplication, viz. $f(t) := e(m(t)) = x(t)(m(t) + z(t))$, where $f(t)$ is the encrypted signal that will be used to drive the chaotic system $\mathbf{u}$ at the receiver end.

Figure 5.12 shows the cryptosystem structure which is similar to the one given in the previous section. The message signal is encrypted using the above scheme to generate $f(t)$. $s(t)$ is the

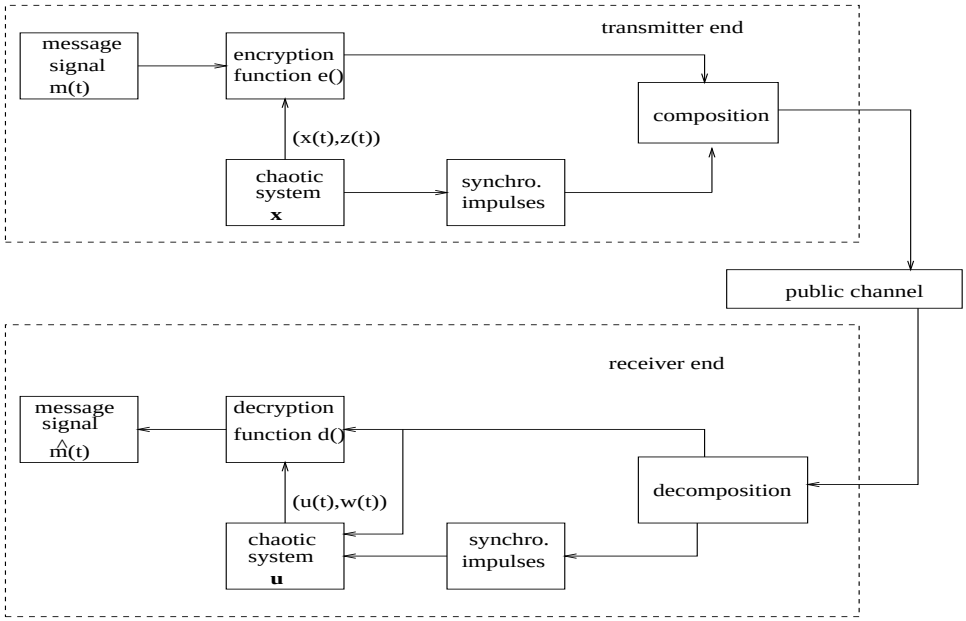

Figure 5.12: Proposed cryptosystem.

transmitted signal; it consists of the sequence of time frames described in the previous section and in Figure 5.10. When each time frame of $s(t)$ is decomposed into the encrypted message $f(t)$ and the synchronizing impulses, the signal $f(t)$ is used to drive the system $\mathbf{u}$, whereas the impulses are used to impulsively synchronize $\mathbf{u}$ with $\mathbf{x}$. By Theorem 2.2.1, the synchronization between $\mathbf{x}$ and $\mathbf{u}$ will be achieved, and we will have $u(t) \approx x(t)$, $v(t) \approx y(t)$ and $w(t) \approx z(t)$. Thus, the decryption process becomes feasible and the two signals, $u(t)$ and $w(t)$, may be used to recover the original message in the following way

$$m(t) \approx \widehat{m}(t) = d(f(t)) = \frac{f(t)}{u(t)} - w(t).$$

As a numerical example of the above scheme, we shall try to encrypt the message signals given by $m_1(t) = 0.02\sin(t)\sin(100t)$ which possesses high frequency and then we shall do the same for the message signal $m_2(t) = 2sin(4t)$ which possesses small frequency. This will be done using the two chaotic systems $\mathbf{x}$ and $\mathbf{u}$ given by (2.25) and (2.26), respectively. We shall start first with $m_1(t)$ and with the case when $\mu = \nu = 0$ and $B_k = B = -\text{diag}(0.1, 0.06, 0.02)$, for all $k = 1, 2, \ldots$. The simulations of the original message $m_1(t)$ and the decrypted message $m_1(t)$ are shown in Figures 5.13(a) and 5.13(b), respectively. Moreover, and most importantly, in the case

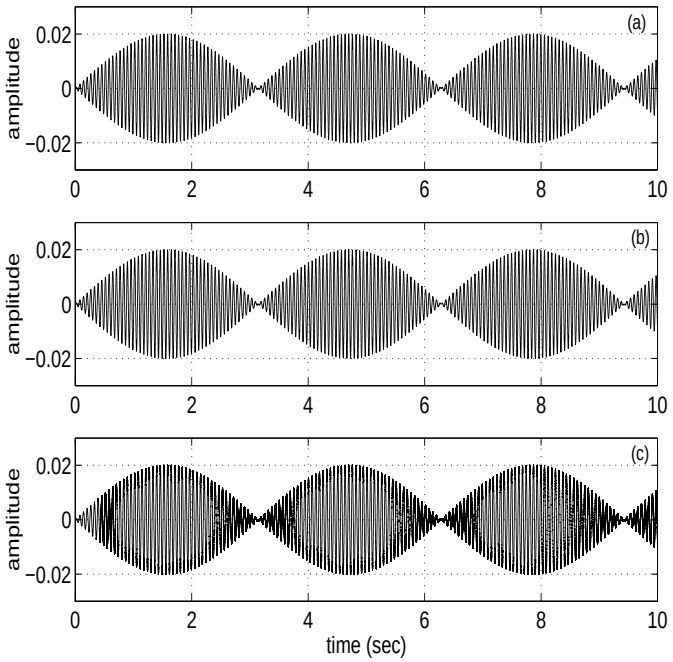

Figure 5.13: Accuracy of the decryption process: (a) Original message $m_1(t)$. (b) Decrypted message $m_1(t)$ for $\mu = \nu = 0$. (c) Decrypted message $m_1(t)$ for $\mu = \nu = 0.01$.

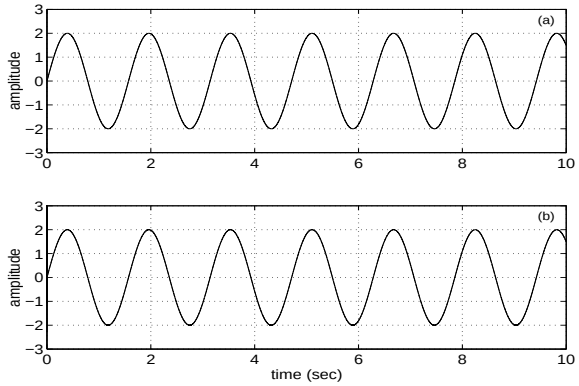

Figure 5.14: Accuracy of the decryption process. (a) Original message $m_2(t)$. (b) Decrypted message $m_2(t)$ for $\mu = \nu = 0.01$.

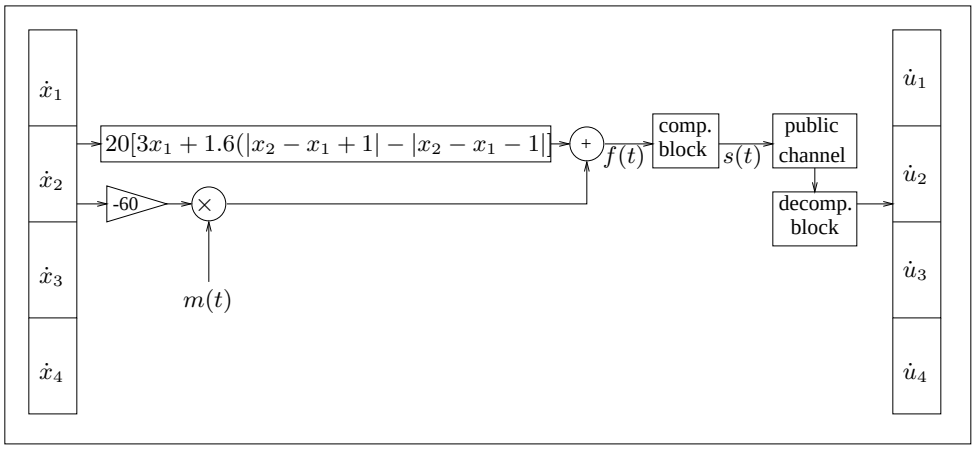

Figure 5.15: Encryption process of $m(t)$ using modulating and masking techniques.

when $\mu, \nu = 0.01$, the encryption and the decryption of $m_1(t)$ show excellent and very accurate results in comparison with the masking method proposed in [22], as shown in Figure 5.13(c). Accurate results are also obtained for the low frequency-large amplitude signal $m_2(t)$, as shown in Figure 5.14. i.e., this scheme is more robust and performs equally well with low-frequency and high-power-level type of messages. Clearly, the simulations show very robust results towards parameter mismatch.

Regarding delay, we shall now construct another cryptosystem very similar to the one just presented, except that the chaotic signals are generated by hyperchaotic systems installed at the transmitter and at the receiver ends. We shall apply the results of Sections 3.2 and 3.3, to show how robust this cryptosystem is towards delay. In particular, Theorems 3.2.1 and 3.2.2, will be used to provide us with the appropriate tools to verify that the hyperchaos-based cryptosystem will not be affected when bounded delays are present.

The proposed cryptosystem is shown in Figure 5.15. In this case, two hyperchaotic Chua's oscillators $\mathbf{x}$ and $\mathbf{u}$, described by equation (1.8), are used to mask-modulate and unmask the message signal $m(t)$, respectively, and are included in this cryptosystem. The hyperchaotic system $\mathbf{x} = (x_1, x_2, x_3, x_4)^T$ is at the transmitter end, whereas the hyperchaotic system $\mathbf{u} = (u_1, u_2, u_3, u_4)^T$ is at the receiver end. Identical to the procedure described above, the masking-modulating process of $m(t)$ is done through two operations: multiplication and addition, viz. $f(t) := e(m(t)) = (-60x_2(t)m(t)) + 20[3x_1 + 1.6(|x_2 - x_1 + 1| - |x_2 - x_1 - 1|)]$, where $f(t)$ is the encrypted signal that will be used to drive the hyperchaotic system $\mathbf{u}$ at the receiver end.

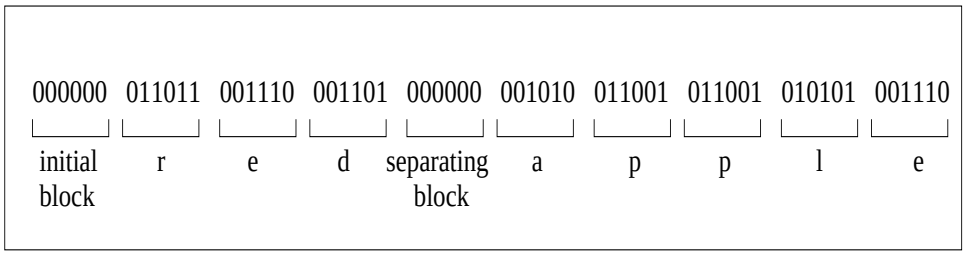

Figure 5.16: Binary representation of the text "red apple".

Binary representation of the English alphabet								
Letter	Value	Binary	Letter	Value	Binary	Letter	Value	Binary
A	10	1010	J	19	10011	S	28	11100
B	11	1011	K	20	10100	T	29	11101
C	12	1100	L	21	10101	U	30	11110
D	13	1101	M	22	10110	V	31	11111
E	14	1110	N	23	10111	W	32	100000
F	15	1111	O	24	11000	X	33	100001
G	16	10000	P	25	11001	Y	34	100010
H	17	10001	Q	26	11010	Z	35	100011
I	18	10010	R	27	11011			

Table 5.1: The binary representation of the English alphabet.

Once more, $s(t)$ is the transmitted signal consisting of the sequence of time frames of length P, shown in Figure 5.10. At the receiver, each time frame of $s(t)$ is decomposed into the encrypted message $f(t)$ and the synchronizing impulses. At this point, $f(t)$ is used to drive the system $\mathbf{u}$, whereas the impulses are used to impulsively synchronize $\mathbf{u}$ with $\mathbf{x}$, exactly in the same manner as the scheme shown in Figure 5.12. When synchronization is achieved, we have $\mathbf{x} \approx \mathbf{u}$. Thus the decryption process of $f(t)$ becomes feasible by applying the operation

$$m(t) \approx \widehat{m}(t) = d(f(t)) = \frac{f(t) - 20[3u_1 + 1.6(|u_2 - u_1 - 1| - |u_2 - u_1 + 1|)]}{-60u_2}.$$

We shall present a numerical example involving the above scheme and using the plain text "red apple". The basic idea of generating a signal $m(t)$ representing any plain text is to assign

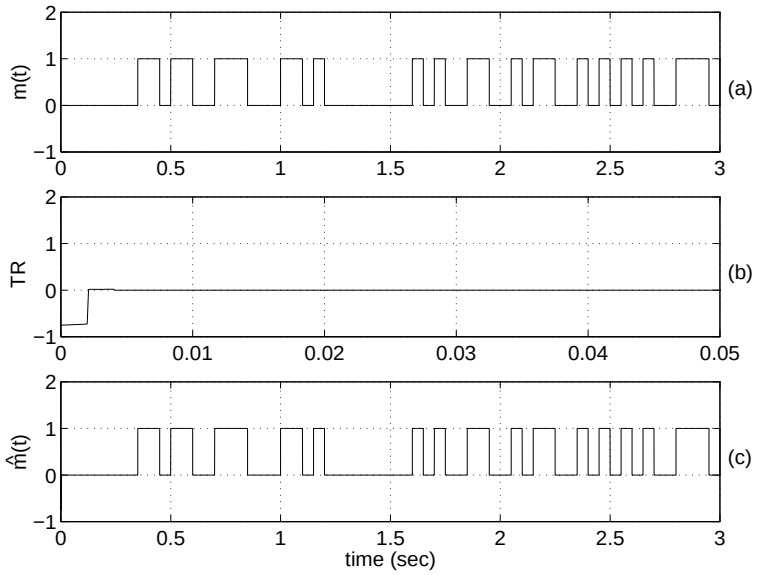

Figure 5.17: (a) Original information signal $m(t)$. (b) Transient region (TR). (c) Decrypted signal $\widehat{m}(t)$.

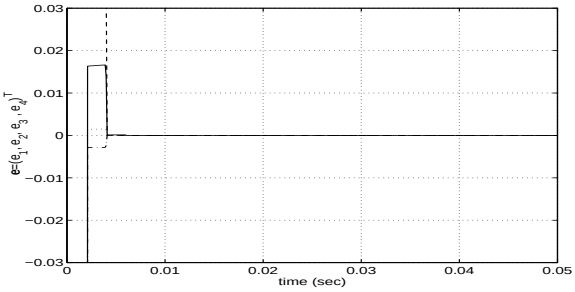

Figure 5.18: Components of the error dynamics $\mathbf{e}$ approaching zero as $t \to \infty$.

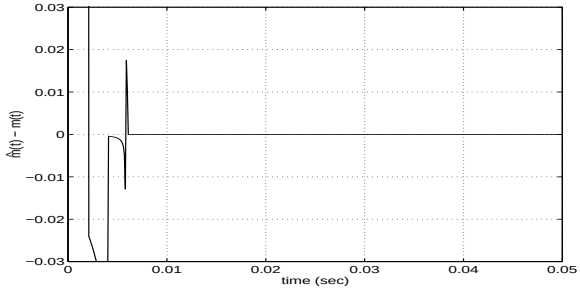

Figure 5.19: The difference $\widehat{m}(t) - m(t)$.

numbers to the English alphabet. For the letter 'A', we assign the number 10, for the letter 'B', we assign the number 11, and so on till we reach the last letter 'Z' whose assigned value is 35, as shown in Table 5.1. These numbers are transfered to their binary representation and a piecewise continuous signal $m(t)$ consisting of a sequence of step functions is generated to reflect these binary representations of any plain text. The way the signal $m(t)$ is constructed is done by forming a sequence of steps and blocks. Each block consists of 6 steps, where each step has length 0.05 sec. and height (or magnitude) equal to 0 or 1 depending on the value of the binary digit in the binary representation of the plain text. Each block represents the binary representation of one English letter only. If the letter has binary representation shorter than six digits (or steps), the missing steps are assigned the value 0 and placed on the left side of the block. For example, the letter 'E' has the binary representation 1110, which has 4 digits. Therefore the block for this letter will be represented by a set of six steps with the value 001110. The signal $m(t)$ becomes complete when it is preceded by a block of 0's (i.e., the first block of $m(t)$ is a set of six steps of magnitude 0), in order to avoid the transient region (TR) of impulsive synchronization, and the words are separated by blocks of 0's. Using the above set up, the binary representation of the plain text "red apple" becomes the sequence shown in Figure 5.16 and the piecewise continuous signal $m(t)$, representing this plain text, is shown in Figure 5.16 (a). Certainly, by implementing the cryptosystem described earlier, there will be two types of delay involved in the system. Delay in the impulses, denoted by r_i, for all $i = 1, 2, \ldots$, and in the differential system, denoted by $\widetilde{r}$, identical to those discussed in Chapter 3. We shall concern ourselves, however, in this numerical set up with the first type of delay r_i. i.e., we shall assume that the transmission delay is zero and we just have sampling delay. For an accurate decryption of the signal $f(t)$, identical synchronization between the two hyperchaotic systems, at the transmitter and receiver ends, is required. Now choosing the matrices B_i, to be $-I$, where I is the identity matrix, the delay terms $r_i = 0.0008$ ($\widetilde{r} = 0$) and $\Delta_i = 0.002$, for all $i = 1, 2, \ldots$, and using the Runge-Kutta method of step-size 0.0001 for integration, the numerical simulation of the error dynamics $\mathbf{e}$ shows identical synchronization starting from time 0.004 sec., as predicted by Theorem 3.2.2 (see Figure 5.18). Furthermore, the simulation of $\widehat{m}(t)$ is identical to the graph of $m(t)$, as shown in Figure 5.17 (c), where Figure 5.17 (b) shows the transient region (TR). This can be seen in Figure 5.19 which shows the graph of $\widehat{m}(t) - m(t)$ decaying to zero as $t \to \infty$. When $\widehat{m}(t)$ is retrieved at the receiver end, transferring the signal into a plain text is done through the same procedure as the one used to construct $m(t)$, i.e, by dividing the signal into blocks of six steps and reading the steps inside each block. The plain text "red apple" can therefore be recovered.

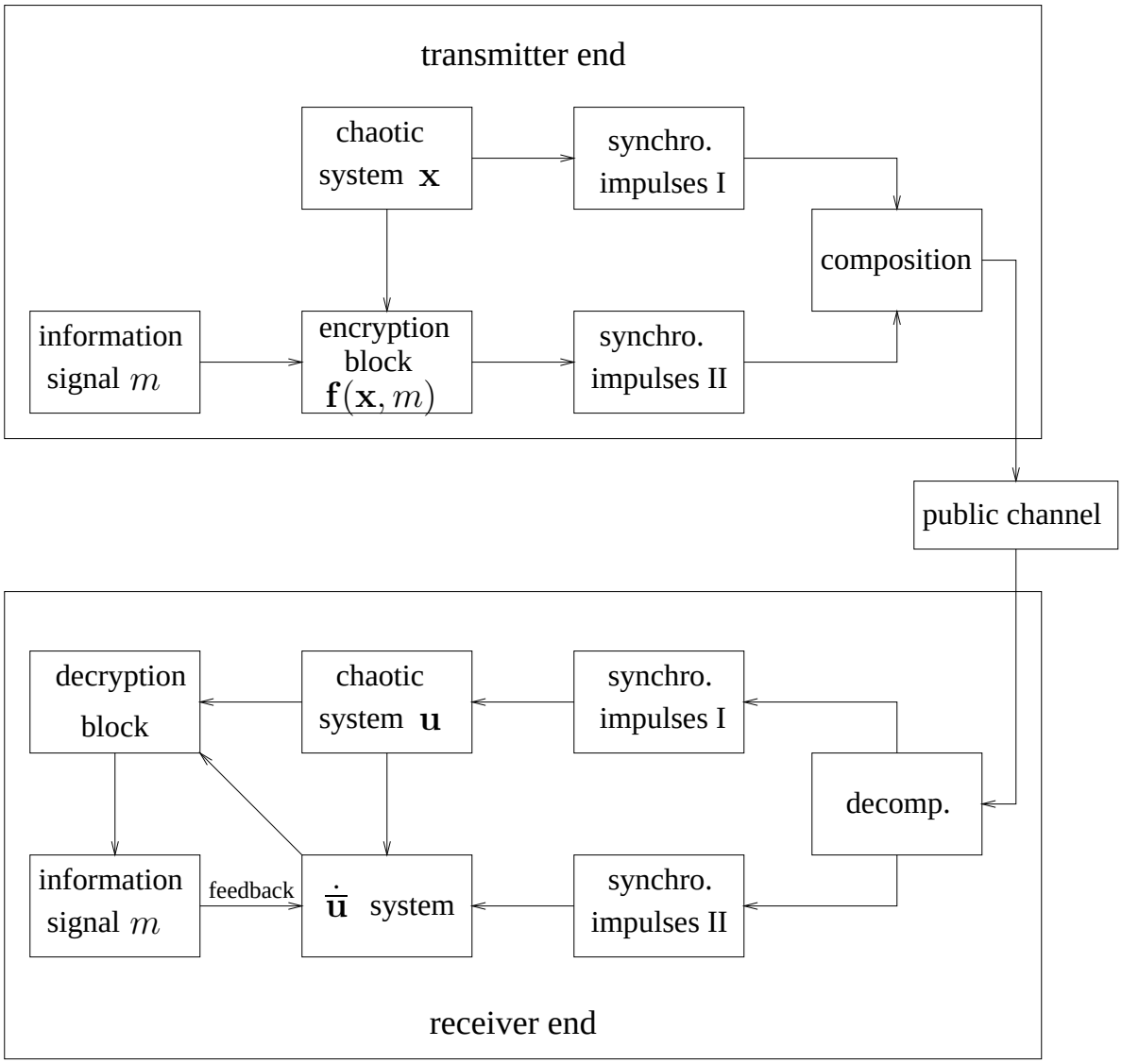

Figure 5.20: Induced-message cryptosystem.

After reflecting on the robustness of impulsive cryptosystems, it still remains to improve the security and the performance of the models discussed in this section and the model described in the previous section which was first proposed by Yang et al., [114–116]. The basic idea is to construct a new model that overcomes several issues related to the time-frame transmission process and improves the security of the transmission. Our following argument and discussion will depend mainly on Theorem 2.2.2 and the synchronization example employing the Lorenz chaotic system described afterwards, i.e., involving equations (2.34), (2.35), (2.36) and (2.37).

In Section 2.2, it has been demonstrated that the error dynamics $\mathbf{e}$ and $\dot{\overline{\mathbf{e}}}$, given by systems (2.38) and (2.39), are both uniformly Lagrange stable, for $q = 1$, provided that the conditions of Theorem 2.2.2 are satisfied. In other words, $\lim_{t\to\infty} \mathbf{e}(t) = \lim_{t\to\infty} \dot{\overline{\mathbf{e}}}(t) = \mathbf{0}$, a property which is considered to be the cornerstone of several chaos-based secure communication schemes. Certainly, we are interested in exploring the applications of this property in transmitting secret information between different parties. Figure 5.20 shows a new proposed cryptosystem, slightly different from the two cryptosystems shown in Figures 5.9 and 5.12, consisting of a transmitter, a receiver and a public channel for communication. The transmitter and the receiver each contains a chaotic system, $\mathbf{x}$ and $\mathbf{u}$, respectively, to generate the encrypting key signals and to drive their derivative systems $\dot{\mathbf{x}}$ and $\dot{\overline{\mathbf{u}}}$, installed at the transmitter and the receiver ends, respectively. The system $\dot{\mathbf{x}}$ is used as the encryption block to encrypt the information signal $f(t)$ at the transmitter end. In addition, the transmitter and the receiver each contains two synchronization impulses blocks. The first block is used to synchronize $\mathbf{u}$ with $\mathbf{x}$ and the other is used to synchronize $\dot{\overline{\mathbf{u}}}$ with $\dot{\mathbf{x}}$. The transmitter contains a composition block which combines the synchronization impulses from the two synchronization impulses blocks. This combining process is done through time frames each of which has length $2Q$ seconds. The first Q seconds are loaded with the impulses to synchronize $\mathbf{x}$ and $\mathbf{u}$, whereas the second Q seconds are loaded with the impulses needed to synchronize $\dot{\mathbf{x}}$ and $\dot{\overline{\mathbf{u}}}$. These time frames are sent across the public channel and are decomposed at the decomposition block at the receiver end into two Q seconds. The first Q seconds are fed into the system $\mathbf{u}$, to recover the key signals, and the second Q seconds are fed into the system $\dot{\overline{\mathbf{u}}}$, to induce the encrypted signal. At the decryption block, the recovered key signals are used to decrypt the induced encrypted information signal by applying the inverse of $\mathbf{f}$, $\mathbf{f}^{-1}$. Then the decrypted signal $m(t)$ is fed back into the block $\dot{\overline{\mathbf{u}}}$ for better and faster recovery.

The encryption-decryption process of the above model may be described as follows. The encryption block at the transmitter end applies conventional cryptographic techniques to the information signal $m(t)$ to formulate the encrypted signal $\mathbf{f}(\mathbf{x}, \tilde{m}(t), 1)$, where $\tilde{m}(t) = m(t)\exp(-\theta t)$,

for some chosen $\theta > 0$, and $\mathbf{f}$ is the nonlinear expression on the right hand side of equation (2.34) with $a = 1$. Thus the complexity of the encryption is increased. However, at the receiver end the chaotic system $\dot{\overline{\mathbf{u}}}$ is installed to synchronize with the system $\dot{\mathbf{x}}$ through applying impulses generated by the system $\dot{\mathbf{x}}$. Meanwhile the system $\dot{\overline{\mathbf{u}}}$ is self-generated and driven by the components of $\mathbf{u}$ and the decrypted signal $\tilde{m}(t)$, by applying message feedback, so that it will have a formulation identical to the system $\dot{\mathbf{x}}$ in order for both to impulsively synchronize. By Theorem 2.2.2, the error dynamics $\dot{\overline{\mathbf{e}}}$, given by system (2.39), is uniformly Lagrange stable. It should be noted that the impulsive synchronization still works for an arbitrary mapping $\mathbf{h} \neq \mathbf{f}$, and thus the complexity of the encryption process of the information signal can be increased by increasing the complexity and the non-linearity of $\mathbf{h}$. However, by choosing $\mathbf{h} \neq \mathbf{f}$, the transmission of the information signal to the receiver end requires two sequences of synchronizing impulses in addition to the sequence of impulses needed to recover the key signals (i.e., a total of three sequences for a complete recovery). This is unlike when $\mathbf{h} = \mathbf{f}$, which requires only one sequence to induce the encrypted signal. In addition, upon choosing $\mathbf{h} \neq \mathbf{f}$, we need to consider the total derivative of $\mathbf{h}$ with respect to t when formulating the system $\overline{\mathbf{x}}$. In other words the encryption block at the transmitter end will involve the system

$$\dot{\overline{\mathbf{x}}} = \frac{\partial \mathbf{h}}{\partial t}(\mathbf{x}, \tilde{m}(t)).$$

It can be seen that the keys and the encrypted signal are not sent across the public channel. They are embedded inside the impulses and then induced at the receiver end using the impulses. The new system is therefore called the induced-message cryptosystem.

One advantage of the induced-message cryptosystem is that it may overcome the problem arising from the time frame congestion problem presented in [41, 43–45, 83]. These papers employ an impulsive cryptosystem whose scheme is identical to the one described in the previous section, as shown in Figure 5.9, and the transmission is based on the time-frame process, shown in Figure 5.10 [114–116]. Recall that the transmitted signal consisted of a sequence of time frames, each of which had a length of P seconds, and is made up of two regions. The first region is the synchronization region of length Q seconds. It consists of the synchronization impulses needed to impulsively synchronize the two chaotic systems in both the transmitter and receiver. The second region contains the encrypted message signal and has a length of $P - Q$ seconds. Since Q is taken to be small compared to T, the lost of time in packing message signals is negligible [115]. The first experimental results on impulsive synchronization were presented in [83]. In the experiment, two Chua's oscillators were effectively synchronized by using narrow impulses ($Q/T = 0.16\%$,

$1/T = 18\text{kHz}$). It was found, in [41, 43–45], that the minimum length of the interval Q increases in proportion to the frame length as it increases. In fact, it was experimentally established that for $5 \times 10^{-5}\text{s} \leq T \leq 5 \times 10^{-3}\text{s}$, the ratio $Q/T \geq 50\%$ can achieve almost-identical synchronization, and thus the lost time in packing the message signals is no longer negligible. It was further realized that the situation becomes worse when implementing hyperchaotic systems where two impulsive synchronization regions (each of which is of length Q) are required for almost-identical synchronization (e.g., for $1.3 \times 10^{-5}\text{s} \leq T \leq 2 \times 10^{-5}\text{s}$, $2Q/T = 100\%$). Therefore, it is more desirable to eliminate this problem by not transmitting the encrypted signal in the first place. We have shown that, in the induced-message cryptosystem proposed above, we are able to accomplish this property of not transmitting the encrypted signal. Instead, two sequences of synchronizing impulses are transmitted only. One sequence is needed to recover the key signals and the other sequence is required to induce the encrypted signal. Thus we reach the objective of increasing the security of the impulsive cryptosystem and prevent the frames from being congested by the synchronization region.

In the following simulations, a fourth-order Runge-Kutta method with step size 10^{-5} is used. The system parameters are $\sigma = 10$, $r = 28$, $b = 8/3$, $B_k = B = -\text{diag}(0.5, 0.6, 0.2)$, the period of the impulses is $\Delta_k = \Delta = 0.002$, $k = 1, 2, \ldots$, and the initial conditions are $(x_0, y_0, z_0) = (3.07, -2.37, 0.88)$, $(u_0, v_0, w_0) = (1.46, -1.87, 0.5)$ and $(\dot{\overline{u}}_0, \dot{\overline{v}}_0, \dot{\overline{w}}_0) = (3.9,\ 0.74, -1.62)$. In the first example, we take the information signal $m_2(t) = 2\sin(4t)$, which has large amplitude and low frequency, as shown in Figure 5.14 (a). In this case $\tilde{m}_2(t) = 2\sin(4t)\exp(-\theta t)$, where θ is taken to be 1. The encryption process is identical to the one described in Figure 2.8. i.e.,

$$\mathbf{h}(\mathbf{x}, \tilde{m}_2(t)) = \mathbf{f}(\mathbf{x}, \tilde{m}_2(t), 1),$$

given by equation (2.34). With the arguments in Section 2.2 and in this section, we know that $\mathbf{u} \to \mathbf{x}$ and $\dot{\overline{\mathbf{u}}} \to \dot{\mathbf{x}}$. Therefore the key signals x, y and z can be recovered by obtaining the signals u, v and w. Moreover, with the process of feeding back the decrypted message $\tilde{m}_2(t)$ into the system $\dot{\overline{\mathbf{u}}}$, the state variable $\dot{\overline{v}} \to \dot{y} = f_2(t) = e(\tilde{m}_2(t)) = rx - y - (z + \tilde{m}_2(t))x$ ($f_2(t)$ is the encrypted signal), which will allow $\tilde{m}_2(t)$ to be recovered by simply using the following operation

$$\tilde{m}_2(t) \approx d(f_2(t)) - \left[w + \frac{\dot{\overline{v}} - ru + v}{u} \right].$$

Then $m_2(t)$ can be obtained by $m_2(t) = \tilde{m}_2(t)\exp(\theta t)$. Figure 5.21 shows the result of the decryption process of the induced message $m_2(t) = 2\sin(4t)$, and Figure 5.22 shows the error

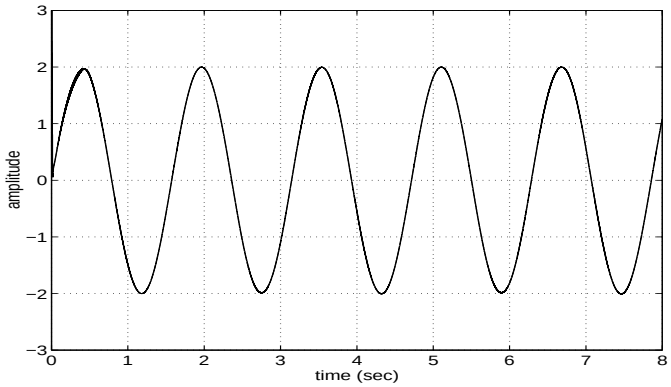

Figure 5.21: Decrypted message $m_2(t) = 2\sin(4t)$.

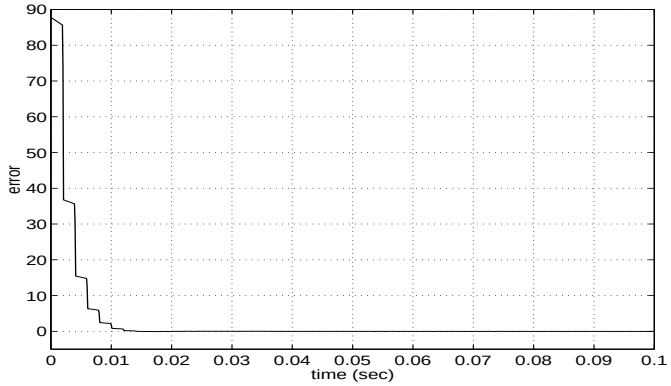

Figure 5.22: Exponential decay of the error between the original and decrypted messages, given by $m_2(t)$.

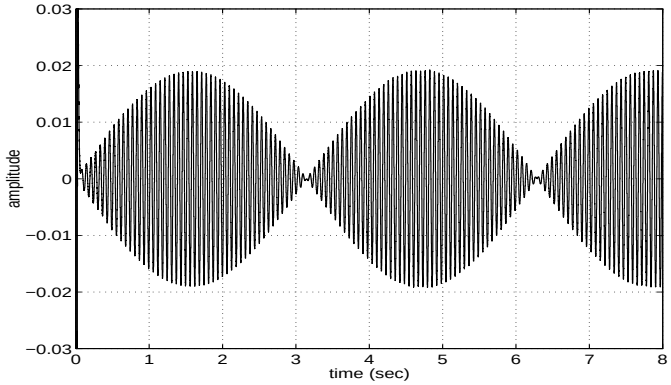

Figure 5.23: Decrypted message $m_1(t) = 0.02\sin(t)\sin(100t)$.

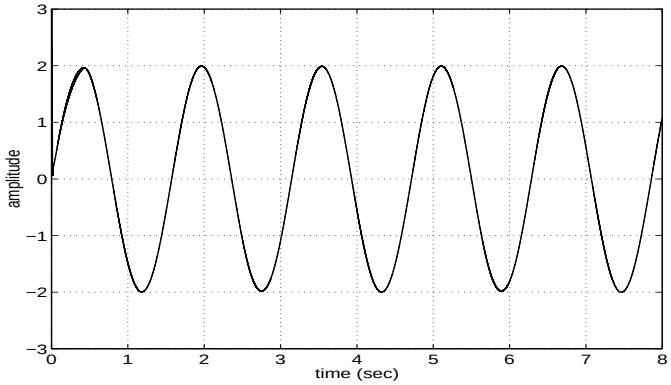

Figure 5.24: Accurate decryption of the message $m_2(t) = 2\sin(4t)$ for $\theta = 0$.

between the original message and the decrypted message decaying exponentially with time. Now similar and accurate results may be obtained when considering the other information signal $m_1(t) = 0.02\sin(t)\sin(100t)$, which possesses low amplitude and very high frequency, as shown in Figures 5.13 (a) and 5.23.

It should be mentioned that the parameter θ has a very significant role in the dynamics of the induced-message cryptosystem. Increasing the value of this parameter will increase the accuracy of the decryption process and decrease the error between the real information signal and the induced one. In other words, the larger the values of θ, the faster the convergence and the smaller the error. However, due to the software numerical integration errors, the decryption of the information signals may not be successful. This is due to the fact that, for large θ, $\exp(-\theta t)$ is driven to zero very fast with time and the information signal may be lost. Therefore the parameter θ has been chosen to be relatively small in the numerical integration process to recover the information signal. Figure 5.24 shows that even with $\theta = 0$ and without message feedback, the message signal $m_2(t) = 2\sin(4t)$ can still be accurately recovered. This also indicates that the induced-message cryptosystem is very robust.

5.3 Generalization to Partial Differential Equations

Due to the fact that PDE's have inherently complex behaviour associated with them and that it takes them usually longer to be solved numerically when compared to ODE's, it is believed that PDE's may lead to distinct advantages in masking information for secure communication (e.g., many more frequencies are involved in the mask when a PDE is used). Therefore there has been

several attempts to apply this theory to communication as a promising tool towards securing information transmission [29, 31, 32]. In this section, we investigate the possibility of making multichannel (ten channels or a hundred channels, for instance) spread-spectrum communication by synchronizing spatiotemporal chaos. The communication efficiency can be greatly enhanced since a large number of informative signals can be transmitted and received simultaneously. To fulfill this task, the operating spatiotemporal systems must have the following properties.

1. The chaotic motions of two identical systems can be synchronized by using control keys as infrequently as possible. The most convenient situation is that this spatiotemporal chaos can be synchronized by using a single key.

2. The chaotic signals transmitted from different channels must be independent (or, say, uncorrelated) from each other, then the interferences between different transmitted signals can be reduced to the lowest level.

3. The key sequences and the transmitted chaotic signals must be high-dimensional hyperchaos so that any imitation of keys and attacks against the transmitted signals are extremely difficult.

It was established in [106, 109] that certain PDE systems well possess these properties.

The study of communication security, by employing spatiotemporal chaotic systems generated by PDE's, is still under investigation for possible design of a secure communication scheme. It is still an open research topic with several potential ideas. For example, in [31, 32], the potential chaotic-optical wavefronts (which exhibits spatiotemporal chaotic behaviour) as information carriers in parallel communication systems, was investigated. It was shown, numerically, that broad-area non-linear ring cavities, generate spatiotemporally chaotic signals which may allow encryption and decryption of data in space and time. Furthermore, in [106], chaotic spatiotemporal chaotic dynamics, generated by non-linear set of coupled partial differential equations which are synchronized via a scalar complex variable, were used to design communication security schemes which are high-dimensional . It was established that those schemes were robust to noise. In addition, it was discovered that the added dimensionality created a new quasisynchronous state, enabling the transmission of multiple messages through a single scalar complex channel. However, the idea of implementing impulsive spatiotemporal synchronization in designing communication security schemes has not been yet investigated.

We shall attempt in this section to present two ways of designing multichannel communication security schemes based on impulsive spatiotemporal synchronization. These schemes will

just present the idea of generalizing the concept of impulsive cryptosystems, discussed in the previous section, to include spatiotemporal chaotic systems instead of low dimensional chaotic or hyperchaotic systems. Certainly, the questions regarding security, robustness, delay and implementation remain to be checked to see the practicality of these systems and if they provide better approach towards secure communications.

We begin our discussion by presenting the following cryptosystem shown in Figure 5.25. As described in the schemes employing low dimensional chaotic and hyperchaotic systems for secure communication, we shall have, in this case, two identical spatiotemporal chaotic systems: $\mathbf{u}$ at the transmitter end and $\mathbf{v}$ at the receiver end. The spatiotemporal chaotic system used in this model will be the Grey-Scott model, given by (4.26). Furthermore, in the new cryptosystem, the transmitter and the receiver each possesses an integrator to integrate the solutions of the drive and response systems, respectively, with respect to the spatial dimension x (the drive and response systems are the Grey-Scott models). At the transmitter end, the integrated chaotic signal $||\mathbf{u}||_2$ is used to encrypt the message signal $m(t)$ using any complicated conventional cryptographic technique such as the n-shift cipher, given by equation (5.2). For illustrative purposes, we shall just apply a masking technique for encrypting $m(t)$. i.e., we shall generate the encrypted signal $f(t) = ||\mathbf{u}(t,x)||_2 + m(t)$. Recall that, in Section 4.4, we have discussed theoretically the impulsive synchronization of two identical Grey-Scott models. Then, in Section 4.5, a numerical analysis of the Lyapunov exponents of the error dynamics between two Grey-Scot models, one of which drives the other through 32 spatial points out of 256 points (i.e., not along the whole spatial dimension x) was also investigated. The analysis revealed that the largest Lyapunov exponent of the error dynamics is negative and the synchronization is feasible provided that the impulse duration $\Delta = 0.1$ and impulse magnitude $Q_k = Q = \text{diag}(0, -0.5)$, $k = 0, 1, \ldots$, which are applied at 32 spatial points along the spatial dimension x in the direction of e_2 only. Investing this property in our new cryptosystem, we are able to send the values of the 32 spatial impulsive points at each moment τ_k, $k = 1, 2, \ldots$, and the encrypted signal $f(t)$ across two separate public channels to the receiver end. The impulses will be used to drive the response system $\mathbf{v}$ at the receiver end and the two Grey-Scot models will consequently synchronize. The integrator will generate the chaotic signal $||\mathbf{v}||_2$ which we already know will eventually satisfy the limiting property $\lim_{t\to\infty} ||\mathbf{v}||_2 = ||\mathbf{u}||_2$. Hence the chaotic signal $||\mathbf{v}||_2$ may be used now to retrieve the encrypted signal $m(t)$ by applying the operation

$$m(t) \approx \hat{m}(t) = f(t) - ||\mathbf{v}||_2.$$

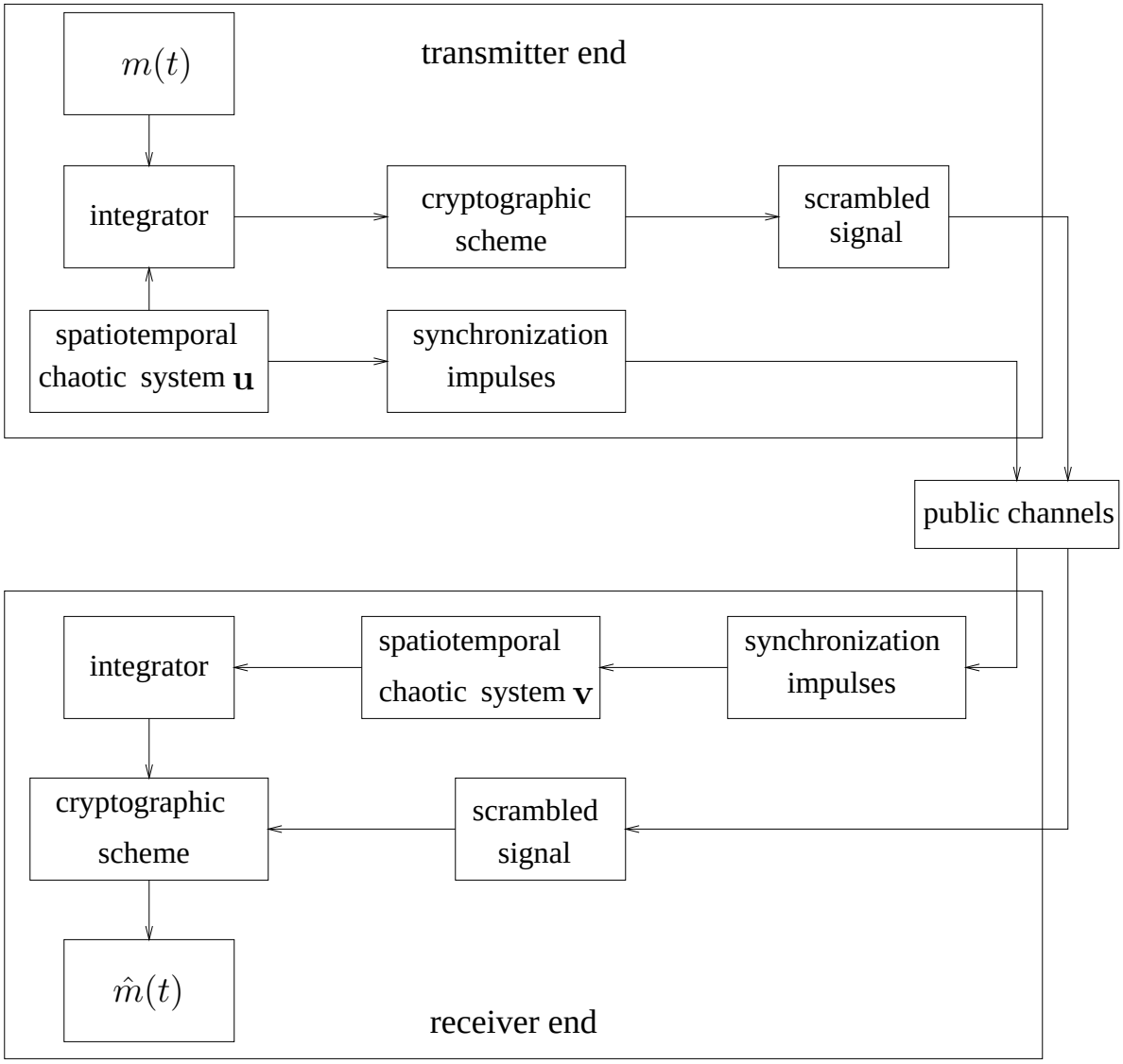

Figure 5.25: Scheme of the spatiotemporal-chaos-based cryptosystem.

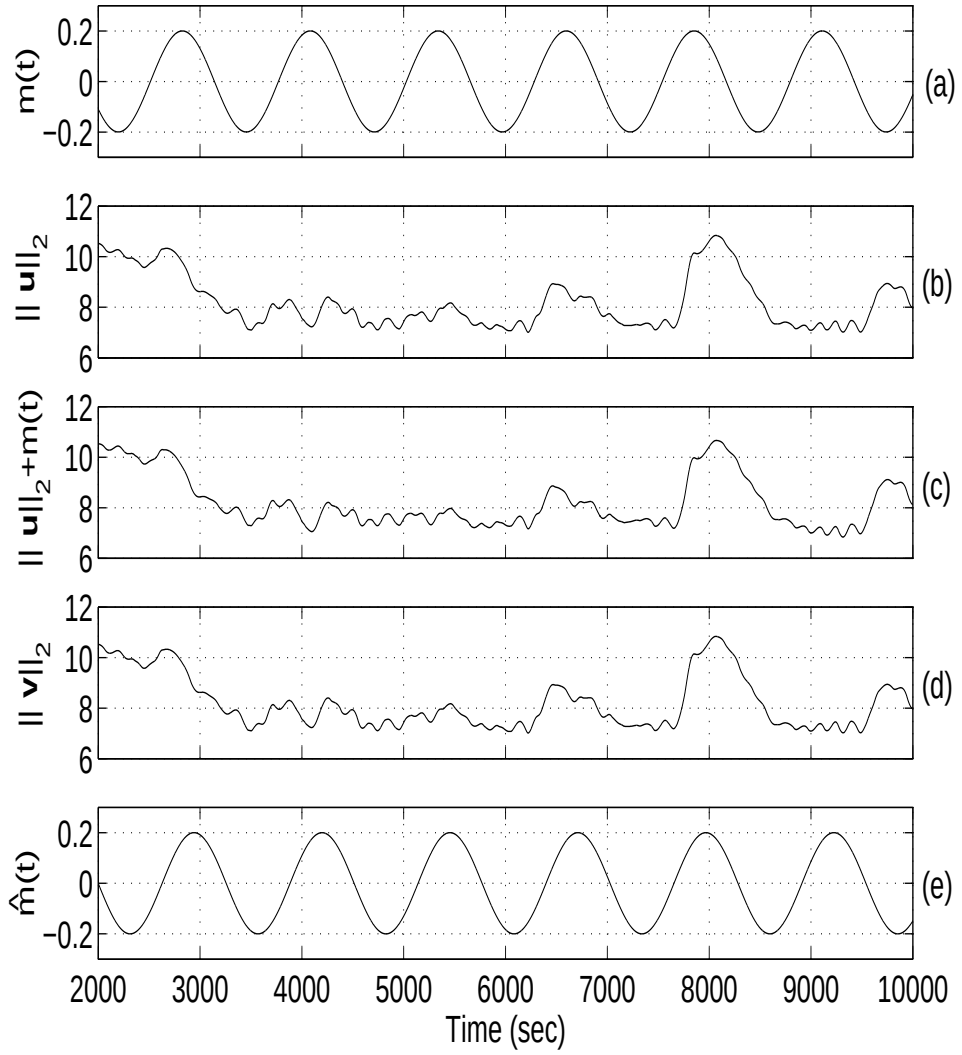

Figure 5.26: Encryption/decryption of $m(t) = 0.2\sin(t/200)$ using masking methods by a spatially integrated spatiotemporal chaotic signal for $\Delta = 0.1$ and $Q_k = Q = \text{diag}(0, -0.5)$ with impulses applied at 32 spatial points in the direction of e_2 only: (a) Original message $m(t)$. (b) Chaotic signal $||\mathbf{u}||_2$ at the transmitter end. (c) Masking the signal $m(t)$ using $||\mathbf{u}||_2$. (d) Chaotic signal $||\mathbf{v}||_2$ at the receiver end. (e) Retrieved signal $\hat{m}(t)$.

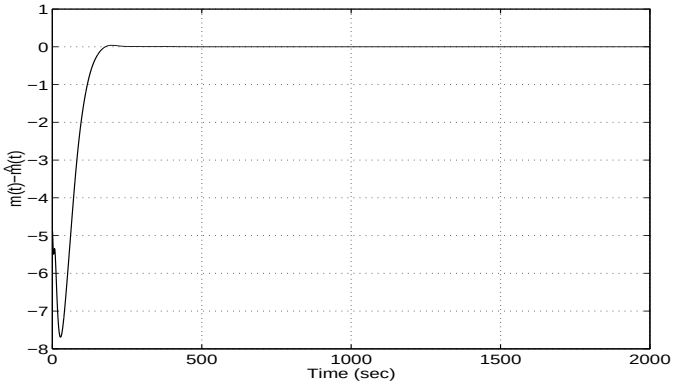

Figure 5.27: The difference $m(t) - \hat{m}(t)$ decaying to zero.

In Figure 5.26, we have used a forward Euler integration of the finite difference equations generated from the discretization of the two Grey-Scott models to obtain the simulations. In the first simulation, Figure 5.26 (a), we show the graph of the original message signal $m(t) = 0.2\sin(t/200)$. In the second and third simulations, Figure 5.26 (b) and (c), we show the graph of $||\mathbf{u}||_2$ and $||\mathbf{u}||_2 + m(t)$, respectively. Notice the two graphs in (b) and (c) are almost identical. In the fourth simulation, Figure 5.26 (d), the graph of the response system is shown and finally in Figure 5.26 (e) the graph of the decrypted signal $\hat{m}(t)$ is displayed showing accurate results away from the transient region. Figure 5.27 confirms this by showing the convergence of the difference $m(t) - \hat{m}(t)$ to zero.

The second cryptosystem we shall propose next is based on the idea of transferring the system of PDE's to a system of ODE's, by applying the numerical method of lines, discussed in Section 4.5. As we said before, the idea of the numerical method of lines is to apply finite difference methods to discretize the spatial partial derivatives and transfer the temporal partial derivative to ordinary derivatives. The resulting system of differential equations will become a system of coupled ODE's whose dynamics is an approximation of the original system of PDE's. Thus, when applying the numerical method of lines to a pair Grey-Scott models, with periodic boundary conditions, for example, by discretizing the second spatial partial derivatives $\partial^2 u/\partial x^2$ and $\partial^2 v/\partial x^2$, at the transmitter and receiver, respectively, the resulting system of 2×257 coupled ODE's will

be given by (see equations (4.51) and (4.52))

$$\left\{\begin{array}{rcl} \dot{u}_1^{(0)} &=& -u_1^{(0)}\left(u_2^{(0)}\right)^2 + a(1-u_1^{(0)}) + d_1\dfrac{2u_1^{(0)} - 5u_1^{(1)} + 4u_1^{(2)} - u_1^{(3)}}{(\Delta x)^2} \\ \dot{u}_1^{(j)} &=& -u_1^{(j)}\left(u_2^{(j)}\right)^2 + a(1-u_1^{(j)}) + d_1\dfrac{u_1^{(j+1)} - 2u_1^{(j)} + u_1^{(j-1)}}{(\Delta x)^2} \\ \dot{u}_2^{(j)} &=& u_1^{(j)}\left(u_2^{(j)}\right)^2 - (a+b)u_2^{(j)} + d_2\dfrac{u_2^{(j+1)} - 2u_2^{(j)} + u_2^{(j-1)}}{(\Delta x)^2} \\ \dot{u}_1^{(256)} &=& -u_1^{(256)}\left(u_2^{(256)}\right)^2 + a(1-u_1^{(256)}) + d_1\dfrac{2u_1^{(256)} - 5u_1^{(255)} + 4u_1^{(254)} - u_1^{(253)}}{(\Delta x)^2} \end{array}\right. \tag{5.3}$$

at the transmitter end, whereas at the receiver end, we have

$$\left\{\begin{array}{rcl} \dot{v}_1^{(0)} &=& -v_1^{(0)}\left(v_2^{(0)}\right)^2 + a(1-v_1^{(0)}) + d_1\dfrac{2v_1^{(0)} - 5v_1^{(1)} + 4v_1^{(2)} - v_1^{(3)}}{(\Delta x)^2} \\ \dot{v}_2^{(j)} &=& -v_1^{(j)}\left(v_2^{(j)}\right)^2 + a(1-v_1^{(j)}) + d_1\dfrac{v_1^{(j+1)} - 2v_1^{(j)} + v_1^{(j-1)}}{(\Delta x)^2} \\ \dot{v}_2^{(j)} &=& v_1^{(j)}\left(v_2^{(j)}\right)^2 - (a+b)v_2^{(j)} + d_2\dfrac{v_2^{(j+1)} - 2v_2^{(j)} + v_2^{(j-1)}}{(\Delta x)^2} \\ \dot{v}_1^{(256)} &=& -v_1^{(256)}\left(v_2^{(256)}\right)^2 + a(1-v_1^{(256)}) + \\ && d_1\dfrac{2v_1^{(256)} - 5v_1^{(255)} + 4v_1^{(254)} - v_1^{(253)}}{(\Delta x)^2} \\ v_2(\tau_k^+)^{(8*\kappa)} &=& v_2(\tau_k)^{(8*\kappa)} + \epsilon(u_2(\tau_k)^{(8*\kappa)} - v_2(\tau_k)^{(8*\kappa)}), \end{array}\right. \tag{5.4}$$

for $j = 1, 2, \ldots, 255$, $\kappa = 1, 2, \ldots, 32$ and $\epsilon = -0.5$. In other words, the new state variables $v_1^{(j)}$ and $v_2^{(j)}$ are impulsively synchronized with the state variables $u_1^{(j)}$ and $u_2^{(j)}$, for $j = 0, 1, \ldots, 256$, by impulsively driving $v_1^{(8*\kappa)}$ and $v_2^{(8*\kappa)}$ by the discrete values of $u_1^{(8*\kappa)}$ and $u_2^{(8*\kappa)}$, $\kappa = 1, 2, \ldots, 32$, at the moments τ_k, $k = 1, 2, \ldots$. The new system of coupled ODE's, given by (5.3), has positive

Lyapunov exponents and exhibits spatiotemporal chaos which is considered more complex than the behaviour of low dimensional chaotic and hyperchaotic systems. This more complex behaviour provides a promising tool towards establishing more secure communication schemes. Clearly, system (5.3) can be used, as we did in Sections 5.1 and 5.2, to design impulsive cryptosystems identical to those ones illustrated by Figures 5.9, 5.12 and 5.20.

Let us, for example, use the impulsive cryptosystem, shown in Figure 5.9, and masking methods as a conventional cryptographic technique, to test the ability to combine systems (5.3) and (5.4) with this cryptosystem. Using the message signal $m(t) = 0.2\sin(t/200)$ and the state variables $u_1^{(92)}$ as a masking signal to generate the encrypted signal $f(t) = u_1^{(92)} + m(t)$ and transmitting the resulting signal, together with the impulses to the receiver through public channels, we obtain the following results. The simulations in Figure 5.28 are obtained by using fourth order Runge-Kutta method to integrate systems (5.3) and (5.4) with respect to time. The original message signal $m(t)$ and the chaotic signal $u_1^{(92)}(t)$ are shown in Figure 5.28 (a) and (b), respectively. In Figure 5.28 (c), the encrypted signal $f(t) = u_1^{(92)}(t) + m(t)$ is shown. When the two spatiotemporal chaotic systems $(\mathbf{u}_1(t), \mathbf{u}_2(t))^T = (u_1^{(0)}, u_1^{(1)}, \ldots, u_1^{(256)}, u_2^{(0)}, u_2^{(1)}, \ldots, u_2^{(256)})^T$, at the transmitter end, synchronize impulsively with the spatiotemporal chaotic system $(\mathbf{v}_1(t), \mathbf{v}_2(t))^T = (v_1^{(0)}, v_1^{(1)}, \ldots, v_1^{(256)}, v_2^{(0)}, v_2^{(1)}, \ldots, v_2^{(256)})^T$, at the receiver end, we will have $\lim_{t\to\infty} v_1^{(92)} = u_1^{(92)}$. The convergence follows from the fact that the largest Lyapunov exponent of the error dynamics between systems (5.3) and (5.4) is negative, as illustrated in Section 4.5. The simulation of the signal $v_1^{(92)}$ is shown in Figure 5.28 (d) which shows almost identical behaviour to the simulation of the signal $u_1^{(92)}$. Thus retrieving the signal $m(t)$ becomes feasible by applying once more the operation

$$m(t) \approx \hat{m}(t) = f(t) - v_1^{(92)}(t).$$

Figure 5.28 (e) shows the propagation of the decrypted signal $\hat{m}(t)$ which exhibits very accurate decryption process. Finally, Figure 5.29 displays the difference $m(t) - \hat{m}(t)$ decaying to zero to confirm our prediction of convergence.

Thus, from the above discussion, spatiotemporal chaos may provide us with a better impulsive cryptosystem in the sense of designing a more secure and more reliable secure communication schemes. Certainly, it will remain to check if this conjecture is true and see how implementable such spatiotemporal-chaos-based cryptosystems are. This will open the door for more required research work in this area that we will leave for future research work.

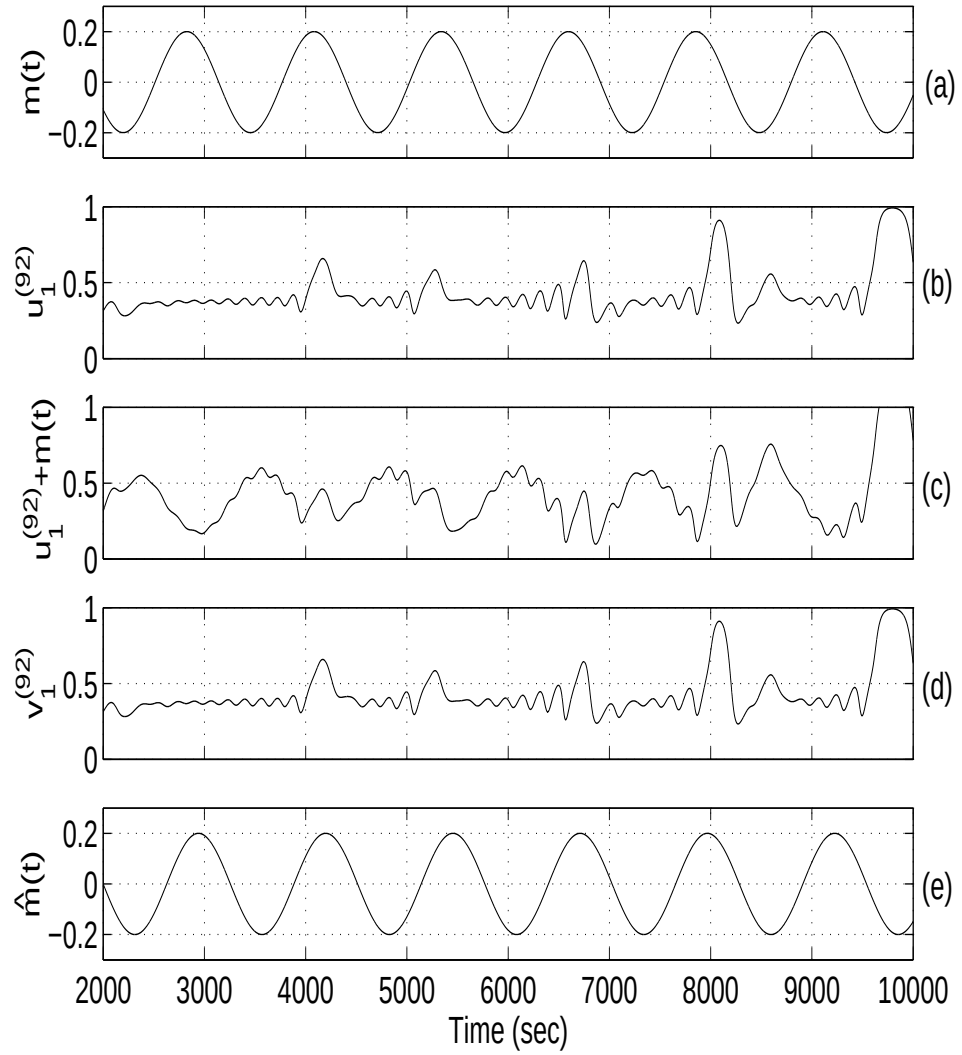

Figure 5.28: Encryption/decryption of $m(t) = 0.2\sin(t/200)$ by applying masking methods using the signal $u_1^{(92)}$ for $\Delta = 0.1$ and $\epsilon = -0.5$: (a) Original message $m(t)$. (b) Chaotic signal $u_1^{(92)}$ at the transmitter end. (c) Masking the signal $m(t)$ using $u_1^{(92)}$. (d) Chaotic signal $v_1^{(92)}$ at the receiver end. (e) Retrieved signal $\hat{m}(t)$.

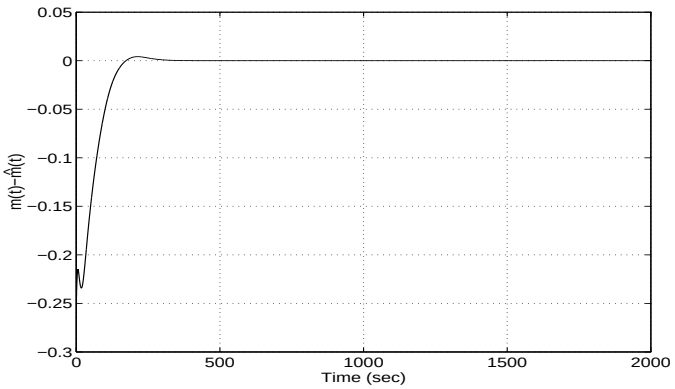

Figure 5.29: The difference $m(t) - \hat{m}(t)$ decaying to zero.

Chapter 6

Conclusions and Discussions

It was established in this thesis that we are able to combine impulsive control theory with chaos synchronization. The theory led us eventually to develop a new technique, called impulsive synchronization, to externally control the general behaviour of chaotic, hyperchaotic and spatiotemporal chaotic systems. In other words, in the presence of two chaotic, hyperchaotic or spatiotemporal chaotic systems, the behaviour of one system was manipulated, by applying impulsive synchronization, in such a way that this system, the response system, was forced to behave in accordance with the behaviour of the other system, the drive system. The performance of this method of synchronization was tested to check for robustness towards parameter mismatch and towards delay, including sampling and transmission delays. We found out that impulsive synchronization possesses this robustness property under certain conditions when dealing with chaotic and hyperchaotic systems. Due to the fact that parameter mismatch and delay issues are inevitable problems, robustness becomes evidently important when dealing with impulsive synchronization. The conditions required to guarantee this robustness property were expressed in this thesis as sufficient conditions for convergence of the error dynamics, between the chaotic and hyperchaotic systems involved, to zero. The mathematical description of convergence was given in terms of Lagrange stability and/or equi-attractivity in the large property. Depending on the stability property we had into our consideration, the sufficient conditions, corresponding to each stability property, were derived to establish theoretically that impulsive synchronization is robust when dealing with chaotic and hyperchaotic systems. The numerical analysis of impulsive synchronization employing Lyapunov exponents confirmed our theoretical results and gave another approach to deal with this synchronization method. However, with the presence of delay, it

still remains to develop a technique to investigate the Lyapunov exponents of the synchronization errors between the chaotic or hyperchaotic systems involved. This technique will be an extension of the method developed when delay was neglected.

The application of impulsive synchronization to secure communication were also discussed in this thesis. We showed that several impulsive cryptosystems can be designed to transmit secret information across public channel or channels. Due to the ability of impulsive synchronization to be combined with conventional cryptographic techniques and its robustness, it provided us with a very promising tool for the purpose of building a communication security scheme. We extended the work done in this area by proposing the induced-message cryptosystem which provides more security than the model proposed in [114–116], and solves the time-frame congestion problem. We finally extended this work to employ spatiotemporal chaotic systems and showed that the possibility of employing spatiotemporal chaotic systems in impulsive cryptosystems to increase their security is very feasible and quite promising.

There are still many unanswered questions regarding impulsive synchronization in general and its applications, in particular when dealing with spatiotemporal chaotic systems. Some of these questions open the door for more future research work in this are. For example: Is impulsive synchronization robust in the presence of parameter mismatch when dealing with spatiotemporal chaotic systems? What happens when delay is present in such systems? How much security can impulsive cryptosystems, based in spatiotemporal chaos, provide and how implementable are they? Is it possible to establish the numerical results, obtained concerning the Lyapunov exponents when dealing with spatiotemporal chaotic systems, theoretically? These questions remain unanswered and require more investigation and more exploration. In fact, the lack of general formulation to describe many spatiotemporal chaotic systems make answering such questions very hard and require dealing with each spatiotemporal chaotic system individually.

Bibliography

[1] R. E. Amritkar and N. Gupte, "Synchronization of Chaotic Orbits: The Effect of a Finite Time Steps", Physical Review E., **47**(6), 3889-3895, 1993.

[2] L. Arnold, H. Crauel and J.-P. Eckmann, "Lyapunov Exponents", Springer-Verlag, Proceedings, Oberwolfach, 1990.

[3] L. Arnold and V. Wihstutz, "Lyapunov Exponents", Springer-Verlag, Proceedings, Bremen, 1984.

[4] D. Bainov, Z. Kamont and E. Minchev, "On the Impulsive Partial Differential-Functional Inequalities of First Order", Utilitas Mathematica, **48**, 107-128, 1995.

[5] D. Bainov, Z. Kamont and E. Minchev, "On the Stability of Solutions of Impulsive Partial Differential Equations of First Order", Advances in Mathematical Sciences and Applications, **6**(2), 589-598, 1996.

[6] D. Bainov and E. Minchev, "On the Stability of Solutions of Impulsive Partial Differential-Functional Equations of First Order via Lyapunov Functions", Non-Linear Phenomenon in Complex Systems, **30**(2), 109-116, 2000.

[7] D. Bainov and P. Simeonov, "Impulsive Differential Equations: Periodic Solutions and Applications", Longman Group UK Limited, 1993.

[8] G. Ballinger and X. Z. Liu, "On Boundedness of Solutions of Impulsive Systems", Non-Linear Studies, **4**(1), 121-131, 1997.

[9] G. H. Ballinger and X. Z. Liu, "Existence and Uniqueness Results for Impulsive Delay Differential Equations" Dynamics of Continuous, Discrete and Impulsive Systems, **5**, 579-591, 1999.

[10] G. H. Ballinger and X. Z. Liu, "Existence, Uniqueness and Boundedness Results for Impulsive Delay Differential Equations", Applicable Analysis, **74**(1-2), 71-93, 2000.

[11] Th. Beth, D. E. Lazic and A. Mathias, "Cryptanalysis of Cryptosystems Based on Remote Chaos Replication", Advances in Cryptology-CRYPTO'94, 318-331, 1994.

[12] S. Boccaletti, J. Bragard and F. T. Arecchi, "Controlling and Synchronizing Space Time Chaos", Physical Review E., **59**(6), 6574-6578, 1999.

[13] S. Boccaletti, J. Bragard, F. T. Arecchi and H. Mancini, "Synchronization in Non-Identical Extended Systems", Physical Review Letters, **83**(3), 536-539, 1999.

[14] W. E. Boyce and R. C. DiPrima, "Elementary Differential Equations and Boundary Value Problems", John Wiley & Sons, Inc., 1991.

[15] T. A. Burton, "Stability and Periodic Solutions of Ordinary and Functional Differential Equations", Academic, New York, 1985.

[16] T. L. Carroll and L. M. Pecora, "Using Multiple Attractor Chaotic Systems for Communication", Chaos, **9**(2), 445-451, 1999.

[17] T. L. Carroll and L. M. Pecora, "Synchronization Non-Autonomous Chaotic circuits", IEEE Transactions on Circuits and Systems-II: Analog and Digital Signal Processing, **40**(10), 646-650, 1993.

[18] T. L. Carroll and L. M. Pecora, "Cascading Synchronized Chaotic Systems", Physica D, **67**, 126-140, 1993.

[19] T. L. Carroll and L. M. Pecora, "Synchronizing Chaotic Circuits", IEEE Transactions on Circuits and Systems, **38**(4), 453-456, 1991.

[20] T. E. Carter, "Optimal Impulsive Space Trajectories Based on Linear Equations", Journal of Optimization Theory and Applications, **70**(2), 277-297, 1991.

[21] M. C. Cross and P. C. Hohenberg, "Pattern Formation Outside of Equilibrium", Reviews of Modern Physics, **65**(8), 851-1112, 1993.

[22] K. M. Cuomo and A. V. Oppenheim, "Chaotic Signals and Systems for Communications", IEEE International Conference on Acoustics, Speech and Signal Processing, **3**, 137-140, 1993.

[23] K. M. Cuomo and A. V. Oppenheim, "Circuit Implementation of Synchronized Chaos with Applications to Communications", Physical Review Letters, **71**(1), 65-68, 1993.

[24] K. M. Cuomo, A. V. Oppenheim and S. H. Strogatz, "Synchronization of Lorenz-Based Chaotic Circuit with Applications to Communications", IEEE Transactions on Circuits and Systems-II: Analog and Digital Signal Processing, **40**(10), 626-633, 1993.

[25] F. Dachselt and W. Schwarz, "Chaos and Cryptography", IEEE Transactions on Circuits and Systems-I: Fundamental Theory and Applications, **48**(12), 1498-1509, 2001.

[26] R. L. Devaney, "An Introduction to Chaotic Dynamical Systems", Addison-Wesley Publishing Company, Inc., 1989.

[27] L. H. Erbe, H. I. Freedman, X. Z. Liu and J. H. Wu, "Comparison Principles for Impulsive Parabolic Equations with Applications to Models of Single Species Growth", Journal of the Australian Mathematical Society, Series B, **32**, 382-400, 1991.

[28] G. Franceschini, S. Bose and E. Schöll, "Control of Chaotic Spatiotemporal Spiking by Time-Delay Auto-synchronization", Physical Review E., **60**(5), 5426-5434, 1999.

[29] B. Fraser, P. Yu and T. Lookman, "Secure Communications Using Chaos Synchronization" Physics in Canada, Special Issue on Non-Linear Dynamics, **57**(2), 155-161, 2001.

[30] A. Friedman, "Foundations of Modern Analysis", Dover Publications, Inc., NY, 1970.

[31] J. García-Ojalvo and R. Roy, "Parallel Communication with Optical Spatiotemporal Chaos", IEEE Transactions on Circuits and Systems-I: Fundamental Theory and Applications, **48**(12), 1491-1497, 2001.

[32] J. García-Ojalvo and R. Roy, "Spatiotemporal Communication with Synchronized Optical Chaos", Physical Review letters, **86**, 5204-5207, 2001.

[33] G. Grassi and S. Mascolo, "Non-Linear Observer Design to Synchronize Hyperchaotic Systems via a Scalar Signal", IEEE Transactions on Circuits and Systems-I: Fundamental Theory and Applications, **44**(10), 1011-1014, 1997.

[34] G. Grassi and S. Mascolo, "A System Theory Approach for Designing Cryptosystems Based on Hyperchaos", IEEE Transactions on Circuits and Systems-I: Fundamental Theory and Applications, **46**(9), 1135-1138, 1999.

[35] G. Grassi and S. Mascolo, "Synchronizing Hyperchaotic Systems by Observer Design", IEEE Transactions on Circuits and Systems-II: Analog and Digital Signal Processing, **46**(4), 478-483, 1999.

[36] Z. H. Guan, C. W. Chan, Y. T. Leung and G. Chen, "Robust Stabilization of Singular-Impulsive-Delayed Systems with Non-Linear Perturbations", IEEE Transactions on Circuits and Systems-I: Fundamental Theory and Applications, **48**(8), 2001.

[37] D. Gulick, "Encounters with Chaos", McGraw-Hill Inc.,1992.

[38] T. Habutsu, Y. Nishio, I. Sasase and S. Mori, "A Secret Key Cryptosystem by Iterating a Chaotic Map", Advances in Cryptology-CRYPTO'91, 127-140, 1991.

[39] K. S. Halle, C. W. Wu, M. Itoh and L. O. Chua, "Spread Spectrum Communication Through Modulation of Chaos", International Journal of Bifurcation and Chaos, **3**(2), 469-477, 1993.

[40] J. F. Hurley, "Multivariable Calculus", Saunders College Publishing, Philadelphia, 1981.

[41] M. Itoh, "Experimental Study of Impulsive Synchronization", Proceedings of the 1999 IEEE International Symposium on Circuits and Systems, Orlando, 410-413, 1999.

[42] M. Itoh and H. Murakami, "New Communication Systems via Chaotic Synchronizations and Modulations", The Institute of Electronics, Information and Communication Engineers, Transactions on Fundamentals of Electronics, Communications and Computer Sciences, **E78-A**(3), 285-290, 1995.

[43] M. Itoh, T. Yang and L. O. Chua, "Experimental Study of Impulsive Synchronization of Chaotic and Hyperchaotic Circuits", International Journal of Bifurcation and Chaos, **9**(7), 1393-1424, 1999.

[44] M. Itoh, T. Yang and L. O. Chua, "Conditions for Impulsive Synchronization of Chaotic and Hyperchaotic Systems", International Journal of Bifurcation and Chaos, **11**(2), 551-560, 2001.

[45] M. Itoh, N. Yamamoto, T. Yang and L. O. Chua, "Performance Analysis of Impulsive Synchronization", Proceedings of the 1999 European Conference on Circuit Theory and Design, Stresa, 353-356, 1999.

[46] L. Junge and U. Parlitz, "Control and Synchronization of Spatially Extended Systems", Proceedings of the International Symposium on Non-Linear Theory and its Applications (NOLTA'98) Le Régent, Crans-Montana, Switzerland, 303-306, September 14-17.

[47] L. Junge and U. Parlitz, "Synchronization and Control of Coupled Ginzburg-Landau Equations Using Local Coupling", Physical Review E., **61**(4), 3736-3742, 2000.

[48] L. Junge and U. Parlitz, "Phase Synchronization of Coupled Ginzburg-Landau Equations", Physical Review E., **62**(1), 438-441, 2000.

[49] L. Junge, U. Parlitz, Z. Tasev and L. Kocarev, " Synchronization and Control of Spatially Extended Systems Using Sensor Coupling", International Journal of Bifurcation and Chaos, **9**(12), 2265-2270, 1999.

[50] Z. Kamont and B. Zubic-Kowal, "Numerical Methods for Impulsive partial Differential Equations", Dynamic Systems and Applications, **7**, 29-52, 1998.

[51] W. G. Kelley and A. C. Peterson, "Difference Equations: An Introduction with Applications", Academic Press, 2nd edition, 2001.

[52] A. Khadra, X. Z. Liu and X. Shen, "Robust Impulsive Synchronization and Its Application to Communication Security", International Journal of Dynamics of Continuous, Discrete, and Impulsive systems, Series B, Applications & Algorithms, **10b**(3), 403-417, 2003.

[53] A. Khadra, X. Z. Liu and X. Shen, "Application of Impulsive Synchronization to Communication Security", IEEE Transactions on Circuits and Systems-I: Fundamental Theory and Applications, **50**(3), 341- 351, 2003.

[54] A. Khadra, X. Z. Liu and X. Shen, "Impulsively Synchronizing Chaotic Systems with Delay and Applications to Secure Communication", Automatica, to appear, 35 pages.

[55] A. Khadra, X. Z. Liu and X. Shen, "Robustness Analysis of Impulsive Synchronization of Chaotic Systems with Delayed Impulses", submitted to IEEE Transactions on Circuits and Systems-I: Fundamental Theory and Applications, October 2002, 22 pages.

[56] A. Khadra, X. Z. Liu and X. Shen, "Impulsive Control and Synchronization of Spatiotemporal Chaos Generated by Spatially Extended Systems", submitted to International Journal of Bifurcation and Chaos, September 2003, 26 pages.

[57] H. K. Khalil, "Non-Linear Systems", Prentice-Hall, Inc., 1996.

[58] L. Kocarev, K. S. Halle, K. Eckert, L. O. Chua and U. Parlitz, "Experimental Demonstration of Secure Communications via Chaotic Synchronization", International Journal of Bifurcation and Chaos, **2**(3), 709-713, 1992.

[59] L. Kocarev and U. Parlitz, "Synchronizing Spatiotemporal Chaos in Coupled Non-Linear Oscillators", Physical Review Letters, **77**(11), 2206-2209, 1996.

[60] L. Kocarev, Z. Tasev and U. Parlitz, "Synchronizing Spatiotemporal Chaos of Partial Differential Equations", Physical Review Letters, **79**(1), 51-54, 1997.

[61] L. Kocarev, Z. Tasev, T. Stojanovski and U. Parlitz, "Synchronizing Spatiotemporal Chaos", Chaos, **7**(4), 635-643, 1997.

[62] V. B. Kolmanovskii and V. R. Nosov, "Stability of Functional Differential Equations", Academic Press, Inc., 1986.

[63] V. Lakshmikantham, D. D. Bainov and P. S. Simeonov, "Theory of Impulsive Differential Equations", World Scientific, Singapore, 1989.

[64] V. Lakshmikantham and X. Z. Liu, "Stability Analysis in Terms of Two Measures", World Scientific, Singapore, 1993.

[65] V. Lakshmikantham and X. Z. Liu, "Stability Criteria for Impulsive Differential Equations in Terms of Two Measures", Journal of Mathematical Analysis and Applications, **137**, 591-604, 1989.

[66] V. Lakshmikantham, L. Wen and B. Zhang, "Theory of Differential Equations with Unbounded Delay", Kluwer Academic Publishers, 1994.

[67] R. J. LeVeque, "Numerical Methods for Conservation Laws", Birkhäuser Verlag, Basel, 1990.

[68] R. J. LeVeque, "Finite Volume Methods for Hyperbolic Problems", Cambridge University Press, 2002.

[69] Z. G. Li, C. Y. Wen and Y. C. Soh, "Analysis and Design of Impulsive Control Systems", IEEE Transactions on Automatic Control, **46**, 894-899, 2001.

[70] Z. G. Li, C. Y. Wen, Y. C. Soh and W. X. Xie, "The Stabilization and Synchronization of Chua's Oscillators via Impulsive Control", IEEE Transactions on Circuits and Systems-I: Fundamental Theory and Applications, **48**(11), 1351-1355, 2001.

[71] X. Z. Liu, "Stability Results for Impulsive Differential Systems with Applications to Population Growth Models", Dynamics and Stability of Systems, **9**(2), 163-174, 1994.

[72] X. Z. Liu, "Impulsive Stabilization and Control of Chaotic Systems", Non-Linear Analysis, **47**, 1081-1092, 2001.

[73] X. Z. Liu and G. Ballinger, "On Boundedness of Solutions of Impulsive Systems in Terms of Two Measures", Non-Linear World, **4**, 417-434, 1997.

[74] X. Z. Liu and A. R. Willms, "Impulsive Controllability of Linear Dynamical Systems with Applications to Maneuvers of Spacecraft", Max Planck Institute for Extraterrestrial Physics, **2**, 277-299, 1996.

[75] X. Z. Liu and D. Y. Xu, "Uniform Asymptotic Stability of Abstract Functional Differential Equations", Journal of Mathematical Analysis and Applications, **216**, 626-643, 1997.

[76] T. Matsumoto, L. O. Chua and K. Kobayashi, "Hyperchaos: Laboratory Experiment and Numerical Confirmation", IEEE Transactions on Circuits and Systems-I: Fundamental Theory and Applications, **33**(11), 1143-1147, 1986.

[77] R. K. Miller and A. N. Michel, "Ordinary Differential Equations", Academic Press, Inc., 1982.

[78] A. A. Minai and T. D. Pandian, "Communicating with Noise: How Chaos and Noise Combine to Generate Secure Encryption Keys", Chaos, **8**(3), 621-628, 1998.

[79] F. Morrison, "The Art of Modeling Dynamic Systems; Forecasting for Chaos, Randomness, & Determinism", Multi-science Press, Inc., 1991.

[80] H. Nijmeijer and I. M. Y. Mareels, "An Observer Looks at Synchronization", IEEE Transactions on Circuits and Systems-I: Fundamental Theory and Applications, **44**(10), 1997.

[81] M. J. Ogorzalik, "Taming Chaos: Part I-Synchronization", IEEE Transactions on Circuits and Systems-I: Fundamental Theory and Applications, **40**(10), 693-699, 1993.

[82] M. J. Ogorzalik, "Taming Chaos: Part II-Control", IEEE Transactions on Circuits and Systems-I: Fundamental Theory and Applications, **40**(10), 700-706, 1993.

[83] A. I. Panas, T. Yang and L. O. Chua, "Experimental Results of Impulsive Synchronization Between Two Chua's Circuits", International Journal of Bifurcation and Chaos, **8**(3), 639-644, 1998.

[84] T. S. Parker and L. O. Chua, "Practical Numerical Algorithms for Chaotic Systems", Springer-Verlag, 1989.

[85] U. Parlitz, L. O. Chua, L. Kocarev, K. Halle and A. Shang, "Transmission of Digital Signals by Chaotic Synchronization", International Journal of Bifurcation and Chaos, **2**, 973-977, 1992.

[86] U. Parlitz and S. Ergezinger, "Robust Communication Based on Chaotic Spreading Sequences", Physics Letters A., **188**, 146-150, 1994.

[87] J. E. Pearson, "Complex Patters in a Simple System", Science, **261**, 189-192, 1993.

[88] L. M. Pecora and T. L. Carroll, "Synchronization in Chaotic Systems", Physical Review Letters, **64**(8), 821-824, 1990.

[89] L. M. Pecora and T. L. Carroll, "Driving Systems with Chaotic Signals", Physical Review A., **44**(4), 2374-2383, 1991.

[90] J. H. Peng, E. J. Ding, M. Ding and W Yang, "Synchronizing Hyperchaos with Scalar Transmitted Signal", Physical Review Letters, **76**(6), 904-907, 1996.

[91] J. E. Prussing, "Optimal Impulsive Linear Systems: Conditions and Maximum Number of Impulses", The Journal of the Astronautical Sciences, **43**(2), 195-206, 1995.

[92] D. Ruelle, "Chaotic Evolution and Strange Attractors", Cambridge University Press, 1989.

[93] W. E. Schiesser, "The Numerical Method of Lines: Integration of Partial Differential Equations", Academic Press, Inc.

[94] H. G. Schuster, "Handbook of Chaos Control", WILEY-VCH Verlag GmbH, 1999.

[95] H. Sira-Ramírez and C. Cruz-Hernández, "Synchronization of Chaotic Systems: A Generalized Hamiltonian Systems Approach", International Journal of Bifurcation and Chaos, **11**(5), 1381-1395, 2001.

[96] W. Stallings, "Cryptography and Network Security: Principles and Practice", 2nd edition, Prentice-Hall, Inc., 1999.

[97] T. Stojanovski, L. Kocarev and U. Parlitz, "Driving and Synchronizing by Chaotic Impulses", Physical Review E., **43**(9), 782-785, 1996.

[98] B. Straughan, "The Energy Method, Stability, and Non-Linear Convection", Springer-Verlag New York, Inc., 1992.

[99] M. Sushchick, "Synchronized Chaotic Oscillations", Ph.D. Dissertation, University of California, San Diego, 1996.

[100] J. A. Suykens, P. F. Curran and L. O. Chua "Robust Synthesis for Master-Slave Synchronization of Lur'e Systems", IEEE Transactions on Circuits and Systems-I: Fundamental Theory and Applications, **46**(7), 841-850, 1999.

[101] J. A. Suykens, P. F. Curran, J. Vandewalle and L. O. Chua "Robust Non-Linear H_∞ Synchronization of Chaotic Lur'e Systems", IEEE Transactions on Circuits and Systems-I: Fundamental Theory and Applications, Special Issue on Chaos Synchronization, Control and Applications, **44**(10), 891-904, 1997.

[102] J. A. Suykens, T. Yang and L. O. Chua, "Impulsive Synchronization of Chaotic Lur'e Systems by Measurement Feedback", International Journal of Bifurcation and Chaos, **8**(6), 1371-1381, 1998.

[103] Z. Tasev, L. Kocarev, L. Junge and U. Parlitz, "Synchronization of Kuramoto-Sivashinsky Equations Using Spatially Local Coupling", International Journal of Bifurcation and Chaos, **10**(4), 869-873, 2000.

[104] X. Wang, "Discrete-Time Neural Networks as Dynamical Systems", Ph.D Thesis, University of Southern California, 1992.

[105] X. Wang, "Period-Doublings to Chaos in a Simple Neural Network: An Analytic Proof", Complex Systems, **5**, 411-425, 1991.

[106] J. K. White and J. V. Moloney, "Multichannel Communication Using an Infinite Dimensional Spatiotemporal Chaotic System", Physical Review A, **59**(3), 2422-2426, 1999.

[107] A. Wolf, J. B. Swift, H. L. Swinney and J. A. Vastano, "Determining Lyapunov Exponents from a Time Series", Physica 16D, 285-317, 1985.

[108] C. W. Wu and L. O. Chua, "A Simple Way to Synchronize Chaotic Systems with Applications to Secure Communication Systems", International Journal of Bifurcation and Chaos, **3**(6), 1619-1627, 1993.

[109] J. H. Xiao, G. Hu and Z. Qu, "Synchronization of Spatiotemporal Chaos and Its Application to Multichannel Spread-Spectrum Communication", Physical Review Letters, **77** (20), 4162-4165, 1996.

[110] T. Yang, "Blind Signal Separation Using Cellular Neural Networks", International Journal of Circuit Theory and Applications, **22**, 399-409, 1994.

[111] T. Yang, "Recovery of Digital Signals from Chaotic Switching", International Journal of Circuit Theory and Applications, **23**, 611-615, 1995.

[112] T. Yang, "Impulsive Control Theory", Berlin: Springer-Verlag, Lecture Notes in Control and Information Sciences, **272**, Paperback, August 2001.

[113] T. Yang, "Impulsive Systems and Control: Theory and Applications", Huntington, NY, Nova Science Publishers, Inc., September 2001.

[114] T. Yang and L. O. Chua, "Impulsive Stabilization for Control and Synchronization of Chaotic Systems: Theory and Application to Secure Communication", IEEE Transactions on Circuits and Systems-I: Fundamental Theory and Applications, **44**(10), 976-988, 1997.

[115] T. Yang and L. O. Chua, "Impulsive Control and Synchronization of Non-Linear Dynamical Systems and Application to Secure Communication", International Journal of Bifurcation and Chaos, **7**(3), 645-664, 1997.

[116] T. Yang and L. O. Chua, "Impulsive Control and Synchronization of Chaotic Systems and Secure Communication", Electron. Res., Lab., College of Eng., University of California at Berkeley, Memo. UCB/ERL M97/12, 1997.

[117] T. Yang and L. O. Chua, "Generalized Synchronization of Chaos via Linear Transformations", International Journal of Bifurcation and Chaos, **9**(1), 215-219, 1999.

[118] T. Yang, J. A. Suykens and L. O. Chua, "Impulsive Control of Non-Autonomous Chaotic Systems Using Practical Stabilization", International Journal of Bifurcation and Chaos, **8**(7), 1557-1564, 1998.

[119] T. Yang, C. W. Wu and L. O. Chua, "Cryptography Based on Chaotic Systems", IEEE Transactions on Circuits and Systems-I: Fundamental Theory and Applications, **44**(5), 469-473, 1997.

[120] T. Yang, C. M. Yang and L. B. Yang, "Control of Rössler System to Periodic Motions Using Impulsive Control Methods", Physics Letters A., **232**, 356-361, 1997.

[121] T. Yang, L. B. Yang and C. M. Yang, "Impulsive Synchronization of Lorenz Systems", Physics Letters A, **226**(6), 349-354, 1997.

[122] T. Yang, L. B. Yang and C. M. Yang, "Impulsive Control of Lorenz System", Physica D, **110**, 18-24, 1997.